

Shujun Wang *Editor*

Starch Structure, Functionality and Application in Foods

 Springer

Starch Structure, Functionality and Application in Foods

Shujun Wang
Editor

Starch Structure, Functionality and Application in Foods

 Springer

Editor

Shujun Wang
State Key Laboratory of Food Nutrition &
Safety/School of Food Science &
Engineering
Tianjin University of Science &
Technology
Tianjin, China

ISBN 978-981-15-0621-5 ISBN 978-981-15-0622-2 (eBook)
<https://doi.org/10.1007/978-981-15-0622-2>

© Springer Nature Singapore Pte Ltd. 2020

This work is subject to copyright. All rights are reserved by the Publisher, whether the whole or part of the material is concerned, specifically the rights of translation, reprinting, reuse of illustrations, recitation, broadcasting, reproduction on microfilms or in any other physical way, and transmission or information storage and retrieval, electronic adaptation, computer software, or by similar or dissimilar methodology now known or hereafter developed.

The use of general descriptive names, registered names, trademarks, service marks, etc. in this publication does not imply, even in the absence of a specific statement, that such names are exempt from the relevant protective laws and regulations and therefore free for general use.

The publisher, the authors, and the editors are safe to assume that the advice and information in this book are believed to be true and accurate at the date of publication. Neither the publisher nor the authors or the editors give a warranty, expressed or implied, with respect to the material contained herein or for any errors or omissions that may have been made. The publisher remains neutral with regard to jurisdictional claims in published maps and institutional affiliations.

This Springer imprint is published by the registered company Springer Nature Singapore Pte Ltd.
The registered company address is: 152 Beach Road, #21-01/04 Gateway East, Singapore 189721, Singapore

Contents

History of Starch Research	1
Les Copeland	
Botanical Sources of Starch	9
Shujun Wang and Peng Guo	
Fine Structure of Amylose and Amylopectin	29
Xiangli Kong	
Multiscale Structures of Starch Granules	41
Shujun Wang, Hanbin Xu, and Huiyu Luan	
Amylose–Lipid Complex	57
Qiang Huang, Xu Chen, Shaokang Wang, and Jianzhong Zhu	
Phase Transitions of Starch and Molecular Mechanisms	77
Shujun Wang, Chen Chao, Shiqing Huang, and Jinglin Yu	
Rheological, Pasting, and Textural Properties of Starch	121
Shujun Wang and Fei Ren	
Starch Modification and Application	131
Shujun Wang, Jinwei Wang, Yi Liu, and Xia Liu	
In Vitro Starch Digestion: Mechanisms and Kinetic Models	151
Bin Zhang, Haiteng Li, Shaokang Wang, Shahid Ahmed Junejo, Xingxun Liu, and Qiang Huang	
Digestibility of Starches for Human Health	169
Les Copeland	

History of Starch Research



Les Copeland

Abstract This chapter presents a brief overview of key discoveries that led to our current knowledge of starch. Due to the variability of natural starch, and the significance of this biopolymer to humans in foods and industrial applications, much attention has been given to gaining an understanding of its structure and functional properties. Early uses for starch are considered, as are developments in the growth of the starch industries, and how the molecular structure of starch was revealed.

Keywords Starch · Structure · Functional properties · Application

Starch is the main storage carbohydrate of plants and a biopolymer of considerable significance for humans. It is a macro-constituent of many foods and the main source of energy in the human diet. Starch is also extracted industrially in large quantities for use in manufactured foods, pharmaceuticals and non-edible products. Natural starch is highly variable between and within plant species, resulting in unpredictability of functional properties important for processing and human nutrition. Hence, much attention has been given to seeking an understanding of the structure and properties of starch in relation to functionality and applications. This chapter will highlight key discoveries that have led to our current knowledge of starch.

The importance of starch to humans dates back to the Palaeolithic era, when starchy foods from roots and tubers were likely to have had a significant role in the evolution of modern humans from early hominin ancestors [1]. Starch grains have been identified in archaeological artefacts, including human dental calculus, dating back hundreds of thousands of years, as described in detail in the monograph edited by Torrence and Barton [2] and updated more recently [3, 4]. Although this is a fascinating area of research for archaeological scholars, with relevance for modern

L. Copeland (✉)

School of Life and Environmental Sciences, The University of Sydney, Sydney, NSW, Australia
e-mail: les.copeland@sydney.edu.au

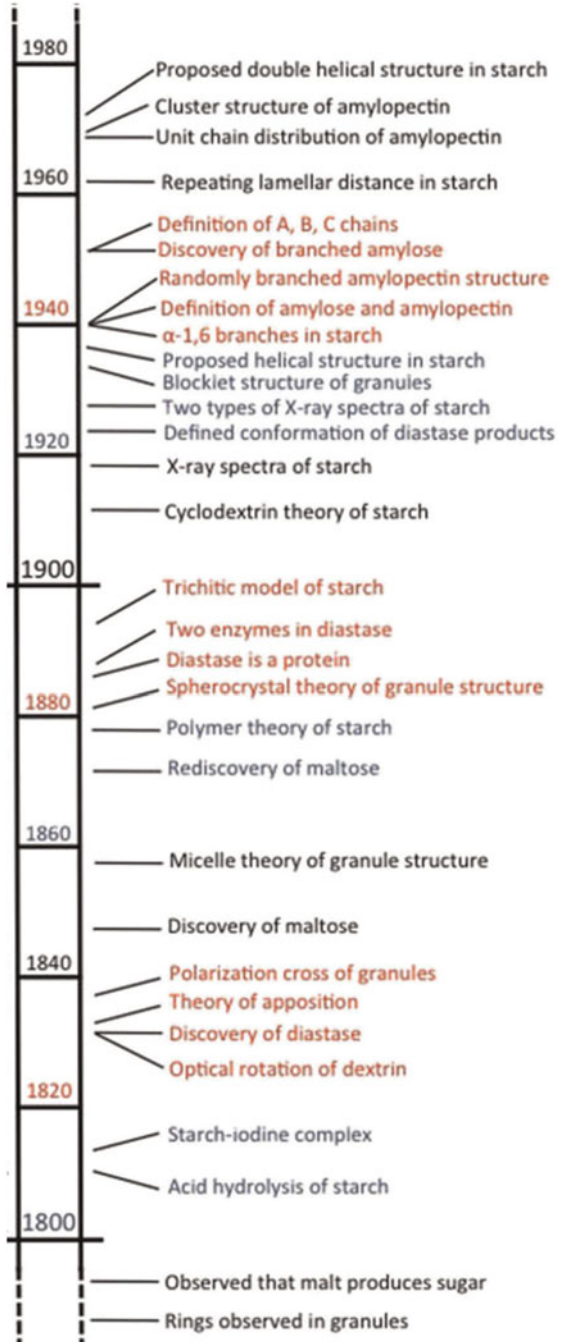
human nutrition and physiology, its consideration is beyond the scope of this discussion.

An early account of the history of research on starch and its uses was written by Herstein [5] to coincide with the centenary in 1911 of the inversion of starch to glucose by dilute acid. More recently, Schwartz and Whistler [6] documented key aspects of the history of starch research, the growth of the starch industries, and the development of specialty starches, for example, waxy, high-amylose and chemically modified starches. However, particularly noteworthy is a series of six definitive essays by Koushik Seetharaman and Eric Bertoft published in 2012 and 2013 under the general title “Perspectives on the history of research on starch” in the journal *Starch-Stärke* [7–12]. These essays tell in considerable detail the story of the discovery of the molecular structure and architectural makeup of starch. They are a lasting tribute to Dr Koushik Seetharaman, whose untimely passing in 2014 was a great loss to the starch community.

With the relatively recent publication of these comprehensive essays, it is not the intention here to provide another detailed account of the history of research on starch. Rather, attention will be drawn to some of the key milestones in the development of our knowledge, as depicted schematically in the timeline shown in Fig. 1. The history of the development of our understanding of the biosynthesis of starch is also beyond the scope of this chapter. This subject has been reviewed extensively, and the reader is directed to a selection of articles for a good overview of developments in this area [13–15].

According to the early historical records described in more detail in the above-mentioned publications, the material we now know as starch was being used in Ancient Egypt by about 800 BCE to stiffening fabrics, as an adhesive to bind together strips of papyrus, and in cosmetics and medicines. The starch used for these purposes was obtained by partial fermentation of wheat grains. According to a description in a Roman treatise dating back as early as 184 BCE, the procedure for preparing starch was to steep grain (usually wheat or barley) in water for 10 days, pressing and mixing with fresh water, filtering through a linen cloth and allowing the slurry to settle. The sedimented material was washed with water and dried in the sun. In the early Roman Empire, Pliny the Elder (23–74 CE) documented how starch, made by boiling freshly ground wheat flour with vinegar, was used for coating papyrus to create a smooth surface, to whiten cloth, powder hair and thicken food sauces. These applications may be examples of early uses of starch modified by acid. There are also records from the fourth century BCE of early Chinese documents coated with finely powdered rice starch to prevent ink penetration, a use of starch that continues today with paper and textiles and is known as sizing. In Mediaeval times, the Dutch established a starch manufacturing process from wheat, mainly for use in laundering as a fabric stiffener. The name starch is likely to have come from this use; starch is derived from the German word *Stärke*, which means strong or stiff. Starch was introduced into England during the reign of Queen Elizabeth I in the mid-sixteenth century. Powdering hair with starch was popular with wealthy Europeans by the mid-eighteenth century.

Fig. 1 Timeline of the development of knowledge of starch (adapted from [12])



Starch was first examined microscopically in 1716 by the Dutch scientist Antonie van Leeuwenhoek. He made detailed hand-drawn sketches that depicted discrete granules, even showing the detail of growth rings. Subsequently in 1745, Beccari of Bologna separated wheat flour into gluten and starch. This was an important achievement, not only in the characterization of starch. It showed for the first time that wheat flour contained a protein component. Proteinaceous material had been thought to be present only in animals, but Beccari's experiment showed it to be also present in vegetable matter [16]. Other early seminal discoveries on the nature of starch included the elemental analysis of potato starch by the Swedish chemist Jöns Berzelius in the early nineteenth century giving the formula $C_6H_{12}O_6$, and Nicolas-Theodore de Saussure of Switzerland in 1835 establishing the relationship between starch and glucose to be 100:110, thereby showing that "starch differed only from sugar by the element of water". The discovery of the element iodine in 1811 by Bernard Courtois, and the subsequent finding that it forms an intense blue colour with starch, led to the development of sensitive indicators for both starch and iodine.

As detailed in the account by Herstein [5], in 1811 a young German chemist, Gottlieb Kirchoff, working at the Academy of Sciences in St. Petersburg, Russia, demonstrated the conversion of starch to glucose by boiling with dilute sulfuric acid. The crystallization of glucose from the sugary syrup obtained opened the way to the industrial production of glucose as a sweetener and eventually for use in fermentations into alcohol and acetic acid. Starch from wheat and potatoes was the main source of glucose in Europe. The industrial production of glucose thrived during the Napoleonic Wars in the nineteenth century with the imposition of trade embargoes on the importation of sugar. The potato starch industry in Germany dates from 1765, and commercial dextrans were made in Germany from 1860. By the beginning of the nineteenth century, roots and tubers were recognized in Europe as alternative sources of starch to cereals. The starch industry expanded in the nineteenth century with the rapid growth of the textile, paper and printing industries and the conversion of starch to dextrans for the production of gum substitutes. Production of glucose from starch until the early 1900s involved acid hydrolysis, with the use of enzymes becoming widespread only in the 1940s and 1950s.

In the USA, industrial production of starch grew rapidly, firstly from wheat (1807) and then from potatoes (1820) and corn (1844). The National Starch Company (now Ingredion) was formed in 1900 by the merger of United Starch Co. and National Starch Manufacturing Co. Waxy maize starch was discovered in China in the early 1900s and was brought to the USA in 1909, but it was not until 1940s that waxy corn was developed into a high-yielding hybrid. High AM corn starch was developed in the USA in the 1940s. From the 1930s, the development of numerous chemical modifications expanded the commercial uses of starch. Fermentation of dextrans obtained by starch by hydrolysis was used in many food and pharmaceutical applications including large-scale fermentation to produce food acids (citric, lactic, malic, gluconic), polyols as low-joule sweeteners and humectants, and amino acids for nutritional supplements in foods and feeds.

Our understanding of the chemical nature of starch as a polymeric material evolved from extensive research in the nineteenth century, as described in the first

essay of the series by Seetharaman and Bertoft [7]. This essay describes how the structure and configuration of glucose, maltose and polysaccharides and the development of our knowledge of the α -1,4 and α -1,6 glycosidic linkages that interconnect the glucose units in starch were elaborated. The second essay by Seetharaman and Bertoft [8] tells about the discovery of diastase (now known as α -amylase) and how it was initially obtained as the active agent from malting barley in 1833. This was the first enzyme to be isolated in the context of sugar production and brewing, and it was an important tool in early studies related to understanding starch structure.

Visualization of starch granules is the subject of the fourth essay by Seetharaman and Bertoft [10]. Following on from Leeuwenhoek's early microscopic observations, a major research emphasis turned to visualizing microscopically the development and architecture of starch granules. This essay describes how the first comprehensive model of the structure of starch granules was developed, leading to an understanding of how the glucan chains are organized into a crystalline geometry and how the concept for the blocklet structure evolved. A series of three landmark articles in 1943 by Rundle, Baldwin and French provided the first evidence that amylose can form crystalline helical complexes with iodine [17–19].

The fifth essay of the series by Seetharaman and Bertoft [11] discusses the stimulation of research on the structure of amylopectin after techniques for the separation of amylose and amylopectin were developed in the 1940s. The understanding of amylopectin structure emerged from research on starch granule crystallinity and lamellar organization. Early hypotheses have evolved into two models, which are usually considered now to explain amylopectin structure. These are the “cluster” model and the “building block backbone” model. The cluster model was originally proposed in 1969 by Nikuni [20] and independently by French in 1972 [21], as represented diagrammatically by Hizukuri in a widely cited paper in 1986 [22]. In this model, the short chains in amylopectin form crystalline clusters, which are interconnected into a tree-like configuration by the long chains of amylopectin. The evidence that led to the proposal of this model is presented in detail by Bertoft [23]. While this model is widely accepted, difficulties in explaining more recent analytical results led to the proposal of the alternative building block backbone model [23]. In this model, long amylopectin chains are linked to each other to form a longer backbone along which the crystalline clusters that make up the building blocks are randomly distributed. A detailed explanation of how starch structural evidence is interpreted in terms of the two models and how they can account for starch granule architecture is presented in Bertoft [23].

The sixth and final essay of the Seetharaman and Bertoft series [12] places the key developments in starch science into a broader historical context of developments in science. As depicted in Fig. 1, this timeline highlights the development of some key techniques in the 1800s that were essential to studying starch.

As the following chapters will show, substantial progress has been made towards an understanding of the structure, properties and functionality of starch. Nevertheless, there are still important gaps in our knowledge of this important biopolymer. Among the aspects requiring greater understanding are the fine structure of the growth rings, particularly the amorphous domains; the location of much of the

amylose in starch granules and how amylose molecules are distributed with respect to amylopectin; the distribution and spacing of branch points; the biosynthesis of amylose and amylopectin molecules; and their assembly into the structural organization of starch granules. The extent of variability between individual granules is another uncertainty that is difficult to resolve due to granules being too small to study by currently available solid-state polymer techniques of diffraction and spectroscopy.

References

1. Hardy K, Brand Miller J, Brown KJ, Thomas MG, Copeland L. The importance of dietary carbohydrate in human evolution. *Q R Biol.* 2015;90(18):251–68.
2. Torrence R, Barton H, editors. Ancient starch research. Walnut Creek: Left Coast Press; 2006.
3. Copeland L, Hardy KA. Archaeological starch. *Agronomy.* 2018;8:4.
4. Mercader J, Akeju T, Brown M, Bundala M, Collins MJ, Copeland L, et al. Exaggerated expectations in ancient starch research and the need for new taphonomic and authenticity criteria. *Facets.* 2018;3(1):777–98.
5. Herstein B. The centenary of glucose and the early history of starch. *J Ind Eng Chem.* 1911;3:158–68.
6. Schwartz D, Whistler RL. History and future of starch. In: BeMiller J, Whistler RL, editors. *Starch Chemistry and Technology.* 3rd ed. Amsterdam: Elsevier Press; 2009. p. 1–10.
7. Seetharaman K, Bertoft E. Perspectives on the history of research on starch. Part I: On the linkages in starch. *Starch-Stärke.* 2012;64(9):677–82.
8. Seetharaman K, Bertoft E. Perspectives on the history of research on starch. Part II: On the discovery of the constitution of diastase. *Starch-Stärke.* 2012;64(10):765–9.
9. Seetharaman K, Bertoft E. Perspectives on the history of research on starch. Part III: On the era of confusion due to terminology. *Starch-Stärke.* 2012;64(11):841–5.
10. Seetharaman K, Bertoft E. Perspectives on the history of research on starch. Part IV: On the visualization of granule architecture. *Starch-Stärke.* 2012;64(12):929–34.
11. Seetharaman K, Bertoft E. Perspectives on the history of research on starch. Part V: On the conceptualization of amylopectin structure. *Starch-Stärke.* 2013;65(1-2):1–7.
12. Seetharaman K, Bertoft E. Perspectives on the history of research on starch. Part VI: Postscriptum. *Starch-Stärke.* 2013;65(1-2):107–11.
13. Myers AM, Morell MK, James MG, Steven G, Ball SG. Recent progress toward understanding biosynthesis of the amylopectin crystal. *Plant Physiol.* 2000;122(4):989–77.
14. Samuel C, Zeeman SC, Kossmann J, Smith AM. Starch: Its metabolism, evolution, and biotechnological modification in plants. *Annu Rev Plant Biol.* 2010;61(1):209–34.
15. Tetlow IJ, Emes MJ. Starch biosynthesis in the developing endosperms of grasses and cereals. *Agronomy.* 2017;7(4):81.
16. Beach EB. Beccari of Bologna: The discoverer of vegetable protein. *J Hist Med Allied Sci.* 1961;16:354–73.
17. Rundle RE, Baldwin RR. The configuration of starch and the starch-iodine complex. I. The dichroism of flow of starch iodine solutions. *J Am Chem Soc.* 1943;65:554–8.
18. Rundle RE, French D. The configuration of starch and the starch-iodine complex. II. Optical properties of crystalline starch fractions. *J Am Chem Soc.* 1943;65:558–61.
19. Rundle RE, French D. The configuration of starch in the starch-iodine complex. III. X-ray diffraction studies of the starch-iodine complex. *J Am Chem Soc.* 1943;65:1707–10.
20. Nikuni Z. Studies on starch granules. *Starch-Stärke.* 1978;30:105–11.
21. French D. Fine structure of starch and its relationship to the organization of starch granules. *J Jap Soc Starch Sci.* 1972;19:8–25.

22. Hizukuri S. Polymodal distribution of the chain lengths of amylopectins, and its significance. *Carbohydr Polym.* 1986;147:342–7.
23. Bertoft E. Understanding starch structure: Recent progress. *Agronomy.* 2017;7(3):56.

Botanical Sources of Starch



Shujun Wang and Peng Guo

Abstract Native starch granules are mainly stored in the endosperm of cereals, parenchyma of tubers, and cotyledons of legume seeds. The wide range of botanical sources of starches lays a great foundation for their industrial production and applications. Starch occurs naturally as insoluble, semicrystalline granules, made up of amylose and amylopectin. The differences in the characteristics of amylose and amylopectin, and the way they are organized within granules, give rise to considerable variability in the size, shape, and functional properties of starch granules, between and within species. Starches from traditional harvested crops, tubers, and pulses have been extensively studied and used, while the new cultivars and novel sources are also receiving extensive attention due to some unique properties. This chapter gives a general overview of starch from several common crop plants (corn, wheat, cassava, sweet potato, rye, barley, oat, rice, and pulses) and novel sources (medicinal plants and fruits). The granular morphology, characteristics of amylose and amylopectin, crystalline structure, and some typical functional properties are summarized briefly.

Keywords Starch · Botanical source · Crops · Tubers · Pulses · Novel sources

S. Wang (✉)

State Key Laboratory of Food Nutrition and Safety, College of Food Science and Engineering,
Tianjin University of Science and Technology, Tianjin, China
e-mail: sjwang@tust.edu.cn

P. Guo

State Key Laboratory of Food Nutrition and Safety, College of Food Science and Engineering,
Tianjin University of Science and Technology, Tianjin, China

School of Agricultural Engineering and Food Science, Shandong University of Technology,
Zibo, Shandong, China

© Springer Nature Singapore Pte Ltd. 2020

S. Wang (ed.), *Starch Structure, Functionality and Application in Foods*,
https://doi.org/10.1007/978-981-15-0622-2_2

1 Introduction

Starch is the major carbohydrate reserve component of higher plants, which is synthesized in plastids in photosynthetic and non-photosynthetic cells [1]. One of the most abundant and universally distributed forms is transient starch, which serves as a reserve to supply sucrose to non-photosynthetic tissues; the other form of starch is for long-term storage present in endosperm of cereals, parenchyma of tubers, and cotyledons of legume seeds. Starch occurs naturally as insoluble, semicrystalline granules, made up of two polymers of D-glucose: the essentially unbranched amylose (AM) and the highly branched amylopectin (AP). Differences in the amounts of these two molecules, and the way they are organized within granules, give rise to considerable variability, between and within species, in the size, shape, and properties of starch granules. Most native starches contain 20–30% AM and 70–80% AP, although natural variants outside this range occur widely [2]. Variation in amylose (or amylopectin) content of different sources might be due to the difference in species and cultivar, physiological state, and growing environment. For example, the amylose contents of stem starch (tuber, rhizome, and corm) and root starch are in a range of 20–35% and 12–35%, respectively, most commonly from 20% to 35%. Of note is that the analytical methods have significant effects on amylose content. Amylose content is measured as apparent amylose content and absolute/total amylose content. Apparent amylose is measured in the presence of any amylose complexing monoacyl lipids which may be present, whereas the total amylose is measured on lipid-free starch, precipitated from dimethyl sulfoxide solution with ethanol [3]. Moreover, the long-branched chains of amylopectin could also bind iodine and produce blue color, which would cause discrepancy between apparent and absolute amylose content [4, 5]. The ratios of amylose and amylopectin in starch from different sources can greatly affect the functional properties and susceptibility to physicochemical modifications [6, 7]. For example, waxy corn starch structure and functionality are affected less by annealing compared to amylose-containing starch [8]. Meanwhile, annealing treatment has been shown to decrease the amylose content of peas [9], wheat [10], normal corn, high-amylose corn, and potato starches [11].

Native starch granules are characterized at different structural scales ranging from the nanometer-sized glucan chains connected by glucose units to intact granules of micrometer dimensions. The complex structure of starch granules is the major determinant of starch functionality for food processing and human nutrition [12]. The double helices formed by branched chains of amylopectin are organized in parallel to form A- and B-type crystallinities [13]. These crystalline structures differ between starches from different botanical sources. A-type crystalline starch has two strong diffraction peaks at about 15° and 23° (2θ) and a doublet at around 17° and 18° (2θ), whereas B-type starch has one strong diffraction peak at around 17° (2θ), a few smaller peaks at around 15° , 22° , and 24° (2θ), and a characteristic peak at about 5.6° (2θ). In comparison, C-type starch has characteristics of both A- and B-type crystallinity [14]. The cereal starches mainly contain A-type crystallinity,

Table 1 Granule characteristics of some commercial starches

Sources	Granular shape	X-ray diffraction type	Relative crystallinity (%)	Apparent amylose content (%)
Wheat	Lenticular-shaped, small round	A	33.5	32.0 [21]
Barley	Lenticular-shaped, small round	A	35.2	30.0 [21]
Corn	Round, polygonal	A	31.0	23.4 [22]
Rice	Polygonal	A	37.1	13.2 [22]
Cassava	Round, irregular	A or C _A	35.8	17.9 [22]
Sago	Oval, spherical	A	32.9	21.9 [22]
Taro	Polygonal	A	35.3	16.3 [22]
Potato	Oval, spherical	B	29.8	18.0 [22]
Water yam	Rod like, round	B or C	29.5	20.8 [22]
Edible canna	Oval, elliptical	B	27.2	27.9 [22]
Chickpea	Oval, spherical	C	17.6	20.7 [23]
Navy bean	Oval, round, elliptical	C	19.5	26.1 [23]
Pinto bean	Oval, round, irregular	C	25.5	29.6 [23]
Smooth pea	Oval, round, irregular	C	19.9	22.0 [23]
Lentil	Round, oval	C	18.7	22.1 [23]

plant tubers and some high-amylose cereal seeds have B-type starches, and legume seeds and some rhizomes contain mainly C-type starches [15–17]. Starch granules in storage organs of higher plants vary in composition, shape, and size, depending on the tissue and plant source [18], and the particle size of starch granules in storage tissues changes with the maturation period. Variations in granule size (1–100 μm in diameter), shape (round, lenticular, polygonal), size distribution (uni- or bimodal), association as individual (simple) or granule clusters (compound), and composition (α -glucan, lipid, moisture, protein, and mineral content) reflect the botanical origin [19]. The granule characteristics of some commercial starches are given in Table 1. The variability of starch originates from the biosynthesis, which is controlled by multiple genes that are subject to developmental controls and environmental influences [1]. Depending on the plant species or cultivar, the growing environment, and genetic variations, starches vary in physicochemical properties significantly [20]. Genetic modification to obtain starches differing in their industrially relevant characteristics has been successful for some cereal crops such as corn and rice and may play a significant role in improving the quality of different food products and could replace chemically modified starches.

The botanical sources of starches are diverse [21]. Corn/maize (*Zea mays* L.), cassava (also known as tapioca—*Manihot esculenta* Crantn.), sweet potato

(*Ipomoea batatas* L.), wheat (*Triticum aestivum* L.), and potato (*Solanum tuberosum* L.) are the major sources of starch, while rice (*Oryza sativa* L.), barley (*Hordeum vulgare* L.), sago (*Cycas* spp.), arrowroot (*Tacca leontopetaloides* (L.) Kuntze), and buckwheat (*Fagopyrum esculentum* Moench) contribute lesser amounts to the total global production [18], estimated at approximately 84 million tons in 2015 [22]. Many plant species containing starch differing in functionality (thermal, retrogradation, pasting and nutritional properties) are grown throughout the world. These functional properties are related to starch composition, morphology, and structure, which vary with genetics and agronomic and environmental conditions. The availability of starches from various botanical sources is essential for its many applications. Starches with desirable functional properties could play a significant role in improving the quality of different food products and could replace chemically modified starches that are currently being used in a number of products. Extensive research has focused on the different structural and physicochemical properties and nutritional effects in relation to their botanical sources [5, 21, 23–26]. In addition to traditional harvested cereal crops, tubers, and pulses, new cultivars and novel sources, such as fruit starch [27–29] and medicinal plants [30–34], have gained attention due to some unique properties. This chapter generally covers several common starch cultivars, as well as some novel cultivars, in which their granular morphology, characteristics of amylose/amylopectin, crystalline structure, and some typical functional properties are briefly summarized.

2 Starch from Different Botanical Sources

2.1 Cereals

Corn Starch Starch for industrial purposes is extracted predominantly from corn, but significant amounts are also extracted from a range of other species. The types of corn (maize, *Zea mays* L.) available today include popping corn, sweet corn, dent corn, flint corn, and flour corn. The availability of corn at low prices, its storability, and its high starch content have led to its use as a major source of starch production. Normal corn starch is generally made up of about 25% amylose and 75% amylopectin. Plants can be bred that produce starches with AM to AP contents outside the “normal” range (~25% AM and ~75% AP); for example, corn can be grown with an AM content as high as 85% (high amylose maize) or as low as zero (waxy corn). Previous studies have reported the waxy, normal, and high-amylose maize starch containing 2.0%, 23.0%, and 85.0% apparent amylose content [35].

Normal and waxy maize starches are composed of various granules with shapes from small spherical to large polyhedral and with the average particle size ranging from 3 to 20 μm . There are clearly evident pores with varying size and depth on the surface of some starch granules [8]. Unlike waxy and normal maize starches, high-amylose maize starch is consisted of two types of granules: small oval granules and large elongated granules. High-amylose maize starch was reported to contain about

7–32% of elongated granules formed by fusion of several small granules [36]. In addition, normal and waxy maize starches displayed A-type X-ray diffraction pattern, whereas high-amylose maize starch displayed B-type. The gelatinization temperature range of waxy and normal maize generally occurs between 60 and 80 °C. In contrast, the high-amylose maize starch exhibits a broad and undefined endothermic transition, which terminates at a high temperature [8].

Wheat Starch Wheat is one of the most grown, consumed, and traded food grains worldwide. It constitutes a major portion of human diet worldwide due to its agronomic adaptability, ease of storage, nutritional qualities, as well as the ability of its flour to prepare a variety of palatable and satisfying foods [37]. Wheat is often classified into two main varieties, *Triticum aestivum* (referred to as bread wheat) and *Triticum durum* (often termed pasta wheat). *Triticum aestivum* is the most commonly grown species of wheat, accounting for 90–95% of annual total production. *Triticum durum* is another commonly grown species contributing to ~40 million tons of global wheat production [38, 39]. Starch comprises about 60–75% of grain and 70–80% of wheat flour. As the main storage carbohydrate in wheat grains, starch contributes to above 50% of energy intake in Western world and up to 90% for those eating wheat as a staple food [12]. Wheat starch is often produced by wet milling or mashing to remove non-starch components. According to amylose content, wheat is also classified into waxy (less than 5% amylose), normal (20–35%), and high-amylose (greater than about 40%) wheat. Starches isolated from 23 bread wheats (*Triticum aestivum*) and 26 durum wheats (*Triticum durum*) contain 26.3–30.6% total amylose and 19.3–25.1% apparent amylose [40].

Wheat starch has a bimodal granule-size distribution consisting of large lenticular-shaped A-granules and small round B-granules, representing about 75% and 25% by weight, respectively [41, 42]. The bimodal distribution of granule size could also be observed for other *Triticeae* starches (barley, rye, and triticale), but not by other cereal, root, tuber, or legume starches [43]. Wheat starch granules have also been classified into three size ranges, A-type granules (>15 μm), B-type granules (5–15 μm), and C-type granules (<5 μm), using image analysis and laser diffraction technology in another report [43]. Granule diameters, total phosphorus, total amylose, lipid-complexed amylose chains, crystallinity, gelatinization temperature range, gelatinization enthalpy, swelling factor, and amylose leaching, in normal, waxy, and high-amylose bread wheat starches ranged from 2 to 38 μm , 0.007% to 0.058%, 26.9% to 32.3%, 13.4% to 18.7%, 28.6% to 42.8%, 12.7 to 14.3 °C, 11.3 to 13.3 J/g, 27.6% to 72.2%, and 22.2% to 26.2%, respectively [10]. Alkali treatment can significantly alter the functionality and in vitro digestibility of bread wheat starch granules by removing the surface proteins and lipids rather than significantly altering the internal structure of starch granules [44]. A-type granules exhibit lower levels of phosphorus, lipid-complexed amylose, and apparent amylose, compared with B-type, and the wheat starch pasting behavior was suggested to be attributed to the A-/B-type granule ratio [45]. The lenticular or disk shape of A-granules from *Triticeae* starches is unique compared with most botanical sources, except in some lesser known starches [46].

Rye Starch Rye is commonly used in producing sour dough breads and crisp breads. Rye starch is difficult to isolate due to the high pentosan content and the poor gluten-forming ability of rye flours [47]. Rye starches, like those of wheat, triticale, and barley, commonly have around 22–25% amylose content and are composed of large (A-type) and small (B-type) granules with diameters of 23–40 μm and less than 10 μm , respectively [48, 49]. Rye starch gives an A-type X-ray diffraction pattern with estimated degree of crystallinity of 15–17% [48].

Barley Starch Barley starch contributes 75–80% of the total barley endosperm kernel weight, within compact barley protein matrix. The amylose content of barley starches ranges widely depending on genotype. Amylose contents of prime starches from non-waxy and high-amylose barley, determined by calorimetric method, were 24.6% and 48.7%, respectively, whereas waxy starch contained only a trace (0.04%) of amylose [50]. Amylose content of Chinese hull-less barley cultivars ranged from 23.1% to 30.0% and swelling power and water solubility index ranged from 12.8 to 19.9 g/g and 12.7% to 23.7%, respectively [51]. The barley starch granules also display a bimodal distribution comprised of large disc-shaped granules and small spherical granules [41]. Generally, the weight average molecular weight of barley amylopectin was 1.15×10^6 g/mol, lower than that of maize amylopectin (19.3×10^6 g/mol) [52]. The amount of amylopectin unit chains with DP > 36 ranged from 9.83% to 16.66% among 14 barley starches [51]. The average chain length (CL) of amylopectin among 6 barley genotypes ranges from 16.2% to 20.4% glucosyl residues, with the large granules having more amylopectin unit chains of DP > 25 and longer chain length than the small granules [41]. Amylopectins of barley starch have a lower amount of long chains and higher amount of short chains, compared to those of maize and rice. The degree of crystallinity of starch granules has been reported to vary greatly from 37.0% to 44.3% (6 genotypes) [53], 10.7% to 43.2% (7 genotypes) [54], and 10.1% to 13.3% (14 genotypes) [51].

Oat Starch Oat is an important grain crop for humans and is grown mainly in Russia, Canada, the United States, Finland, Australia, and China [55]. Oat has two major cultivated species, *Avena sativa* L. (hulled oat) and *Avena nuda* L. (naked oat). Naked oat is not only commonly grown and consumed in north China, such as Shanxi, Gansu, Jilin, and Hebei provinces, but also serves as a traditional Chinese medicine [56]. In contrast, hulled oat is grown widely in western countries and consumed in the form of rolled oats and steel-cut groats. Oat is recognized as a low or medium Glycemic Index (GI) food, depending on the processing protocols or cooking practices. As the major glycemic carbohydrate, starch accounts for above 60% of the dry matter of the grains, with amylose content in the range of 25.2–29.4% [57], and A-type crystalline polymorphs representative of cereal starches [58]. Oat starch granules tend to exist in clusters of individual granules. The granules range from irregular to polygonal in shape and have average diameters of 7.0–7.8 μm [58], much smaller than for wheat, rye, barley, and corn starch granules.

Rice Starch Rice (*Oryza sativa* L.) is one of the most widely grown cereal crops for food. Undamaged rice is mostly consumed as cooked polished grains for staple food

in many countries, whereas broken rice grains are commonly milled or ground into flour and used as an ingredient in baby foods, noodles, puddings, and many Asian cuisines. The largest component in rice grains is starch (>80%, db), which is an important factor determining the quality of rice products [59]. As a major dietary source of carbohydrate, rice plays an important role in modulating the level of postprandial glucose in bloodstream. Rice is considered a high GI food due to the fast digestion of starch, and thus understanding factors that determine its digestibility is of particular nutritional interest. From the perspective of industrial applications, rice starch is underutilized because of its high cost of production compared with other commercial starches.

According to grain shapes and texture, Asian rice is usually categorized into *Indica*, *Japonica*, and *waxy* rice. In general, *Indica* rice has a higher amount of amylose than *Japonica* rice, making it unacceptable to consumer due to poor cooking and eating quality [60]. So far, hybrid *Indica* rice with low amylose content has been developed successfully in China to improve the quality [61, 62]. Rice starch granules are round, angular, and polygonal and have dimensions in the range of 3–10 μm [63]. Amylose has a number-average degree of polymerization (DP_n) of 920–1110 and is slightly branched with 2–5 chains on average. Amylopectin has 5–6% α -(1,6)-bonds and a DP_n of 8200–12,800 [64]. *Japonica* rice and *waxy* rice starches have a larger proportion of short A chains and a smaller proportion of intermediate B1 chains and long B3 chains compared with *Indica* hybrid rice starch [64].

2.2 Tubers and Roots

Potato Starch Potato (*Solanum tuberosum* L.) is the fourth most important food crop in the world after wheat, rice, and maize, playing a vital role for global food security [65, 66]. Potatoes are a major source of carbohydrate in the Western world, and consumption is increasing rapidly in developing countries. Potatoes are consumed as vegetables and also as raw materials for processing into products, such as snacks, breads, starch, and its derivatives. Potatoes are also a popular source of dietary carbohydrate worldwide and generally considered a high glycemic index (GI) food [67].

Potato starch is the main component of potato tubers and generally occupies 66–80% of a dry weight basis [68]. The chemical composition of potato starches from ten potato cultivars grown under the same conditions showed that protein, amylose, and phosphorus contents ranged from 0.30% to 0.34%, 25.2% to 29.1%, and 52.6 to 66.2 mg/100 g (dry basis), respectively [65]. Other studies reported that total phosphorous content ranged from 59.0 to 71.0 mg/100 g (dry basis) for isolated potato starch from potatoes grown in different locations in Canada [68]. Potato starches with a high degree of phosphorylation are highly desirable because it confers good functional properties of native potato starch for industrial applications without environmentally unfriendly chemical processes [69]. Potato starch has a

broad granule size ranging from 5 to 100 μm , with a mean diameter of 23–30 μm . The granule shapes are observed to be oval and irregular or cuboidal [26].

Native potato starches exhibit a typical B-type X-ray diffraction pattern (characteristic of root and tuber starches). The relative crystallinity reported varies from 15% to 45%, depending not only on the origin and the moisture content of starch but also on the technique and calculation methods used [70]. The chain length distribution profile of amylopectin from different potato cultivars showed that the chains with DP 13–24 and DP 6–12 have the highest (47–51%) and the lowest percentage (7–9%), respectively [71].

Potato starch has the unique properties among other commercially available starches, such as the large granule size, purity, relatively long amylose and amylopectin chain lengths, presence of phosphate ester groups on amylopectin, high swelling power and pasting viscosity, high clarity of starch paste, neutral flavor, and ability to form thick viscoelastic gels upon heating and subsequent cooling [65]. As such, potato starch has been utilized extensively in food and nonfood industries, as thickening agent, food materials, pharmaceutical filler, or excipients [72, 73]. Moreover, raw potato starch has greater resistance towards acid and enzymic hydrolysis compared with other normal starches, which is associated with higher phosphorous content, B-type crystallites, and a larger amount of long amylopectin chains [74].

Cassava Starch Cassava (*Manihot esculenta* Crantz), also known as tapioca, manioc, or yuca, is a perennial woody shrub with tuberous roots in the spurge family (Euphorbiaceae) [75]. Typical mature roots have on average composition of 30–40% dry matter, 30–35% carbohydrate, 1–2% fat, 1–2% fiber, and 1–2% protein, with trace quantities of vitamins and minerals. Cassava is considered as a reliable crop for food security and industrial applications, due to its admirable production in harsh natural conditions [76]. It should be noted that the toxicity of cassava cannot be ignored due to the presence of cyanogenic glucosides. Hence, proper processing is required to effectively detoxify cassava when it is used in the human diet or as animal feed [75].

Starch contributes up to 70% (db) of dried cassava roots [77] and determines the major quality of cassava-based products. Amylose content of cassava starch ranges widely from 0% to 30%. For example, wide variation of amylose content (15.2–26.5%) has been observed for 4050 cassava genotypes collected worldwide [78]. The shape of the granules is oval, truncated, and rounded, and the granule size is in the range of 2–32 μm [72, 79, 80]. Cassava starch granules exhibit a smoother surface compared with potato granules [81]. The molecular weight of cassava amylose was reported to have DP (degree of polymerization) of 1035–1202 (in 4 genotypes harvested in 4 different months) [73], $2.44\text{--}2.70 \times 10^5$ (in 5 genotypes) [82], and 2050–4390 (in 4 genotypes) [83]. The ratio of weight average molar mass to the number average molar mass (M_w/M_n), reflecting the heterogeneity of the amylopectin size (dispersity index of amylopectin), was reported to be 1.25–2.23 for 8 cassava genotypes [84]. The percentages were 9.3–11.6%, 28.8–30.9%, 47.9–49%, 12.3–13%, and 8.6–9.4% for amylopectin branches with DP 6–9, DP

6–12, DP 13–24, DP 25–36, and DP > 37, respectively (4 genotypes) [79]. Cassava starch mainly exhibits A- or C_a-type X-ray diffraction pattern [72, 79], albeit a small amount of B-type starch is also present in C_a-type starch [84]. Great diversity in gelatinization properties has been reported, for instance, the ranges of T_o , T_p , T_c , and ΔH for 12 genotypes were 61.1–71.3 °C, 66.8–74.9 °C, 78.4–85 °C, and 15.1–16.4 J/g, respectively [85].

Cassava starch has medium swelling power compared to potato and cereal starches. The swelling volume of different varieties of cassava starches varies from 25.5 to 41.8 g/g. Cassava starch has a higher solubility compared to other tuber starches, which can be attributed partially to the high swelling power. The solubility of starch from different cassava varieties varies from 17.2% to 27.2%. Compared to cereal starches, cassava starch has better gel stability, which is of importance in food applications [86].

Yam Starch Yam (*Dioscorea* spp.) is one of the most important root and tuber crops and an edible starchy tuber, which is of cultural, economic, and nutritional importance in the tropical and subtropical regions of the world. The most commonly cultivated species include *D. alata* (water yam), *D. cayenensis* (yellow yam), *D. esculenta* (lesser yam), *D. opposita* (Chinese yam), *D. rotundata* (white yam), and *D. trifida* (cush-cush yam) [87].

Yam starch accounts for about 60–80% of the dry matter of yam tuber, and it is a main factor in determining the physicochemical, rheological, and textural characteristics of food products from different yam species [88, 89]. The size of individual yam starch granules ranges from around 1 µm up to 90 µm, and most have monomodal size distribution. Yam starch presents round, oval, polyhedral, and polygonal granules with small fissures on the surface. Genotypes from various yam species showed that the amylose content ranges from 1.4% to 50% [90, 91], with lower amounts of amylose (<20%) observed for *D. dumetorum* and *D. esculenta*, than for *D. alata*, *D. rotundata*, *D. cayenensis-rotundata*, and *D. cayenensis* (AM > 20%) [89, 92]. Most of studied yam starches have B- or C-type polymorph (*D. alata*, *D. cayenensis-rotundata*), with some species showing A-type polymorph (*D. dumetorum*, *D. zingiberensis*) [89, 93, 94]. Great variations in the degree of crystallinity (ranging from 24% to 53%) occur between the various species and within the same species [87]. Yam starches have higher gelatinization temperatures (T_o , T_p , and T_c) than other tuber and root starches such as potato, sweet potato, and cassava starches [87].

Sweet Potato Starch Sweet potato (*Ipomoea batatas* L. Lam) is a tuberous rooted perennial plant in the family Convolvulaceae (morning glory). Sweet potato starch is high-yielding, but its industrial applications are still limited. Starch is the major component of sweet potato roots, accounting for around 50–80% of the dry matter of roots. The degree of polymerization of sweet potato amylose is in the range of 3400–4400, while amylopectin has an average unit chain length of DP 21–22 [95]. Sweet potato starch possesses A-type, C-type, or a mixture of A- and C-type crystalline pattern [96]. The absolute crystallinity for sweet potato starch was 38% [95]. Apparent amylose (AAM) content measured by iodine-binding assay ranged

from 23.3% to 26.5%, whereas AAM content measured by gel permeation chromatography after debranching ranged from 17.5% to 23.9% [97].

2.3 Pulses

Pulses are the edible seeds of leguminous plants including lentil (*Lens culinaris* L.), bean (*Phaseolus vulgaris* L.), pea (*Pisum sativum* L.), and chickpea (*Cicer arietinum* L.) [14]. Pulses are the second major food source for human next to cereals and play an important role in the human diet in developing countries [27, 98]. Most pulse starch granules are described as round or spherical, oval, or irregular shapes. Granule surfaces of pulse starch are generally smooth with no evidence of fissures or pinholes [99, 100]. The granule size of pulse starch ranges from about 1.0–100.0 μm , with major distribution occurring between 5.0 and 30.0 μm [101]. The amylose content of the legume seed starch varies in the range of 17–52% [102]. The weight average molar mass of soya bean amylopectin ranges from 5.1 to 11.3×10^8 g/mol. Amylopectin average branch chain length, determined by anion-exchange chromatography, is in the range of DP 20.4–20.9 [101]. Other studies on the structure and physicochemical properties of pulse starches isolated from different cultivars of faba bean, black bean, and pinto bean have reported that the apparent amylose, phosphorus, and bound lipid contents ranged from 25.8% to 33.6%, 0.004% to 0.009%, and 0.13% to 0.15%, respectively [103]. The total amylose content starches from four cultivars of field pea (*Pisum sativum* L.) ranged from 48.8% to 49.6%, of which 10.9–12.3% was complexed by native lipid. The degree of polymerization (DP) of amyloses ranged from 1300 to 1350. The chain length distributions of debranched amylopectins of field pea starches showed that the proportion of short branch chains, of DP 6–12 ranged from 16.2% to 18.6% [104].

The XRD pattern of the pulse seed starch granules shows the characteristics of C-type starch granules [104, 105]. The B-type crystallites are proposed to be located predominantly in the center of the granules, with the A-type crystallites more abundant towards the periphery [15, 106]. Depending on the proportion of A- and B-type polymorphs, C-type starch can further be divided into three types: C_A-type (closer to A-type), C_C-type (typical C-type), and C_B-type (closer to B-type) [14]. XRD pattern of C_C-type starch exhibits a singlet at about 17° and 23° (2θ) and a few small peaks at around 5.6° and 15° (2θ). The diffraction patterns of C_A- and C_B-type starches are similar to that of C_C-type, but there is a shoulder peak at about 18° (2θ) and a strong singlet at 23° (2θ) for C_A-type starch and two shoulder peaks at about 22° and 24° (2θ) for C_B-type starch [14]. For example, a detailed study on the starches from faba beans, black beans, and pinto beans showed that the B-type polymorphic content in C-type diffraction pattern ranged from 20.6% to 26.3%, 15.4% to 17.7%, and 7.9% to 17.3%, respectively [103]. However, certain pea mutants show different proportions of A- and B-type polymorphs within the starch granule, which can be used as useful models to understand the development of the different polymorphs [107, 108].

2.4 Others

Fruit Starch Unlike starches from cereals, tubers, roots, and pulses, fruit starches have been studied extensively over the decades on the relationship between sugar and starch metabolism and fruit softening, in order to provide basis for developing better storage technology for post-harvested fruits (e.g., tomato, apple, banana, winter squash, etc.) [109]. Recently, starches from fruits have been studied in terms of their structure and functionality related to food applications. Generally, the starch content in fruits varies greatly, which may be attributed to the different harvest time and degradation of starch during maturation. Some winter squash fruit could contain up to 65% dry weight starch content [110], and tomato was reported to contain substantial starch of 20% dry weight at 20 days post-anthesis [111]. Moreover, a range of crystalline structures can be found in the starch-storing tissues of different cultivars. For example, the columella and pericarp of tomato fruits are the primary sites of starch storage in immature fruits with different starch features [112], and the starch features differed between columella and pericarp at the same physiological stage [113]. Tomato fruit starches are described as C-type, and the degree of crystallinity is 40.1% and 30.7% in columella and pericarp tissue from tomato, respectively [113].

Like many other fruits, apples also accumulate starch at early stages of maturation and progressively degrade the starch to increase sweetness during ripening [114]. The total starch increased up to around 20–30 mg per fruit basis 110 days after anthesis for “Royal Gala” apple species and 130 days after anthesis for “Fuji” apple species [115]. Starch content of apple fruits of different cultivars varied from 44.0% to 53.2% (db) [116]. Apple starch showed similar granule morphology to squash fruit starch [101] and kiwifruit starch [111], all exhibiting mainly spherical or dome-shaped and split granules with the diameter ranging between 2 and 12 μm [116]. Apple starch has a C_A-type X-ray diffraction pattern with crystallinity of 40–47%. The apparent amylose content of starches from six apple cultivars ranged from 40% to 48%, and the average branch chain length of amylopectin was reported as DP 27.9–29.6. The weight average molecular weight of amylopectin ranged from 4.6×10^8 to 11.1×10^8 [117].

Bananas (*Musa* spp.) including plantains are the second most important fruit crop after citrus, accounting for ~16% of the world fruit production. For green bananas, starch is the mostly available carbohydrate, and the total starch in green banana flours varied from 69 to 82 g/100 g on a dry weight basis [118]. In a previous study, the amylose content of different banana starches was from 15 to 23 g/100 g (db), and the relative crystallinity was 2.0–12.2% [118]. Banana starch has A-, B-, or C-type crystalline pattern, depending on the varieties, the growing conditions, and the isolation technique [28, 119]. Starch granules from various banana types appear as elongated ovals with ridges [28]. Banana amylopectin exhibits a lower proportion of short chains DP 6–12 (21.6%), a higher proportion of long chains DP > 36 (21.4%), and also a higher proportion of very long chains, which is significantly different from corn or potato amylopectin [119]. The distribution of the short chains (DP 6–12) is

characteristic for banana amylopectins and was characterized as a “fingerprint” of the starches [119]. For cooked banana starch, higher reassociation of the long chains upon cooling could lead to a slower rate of starch digestion [119]. Native banana starch is highly resistant to enzymatic hydrolysis, partially attributed to the external thick layer of granules impeding enzyme penetration into granules [120]. Natural banana starch has potential for various applications, due to its superior property comparable to a lightly cross-linked starch [121]. Phosphorylated banana starch showed better paste clarity and freeze-thaw stability, while hydroxypropylated banana starch showed higher water-binding capacity than native starch [122].

Medicinal Plant Starch The starches from the major common crops have been studied extensively. However, the starches from medicinal plant sources are usually discarded during the isolation and separation of the small-molecule bioactive compounds. With the developments of starch industries, new starches with distinct properties are being paid more and more attention.

The bulbs of *Fritillaria* species, Beimu, have been used as important antitussive, expectorant, and antihypertensive drugs in traditional Chinese medicine for thousands of years [32]. Starch is the main component of the bulbs of *Fritillaria* species, which accounts for approximately 80% of the total biomass [123]. The amylose content of different *Fritillaria* starches ranged from 18.8% to 30.2% [33, 124]. *Fritillaria* starch granules are predominantly oval, elliptical, and polygonal, with granule size ranging from 5 to 50 μm . X-ray diffraction patterns demonstrated that most *Fritillaria* starches show a characteristic B-type, while the *F. cirrhosa* starch shows a typical C_B-type pattern [31]. The degree of starch crystallinity was reported in the range of 33.9–54.9% for different *Fritillaria* species [30, 31, 124].

Dioscorea opposita Thunb. (Chinese yam) is one of the most important rhizome species and has also been used as an important invigorant in traditional Chinese medicine for years. In the rhizome of *D. opposita* cultivars, starch accounts for 20–60% content in the total biomass [125, 126]. Starches isolated from *D. opposita* Thunb. cultivars exhibit mainly from round or oval to elliptic or pie-like shapes with diameters ranging between 5–20 and 20–60 μm , respectively, for small and large granules [125, 127]. The starches separated from different *D. opposita* Thunb. cultivars have amylose content of 10.0–23.0% and show a typical C-type XRD pattern with crystallinity ranging from 31% to 50% [125–127]. The B-type polymorph is proposed to be mainly located in the center region of the granules, surrounded by the peripheral A-type polymorph [106, 128]. Chinese yam starches were found to significantly decrease the serum total cholesterol, triglyceride, and LDL-cholesterol levels in hyperlipidemic rats [129].

3 Conclusions

Starches from common botanical sources (cereals, tubers, roots, and pulses) and some novel sources are summarized in terms of their morphology, chemical composition, amylose/amylopectin ratio, structural characteristics, and physicochemical properties. In recent years, more and more starches from novel sources are studied, with the aim of understanding the structure-function relationship and exploring the potential industrial applications. The wide range of botanical sources of starches lays a great foundation for their industrial production and applications.

Acknowledgments The authors gratefully acknowledge the financial support from the National Natural Science Foundation of China (31871796) and Natural Science Foundation of Tianjin City (17JJCQJC45600).

References

1. Zeeman SC, Kossmann J, Smith AM. Starch: Its metabolism, evolution, and biotechnological modification in plants. *Annu Rev Plant Biol.* 2010;61:209–34.
2. Wang S, Copeland L. Molecular disassembly of starch granules during gelatinization and its effect on starch digestibility: A review. *Food Funct.* 2013;4:1564–80.
3. Morrison WR, Laignelet B. An improved colorimetric procedure for determining apparent and total amylose in cereal and other starches. *J Cereal Sci.* 1983;1:9–20.
4. Zhu T, Jackson DS, Wehling RL, Geera B. Comparison of amylose determination methods and the development of a dual wavelength iodine binding technique. *Cereal Chem.* 2008;85:51–8.
5. Ashogbon AO. Contradictions in the study of some compositional and physicochemical properties of starches from various botanical sources. *Starch-Stärke.* 2018;70:1600372.
6. Klucinec JD, Thompson DB. Amylopectin nature and amylose-to-amylopectin ratio as influences on the behavior of gels of dispersed starch. *Cereal Chem.* 2007;79:24–35.
7. Fredriksson H, Silverio J, Andersson R, Eliasson AC, Åman P. The influence of amylose and amylopectin characteristics on gelatinization and retrogradation properties of different starches. *Carbohydr Polym.* 1998;35:119–34.
8. Wang S, Wang J, Yu J, Wang S. A comparative study of annealing of waxy, normal and high-amylose maize starches: The role of amylose molecules. *Food Chem.* 2014;164:332–8.
9. Wang S, Jin F, Yu J. Pea starch annealing: New insights. *Food Bioprocess Technol.* 2013;6:3564–75.
10. Lan H, Hoover R, Jayakody L, Liu Q, Donner E, Baga M, et al. Impact of annealing on the molecular structure and physicochemical properties of normal, waxy and high amylose bread wheat starches. *Food Chem.* 2008;111:663–75.
11. O'Brien S, Wang YJ. Susceptibility of annealed starches to hydrolysis by α -amylase and glucoamylase. *Carbohydr Polym.* 2008;72:597–607.
12. Wang S, Li C, Copeland L, Niu Q, Wang S. Starch retrogradation: A comprehensive review. *Rev Food Sci Food Saf.* 2015;14:568–85.
13. Pérez S, Bertoft E. The molecular structures of starch components and their contribution to the architecture of starch granules: A comprehensive review. *Starch-Stärke.* 2010;62:389–420.
14. He W, Wei C. Progress in C-type starches from different plant sources. *Food Hydrocolloids.* 2017;73:162–75.

15. Bogracheva TY, Ring SG, Hedley CL, Morris VJ. The granular structure of C-type pea starch and its role in gelatinization. *Biopolymers*. 1998;45:323–32.
16. Norman WHC, Leping T. Variation in crystalline type with amylose content in maize starch granules: An X-ray powder diffraction study. *Carbohydr Polym*. 1998;36:277–84.
17. Hoover R. Composition, molecular structure, and physicochemical properties of tuber and root starches: A review. *Carbohydr Polym*. 2001;45:253–67.
18. Ratnayake WS, Jackson DS. Starch: Sources and processing. *Encyclop Food Sci Nutr*. 2003;5567–72.
19. Tester RF, Karkalas J, Qi X. Starch-composition, fine structure and architecture. *J Cereal Sci*. 2004;39:151–65.
20. Vamadevan V, Bertoft E. Structure-function relationships of starch components. *Starch-Stärke*. 2014;67:55–68.
21. Ashogbon AO, Akintayo ET. Recent trend in the physical and chemical modification of starches from different botanical sources: A review. *Starch-Stärke*. 2014;66:41–57.
22. Waterschoot J, Gomand SV, Fierens E, Delcour JA. Production, structure, physicochemical and functional properties of maize, cassava, wheat, potato and rice starches. *Starch-Stärke*. 2015;67:14–29.
23. Srichuwong S, Sunarti TC, Mishima T, Isono N, Hisamatsu M. Starches from different botanical sources. I: Contribution of amylopectin fine structure to thermal properties and enzyme digestibility. *Carbohydr Polym*. 2005;60:529–38.
24. Jenkins PJ, Cameron RE, Donald AM. A universal feature in the structure of starch granules from different botanical sources. *Starch-Stärke*. 1993;45:417–20.
25. Schirmer M, Höchstätter A, Jekle M, Arendt E, Becker T. Physicochemical and morphological characterization of different starches with variable amylose/amylopectin ratio. *Food Hydrocolloids*. 2013;32:52–63.
26. Singh N, Singh J, Kaur L, Sodhi NS, Gill BS. Morphological, thermal and rheological properties of starches from different botanical sources. *Food Chem*. 2003;81:219–31.
27. Kaur M, Singh N, Sandhu KS, Guraya HS. Physicochemical, morphological, thermal and rheological properties of starches separated from kernels of some Indian mango cultivars (*Mangifera indica* L.). *Food Chem*. 2004;85:131–40.
28. Zhang P, Whistler RL, Bemiller JN, Hamaker BR. Banana starch: Production, physicochemical properties, and digestibility—a review. *Carbohydr Polym*. 2005;59:443–58.
29. Li D, Zhu F. Physicochemical properties of kiwifruit starch. *Food Chem*. 2017;220:129–36.
30. Wang S, Gao W, Chen H, Xiao P. New starches from *Fritillaria* species medicinal plants. *Carbohydr Polym*. 2005;61:111–4.
31. Wang S, Gao W, Jiang W, Xiao P. Crystallography, morphology and thermal properties of starches from four different medicinal plants of *Fritillaria* species. *Food Chem*. 2006;96:591–6.
32. Wang S, Gao W, Chen H, Xiao P. Studies on the morphological, thermal and crystalline properties of starches separated from medicinal plants. *J Food Eng*. 2006;76:420–6.
33. Wang S, Yu J, Gao W, Pang J, Yu J, Xiao P. Characterization of starch isolated from *Fritillaria* traditional Chinese medicine (TCM). *J Food Eng*. 2007;80:727–34.
34. Man J, Cai J, Cai C, Huai H, Wei C. Physicochemical properties of rhizome starch from a traditional Chinese medicinal plant of *Anemone altaica*. *Carbohydr Polym*. 2012;89:571–7.
35. Tester RF, Debon SJJ, Sommerville MD. Annealing of maize starch. *Carbohydr Polym*. 2000;42:287–99.
36. Jiang HX, Campbell M, Blanco M, Jane JL. Characterization of maize amylose-extender (*ae*) mutant starches: Part II. Structures and properties of starch residues remaining after enzymatic hydrolysis at boiling-water temperature. *Carbohydr Polym*. 2010;80:1–12.
37. Guo P, Yu J, Wang S, Wang S, Copeland L. Effects of particle size and water content during cooking on the physicochemical properties and in vitro starch digestibility of milled durum wheat grains. *Food Hydrocolloids*. 2018;77:445–53.

38. Gélinas P, McKinnon C. Gluten weight in ancient and modern wheat and the reactivity of epitopes towards R5 and G12 monoclonal antibodies. *Int J Food Sci Technol.* 2016;51:1801–10.
39. Sobota A, Rzedzicki Z, Zarzycki P, Kuzawińska E. Application of common wheat bran for the industrial production of high-fibre pasta. *Int J Food Sci Technol.* 2015;50:111–9.
40. Soulaka AB, Morrison WR. The amylose and lipid contents, dimensions, and gelatinisation characteristics of some wheat starches and their A- and B-granule fractions. *J Sci Food Agric.* 2010;36:709–18.
41. Ao Z, Jane J. Characterization and modeling of the A- and B-granule starches of wheat, triticale, and barley. *Carbohydr Polym.* 2007;67:46–55.
42. Hyunseok K, Kerry H. Physicochemical properties and amylopectin fine structures of A- and B-type granules of waxy and normal soft wheat starch. *J Cereal Sci.* 2010;51:256–64.
43. Wilson JD, Bechtel DB, Todd TC, Seib PA. Measurement of wheat starch granule size distribution using image analysis and laser diffraction technology. *Cereal Chem.* 2007;83:259–68.
44. Wang S, Luo H, Zhang J, Zhang Y, He Z, Wang S. Alkali-induced changes in functional properties and in vitro digestibility of wheat starch: The role of surface proteins and lipids. *J Agric Food Chem.* 2014;62:3636–43.
45. Shinde SV, Nelson JE, Huber KC. Soft wheat starch pasting behavior in relation to A- and B-type granule content and composition. *Cereal Chem.* 2003;80:91–8.
46. Jane JL, Kasemsuwan T, Leas S, Zobel H, Robyt JF. Anthology of starch granule morphology by scanning electron microscopy. *Starch-Stärke.* 1994;46:121–9.
47. Autio K, Eliasson AC. Rye starch. In: BeMiller J, Whistler R, editors. *Starch.* 3rd ed. New York: Academic Press; 2009. p. 579–87.
48. Schierbaum DSF, Radosta S, Richter M, Kettlitz B, Dipl Krist CG. Studies on rye starch properties and modification. Part I: Composition and properties of rye starch granules. *Starch-Stärke.* 1991;43:331–9.
49. Gomand SV, Verwimp T, Goesaert H, Delcour JA. Structural and physicochemical characterisation of rye starch. *Carbohydr Res.* 2011;346:2727–35.
50. Czuchajowska Z, Klamczynski A, Paszczynska B, Baik BK. Structure and functionality of barley starches. *Cereal Chem.* 1998;75:747–54.
51. Kong X, Kasapis S, Zhu P, Sui Z, Bao J, Corke H. Physicochemical and structural characteristics of starches from Chinese hull-less barley cultivars. *Int J Food Sci Technol.* 2016;51:509–18.
52. Luisarturo BP, Sandral RA, Edith AA, Mirnam SR. Solubilization effects on molecular weights of amylose and amylopectins of normal maize and barley starches. *Cereal Chem.* 2009;86:701–5.
53. Waduge RN, Hoover R, Vasanthan T, Gao J, Li J. Effect of annealing on the structure and physicochemical properties of barley starches of varying amylose content. *Food Res Int.* 2006;39:59–77.
54. Li W, Xiao X, Zhang W, Zheng J, Luo Q, Ouyang S, et al. Compositional, morphological, structural and physicochemical properties of starches from seven naked barley cultivars grown in China. *Food Res Int.* 2014;58:7–14.
55. Xu D, Ren G, Liu L, Zhu W, Liu Y. The influences of drying process on crude protein content of naked oat cut herbage (*Avena nuda* L.). *Dry Technol.* 2014;32:321–7.
56. Hu XZ, Zheng JM, Li XP, Xu C, Zhao Q. Chemical composition and sensory characteristics of oat flakes: A comparative study of naked oat flakes from China and hulled oat flakes from western countries. *J Cereal Sci.* 2014;60:297–301.
57. Gudmundsson M, Eliasson AC. Some physico-chemical properties of oat starches extracted from varieties with different oil content. *Acta Agric Scand Sect A.* 2009;39:101–11.
58. Hoover R, Smith C, Zhou Y, Ratnayake RMWS. Physicochemical properties of Canadian oat starches. *Carbohydr Polym.* 2003;52:253–61.

59. Hasjim J, Li E, Dhital S. Milling of rice grains: Effects of starch/flour structures on gelatinization and pasting properties. *Carbohydr Polym.* 2013;92:682–90.
60. Tian R, Jiang GH, Shen LH, Wang LQ, He YQ. Mapping quantitative trait loci underlying the cooking and eating quality of rice using a DH population. *Mol Breed.* 2005;15:117–24.
61. Kuang Q, Xu J, Wang K, Zhou S, Liu X. Structure and digestion of hybrid Indica rice starch and its biosynthesis. *Int J Biol Macromol.* 2016;93:402–7.
62. Ni D, Zhang S, Sheng C, Yong X, Li L, Hao L, et al. Improving cooking and eating quality of Xieyou57, an elite indica hybrid rice, by marker-assisted selection of the Wx locus. *Euphytica.* 2011;179:355–62.
63. Ashogbon AO, Akintayo ET. Morphological, functional and pasting properties of starches separated from rice cultivars grown in Nigeria. *Int Food Res J.* 2012;19:181–7.
64. Wang S, Li P, Yu J, Guo P, Wang S. Multi-scale structures and functional properties of starches from Indica hybrid, Japonica and waxy rice. *Int J Biol Macromol.* 2017;102:136–43.
65. Alvani K, Xin Q, Richard FT, Colin ES. Physico-chemical properties of potato starches. *Food Chem.* 2011;125:958–65.
66. Tong C, Ahmed S, Pang Y, Xin Z, Bao J. Fine structure and gelatinization and pasting properties relationships among starches from pigmented potatoes. *Food Hydrocolloids.* 2018;83:45–52.
67. Ek KL, Wang S, Copeland L, Brand-Miller JC. Discovery of a low-glycaemic index potato and relationship with starch digestion in vitro. *Br J Nutr.* 2014;111:699–705.
68. Chung H-J, Li X-Q, Kalinga D, Lim S-T, Yada R, Liu Q. Physicochemical properties of dry matter and isolated starch from potatoes grown in different locations in Canada. *Food Res Int.* 2014;57:89–94.
69. Singh N, Isono N, Srichuwong S, Noda T, Nishinari K. Structural, thermal and viscoelastic properties of potato starches. *Food Hydrocolloids.* 2008;22:979–88.
70. Cooke D, Gidley MJ. Loss of crystalline and molecular order during starch gelatinisation: Origin of the enthalpic transition. *Carbohydr Res.* 1992;227:103–12.
71. Ek KL, Wang S, Brand-Miller J, Copeland L. Properties of starch from potatoes differing in glycemic index. *Food Funct.* 2014;5:2509–15.
72. Defloor I, Dehing I, Delcour JA. Physico-chemical properties of cassava starch. *Starch-Stärke.* 1998;50:58–64.
73. Srirath K, Santisopasri V, Petchalanuwat C, Kurotjanawong K, Piyachomkwan K, Oates CG. Cassava starch granule structure-function properties: Influence of time and conditions at harvest on four cultivars of cassava starch. *Carbohydr Polym.* 1999;38:161–70.
74. Jane J-L, Wong K-S, McPherson AE. Branch-structure difference in starches of A- and B-type X-ray patterns revealed by their Naegeli dextrans. *Carbohydr Res.* 1997;300:219–27.
75. Hillocks RJ, Thresh JM, Bellotti A, editors. *Cassava: Biology, Production and Utilization.* New York: CABI Publish Press; 2002.
76. Alves AAC. Cassava botany and physiology. In: Hillocks RJ, Thresh JM, Bellotti AC, editors. *Cassava Biology Production and Utilization.* New York: CABI Publish Press; 2002. p. 67–89.
77. Olomo V, Ajibola O. Processing factors affecting the yield and physicochemical properties of starch from cassava chips and flour. *Starch-Stärke.* 2010;55:476–81.
78. Sánchez T, Salcedo E, Ceballos H, Dufour D, Mafía G, Morante N, et al. Screening of starch quality traits in cassava (*Manihot esculenta* Crantz). *Starch-Stärke.* 2010;61:12–9.
79. Rolland-Sabaté A, Sanchez T, Buléon A, Colonna P, Ceballos H, Zhao SS, et al. Molecular and supra-molecular structure of waxy starches developed from cassava (*Manihot esculenta* Crantz). *Carbohydr Polym.* 2013;92:1451–62.
80. Moorthy SN, Wenham JE, Jmv B. Effect of solvent extraction on the gelatinisation properties of flour and starch of five cassava varieties. *J Sci Food Agric.* 2015;72:329–36.
81. Lesław J, Fortuna T, Krok F. Non-contact atomic force microscopy of starch granules surface. Part I. Potato and tapioca starches. *Starch-Stärke.* 2003;55:1–7.

82. Charles AL, Chang YH, Ko WC, Sriroth K, Huang TC. Influence of amylopectin structure and amylose content on the gelling properties of five cultivars of cassava starches. *J Agric Food Chem.* 2005;53:2717–25.
83. Charoenkul N, Uttapap D, Pathipanawat W, Takeda Y. Molecular structure of starches from cassava varieties having different cooked root textures. *Starch-Stärke.* 2010;58:443–52.
84. Rollandsabaté A, Sánchez T, Buléon A, Colonna P, Jaillais B, Ceballos H, et al. Structural characterization of novel cassava starches with low and high-amylose contents in comparison with other commercial sources. *Food Hydrocolloids.* 2012;27:161–74.
85. Charoenkul N, Uttapap D, Pathipanawat W, Takeda Y. Physicochemical characteristics of starches and flours from cassava varieties having different cooked root textures. *LWT-Food Sci Technol.* 2011;44:1774–81.
86. Moorthy SN. Tropical sources of starch. In: Eliasson AC, editor. *Starch in Food: Structure, Function and Applications.* New York: Woodhead Press; 2004. p. 321–59.
87. Zhu F. Isolation, composition, structure, properties, modifications, and uses of yam starch. *Compr Rev Food Sci Food Saf.* 2015;14:357–86.
88. Otegbayo B, Bokanga M, Asiedu R. Physicochemical properties of yam starch: Effect on textural quality of yam food product (*pounded* yam). *J Food Agric Environ.* 2011;9:145–50.
89. Amani N, Buléon A, Kamenan A, Colonna P. Variability in starch physicochemical and functional properties of yam (*Dioscorea* sp) cultivated in Ivory Coast. *J Sci Food Agric.* 2004;84:2085–96.
90. Pérez E, Gibert O, Rolland-Sabaté A, Jiménez Y, Sánchez T, Giraldo A, et al. Physicochemical, functional, and macromolecular properties of waxy yam starches discovered from “Mapuey” (*Dioscorea trifida*) genotypes in the Venezuelan Amazon. *J Agric Food Chem.* 2011;59:263–73.
91. Rolland-Sabaté A, Georges Amani NG, Dufour D, Guilois S, Colonna P. Macromolecular characteristics of ten yam (*Dioscorea* spp.) starches. *J Sci Food Agric.* 2003;83:927–36.
92. Otegbayo B, Oguniyan D, Akinwumi O. Physicochemical and functional characterization of yam starch for potential industrial applications. *Starch-Stärke.* 2014;66:235–50.
93. Zhou Q, Shi W, Meng X, Liu Y. Studies on the morphological, crystalline, thermal properties of an under utilized starch from yam *Dioscorea zingiberensis* CH Wright. *Starch-Stärke.* 2013;65:123–33.
94. Jayakody L, Hoover R, Liu Q, Donner E. Studies on tuber starches. II. Molecular structure, composition and physicochemical properties of yam (*Dioscorea* sp.) starches grown in Sri Lanka. *Carbohydr Polym.* 2007;69:148–63.
95. Takeda Y, Tokunaga N, Takeda C, Hizukuri S. Physicochemical properties of sweet potato starches. *Starch-Stärke.* 1986;38:345–50.
96. Moorthy SN. Physicochemical and functional properties of tropical tuber starches: A review. *Starch-Stärke.* 2015;54:559–92.
97. Zhu F, Yang X, Cai YZ, Bertoft E, Corke H. Physicochemical properties of sweetpotato starch. *Starch-Stärke.* 2011;63:249–59.
98. Tharanathan RN, Mahadevamma S. Grain legumes—a boon to human nutrition. *Trends Food Sci Technol.* 2003;14:507–18.
99. Hoover R, Ratnayake WS. Starch characteristics of black bean, chick pea, lentil, navy bean and pinto bean cultivars grown in Canada. *Food Chem.* 2002;78:489–98.
100. Chung HJ, Liu Q, Donner E, Hoover R, Warkentin TD, Vandenberg B. Composition, molecular structure, properties, and in vitro digestibility of starches from newly released Canadian pulse cultivars. *Cereal Chem.* 2008;85:471–9.
101. Stevenson DG, Doorenbos RK, Jane JL, Inglett GE. Structures and functional properties of starch from seeds of three soybean (*Glycine max* (L.) Merr.) varieties. *Starch-Stärke.* 2006;58:509–19.
102. Wani IA, Sogi DS, Hamdani AM, Gani A, Bhat NA, Shah A. Isolation, composition, and physicochemical properties of starch from legumes: A review. *Starch-Stärke.* 2016;68:834–45.

103. Ambigaipalan P, Hoover R, Donner E, Liu Q, Jaiswal S, Chibbar R, et al. Structure of faba bean, black bean and pinto bean starches at different levels of granule organization and their physicochemical properties. *Food Res Int.* 2011;44:2962–74.
104. Ratnayake WS, Hoover R, Shahidi F, Perera C, Jane J. Composition, molecular structure, and physicochemical properties of starches from four field pea (*Pisum sativum* L.) cultivars. *Food Chem.* 2001;74:189–202.
105. Sarko A, Wu HH. The crystal structures of A-, B- and C-polymorphs of amylose and starch. *Starch-Stärke.* 1978;30:73–8.
106. Wang S, Yu J, Zhu Q, Yu J, Jin F. Granular structure and allomorph position in C-type Chinese yam starch granule revealed by SEM, ¹³C CP/MAS NMR and XRD. *Food Hydrocolloids.* 2009;23:426–33.
107. Bogracheva TY, Cairns P, Noel TR, Hulleman S, Wang TL, Morris VJ, et al. The effect of mutant genes at the *r*, *rb*, *rug3*, *rug4*, *rug5* and *lam* loci on the granular structure and physicochemical properties of pea seed starch. *Carbohydr Polym.* 1999;39:303–14.
108. Hedley CL, Bogracheva TY, Wang TL. A genetic approach to studying the morphology, structure and function of starch granules using pea as a model. *Starch-Stärke.* 2015;54:235–42.
109. Schaffer AA, Levin I, Oguz I, Petreikov M, Bar M. ADPglucose pyrophosphorylase activity and starch accumulation in immature tomato fruit: The effect of a *Lycopersicon hirsutum*-derived introgression encoding for the large subunit. *Plant Sci.* 2000;152:135–44.
110. Stevenson DG, Yoo SH, Hurst PL, Jane JL. Structural and physicochemical characteristics of winter squash (*Cucurbita maxima* D.) fruit starches at harvest. *Carbohydr Polym.* 2005;59:153–63.
111. Brampton T, Asquith M, Parke B, Barraclough AJ, Hughes WA. Localisation of starch granules in developing tomato fruit. *Acta Hort.* 1994:415–8.
112. Schaffer AA, Petreikov M. Sucrose-to-starch metabolism in tomato fruit undergoing transient starch accumulation. *Plant Physiol.* 1997;113:739–46.
113. Luengwilai K, Beckles DM. Structural investigations and morphology of tomato fruit starch. *J Agric Food Chem.* 2008;57:282–91.
114. Warrington IJ, Fulton TA, Halligan EA, De Silva HN. Apple fruit growth and maturity are affected by early season temperature. *J Am Soc Hortic Sci.* 1999;124:468–77.
115. Brookfield P, Murphy P, Harker R, Macrae E. Starch degradation and starch pattern indices; interpretation and relationship to maturity. *Postharvest Biol Technol.* 1997;11:23–30.
116. Carrín ME, Ceci LN, Lozano JE. Characterization of starch in apple juice and its degradation by amylases. *Food Chem.* 2004;87:173–8.
117. Stevenson DG, Domoto PA, Jane J-L. Structures and functional properties of apple (*Malus domestica* Borkh) fruit starch. *Carbohydr Polym.* 2006;63:432–41.
118. Kumar PS, Saravanan A, Sheeba N, Uma S. Structural, functional characterization and physicochemical properties of green banana flour from dessert and plantain bananas (*Musa* spp.). *LWT-Food Sci Technology.* 2019;116:108524.
119. Zhang P, Hamaker BR. Banana starch structure and digestibility. *Carbohydr Polym.* 2012;87:1552–8.
120. Cummings JH, Englyst HN. Measurement of starch fermentation in the human large intestine. *Can J Physiol Pharmacol.* 1991;69:121–9.
121. Eggleston G, Swennen R, Akoni S. Physicochemical studies on starches isolated from plantain cultivars, plantain hybrids and cooking bananas. *Starch-Stärke.* 1992;44:121–8.
122. Waliszewski KN, Aparicio MA, Bello LA, Monroy JA. Changes of banana starch by chemical and physical modification. *Carbohydr Polym.* 2003;52:237–42.
123. Gao W, Fan L, Paek K-Y. Ultrastructure of amyloplasts and intercellular transport of old and new scales in *Fritillaria ussuriensis*. *J Plant Biol.* 1999;42:117–23.
124. Li X, Gao W, Jiang Q, Hao J, Guo X, Huang L. Physicochemical, morphological, structural, and thermal characteristics of starches separated from *Bulbus fritillaria* of different cultivars. *Starch-Stärke.* 2012;64:572–80.

125. Wang S, Yu J, Gao W, Liu H, Xiao P. New starches from traditional Chinese medicine (TCM)-Chinese yam (*Dioscorea opposita* Thunb.) cultivars. *Carbohydr Res.* 2006;341:289–93.
126. Wang S, Liu H, Gao W, Chen H, Yu J, Xiao P. Characterization of new starches separated from different Chinese yam (*Dioscorea opposita* Thunb.) cultivars. *Food Chem.* 2006;99:30–7.
127. Wang S, Gao W, Liu H, Chen H, Yu J, Xiao P. Studies on the physicochemical, morphological, thermal and crystalline properties of starches separated from different *Dioscorea opposita* cultivars. *Food Chem.* 2006;99:38–44.
128. Wang S, Yu J, Yu J, Liu H. The partial characterization of C-type rhizome *Dioscorea* starch granule during acid hydrolysis. *Food Hydrocolloids.* 2008;22:531–7.
129. Wang S, Yu J, Liu H, Chen W. Characterisation and preliminary lipid-lowering evaluation of starch from Chinese yam. *Food Chem.* 2008;108:176–81.

Fine Structure of Amylose and Amylopectin



Xiangli Kong

Abstract Starch granules consist of two types of polymeric components, essentially linear amylose and branched amylopectin. Ratios and fine structure of these two polymers determine the starch functional properties and starch applications in food and non-food industries. Amylose fine structure can be characterized by two features, molecular size and structure of branching. Amylopectin consists of numerous short chains, with a chain length of ~6–35 glucosidic units, of α -(1, 4)-linked D-glucose residues, which are interlinked to form clusters defined as groups of chains through their reducing end side by α -(1, 6)-linkages, and the macromolecule of amylopectin exhibits a heavily branched structure built from about 95% (1→4)- α - and 5% (1→6)- α -linkages. Chain length profile and cluster model of amylopectin can provide a useful conceptual basis for understanding the structure of the amylopectin and guide current thinking related to amylopectin biosynthesis and physical behavior. This chapter reviews the structural characteristics of amylose and amylopectin.

Keywords Amylose · Amylopectin · Fine structure · Cluster model · Branch chains

1 Introduction

Two primary types of polymeric components, amylose and amylopectin, constitute starch. Both these biomacromolecules consist solely of α -D-glucosidic units linked together through α -(1→4) and α -(1→6) bonds. The molecular size of amylopectin is much larger than that of amylose. Amylopectin is the main component by weight, whereas amylose content varies between 15% and 30% for most starches [1]. Waxy starches contain very little or zero amylose, and some high amylose starches contain much higher content (>50%) of amylose, including amylose-only genetically

X. Kong (✉)

College of Agriculture and Biotechnology, Zhejiang University, Hangzhou, China

e-mail: xlkong@zju.edu.cn

© Springer Nature Singapore Pte Ltd. 2020

S. Wang (ed.), *Starch Structure, Functionality and Application in Foods*,

https://doi.org/10.1007/978-981-15-0622-2_3

modified starch [2]. Ratios and fine structure of these two polymers determine the starch functional properties [3–9] and finally its applications in the food industry.

2 Fine Structure of Amylose

The double helical structure of deoxyribonucleic acid is very well known; however, the first helical structure of a biomacromolecule was probably proposed for amylose [10]. The nomenclature “amylose” was used since this linear, slightly branched molecule was fractionated from starch by an aqueous leaching method [11, 12]. Amylose contains around 99% (1→4)- α - and 1% (1→6)- α -linkages, making a relatively long, mostly linear polysaccharide that differs in size and structure depending on botanical origins [13]. The molecular size and structure of branching are two features currently employed to characterize amylose fine structure. The molecular size of amylose is indicated by molecular size or degree of polymerization (DP) depending on analytical methods.

2.1 Analytical Methods

Amylose is able to form a helical inclusion complex with iodine presenting a deep blue color, which is used to measure amylose content. However, the longer chains (DP > 60) in amylopectin can also bind with iodine, resulting in overestimation of the content of amylose. On the other hand, amylose forms complexes with phospholipids and free fatty acids hindering iodine combination, causing underestimation of the amylose content. Therefore, the content of amylose determined by this method was named to be amylose equivalents or apparent amylose [14]. Hence, other methods, for example, differential scanning calorimetric (DSC) method based on the complex formation between amylose and added excess phospholipid, lectin-binding (concanavalin A) method, and size-exclusion chromatography (SEC) or gel permeation chromatography (GPC) methods based on molecular size difference between amylose and amylopectin, were also developed and compared [15–19]. Near-infrared transmittance spectroscopy (NIRS) was suggested to partly replace the wet chemical analytical methods and has applications in breeding programs requiring rapid screening [20].

Average values of molecular weight or DP are generally expressed due to the polydispersity of amylose and can be described as either weight- or molar-based, according to the principle of the analytical method used [21]. The modified Park-Johnson method and the bicinchoninic acid method, which have high sensitivity for determining reducing residues, can give molar-based values. However, the light scattering technique offers weight-based values [22]. Besides the average values of molecular weight, the weight- or molar-based distribution of amylose can be

determined by gel permeation chromatography (GPC) or high-performance size-exclusion chromatography [21].

2.2 Structural Characteristics of Amylose

The average molecular weight of amylose from various starches ranges between 1.3×10^5 and 5×10^5 with polydispersity, and some amylose molecules possess 5–20 chains making the molecules slightly branched. The molecular sizes of branched amyloses are commonly larger than those of linear ones, but the chain length present in linear amylose is longer than average chain length in branched ones. Mono-modal size distribution of amylose was observed on a weight basis [23], whereas mono- or polymodal size distributions were detected on a molar basis [24]. The DP values of elution positions at which 10% and 90% of the amylose was eluted on weight or molar basis can be used to describe distribution of apparent DP. For cereal amyloses, the apparent DP distribution was 2000–4000 at 10% and 200–300 at 90% on a molar basis. For potato amylose, the values were 9800 and 970, respectively. For sweet potato amylose, the values were 7900 and 440, respectively [24]. The amyloses from tapioca and potato were observed to show broad distributions; however, a narrow distribution was detected for amylose from kudzu. The apparent DP distribution showed 200–20,000 on weight bases, however, with some exceptions [23, 25].

The classical measurement of linearity was the susceptibility of amylose to complete enzymolysis by using β -amylase. The enzyme β -amylase splits the α -(1,4)-glucosidic linkages starting from the non-reducing end of the chain and releases maltose; however, this enzyme cannot hydrolyze the α -(1,6)-glucosidic bonds. The fact that β -amylase cannot hydrolyze amylose completely, and that the combined action of debranching enzyme and β -amylase increases β -amylolysis limit of amylose, indicates the existence of α -(1,6)-glucosidic bonds in amylose molecules. A large percentage of the amylose fraction, varying from 10% to 70%, comprises slightly branched macromolecules depending on botanical sources [26–28], with each molecule containing 5–20 chains.

The amylose unit chains were categorized into A-, B-, and C-chains, with the C-chain termed as the main chain and A- and B-chains as side chains [21]. The CL of branched amylose C-chain from maize was observed to range from 200 to 710, by using an isotopic tritium labelling method at the reducing end [29]. Takeda and coworkers investigated the amylose branch pattern by producing β -limit dextrans of amyloses with β -amylase action [25, 28, 29]. This enzyme can hydrolyze both the external chains of branched amylose and linear amylose; therefore the number-based percentage of branched amylose can be determined. By using aqueous n-butanol to separate the amylose in maize, the supernatant was observed to contain minor amounts of high-molecular-weight, branched material with short chains forming undeveloped clusters [28]. Subsequently, Takeda et al. reported similar findings for rice amylose [29]. In their report, the authors debranched rice amylose by using

isoamylase, and after labelling the unit chains with tritium, typical long chains and short chains (peak at DP 21) in rice amylose were observed. The short chains found in amylose had similar lengths to typical amylopectin chains. The number ratio of chains with different lengths was 8 (DP > 200):6 (DP30-200):40 (DP10-30). Through the 2-aminopyridine labelling method, the short chains were further confirmed to be present in rice amylose [30]. The conclusion that there were differences in the short chains branching pattern between amylose and amylopectin was made by Hanashiro et al., based on the patterns of chain distribution [30]. Using atomic force microscopy to image the amylose structure at a molecular level, molecules with only one long side chain forming one branch and molecules with short side chains forming multiple branches were observed [31].

The branch pattern of amylose can be characterized by several approaches [21]:

1. β -amylolysis limit, which is described as the proportion of maltose hydrolyzed by β -amylase from amylose. The β -amylase can only hydrolyze amylose molecules from the non-reducing ends and release maltose. However, this enzyme has no capability to bypass (1 \rightarrow 6)- α -linkages in branched amyloses; therefore, the area between the outmost branched linkages and reducing end is left and termed as β -limit dextrin. The percentage of linear amyloses, the molar ratio of side chains in branched amyloses, and the position of branches will affect β -limit dextrin [21]. β -Amylolysis limit values of amyloses were observed from 70% to 90% for starches from diverse origins [28, 32]. In comparison, the β -amylolysis limit values of branched amyloses were shown to be \sim 40% by calculating both the number percentage of the branched amyloses and β -amylolysis limit values [33].
2. Proportion of branched and linear amyloses, based on weight or number. The molar-based percentage can be determined by measuring labelled reducing terminals released from β -amylase hydrolysis [29, 30]. Some structural parameters, such as the branch number in one amylose molecule and β -limit value of amylose, can be better interpreted by the molar percentage of branched amyloses. The number-based percentage of branched amyloses was observed to range from 15% to 70%, and the typical percentage was 20–50%. Although the linear and branched amylose molecules cannot be separated by a method, the weight-based percentage can be estimated from molar-based ratio, branched amylose DP_n , and whole amylose DP_n [33].
3. Chain length, which is described to be the number of glucose units in a linear chain after debranching. The length of chain is normally determined from a mixture of linear-chain fraction with various lengths; therefore, the chain length values are given as molar-based average chain length or weight-based average chain length. The molar-based average chain length can be calculated from the ratio of total glucose units to non-reducing ends. The chain length for linear chains of amylose after debranching shows a very wide range with over 2–3 orders of magnitude. Therefore, the molar-based average chain length value will be influenced to a large extent by the occurrence of only one short or long chain. As a consequence, the distinctions of average chain length among different amylose samples should be explained cautiously [21].

4. Number of chains (NC), which is the number of linear chains in one amylose molecule after debranching. The number of chains in amylose can be calculated from the ratio of non-reducing ends to reducing ends. For linear amylose, the number of chains is one, because the molecules of linear amylose comprise one reducing end and one non-reducing end [21]. However, for branched amylose, the number of chains is greater than one attributing to the existence of side chains. The number of side chains in one amylose molecule can be calculated by using the number of chains minus one. The number of chains for amylose molecules ranges between about two and ten. However, the number of chains is calculated from the mixture of branched and linear amylose molecules depending on the fractionation process of amylose from starch; therefore, this value cannot reveal the authentic branching pattern. The high proportion of linear amylose will decrease the number of chains in amylose molecules.
5. Extent of debranching. The amylopectin molecules can be debranched completely by bacterial debranching enzymes, whereas the amylose molecules cannot be debranched completely by these enzymes. The number-based ratio of α -(1 \rightarrow 6) bonds cleaved by the debranching enzymes was used to describe the extent of debranching for amylose. The value describing the extent of debranching can be estimated by the number ratio of reducing ends hydrolyzed after debranching to the non-reducing ends of amylose side chains. Until now, it remains unknown about the mechanism of only partial debranching for amylose molecules with debranching enzymes [21].

3 Fine Structure of Amylopectin

The main component in normal type starches is amylopectin, which plays a key role in the internal structure of starch granules and presents a semicrystalline form [34]. Amylopectin is composed of many short chains of α -(1, 4)-linked D-glucosyl units (chain length of \sim 6–35 glucose units) interlinked to form clusters [35]. These clusters are defined as groups of chains linked through their reducing end by α -(1, 6)-linkages; they exhibit a highly branched structure with about 95% α -(1 \rightarrow 4) and 5% α -(1 \rightarrow 6) bonds. The molecular size distribution of amylopectin can be analyzed by size-exclusion chromatography (SEC), gel permeation chromatography (GPC), or asymmetrical flow field-flow fractionation (AF4) as size separation methods coupled with differential refractive index (RI) detector or multi-angle laser light scattering (MALLS) detector as size characterization methods. The amylopectin molecule, with a molecular weight average (M_w) of 1×10^7 – 1×10^9 , is about 1–3 orders of magnitude larger than amylose [36], depending on the plant origin, analytical methods, and the solvent used for the amylopectin [37]; however, the number-based average values (M_n) are determined to be only 10^5 – 10^6 , so the polydispersity index (M_w/M_n) of amylopectin macromolecules is rather large [1]. The component of amylopectin from a wide range of starches is categorized into three fractions according to molecular size. The largest molecules in size have the degree of

polymerization (DP_n) of 13,400–26,500 with number-based average, while the intermediate molecules in size have DP_n of 4400–8400, and the smallest amylopectin molecules have DP_n of 700–2100. Among them, the percentage of the largest molecules (DP_n : 13,400–26,500) was the highest [37]. The same as amylose, the shape, size, structural properties, and polydispersity of the amylopectin molecules depend on botanical sources.

3.1 Unit Chain Length of Amylopectin

The structural characteristics of amylopectin are usually depicted by unit chain length profile. The distribution of the amylopectin unit chains after debranching can be analyzed by size-exclusion chromatography (SEC), high-performance anion-exchange chromatography with pulsed amperometric detection (HPAEC-PAD), or fluorophore-assisted carbohydrate electrophoresis (FACE). Essentially, the unit chains of amylopectin are classified into two categories, which are A-chains (not substituted with other chains) and B-chains (termed as chains substituted with other chains) [3]. Based on the comparison between debranched amylopectin from 11 plant origins, the unit chains were suggested to be fractionated into 4 fractions according to the length of unit chains, which are fa (DP 6–12), fb₁ (DP 13–24), fb₂ (DP 25–36), and fb₃ (DP > 36). These four fractions constitute the amylopectin polymodal chain length distribution. The unit chain length distribution can also be acquired from ϕ , β -limit dextrans produced by continuous hydrolysis with phosphorylase *a* and β -amylase; in this products all A-chains are present as maltosyl stubs; however, all B-chains are longer than that [38]. Therefore, the A-chains can be estimated from the quantity of maltose produced from ϕ , β -limit dextrans debranching. The B-chains can be further categorized into B1-, B2- and B3-chains; in addition, the B1-chains are sub-grouped into B1a- and B1b-chains, wherein the former ones are subdivided into B1a(s)- and longer B1a(l)-chains [1]. Typical chain length distributions of amylopectin and ϕ , β -limit dextrin, based on weight, are presented in Fig. 1.

The length and the size distribution of the unit chains in amylopectin is the most common structural parameter to be measured, although not necessarily the most informative. The chain categories are distinguished from each other based on profiles of unit chains developed from experimental data, specifically, the actions of different starch-degrading enzymes. Two exo-acting enzymes are commonly employed for amylopectin structure analysis: (1) phosphorylase *a* (the enzyme in the muscle and liver involved in glycogen metabolism), which can remove one glucose residue from the non-reducing ends successively by producing glucose 1-phosphate through a phosphorolytic mechanism; (2) β -amylase, which produces maltose by hydrolysis from non-reducing terminals. Both of the enzymes cannot split the (1→6)- α -linkage branches. Firstly, ϕ -limit dextrin (ϕ -LD) is produced by hydrolysis with the enzyme of phosphorylase *a*; all A-chains have been cleaved into maltotetraose stubs in the ϕ -LD. Then the enzyme of β -amylase is employed to act on the ϕ -LD, whereafter

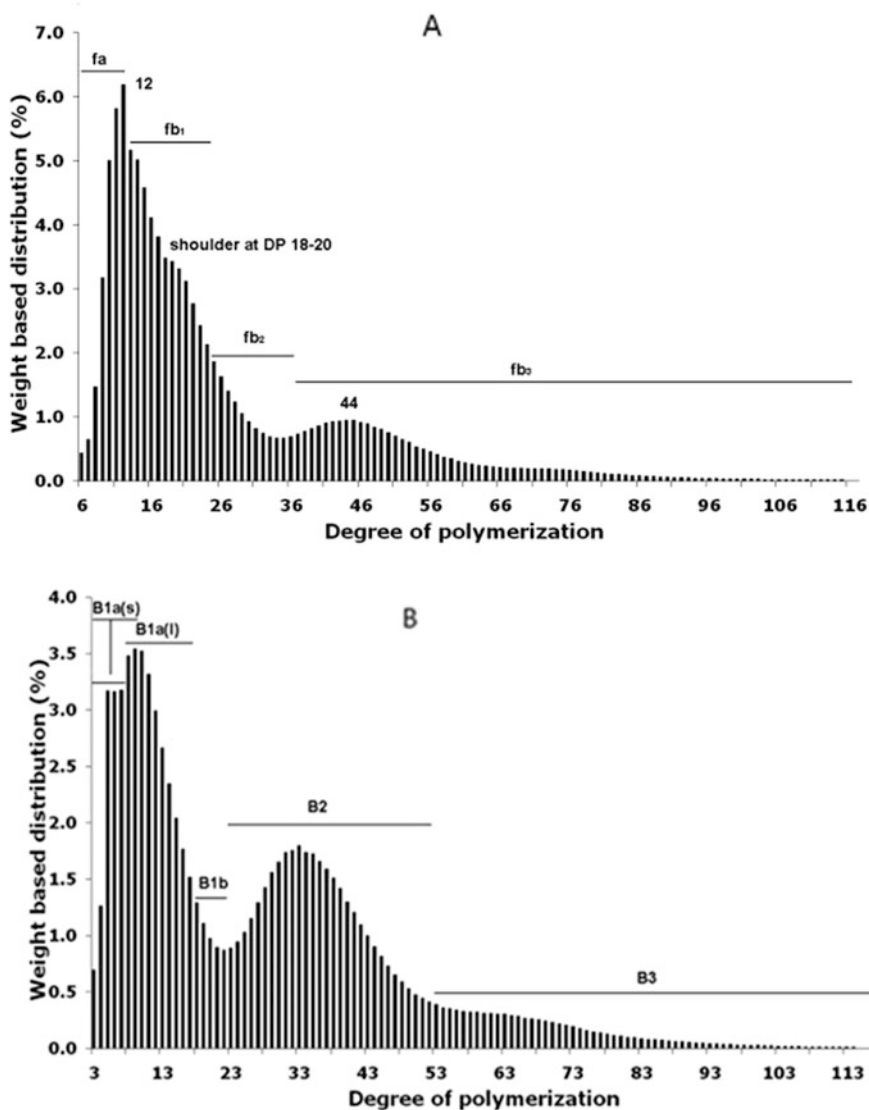


Fig. 1 Typical chain length profile of (a) amylopectin and (b) ϕ,β -limit dextrin. Reproduced from [3] with permission from the Elsevier Ltd. (2008)

one additional maltose residue for each chain is cleaved from non-reducing ends, so all A-chains remain as maltosyl stubs in the final products called ϕ,β -LD. In the β -limit dextrin, the chain length of external stubs is dependent on even or odd number of glucosyl units on the original external segments, as a consequence, the A-chains in β -limit dextrin remain as DP 2 or 3 (Fig. 2) [39]. Two debranching enzymes, namely, isoamylase and pullulanase, are used to cleave the branch points

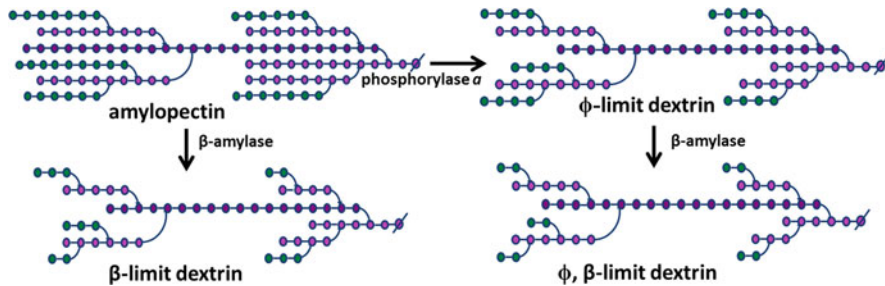


Fig. 2 Production of β -limit dextrin and ϕ , β -limit dextrin from amylopectin by phosphorylase α and β -amylase. Reproduced from [39] with permission from the Elsevier Ltd. (2017)

and obtain the unit chains with short length. These two enzymes have distinct action patterns on molecules of branched oligosaccharide but also on intact molecules of amylopectin. Pullulanase can completely hydrolyze the polysaccharide pullulan and, furthermore, hydrolyze maltosyl chain stubs more effectively; however, isoamylase has no enzymatic activity on pullulan but can cleave the whole molecule of amylopectin more effectively.

3.2 The Cluster Model

To characterize the structural properties of amylopectin, the chain length distribution is usually measured. However, the amylopectin cluster model, which can give a meaningful conceptual basis for understanding the structure of the biomacromolecule and guide present understanding related to the biosynthesis of amylopectin and physical properties, needs to be investigated [40]. The unit chains consisted in amylopectin were firstly proposed to be organized as clusters by Nikuni [41]. However, this concept was published in the journal of *Starch-Stärke* in English after almost 10 years [42]. During this period, the cluster model was also proposed by two research groups, independently [43, 44]. The chain length profile of amylopectin shows bimodal distribution and is composed of both long and short chains, of which the short chains form clusters, whereas the long chains can be proposed to interlink the clusters. Consequently, the ratio of short chains to long chains in the molecule of amylopectin can be used as an index for the size of clusters in the form of the number of chains averagely consisted in the clusters [39].

Lower-molecular-weight dextrans from the macromolecule of amylopectin can be released by cleaving longer internal chain segments through endo-acting enzyme. The long segments observed between the clusters pave the way for isolating the clusters from amylopectin for further structural analysis [1]. The clusters were isolated by using maltotetraose-forming amylase from *Pseudomonas stutzeri* [45] and cyclodextrin glycosyltransferase from *Klebsiella pneumoniae* [46]. The other reported clusters were isolated by using the α -amylase from *Bacillus*

amyloliquefaciens (or *B. subtilis*) and analyzed by Bertoft and his co-workers [39]. The DP value of clusters in the form of ϕ, β -LDs produced with the α -amylase of *B. amyloliquefaciens* ranges from approximately DP 10–15 up to 660–850 [47]. The long segments between clusters are hydrolyzed in order to produce clusters. Thereafter, the produced clusters are much highly branched than the macromolecule itself, and they are composed of much more short chains. However, some crucial structural characteristics of clusters contradict with the classical cluster model [47]; more recently, the building block backbone model was raised. In this model, the biopolymer has a backbone composed of mainly interconnected B₂- and B₃-chains, but the existence of shorter B₁-chains is not ruled out. A- and B₁-chains with short chain length extend from the backbone and arrange into building blocks with very small, tightly branched units; in this new model, the building blocks are the basic structural units, compared to clusters as the basic structural units in the cluster model [39].

4 Conclusions

Research on amylose and amylopectin has been ongoing for 80 years since these two components were identified. However, a consensus on their molecular structure has not been reached, which might be attributed to the large size of amylose and amylopectin and their great variation from diverse sources. The most powerful approach currently available to analyze fine structure of amylose and amylopectin is based on enzymatic hydrolysis. It could be foreseen that the understanding on fine structure of amylose and amylopectin will be deepened in the future as new techniques are developed.

References

1. Bertoft E. Understanding starch structure: Recent progress. *Agronomy*. 2017;7(3):56.
2. Carciofi M, Blennow A, Jensen SL, Shaik SS, Henriksen A, Buléon A, Holm PB, Hebelstrup KH. Concerted suppression of all starch branching enzyme genes in barley produces amylose-only starch granules. *BMC Plant Biol*. 2012;12:223.
3. Kong X, Bertoft E, Bao J, Corke H. Molecular structure of amylopectin from amaranth starch and its effect on physicochemical properties. *Int J Biol Macromol*. 2008;43:377–82.
4. Syahariza ZA, Sar S, Hasjim J, Tizzotti MJ, Gilbert RG. The importance of amylose and amylopectin fine structures for starch digestibility in cooked rice grains. *Food Chem*. 2013;136:742–9.
5. Wang K, Hasjim J, Wu AC, Henry RJ, Gilbert RG. Variation in amylose fine structure of starches from different botanical sources. *J Agric Food Chem*. 2014;62:4443–53.
6. Kong X, Zhu P, Sui Z, Bao J. Physicochemical properties of starches from diverse rice cultivars varying in apparent amylose content and gelatinisation temperature combinations. *Food Chem*. 2015;172:433–40.

7. Kong X, Chen Y, Zhu P, Sui Z, Corke H, Bao J. Relationships among genetic, structural, and functional properties of rice starch. *J Agric Food Chem.* 2015;63:6241–8.
8. Kong X, Kasapis S, Zhu P, Sui Z, Bao J, Corke H. Physicochemical and structural characteristics of starches from Chinese hull-less barley cultivars. *Int J Food Sci Technol.* 2016;51:509–18.
9. Li H, Prakash S, Nicholson TM, Fitzgerald MA, Gilbert RG. The importance of amylose and amylopectin fine structure for textural properties of cooked rice grains. *Food Chem.* 2016;196:702–11.
10. Hanes CS. The action of amylases in relation to the structure of starch and its metabolism in the plant. Part IV–VII. *New Phytol.* 1937;36:189–239.
11. Meyer KH, Brentano W, Bernfeld P. Recherches sur l'amidon II. Sur la nonhomogénéité de l'amidon. *Helv Chim Acta.* 1940;23:845–53.
12. Meyer KH, Bernfeld P, Wolff E. Recherches sur l'amidon III. Fractionnement et purification de l'amylose de maïs naturel. *Helv Chim Acta.* 1940;23:854–64.
13. Tester RF, Karkalas J, Qi X. Starch-composition, fine structure and architecture. *J Cereal Sci.* 2004;39:151–65.
14. Chen MH, Bergman CJ. Method for determining the amylose content, molecular weights, and weight- and molar-based distributions of degree of polymerization of amylose and fine-structure of amylopectin. *Carbohydr Polym.* 2007;69(3):562–78.
15. Mestres C, Matencio F, Pons B, Yajid M, Fliedel G. A rapid method for the determination of amylose content by using differential scanning calorimetry. *Starch-Stärke.* 1996;48:2–6.
16. Gibson TS, Solah V, McCleary BV. A procedure to measure amylose in cereal starches and flours with concanavalin. *J Cereal Sci.* 1997;25:111–9.
17. Batey IL, Curtin BM. Measurement of amylose/amylopectin ratio by high-performance liquid chromatography. *Starch-Stärke.* 1996;48:338–44.
18. Blennow A, Bay-Smidt AM, Bauer R. Amylopectin aggregation as a function of starch phosphate content studied by size exclusion chromatography and on-line refractive index and light scattering. *Int J Biol Macromol.* 2001;28:409–20.
19. Noosuk P, Hill SE, Pradipasena P, Mitchell JR. Structure-viscosity relationships for Thai rice starches. *Carbohydr Polym.* 2003;55:337–44.
20. Campbell MR, Yeager H, Abdubek N, Pollak LM, Glover DV. Comparison of methods for amylose screening among amylose-extender (*ae*) maize starches from exotic backgrounds. *Cereal Chem.* 2002;79:317–21.
21. Hanashiro I. Fine structure of amylose. In: Nakamura Y, editor. *Starch: Metabolism and Structure.* Tokyo: Springer; 2015. p. 41–60.
22. Miles MJ, Morris VJ, Ring SG. Gelation of amylose. *Carbohydr Res.* 1985;135:257–69.
23. Hizukuri S, Takagi T. Estimation of the distribution of molecular weight for amylose by the low-angle laser-light-scattering technique combined with high-performance gel chromatography. *Carbohydr Res.* 1984;134:1–10.
24. Hanashiro I, Takeda Y. Examination of number-average degree of polymerization and molar-based distribution of amylose by fluorescent labeling with 2-aminopyridine. *Carbohydr Res.* 1998;306:421–6.
25. Takeda Y, Hizukuri S, Juliano BO. Purification and structure of amylose from rice starch. *Carbohydr Res.* 1986;148:299–308.
26. Hizukuri S, Takeda Y, Yasuda M, Suzuki A. Multi-branched nature of amylose and the action of debranching enzymes. *Carbohydr Res.* 1981;94:205–13.
27. Manners DJ, Bathgate GN. α -1,4-glucans. Part XX. The molecular structure of the starches from oats and malted oats. *J Inst Brew.* 1969;75(2):169–75.
28. Takeda Y, Hizukuri S, Takeda C, Suzuki A. Structures of branched molecules of amyloses of various origins, and molar fractions of branched and unbranched molecules. *Carbohydr Res.* 1987;165:139–45.
29. Takeda Y, Maruta N, Hizukuri S. Examination of the structure of amylose by tritium labelling of the reducing terminal. *Carbohydr Res.* 1992;227:113–20.

30. Hanashiro I, Sakaguchi I, Yamashita H. Branched structures of rice amylose examined by differential fluorescence detection of side-chain distribution. *J Appl Glycosci.* 2013;60:79–85.
31. Gunning AP, Giardina TP, Faulds CB, Juge N, Ring SG, Williamson G, Morris VJ. Surfactant-mediated solubilisation of amylose and visualisation by atomic force microscopy. *Carbohydr Polym.* 2003;51:177–82.
32. Banks W, Greenwood CT. Physicochemical studies on starches. Part XXXII. The incomplete β -amylolysis of amylose: A discussion of its cause and implications. *Starch-Starke.* 1967;19:197–206.
33. Hizukuri S, Takeda Y, Maruta N, Juliano BO. Molecular structures of rice starch. *Carbohydr Res.* 1989;189:227–35.
34. Bertoft E. Fine structure of amylopectin. In: Nakamura Y, editor. *Starch: Metabolism and Structure.* Tokyo: Springer; 2015. p. 3–40.
35. Bertoft E. Composition of clusters and their arrangement in potato amylopectin. *Carbohydr Polym.* 2007;68:433–46.
36. Buléon A, Colonna P, Planchot V, Ball S. Starch granules: Structure and biosynthesis. *Int J Biol Macromol.* 1998;23:85–112.
37. Takeda Y, Shibahara S, Hanashiro I. Examination of the structure of amylopectin molecules by fluorescent labeling. *Carbohydr Res.* 2003;338:471–5.
38. Hanashiro I, Abe JI, Hizukuri S. A periodic distribution of the chain length of amylopectin as revealed by high-performance anion-exchange chromatography. *Carbohydr Res.* 1996;283:151–9.
39. Bertoft E. Analyzing starch molecular structure. In: Sjö M, Nilsson L, editors. *Starch in Food: Structure, Function and Applications.* 2nd ed. New York: Woodhead Publishing; 2017. p. 97–149.
40. Kong X, Corke H, Bertoft E. Fine structure characterization of amylopectins from grain amaranth starch. *Carbohydr Res.* 2009;344:1701–8.
41. Nikuni Z. Starch and cooking (in Japanese). *Sci Cook.* 1969;2:6–14.
42. Nikuni Z. Studies on starch granules. *Starch-Stärke.* 1978;30:105–11.
43. French D. Fine structure of starch and its relationship to the organization of starch granules. *J Jap Soc Starch Sci.* 1972;19:8–25.
44. Robin JP, Mercier C, Charbonnière R, Guilbot A. Lintnerized starches. Gel filtration and enzymatic studies of insoluble residues from prolonged acid treatment of potato starch. *Cereal Chem.* 1974;51:389–406.
45. Finch P, Sebesta DW. The amylase of *Pseudomonas stutzeri* as a probe of the structure of amylopectin. *Carbohydr Res.* 1992;227:c1–4.
46. Bender H, Siebert R, Stadler-Szöke A. Can cyclodextrin glycosyltransferase be useful for the investigation of the fine structure of amylopectins?: Characterisation of highly branched clusters isolated from digests with potato and maize starches. *Carbohydr Res.* 1982;110:245–59.
47. Bertoft E, Koch K, Åman P. Building block organisation of clusters in amylopectin from different structural types. *Int J Biol Macromol.* 2012;50:1212–23.

Multiscale Structures of Starch Granules



Shujun Wang, Hanbin Xu, and Huiyu Luan

Abstract Native starch is found widely in the form of granules in many tissues of most plant species. Starch granules occur as semi-crystalline complex structure synthesized through coordinated interactions of multiple biosynthetic enzymes, which are influenced by growth environment. The structure of starch granules needs to be explored because of its close relation to functionality and hence applications. This chapter will highlight key features of starch granules, including growth rings, lamellae, blocklets, and helical structures, which have led to knowledge and understanding of properties important for applications of starch products.

Keywords Starch structure · Semi-crystalline · Granules · Growth rings · Helices

1 Introduction

Starch, as the main storage carbohydrate in higher plants, is synthesized in a range of plant tissues of most plant species. Starch granules are biosynthesized in heterotrophic plastids by coordinated interactions of multiple biosynthetic enzymes and reserved in storage organs of grains, seeds, fruits, roots, and tubers. Native starch granules have a very complicated semi-crystalline structure [1], and they have a density of about 1.5 g/mL, higher than that of the fiber (1.2–1.4 g/mL) [2]. Semi-crystalline starch granules are insoluble in water at room temperature, but they can be dispersed and dissolved upon heating [3, 4].

Starch granules are constituted mainly by two glucans, lightly branched amylose and highly branched amylopectin. The fine structure of these polymers is described in chapter “Fine Structure of Amylose and Amylopectin” and will not be discussed in detail here. Amylose, which accounts for 15–35% of normal starch granules in most plants, is mainly constituted of glucose residues joined through α -1,4-linkages

S. Wang (✉) · H. Xu · H. Luan

State Key Laboratory of Food Nutrition & Safety, Tianjin University of Science & Technology, Tianjin, China

e-mail: sjwang@tust.edu.cn

© Springer Nature Singapore Pte Ltd. 2020

S. Wang (ed.), *Starch Structure, Functionality and Application in Foods*,
https://doi.org/10.1007/978-981-15-0622-2_4

with less than 0.5% α -1,6-linkages [5, 6]. The degree of polymerization (DP) of amylose is usually in the range of 500–6000 glucose units [7]. Amylopectin is a highly branched polymer linked mainly by α -1,4-linkages and an average of 5% of α -1,6-bonds at branch points [8]. The DP of amylopectin is in the range of 3×10^5 to 3×10^6 , corresponding to molecular weight of 10^7 – 10^9 , much larger than that of amylose [7, 9, 10]. The chains of amylopectin molecules are often divided into A-, B- and C-chains [8], as firstly defined by Peat et al. [11]. The outermost single chains, which have DP of 6–12, are termed A-chains. B-chains, which are substituted by other chains, are further subdivided into B1 (DP 13–24), B2 (average DP 25–36), and B3+ chains (DP \geq 37) [12]. There is only one C-chain in each amylopectin molecule, which has a broad size distribution from 15 to 120, with a peak around DP 40. Each amylopectin molecule has the sole reducing end and many non-reducing ends [5, 13]. Amylose and amylopectin are arranged into a complicated multiscale structure in starch granules, which has been studied extensively but remains to be investigated further.

Native starch can be characterized on at least five levels of ordered structure from nanometer-scale double helices, lamellae, blocklets, and growth rings to micron-sized granules (Fig. 1) [6, 10, 14]. Additionally, other structural elements such as the hilum, superhelices, amorphous core, and clusters have also been studied but are not well understood [6, 10, 15]. Native starch differs greatly in granule structure between and within botanical species, even from the same cultivar grown under different conditions [16]. The functional properties of starch are determined predominantly by the multiscale structures of starch granules [14, 17]. The extent to which structural changes occur during cooking or processing is the major determinant for the quality of finished food products [15–17]. Other properties of starch granules, such as size [18, 19], surface channels or pores [20], amylose/amylopectin content [21], and chain length distribution of amylopectin [21] also play an important role in starch functionality and digestibility [15–17]. The molecular density of starch [22] and specific surface area [20] could also have an effect on applications of starch.

In this chapter, some recent advances in knowledge of starch granule structure are reviewed. An understanding of the internal structure of starch granules, and its relationship to functionality, will help to improve the industrial applications of starch, including optimizing conditions for physical, chemical, and enzymatic processing.

2 Starch Granules

Native starch granules occur in various shapes including spherical, oval, polygonal, flat, lenticular, elongated, and kidney-shaped, as observed by SEM [6]. The size of starch granules varies from submicron to 100 μm , as shown in Table 1. For example, native rice starch granules display a polyhedral or irregular shape with a typical diameter of 2–8 μm (Fig. 2a). Yam starch granules are oval or disk-like with size between 10 and 30 μm (Fig. 2d). Potato starch granules are spherical or oval with

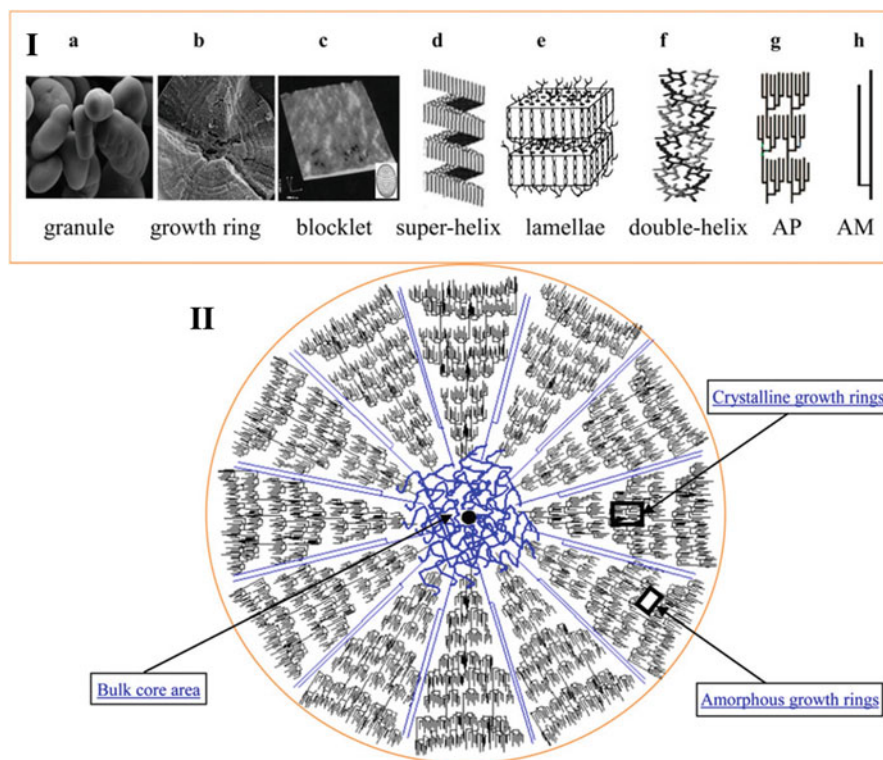


Fig. 1 The hierarchical structure of starch granules (I) and a schematic model representing the distribution of amylose and amylopectin molecules (II). (a) Native pea starch granules as viewed by scanning electron microscopy (SEM); (b) growth rings as observed by SEM; (c) blocklet structures as revealed by atomic force microscope (AFM); (d–h) representations of superhelix, lamellae, double helix, and amylopectin and amylose molecules, respectively. The blue lines in (II) represent amylose molecules, and the black lines represent amylopectin molecules. The structures in (II) are not represented to scale. Reproduced from [10] with permission from Wiley (2015)

granule size ranging from 10 to 75 μm (Fig. 2c). Lotus starch granules contain two distinct types of granules, large oval shapes (15–20 μm across and 40–60 μm long) and small spherical shapes (2–5 μm) [23, 24] (Fig. 2b). A birefringent Maltese cross pattern, observed for almost all native starch granules under polarized light microscopy, is indicative of a radial arrangement of ordered structures. By monitoring the changes of Maltese cross during processing or cooking, starch functionality can be analyzed, such as the degree of gelatinization starch [25].

Generally, the surface of native starch granules, such as those from pea, wheat, yam, lotus, and potato, is smooth without obvious pinholes or depressions. The smooth surface of starch granules is disrupted by cooking or thermal processing, which affects starch functionality and *in vitro* enzymatic digestibility [24, 26]. Some starch granules (e.g., maize, sorghum, and millet) present tiny pores or channels that extend from the outer surface to the interior parts [27–29]. The external pores and

Table 1 Particle size of different starch granules. Reproduced from [6] with permission from Wiley (2010)

Origin	Size (μm)
Small wheat granules	2–3
Large wheat granules	22–36
Small lotus granules	2–5
Large lotus granules	15–60
Potato starch	10–75
Canna starch	Up to 100
Maize starch	5–20
Rice starch	2–8
Yam starch	10–30
Legume starch	10–45
Amaranth; cow cockle; pig weed	Submicrons-2
Taro, Quinoa	Submicrons-2

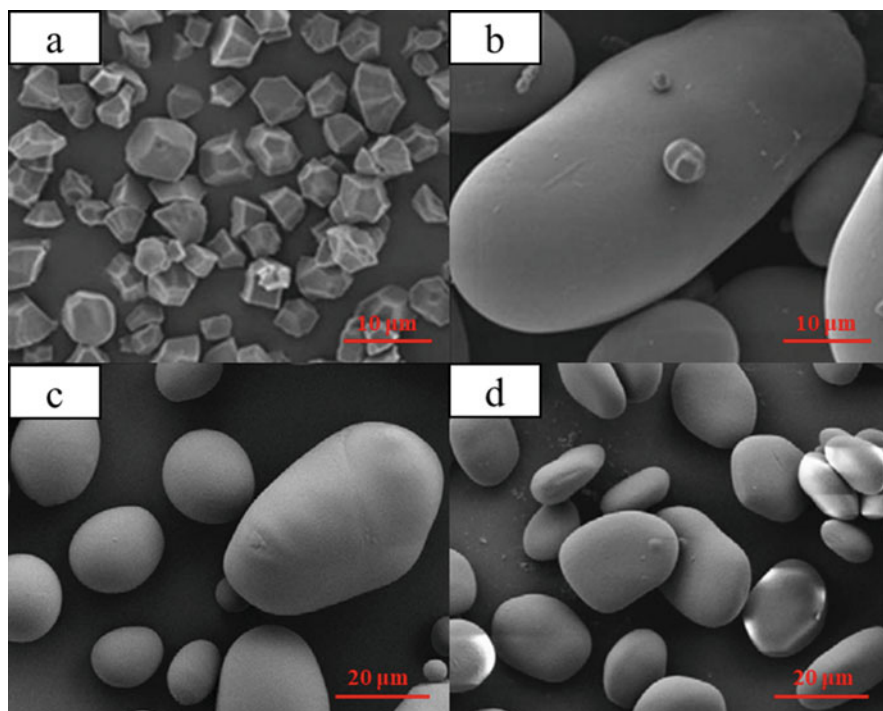


Fig. 2 SEM images of starches. (a) Rice starch; (b) lotus starch; (c) potato starch; (d) yam starch. Reproduced from [23] with permission from the Royal Society of Chemistry (2016) and [24] with permission from Elsevier Ltd. (2017)

channels in sorghum starch granules have diameters of about 0.1–0.3 mm and 0.07–0.1 mm, respectively. These pores and channels are reported to cause high susceptibility of starch granules to enzyme attack [20].

Starch granules also contain small amounts of other components, such as proteins, lipids, and phosphorus. Proteins (0.1–0.7% by weight) and lipids (up to 2%) occur in greater amounts in cereal starches than in other starches, whereas phosphorus is more abundant in potato starch. Proteins are found at both surface and interior of starch granules, including in channels [30]. Lipids, in the form of free fatty acids, lysophospholipids, and complexes with amylose, are also found in many starches [17, 31]. Phosphorus, found mainly in potato starch as phospholipids and phosphate monoesters, has a great effect on starch functional properties. These minor constituents are all reported to affect the functional properties and digestibility of starch [32, 33].

As granule morphology (size and shape) is an important property of starch structure, it is often investigated using light microscopy (LM), SEM, AFM, transmission electron microscope (TEM), and confocal laser scanning microscope (CLSM) [8]. SEM can be used to study the surface morphology of native starch granules or starches after different treatments. TEM is mainly used to examine the internal ultrastructure of native starch granules after ultrathin sectioning or starch nanoparticles or nano-crystalline lamellae [34]. AFM is a high-resolution technique for studying the external and internal structures of starch granules. CLSM also allows characterization of both external and internal structures of starch granules after staining with dyes. Characterizing the morphology of starch granules is of importance for better understanding the structure-function relationship of starch.

3 Growth Rings

Native starch occurs naturally in the form of insoluble and semi-crystalline granules, in which a characteristic hierarchical structure-growth ring can be observed by SEM (Figs. 1b and 3a) [10, 35–37]. These growth rings, as originally defined by French

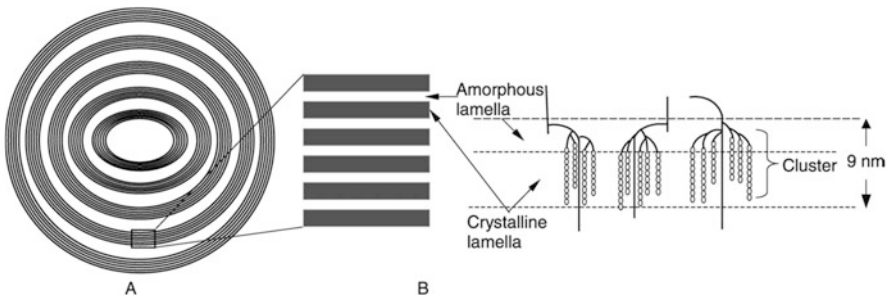


Fig. 3 Diagrammatic representation of the lamellar structure of a starch granule. (a) Stacks of microcrystalline lamellae separated by amorphous growth rings. (b) Magnified view of the amorphous and crystalline regions. Double helical structures formed by adjacent chains of amylopectin give rise to crystalline lamellae. Branching points constitute the amorphous regions. Reproduced from [35] with permission from the Academic Press Inc. (2004)

[38], and usually observed in fragments generated by acid or amylase treatment of starch granules, are considered to represent diurnal deposition of starch. The number and size of the growth rings are mainly dependent on the botanical origin of the starch [39].

Starch granules are composed of semi-crystalline and amorphous growth rings. The alternating and amorphous semi-crystalline growth rings increase in diameter from the bulk core area toward the starch granules surface (Fig. 3), resembling the layers of an onion [35, 36, 40]. The semi-crystalline growth rings were observed to decrease gradually in thickness from 450–550 nm for those closer to the hilum to 80–160 nm for rings near the periphery [40]. The semi-crystalline rings are well characterized by alternating crystalline and amorphous lamellae with a repeat period of 9–10 nm [41]. The amorphous growth rings are mainly made up of extended amylopectin chains that interconnect the crystalline regions, branch points of amylopectin chains, and interspersed amylose molecules. The amorphous growth rings are softer and looser than the crystalline growth rings and display a uniform width of approximately 60–80 nm [40]. The alternating concentric semi-crystalline and amorphous growth rings are attributed to the daily fluctuations in the amount of carbohydrate available as the starch granule grows in the plant [42]. An area surrounding the granule hilum, composed of randomly coiled amylose and the reducing ends of amylopectin, is termed the bulk amorphous core [10, 40], which is still not well understood.

4 Blocklets

Blocklets are observed as protrusions on the surface of starch granules with AFM and SEM (Fig. 1c). The scale of blocklets is between growth rings and lamellae, varying from 20 nm to 500 nm, depending on the botanical starch sources [6, 43]. In general, the blocklets are larger in B-type potato starch granules (diameter of 400–500 nm) than in A-crystalline wheat starch granules (25–100 nm in diameter) [6]. Blocklets normally consist of crystalline and amorphous lamellae that are formed by the clusters of amylopectin molecules. The reducing terminal sides for all the blocklets are toward the hilum of starch granules [44]. Blocklets, present in both amorphous and semi-crystalline growth rings, have a semi-crystalline ultrastructure and consist of several amylopectin molecules [5, 6]. Blocklets are differentiated into normal and defective ones, occurring in the same starch granules [44]. The normal blocklets are present in the hard shells or semi-crystalline growth rings, while the defective blocklets occur in the soft shells or amorphous growth rings. From the perspective of the physicochemical properties of starch granules, the blocklets of two types may be arranged into the two formations, heterogeneous and homogenous shell. Amylopectin plays an important role in blocklet architecture, whereas amylose contributes to the strength and flexibility of starch granule. Despite of these differences, there are some consistent structural features, as follows [44]:

1. In the same plant, most of the blocklets are similar in size and shape, although a range of dimensions may occur.
2. The blocklets occur continuously throughout the granule.
3. The blocklet size may not relate to their granule size and the thickness of growth rings.
4. The blocklet assembly may lead to defects in the amorphous growth rings and may be assembled loosely.
5. There is an interconnecting matrix surrounding groups of blocklets.
6. The blocklets in semi-crystalline and amorphous growth rings are not always continuous structures.

Although the spherical blocklets are observed and thought to be really present in starch, the exact nature of the blocklets and their relationship with other structures (e.g., superhelices) has not been fully understood [6, 10]. As there are no available methods or technology to separate the blocklets, their structure has not been well characterized yet. Even so, the blocklets are still thought to play a role in the organization of starch molecule and in affecting starch functionality.

5 Lamellae

At a smaller scale than blocklets are lamellae (Figs. 1e and 3b), which can be characterized by small-angle X-ray scattering (SAXS). SAXS patterns from all hydrated native starches show a broad scattering peak at $0.06\text{--}0.07 \text{ \AA}^{-1}$ (Fig. 4), which is reciprocally related to the average total thickness (9–10 nm) of the crystalline and amorphous regions in a lamellar arrangement in the granule (known as the lamellar repeat distance, long period or Bragg spacing $d = 2\pi/q$)

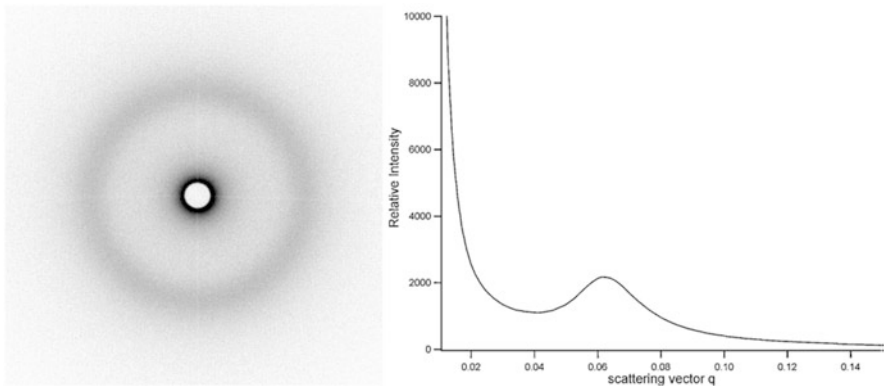


Fig. 4 Scattering pattern from regular maize starch and corresponding SAXS curve showing relative intensity vs. scattering vector. Reproduced from [41] with permission from the Elsevier Ltd. (2011)

[41, 45, 46]. This characteristic appears to be a common feature in the structure of native starch granules, independent of botanical source [47]. The position of the peak depends on the thickness of the lamellae, while the peak area or intensity is mainly related to the electron density difference between crystalline and amorphous lamellae, which reflects the degree of order in semi-crystalline regions [46, 48, 49]. The crystalline lamellae are considered to be generated by double helices of amylopectin side chains and parts of amylose molecules, whereas the amorphous lamellae comprise amylose and the amylopectin branch points [10, 15, 50]. Generally, the thickness of crystalline lamellae is approximately 4–6 nm, whereas that of the amorphous lamellae is 3–6 nm [5, 51]. About 16 repeat lamellae form a dense part of a growth ring with a thickness of 140 nm [42]. For waxy starch, the amorphous lamellae are generally thicker than the crystalline lamellae [52]. It has been found that amylose in the semi-crystalline lamellae can disrupt the order of lamellar structure and result in the defective lamellae with lower scattering intensity [46, 53]. The molecular density of crystalline lamellae is lower in potato starch (1.10 g/cm^3) than in waxy maize (1.22 g/cm^3), probably due to the higher water content of B-type crystalline polymorphs. In contrast, the molecular density of amorphous lamellae is found to be almost similar in potato starch (0.52 g/cm^3) and in waxy maize starch (0.46 g/cm^3) [54].

6 Double Helices

The structural element termed double helix is the smallest-scale ordered structure in starch granules (Fig. 5A). Double helix in normal starch is predominantly made up of amylopectin molecules; whereas in high-amylose starches, amylose also involves in the formation of double helices (and potentially crystalline arrays) [35, 57, 58]. The unbranched (A chains) and singly branched chains (B1 chains) of amylopectin with a degree of polymerization (DP) of at least 10 are thought to intertwine to form double helices [59]. Double helix content in starch granules is usually measured by ^{13}C cross-polarization magic angle spinning/nuclear magnetic resonance (^{13}C CP-MAS/NMR) and ^{13}C -single pulse magic angle spinning (^{13}C SP/MAS) [60, 61]. Each double helix consists of two chains with 6 glucose residues per turn of each strand and a pitch of 2.1 nm with the length about 4–6 nm [5, 9, 35]. The double helix is generally left handed and packed in monoclinic hexagonal or pseudohexagonal unit cell into A- or B-type crystallites, respectively (Fig. 5B or C) [6, 55, 62].

Once double helices are arranged into either A- or B-crystalline forms, they can be identified by characteristic X-ray diffraction (XRD) patterns (Fig. 6). The double helices forming the two crystalline polymorphs have essentially the same structure [2, 59]. However, the packing of these double helices within the A-type polymorphic (crystalline) structure is relatively compact with low water content, while the B-type polymorph has a more open structure containing a hydrated helical core (Fig. 5B and C) [35]. In the A-type crystal, the double helices are refined in a monoclinic unit cell

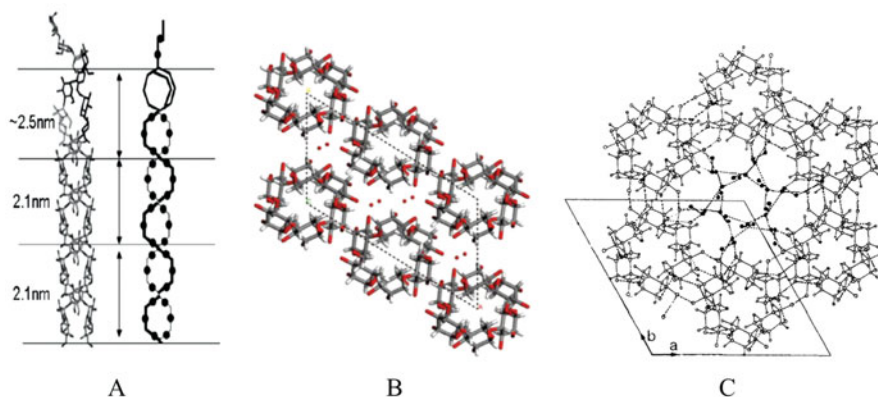


Fig. 5 Schematic representations of double helix and unit cell of A- or B-type crystallites. **(A)** The double helix of crystalline starch. **(B)** Crystallites of A-type starch. Projection of the structure on the (a, b) plane. The dots represent the oxygen atoms of the water molecules. **(C)** Crystallites of B-type starch. Projection of the structure onto the (a, b) plane. The unit cell content and some neighboring double helices are represented in order to show the localization of the water molecules (as black spots) in a channel. Hydrogen bonds are indicated as dashed lines. Reproduced from [6, 55, 56] with permission from Wiley (2010), Wiley (1988), and the American Chemical Society (2009), respectively

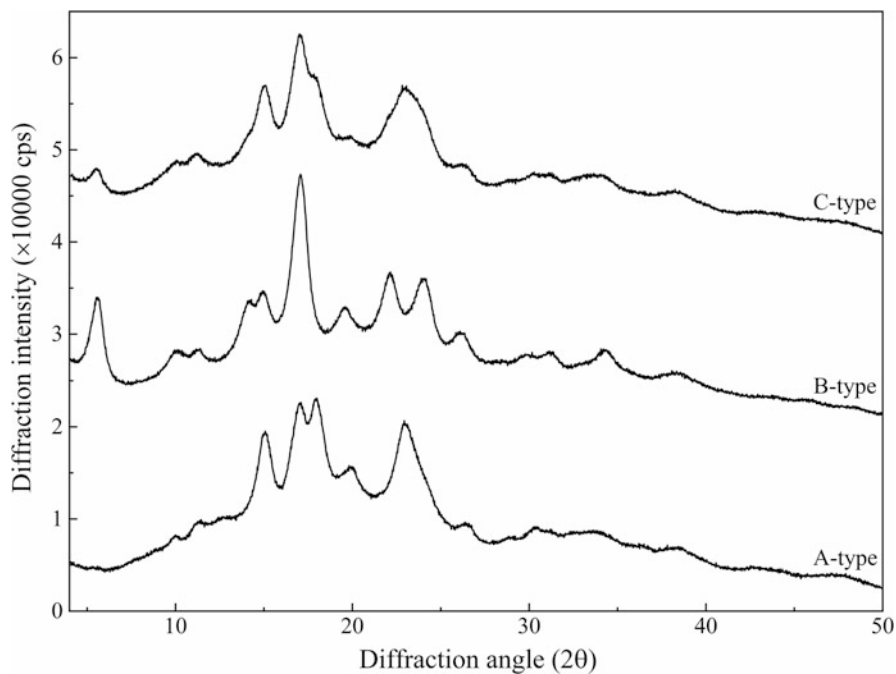


Fig. 6 XRD patterns of three starches: A-type from corn starch; B-type from potato starch; C-type from pea starch

with dimensions $a = 2.083$ nm, $b = 1.145$ nm, c (chain axis and monoclinic axis) = 1.058 nm, and $\gamma = 122.0^\circ$ containing 8 water molecules of each turn (Fig. 5B) [56]. The XRD pattern of the A-type polymorphic structure shows the peaks at 15° , 17° , 18° , and 23° (2θ). The A-type polymorph is found in cereal starches which have a larger population of short branch chains [63]. In the B-type polymorph, the double helices are packed in a hexagonal unit cell with lattice parameters $a = b = 1.85$ nm, $c = 1.04$ nm with 36 water molecules (Fig. 5C) [55]. The B-type polymorph occurs mainly in tuber, root, retrograded, and high-amylose starch (e.g., high-amylose maize and barley starch), which have more long branch chains than A-type starches. The main XRD peaks of these starches occur at 5.6° , 17° , 22° , and 24° (2θ) [63, 64]. A mixture of A- and B-type crystals, present in starches from legumes, some roots, and fruits, is often referred to as a C-type crystal [16, 17]. The relative location and proportion of A-type and B-type crystalline polymorphs in C-type starch differs with starch sources and has a great effect on the properties of C-type starch [17].

7 Other Structures

In addition to the five levels of starch structure mentioned above, other structural features, such as amorphous core, single helix, superhelix, and clusters have also been studied. Hilum is the center from which starch granules grow biosynthetically by apposition [1, 6]. The hilum is surrounded by an amorphous core, which is composed mainly of amylose and few of disordered amylopectin chains [10, 40]. The hilum structure tends to be much more amorphous than the outer layers, confirmed by AFM imaging [65]. The amorphous core is surrounded by concentric semi-crystalline growth rings of decreasing width toward the periphery, alternating with amorphous growth rings of more uniform thickness [10, 40]. Some amylose chains, which are represented as radiating from the core in a spoke-like pattern, may reinforce the granule structure (Fig. 1II). The proportion of the granule occupied by the amorphous core may depend on the amylose content of starch; waxy maize starch granules had the smallest amorphous core area compared to normal and high-amylose maize starches [10, 40, 66].

Amylose single helices occur in left-handed inclusion complexes with certain ligands, such as iodine, fatty acids, alcohols, and flavor compounds [6, 17], which can be studied by ^{13}C cross-polarization magic angle spinning/nuclear magnetic resonance (^{13}C CP-MAS/NMR) and ^{13}C -single pulse magic angle spinning (^{13}C SP/MAS) [60, 61]. These left-handed complexes are insoluble in water and have a V-crystalline form with a characteristic XRD pattern differing from the A- and B-crystal forms. The size of the helix (six, seven, or eight glucose residues per turn) is determined by the nature of the complexing guests [17]. The glucosyl hydroxyl groups of α -1,4-glucose chains are located on the outer surface of the helix, thus leading to the inner core being a hydrophobic cavity lined with methylene groups and glucosidic oxygens.

Superhelix is a super structure of lamellae primarily in potato starch, which is first proposed by Oostergetel and van Bruggen (Fig. 1d) [67]. In this model, the helices form a continuous and regular crystalline network, serving as a skeleton around which the rest of the starch granule is built. The crystalline regions containing the double helical linear segments in the amylopectin form a continuous network consisting of left-handed helices packed in a tetragonal array. Since neighboring helices interpenetrate each other, the crystalline lamellae form a more or less continuous superhelical structure [6, 67]. The direction of the clustered chains and the individual amylopectin molecules is in line with that of the superhelix axis [68]. The basic building blocks of superhelices have a width of approximately 4–5 helices and approximately 18–40 adjacent helices in a helical pitch. The superhelix has an outer diameter of 18 nm, a central cavity with a diameter about 8 nm, and a pitch of 9 nm based on electron optical tomography and cryo-electron diffraction experiments [67, 69]. A single macromolecular superhelix is only comparable to the smallest identified blocklets observed by AFM [68, 70].

Clusters are constructed by the short chains of amylopectin that are interlinked and regularly spaced (Fig. 3b). The regular and widespread chain clustering would be amenable to the formation of double helices, which is confirmed by low and wide-angle X-ray diffraction study [9]. As proposed by Bertoft, a cluster is consisted of a group of chains, in which the branches are separated by internal chain segments shorter than nine glucosyl residues [71]. The number of clusters per amylopectin molecule differs by plant origin and appears to be in the range of 61–120 on average for the large amylopectin, 20–40 for the medium amylopectin, and 4–15 for the small amylopectin [72]. In general, A-crystalline starches tend to have larger clusters than B-crystalline starches. The size distribution of limit dextrins of the clusters in maize, barley, and rice is comparatively broad with peak DP (representing the major part of the clusters on a weight basis) around 100–200 [6]. The number of chains which form a large cluster in waxy rice amylopectin is estimated to 23. Small clusters are proposed to consist of 5–8 chains [73]. The density of branches within clusters is higher in the A-crystalline cereal starches than in the B-crystalline starches [73, 74], but the density in the A-crystalline root starch of cassava is similar or only slightly higher than that in B-type starches [75].

8 Conclusions

Starch granules are made up of a variety of structural elements, such as single chains, helices, superhelices, clusters, lamellae, blocklets, growth rings, and granules varying in size from Ångströms to microns. While significant advancements have been achieved in the study of starch structure, there is still knowledge gap to be filled in the future. Development of new methodology or technology is of crucial importance for better understanding the fine structure of starch granules, as well as for further revealing the structure-function relationship.

References

1. Tetlow IJ. Starch biosynthesis in developing seeds. *Seed Sci Res.* 2010;21(01):5–32.
2. Chen W, Lickfield GC, Yang CQ. Molecular modeling of cellulose in amorphous state. Part I: Model building and plastic deformation study. *Polymer.* 2004;45(3):1063–71.
3. Tester RF, Morrison WR. Swelling and gelatinization of cereal starches. I. Effects of amylopectin, amylose, and lipids. *Cereal Chem.* 1990;67(6):551–7.
4. Wang S, Copeland L. Phase transitions of pea starch over a wide range of water content. *J Agric Food Chem.* 2012;60(25):6439–46.
5. Bertoft E. Understanding starch structure: Recent progress. *Agronomy.* 2017;7(3):56.
6. Pérez S, Bertoft E. The molecular structures of starch components and their contribution to the architecture of starch granules: A comprehensive review. *Starch-Stärke.* 2010;62(8):389–420.
7. Jacobs H, Delcour JA. Hydrothermal modifications of granular starch, with retention of the granular structure: A review. *J Agric Food Chem.* 1998;46(8):2895–905.
8. Buléon A, Colonna P, Planchot V, Ball S. Starch granules: Structure and biosynthesis. *Int J Biol Macromol.* 1998;23(2):85–112.
9. Zobel H. Molecules to granules: A comprehensive starch review. *Starch-Stärke.* 1988;40(2):44–50.
10. Wang S, Copeland L. Effect of acid hydrolysis on starch structure and functionality: A review. *Crit Rev Food Sci Nutr.* 2015;55(8):1081–97.
11. Peat S, Whelan W, Thomas GJ. Evidence of multiple branching in waxy maize starch. *J Chem Soc.* 1952:4536–8.
12. Hanashiro I, Abe J-i, Hizukuri S. A periodic distribution of the chain length of amylopectin as revealed by high-performance anion-exchange chromatography. *Carbohydr Res.* 1996;283:151–9.
13. Hanashiro I, Tagawa M, Shibahara S, Iwata K, Takeda Y. Examination of molar-based distribution of A, B and C chains of amylopectin by fluorescent labeling with 2-aminopyridine. *Carbohydr Res.* 2002;337(13):1211–5.
14. Wang S, Li C, Copeland L, Niu Q, Wang S. Starch retrogradation: A comprehensive review. *Compr Rev Food Sci Food Saf.* 2015;14(5):568–85.
15. Vamadevan V, Bertoft E. Structure-function relationships of starch components. *Starch-Stärke.* 2015;67(1-2):55–68.
16. Copeland L, Blazek J, Salman H, Tang MC. Form and functionality of starch. *Food Hydrocolloids.* 2009;23(6):1527–34.
17. Wang S, Copeland L. Molecular disassembly of starch granules during gelatinization and its effect on starch digestibility: A review. *Food Funct.* 2013;4(11):1564–80.
18. Dhital S, Butardo VM Jr, Jobling SA, Gidley MJ. Rice starch granule amylolysis-differentiating effects of particle size, morphology, thermal properties and crystalline polymorph. *Carbohydr Polym.* 2015;115:305–16.
19. Al-Rabadi GJS, Gilbert RG, Gidley MJ. Effect of particle size on kinetics of starch digestion in milled barley and sorghum grains by porcine alpha-amylase. *J Cereal Sci.* 2009;50(2):198–204.
20. Dhital S, Shrestha AK, Gidley MJ. Relationship between granule size and in vitro digestibility of maize and potato starches. *Carbohydr Polym.* 2010;82(2):480–8.
21. Xu J, Kuang Q, Wang K, Zhou S, Wang S, Liu X, et al. Insights into molecular structure and digestion rate of oat starch. *Food Chem.* 2017;220:25–30.
22. Zhang B, Dhital S, Gidley MJ. Densely packed matrices as rate determining features in starch hydrolysis. *Trends Food Sci Technol.* 2015;43(1):18–31.
23. Wang S, Sun Y, Wang J, Wang S, Copeland L. Molecular disassembly of rice and lotus starches during thermal processing and its effect on starch digestibility. *Food Funct.* 2016;7(2):1188–95.
24. Wang S, Wang J, Wang S, Wang S. Annealing improves paste viscosity and stability of starch. *Food Hydrocolloids.* 2017;62:203–11.

25. Alvarez-Ramirez J, Vernon-Carter EJ, Carrillo-Navas H, Meraz M. Effects of cooking temperature and time on the color, morphology, crystallinity, thermal properties, starch-lipid complexes formation and rheological properties of roux. *LWT-Food Sci Technol.* 2018;91:203–12.
26. Wang S, Wang S, Liu L, Wang S, Copeland L. Structural orders of wheat starch do not determine the in vitro enzymatic digestibility. *J Agric Food Chem.* 2017;65(8):1697–706.
27. Fannon JE, Hauber RJ, BeMiller JN. Surface pores of starch granules. *Cereal Chem.* 1992;69(3):284–8.
28. Fannon JE, Shull JM, Bemiller JN. Interior channels of starch granules. *Cereal Chem.* 1993;70:611.
29. Huber KC, BeMiller JN. Channels of maize and sorghum starch granules. *Carbohydr Polym.* 2000;41(3):269–76.
30. Han X-Z, Benmoussa M, Gray JA, BeMiller JN, Hamaker BR. Detection of proteins in starch granule channels. *Cereal Chem.* 2005;82(4):351–5.
31. Morrison WR, Milligan TP, Azudin MN. A relationship between the amylose and lipid contents of starches from diploid cereals. *J Cereal Sci.* 1984;2(4):257–71.
32. Wang S, Luo H, Zhang J, Zhang Y, He Z, Wang S. Alkali-induced changes in functional properties and in vitro digestibility of wheat starch: The role of surface proteins and lipids. *J Agric Food Chem.* 2014;62(16):3636–43.
33. Nor Nadiha MZ, Fazilah A, Bhat R, Karim AA. Comparative susceptibilities of sago, potato and corn starches to alkali treatment. *Food Chem.* 2010;121(4):1053–9.
34. Putaux J-L, Molina-Boisseau S, Momaur T, Dufresne A. Platelet nanocrystals resulting from the disruption of waxy maize starch granules by acid hydrolysis. *Biomacromolecules.* 2003;4(5):1198–202.
35. Tester RF, Karkalas J, Qi X. Starch-composition, fine structure and architecture. *J Cereal Sci.* 2004;39(2):151–65.
36. Yamaguchi M, Kainuma K, French D. Electron microscopic observations of waxy maize starch. *J Ultrastruct Res.* 1979;69(2):249–61.
37. French D. Organization of starch granules. In: Whistler RL, Bemiller JN, Paschall EF, editors. *Starch: Chemistry and Technology.* 2nd ed. Amsterdam: Academic Press; 1984. p. 183–247.
38. French D. Fine structure of starch and its relationship to the organization of starch granules. *J Jap Soc Starch Sci.* 1972;19(1):8–25.
39. Chen P, Yu L, Simon GP, Liu X, Dean K, Chen L. Internal structures and phase-transitions of starch granules during gelatinization. *Carbohydr Polym.* 2011;83(4):1975–83.
40. Wang S, Blazek J, Gilbert E, Copeland L. New insights on the mechanism of acid degradation of pea starch. *Carbohydr Polym.* 2012;87(3):1941–9.
41. Blazek J, Gilbert EP. Application of small-angle X-ray and neutron scattering techniques to the characterisation of starch structure: A review. *Carbohydr Polym.* 2011;85(2):281–93.
42. Cameron RE, Donald AM. A small-angle X-ray scattering study of the annealing and gelatinization of starch. *Polymer.* 1992;33(12):2628–35.
43. Gallant DJ, Bouchet B, Baldwin PM. Microscopy of starch: Evidence of a new level of granule organization. *Carbohydr Polym.* 1997;32(3):177–91.
44. Tang H, Mitsunaga T, Kawamura Y. Molecular arrangement in blocklets and starch granule architecture. *Carbohydr Polym.* 2006;63(4):555–60.
45. Yang Z, Chaib S, Gu Q, Hemar Y. Impact of pressure on physicochemical properties of starch dispersions. *Food Hydrocolloids.* 2017;68:164–77.
46. Wang S, Li P, Yu J, Guo P, Wang S. Multi-scale structures and functional properties of starches from *Indica* hybrid, *Japonica* and waxy rice. *Int J Biol Macromol.* 2017;102:136–43.
47. Jenkins PJ, Cameron RE, Donald AM. A universal feature in the structure of starch granules from different botanical sources. *Starch-Stärke.* 1993;45(12):417–20.
48. Kuang Q, Xu J, Liang Y, Xie F, Tian F, Zhou S, et al. Lamellar structure change of waxy corn starch during gelatinization by time-resolved synchrotron SAXS. *Food Hydrocolloids.* 2017;62:43–8.

49. Yuryev VP, Krivandin AV, Kiseleva VI, Wasserman LA, Genkina NK, Fornal J, et al. Structural parameters of amylopectin clusters and semi-crystalline growth rings in wheat starches with different amylose content. *Carbohydr Res.* 2004;339(16):2683–91.
50. Li M, Dhital S, Wei Y. Multilevel structure of wheat starch and its relationship to noodle eating qualities. *Compr Rev Food Sci Food Saf.* 2017;16(5):1042–55.
51. Qiao D, Xie F, Zhang B, Zou W, Zhao S, Niu M, et al. A further understanding of the multi-scale supramolecular structure and digestion rate of waxy starch. *Food Hydrocolloids.* 2017;65:24–34.
52. Jenkins P, Donald A. The influence of amylose on starch granule structure. *Int J Biol Macromol.* 1995;17(6):315–21.
53. Koroteeva DA, Kiseleva VI, Krivandin AV, Shatalova OV, Blaszczyk W, Bertoft E, et al. Structural and thermodynamic properties of rice starches with different genetic background: Part 2. Defectiveness of different supramolecular structures in starch granules. *Int J Biol Macromol.* 2007;41(5):534–47.
54. Donald AM, Kato KL, Perry PA, Weigh TA. Scattering studies of the internal structure of starch granules. *Starch-Starke.* 2001;53(10):504–12.
55. Imberty A, Perez S. A revisit to the three-dimensional structure of B-type starch. *Biopolymers.* 1988;27(8):1205–21.
56. Popov D, Buléon A, Burghammer M, Chanzy H, Montesanti N, Putaux JL, et al. Crystal structure of A-amylose: A revisit from synchrotron microdiffraction analysis of single crystals. *Macromolecules.* 2009;42(4):1167–74.
57. Shi Y-C, Capitani T, Trzasko P, Jeffcoat R. Molecular structure of a low-amylopectin starch and other high-amylose maize starches. *J Cereal Sci.* 1998;27(3):289–99.
58. Tester RF, Debon SJJ, Sommerville MD. Annealing of maize starch. *Carbohydr Polym.* 2000;42(3):287–99.
59. Gidley MJ. Factors affecting the crystalline type (A-C) of native starches and model compounds: A rationalisation of observed effects in terms of polymorphic structures. *Carbohydr Res.* 1987;161(2):301–4.
60. Gidley MJ. Molecular mechanisms underlying amylose aggregation and gelation. *Macromolecules.* 1989;22(1):351–8.
61. Tan I, Flanagan BM, Halley PJ, Whittaker AK, Gidley MJ. A method for estimating the nature and relative proportions of amorphous, single, and double-helical components in starch granules by ¹³C CP/MAS NMR. *Biomacromolecules.* 2007;8(3):885–91.
62. Imberty A, Chanzy H, Pérez S, Buléon A, Tran V. The double-helical nature of the crystalline part of A-starch. *J Mol Biol.* 1988;201(2):365–78.
63. Jane JL. Current understanding on starch granule structures. *J Appl Glycosci.* 2006;53(3):205–13.
64. Zobel HF. Starch crystal transformations and their industrial importance. *Starch-Stärke.* 1988;40(1):1–7.
65. Zhu F. Atomic force microscopy of starch systems. *Crit Rev Food Sci Nutr.* 2017;57(14):3127–44.
66. Li JH, Vasanthan T, Hoover R, Rossnagel BG. Starch from hull-less barley: Ultrastructure and distribution of granule-bound proteins. *Cereal Chem.* 2003;80(5):524–32.
67. Oostergetel GT, van Bruggen EF. The crystalline domains in potato starch granules are arranged in a helical fashion. *Carbohydr Polym.* 1993;21(1):7–12.
68. Bertoft E. On the nature of categories of chains in amylopectin and their connection to the super helix model. *Carbohydr Polym.* 2004;57(2):211–24.
69. Waigh TA, Donald AM, Heidelbach F, Riekkel C, Gidley MJ. Analysis of the native structure of starch granules with small angle X-ray microfocus scattering. *Biopolymers.* 1999;49(1):91–105.
70. Baldwin PM, Adler J, Davies MC, Melia CD. High resolution imaging of starch granule surfaces by atomic force microscopy. *J Cereal Sci.* 1998;27(3):255–65.

71. Bertoft E. Composition of building blocks in clusters from potato amylopectin. *Carbohydr Polym.* 2007;70(1):123–36.
72. Takeda Y, Shibahara S, Hanashiro I. Examination of the structure of amylopectin molecules by fluorescent labeling. *Carbohydr Res.* 2003;338(5):471–5.
73. Bertoft E, Koch K. Composition of chains in waxy-rice starch and its structural units. *Carbohydr Polym.* 2000;41(2):121–32.
74. Kong X, Corke H, Bertoft E. Fine structure characterization of amylopectins from grain amaranth starch. *Carbohydr Res.* 2009;344(13):1701–8.
75. Laohaphatanaleart K, Piyachomkwan K, Sriroth K, et al. The fine structure of cassava starch amylopectin: Part 1: Organization of clusters. *Int J Biol Macromol.* 2010;47(3):317–24.

Amylose–Lipid Complex



Qiang Huang, Xu Chen, Shaokang Wang, and Jianzhong Zhu

Abstract Starch and lipids are the two major components in food products, and amylose is an important component in starch granules. In some native and processed starches, amylose may bind with lipids to form amylose–lipid complex, which will significantly affect the starch properties. This chapter introduces three types of methods for amylose–lipid complex formation, i.e., classical, enzymatic, and thermomechanical, and factors affecting complex formation are discussed in detail. The effects of amylose–lipid complexes on starch properties are addressed, including digestibility, solubility, gelatinization properties, rheological properties, and retrogradation. As a new type of resistant starch, the health implications of the amylose–lipid complex are also discussed at the end of this chapter. Amylose–lipid complexes can influence glycemic and insulin levels and reduce risk of colon cancer, and it can also be used for nano-encapsulation of bioactive or sensitive substances.

Keywords Amylose–lipid complex · Amylopectin · Starch properties

1 Introduction

Starch and lipids are major components of foods, which play important roles in the caloric density, texture, and flavor of foods. Starch is mainly made up of two components: amylose and amylopectin. Amylose has mainly linear α -1,4-D-glucan chains and a small number of branched chains connected by α -1,6-glycosidic bonds. Amylopectin is a moderately branched macromolecule composed of backbone chains and side chains that are linked by an average of 5% of α -1,6-glycosidic bonds. Lipids are broadly defined as a group of compounds that are soluble in

Q. Huang (✉) · X. Chen · S. Wang · J. Zhu

School of Food Science and Engineering, Center for Discipline Innovation of Food Nutrition and Human Health (111 Center), Guangdong Province Key Laboratory for Green Processing of Natural Products and Product Safety, South China University of Technology, Guangzhou, China

e-mail: qiangh@scut.edu.cn

organic solvents, which can be further divided into simple lipids, compound lipids, and derived lipids [1].

It is well known that amylose can form helical structure with a series of other substance, such as iodine, lipids (fatty acids, monoglycerides), alcohols and some other fat-soluble bioactive substances [1]. Normally, amylose–lipid complexes can be found in native starch granules and processed starch [2, 3]. The amylose–lipid complex entangles amylopectin molecules, restricting the swelling of starch granules and enzyme hydrolysis [4]. The hydrocarbon chain of the lipid interacts with the hydrophobic moiety of the amylose chain and fills the central cavity of the amylose single helix [3, 5, 6]. Depending on the size of the cross section of the complexing ligand, the number of glucose units per helical turn ranges from six to eight.

The interaction between lipid and amylopectin can also form a single helical complex. The X-ray diffraction pattern indicated that cold-water soluble starch prepared by heating normal maize starch in aqueous ethanol solution exhibited a V-type structure [7, 8]. Notably, the relative crystallinity of the cold-water soluble maize starch is higher than its amylose content, which implies that part of amylopectin forms complexes with the alcohols. The formation of amylopectin–lipid complex restricts the reassociation of amylopectin branches into double helices, as evidenced by the decrease in the degree of starch retrogradation during storage [9]. Amylose–lipid complexes can be classified into two forms according to their crystallinity, namely, the less ordered more amorphous type I and the semicrystalline type II. In general, type I complexes can be obtained by mixing amylose and lipid at a lower temperature (25–60 °C), whereas type II complexes are usually produced at a higher temperature (90–100 °C) [10, 11]. Therefore, type I complex has a lower dissociation temperature (<100 °C) than does the semicrystalline counterpart (>100 °C). Additionally, isothermal annealing treatment can convert the amorphous amylose–lipid complex into semicrystalline complex.

In addition to the four long-recognized sources, namely, physically inaccessible starch (RS 1), native B- or C-type polymorphic starch granules (RS 2), retrograded amylose (RS 3), and chemically modified starch (RS 4) [12, 13], amylose–lipid complexes (ALC) have been proposed as a new source of resistant starch (RS 5), because it has high resistance to amyolytic enzyme hydrolysis [5, 14].

2 Production of Amylose–Lipid Complex

Amylose–lipid complex (ALC) formation is an instant reaction, and the complex can reform after cooking, and it is considered thermally stable [15]. Generally, there are three types of methods for preparing amylose–lipid complexes: classical methods, enzymatic methods, and thermomechanical methods [16]. Base on the material, these could be sub-divided into three major groups, i.e., (1) starting from starch and ligands, (2) starting from amylose and ligands, (3) synthesizing amylose in the presence of the ligands [17].

2.1 *Classical Methods or Starting from Amylose and Ligands*

The classical method involves solubilizing amylose in solvents such as DMSO or KOH followed by the reduction of pH with HCl. The starch dispersion is heated to 121 °C and cooled to between 60 and 90 °C. Dissolved lipids in absolute ethanol are added to the cooled starch solution and then centrifuged. The precipitates are successively washed with hot water to remove free starch and fatty acids. This method yields type I and type II ALC at preparative temperatures of 60 °C and 90 °C, respectively [18].

Classical methods for preparing ALC include different technical variations, such as parboiling [19], autoclaving [20], and shearless heating of amylose/ligand/diluent mixture at elevated temperature (up to 140 °C) [21]. Depending on the preparation conditions, the thickness of crystal lamellae of complex obtained by this method ranges from 5 to 100 nm. One study [22] has shown that distinct nanocrystalline structures could be formed using this classical method, whereas other studies [23] suggested that these methods generally give polydisperse V-amylose populations.

2.2 *Enzymatic Methods for Synthesizing Amylose in the Presence of the Ligands*

Enzymatic methods for ALC preparation are generally classified into two main forms, that is, entirely and partially enzymatic methods. Entirely enzymatic methods commonly use glucose phosphorylase to catalyze synthesis of V-amylose from glucose-1-phosphate in the presence of appropriate hydrophobic ligands. Putseys et al. [24] used glucose-1-phosphate as a primer and a fatty acid with a polymerization enzyme (e.g., phosphorylase) to promote the formation of glycosidic bonds by an enzymatic method. The results indicated that the primer is first polymerized to produce an amylose chain of sufficient length to accommodate the first lipid; further chain extension occurred to form insoluble ALC. Most of the ALC formed by this method were type I.

The application of enzymatic preparation of V-amylose complex mainly refers to the modification of classical V-amylose synthesis, which is mainly achieved by adding an enzyme-catalyzed starch/amylose depolymerization step before or after the formation of the complex [16]. Gelders et al. [23] produced V-amylose complexes by depolymerizing starch using β -amylase before complexing the resultant mixture of dextrans with an appropriate ligand. Increasing the amount of amylose–lipid complex in granular starch can be used to produce RS type 5 [4, 46]. Firstly, swollen starch granules are treated with debranching enzyme (isoamylase or pullulanase) to remove the branch linkages of amylopectin, then the resulting free long branch-chains of amylopectin function similarly to amylose molecules, and therefore, they could effectively complex with fatty acids.

2.3 Thermomechanical Methods Starting from Starch and Ligands

Thermal processing technologies are alternative methods to produce ALC, which include steam-jet cooking [16, 25, 26], homogenization [27], pasting [28–30], and extrusion [31]. The advantage of this technology is that it is green, whereas for lab-scale production of pure ALC, the classical and enzymatic methods are more suitable.

In recent years, a new formation method of V-amylose complex by controlling temperature has attracted many researchers' attention, which was attributed to its easier cycle, less energy and better mouthfeel. A simple method to prepare inclusion complexes by "inserting" ascorbyl palmitate into preformed "empty" V-type amylose helices using high-amylose maize starch or potato amylose as material was reported [32]. Nakazawa and Wang [33] prepared starch-palmitic acid complex by annealing starch in methanol at 30 °C, which could increase the degree of complexation. D'Silva, Taylor, and Emmambux [29] studied the effects of stearic acid on the functional properties of V-amylose complex prepared with teff and maize starches and revealed that the teff starch modified with stearic acid has a promising application in foods with better mouthfeel.

Lauric acid (LA) was used to prepare starch–lipid complexes, which interact with three kinds of maize starches differing in amylose content, i.e., waxy maize starch (WMS), normal maize starch (NMS), and high-amylose maize starch (Hylon V) [34]. Gelatinization and retrogradation of starch can be retarded after the addition of LA [35]. The final product including intact granule ghost is beneficial for recycling. Both the complexation degree and the loss of the amylopectin double helices could affect the relative crystallinity of starch–LA complex [34]. Amylopectin may form complexes with LA at higher reaction temperature [36]. With the increase temperature or amylose content, the melting temperature and enthalpy changes of starch–LA complex enhanced. In addition, higher incubation temperature was conducive to the formation of the more ordered starch–LA complex [37, 38].

3 Factors that Affect ALC Formation

The formation of ALC depends on a multiplicity of factors including type of starch, degree of starch polymerization, the concentration ratio of starch–ligand, the structure of included molecule, and complexation temperature, water content, complexation time, and medium pH [16], as described in the following sections.

3.1 Effect of Starch Type

Amylose content, starch source, and degree of polymerization affect the formation of V-amylose. The effect of crop variety on the V-amylose complexes has been reported. The rice varieties have significant effects on the complex formation during rice parboiling [19]. The effect of starch type or variety on the yield of amylose–lipid complex is mainly attributed to the penetration rate of starch granules by the ligands (lipids), which is due to the differences in the microstructures of starch granules, such as the absence or presence of the surface channels/pores on the granule surface [29]. It has also been reported that starches with higher amylopectin content form fewer or no complexes than those with less amylopectin content [25, 39, 40].

3.2 Effect of Degree of Starch Polymerization

Compared with the number of carbons, V-amylose yield is more sensitive to amylose molecular weight [41]. With the increase of amylose chain, the melting temperature, stability, crystallite size, and level of organization of amylose–lipid complex increase [42]. On the one hand, too long amylose will lead to conformational disorder and to faults of the crystal structure [42]. On the other hand, if too short, it will disturb the formation of the crystal. It appears the ligand determines minimum DP of the complexing ligands. For instance, the minimum amylose size for complexing with palmitic acid is around 30–40 glucosyl residues whereas 20–30 glucosyl residues for lauric and caprylic acids, which is about the chain length to accommodate two fatty acids per chain [41]. It has also been reported that the critical minimum DP of complex formation and precipitation of glycerol monostearate (GMS) and docosanoic acid (C₂₂) was 35 and 40, respectively, regardless of the complexing temperature, which also correspond to the length required for each ligand molecule to accommodate two ligand molecules [42].

3.3 Effect of Starch Moisture Content

Moisture content affects the type of crystalline structure, and it can also influence the extent of type II amylose V-complexes formation at low- and intermediate-moisture conditions. V-amylose complexes are readily formed, during which, water is suggested to be necessary as plasticizer, whereas for high moisture contents, increased water content probably hinders the system from attaining the activation energy required for complex formation, thus inhibiting complex formation and crystallization [19]. In addition, for the same moisture content, starch type and heating conditions (temperature, time, and presence of shearing effects) may also play a role in the complex formation.

3.4 *Effect of Lipid Type, Chain Length, and Unsaturation*

Multiple factors may influence the formation of V-amylose complexes, for instance, the presence of native starch lipids, the acyl chain (hydrophobic component) length, degree of unsaturation, and the type of polar head of the ligand [43–46]. Increasing the unsaturation of fatty acids could promote the formation of less crystalline complexes than fully saturated fatty acids [43, 47]. Studies have shown that *cis*-unsaturated fatty acid complex poorly with amylose, giving low yields and low enthalpies of dissociation [48]. This may be due to the inefficient complexation of fatty acids, which was depicted as nonlinear or kinked due to the *cis*-double bond [49, 50]. Karkalas et al. [43] suggested that the effect of *cis-trans* effect on crystal structure is greater than that on yield. They postulated that the amylose helix needed to be expanded from six glucosyl residues per turn to seven in order to accommodate the unsaturated portion of the acyl chain, as happens with other bulky ligand molecules.

The V-amylose yield decreases with increasing chain length of lipid [51], which was due to the increased activation energy required for the complex formation, and increases as the length of the acyl chain is increasing [51]. Increased hydrophobic interaction between the ligand and amylose helix requires extra energy, which is also responsible for the increased activation energy [52, 53]. However, Goldet et al. [41] suggested under given conditions, the solubility of the ligand was positively correlated with the formation of the V-amylose complex. Thus, they believe longer acyl chains reduce the ability to form complexes. [41].

3.5 *Effect of Ligand Concentration and Solubility*

The degree of complex formation is affected by both ligand concentration and solubility [54]. Reports showed that a ratio of 10:1 (amylose/fatty acid) by weight was found optimal [55, 56]. Studies also demonstrated that for different types of fatty acid, the maximal complex formation occurs at different concentrations [54]. For fatty acids, not only the water solubility of lipids but also critical micellar concentration affects the optimal concentration, above a certain concentration; the lipids tend to self-assemble in preference to form V-amylose complexes [54]. This may be responsible for the different complex formations with stearic acid in different reports [48, 54, 57]. Since the carbon chain length is negatively correlated with the critical micelle concentration of fatty acids and water solubility [54], compared with the shorter-chained fatty acids under the same conditions, the amount of longer-chained lipids required to form complex is less. However, for the complexation of ionic ligands, such as dodecyl trimethylammonium bromide, the higher the ligand concentration, the more difficult for packing. Therefore, complexes with lower dissociation temperatures are prone to complexation reactions due to repulsion of ionic charges [58].

Interaction between ligand and amylose must be in solution; as a result, solubility is a key factor during the complexation. Therefore, the presence of flavor compounds with high solubility may be sufficient to induce complex formation, that is, V₇-amylose. However, for low-solubility flavor molecules, a stable complex can only be formed in the presence of lipids, resulting in a V₆-conformation for the ternary complex [59].

3.6 *Effect of Heat*

During the complex, there are a series of factors affecting the V-amylose crystal structure, such as the complexation temperature, duration of heating, and the cooling rate. For example, several factors such as endpoint heating temperature, the cooling rate, and the final quench temperature play a decisive role in the formation and morphology of the final spherulites during the steam-jet preparation of amylose–lipid complexes [25, 57, 60]. Similarly, heating/barrel temperature also has an important influence on the formation of amylose–lipid complexes during extrusion cooking [61].

Type I complex is obtained by rapid nucleation at lower heating temperature (60 °C), which results in a random distribution of helices without forming distinct crystallites [42]. In contrast, type II complexes are usually formed at higher temperature; typically, the optimal temperature is above 90 °C [42, 62, 63]. At these temperatures, both enthalpies and crystallinities are maximized [64]. There is a high energy barrier between type I and type II complexes, that is, the two types of complexes are in two separate thermodynamic states, and obviously, the formation of type II complex requires higher temperature [44, 55].

The duration of the heating directly determines the type of formed complex, and longer heat treatment is conducive to the formation of complex type II V-amylose rather than type I [44]. While shorter heat treatment mainly induced the formation of type I complexes, a certain amount of type II complex may also form [44]. Correspondingly, the ligands with shorter acyl chains require shorter heating time to form type II V-amylose than those with longer acyl chains [44, 65].

3.7 *Effect of pH*

The pH of the complexation medium is another important factor affecting complex formation. Complexes with neutral lipids (e.g., monoglycerides) tend to form insoluble precipitates in neutral aqueous media; on the contrary, insoluble complexes with ionizable fatty acids only could be formed in the presence of electrolytes at pH value below 7 [43]. The ionizable carboxyl group in fatty acid ligands makes the initial aggregation of complexes more sensitive to pH and salt concentration [43]. When $\text{pH} < \text{pKa}$, fatty acids with short chain (e.g., 8:0) are more easily to

form V-amylose complexes than these with longer chain (>10:0). While when $\text{pH} > \text{pK}_a$, longer-chain fatty acids (>10:0) are more likely to form V-amylose complexes. This may be attributed to the increased solubility of long-chain fatty acids in the form of dissociation or ionization [66].

3.8 Effect of Other Additives and Starch Modifications

It has been reported that other potential amylose complexing agents and acetylation also affect the formation of V-amylose complexes, of which, starch acetylation particularly reduces the complex-forming ability of amylose polymers [67]. Cyclodextrin could also form inclusion complexes by competing with amylose for ligands, during which, a three-in-one complex involving amylose and the ligand may form [68]. The presence of whey protein can effectively reduce the amount of starch-FFA complex and the melting enthalpy of DSC; interestingly, a more crystalline XRD order was observed [69]. It has also been reported that the relative crystallinity and crystal size of V-amylose increase with the addition of sorbitol [70].

4 Functional Properties of ALC

The functional properties of food products will be affected after starch forms complexes with monoglycerides, free fatty acids, and lysophospholipids [43]. Previous studies have shown that the formation of V-type complexes can affect a range of functional properties of starch, for example, the digestibility, flow properties, gel formation, pasting, and retrogradation of starch.

4.1 Effect of Amylose-Lipid Complex on Starch Digestibility

The starch-lipid complex shows higher resistance to amylase hydrolysis than most type-A polymorphic starches and amorphous amylose. Its enzyme resistance is affected by multiple factors, such as the amylose content, the molecular structures of complexing lipid [23], and the crystalline structure of the amylose-lipid complex [10]. Studies have shown that when starch is heated in excess water, the amylose-lipid complex could inhibit the swelling of granules, which further reduces the accessibility of enzyme to hydrolyze the starch granules [71]. The addition of other additives such as soy lecithin, corn oil, palmitic acid (PA), stearic acid (SA), oleic acid (OA) or linoleic acid (LA) could also reduce the starch enzymatic susceptibility when cooking cassava, common or high amylose corn starch [1]. However, similar results were not observed with waxy maize starch. Thus, it can be

concluded that the lipid complex formed during the cooking of non-waxy maize starch is the main reason for its decreased digestibility.

4.2 Effect of Amylose–Lipid Complex on Starch Swelling Capacity and Solubility

Starch–lipid interactions decrease starch swelling capacity [72, 73], solubility, and granule disruption [61, 74–77]. This is due to the formation of an insoluble layer between the additional exogenous pure lipids and surrounding granules, which can effectively prevent water from entering [78]. However, complexation between amylose and these lipids, either at the surface or inside the granule, can also facilitate these phenomena by preventing leaching of soluble carbohydrates [79].

4.3 Effect of Amylose–Lipid Complex on Starch Gelatinization Properties

Starch–lipid interactions increase the gelatinization temperature [80, 81]. The gelatinization behavior is gradually delayed with the increase of chain length and its concentration [80, 82].

The possibility of transitioning to more crystalline complexes that are dissociated at higher temperature was first proposed by Kugimiya et al. [83]. Subsequently, a report indicated that the two DSC endotherms were separated by an exotherm [84]. The exothermal transition indicates that, after dissociation of type I complexes, the helices as nuclei could obtain sufficient mobility to align around the remaining helices [85] resulting in better ordered crystals. However, not all amylose and ligands can go through this crystal perfection. In the case where the amylose chain may be too short, or the ligand is too voluminous, type II semicrystalline amylose–lipid complexes cannot be formed [23, 86], thereby annealing of type I complexes into semicrystalline type II complexes.

4.4 Effect of Amylose–Lipid Complex on Starch Pasting and Viscous Behavior

The formation of amylose–lipid complexes can also affect starch pasting behavior. For instance, in the presence of the complexes, the granule swelling and amylose leaching are inhibited [87–89]; initial viscosity pasting peak is reduced or absent [29, 90]; under high temperature or shear conditions, the viscosity of the cold paste was stable [91]; and no starch gel formation was observed or reduced [29, 92,

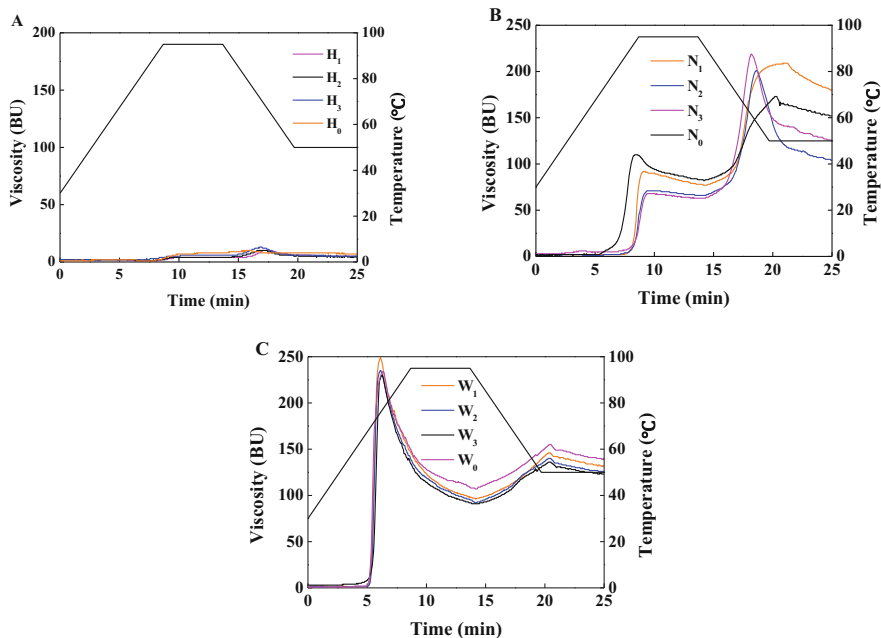


Fig. 1 Brabender viscosity of native maize starch and starch-LA complex (6%, w/w, dry starch base). (a) Hylon V and lauric acid complexed at 80 °C (H₁), 85 °C (H₂) and 90 °C (H₃). (b) Normal maize starch and lauric acid complexed at 60 °C (N₁), 65 °C (N₂) and 70 °C (N₃). (c) Waxy maize starch and lauric acid complexed at 55 °C (W₁), 60 °C (W₂) and 65 °C (W₃). Reproduced from Eliasson and Kare [36] with permission from the Elsevier Ltd. (2013)

93]. This pasting behavior is similar to that of crosslinked starch [91] and provides a possible way to improve the mouthfeel of starch-containing foods [29].

Amylose-lauric acid (LA) complexes showed a pronounced effect on the viscosity profile of normal maize starch (NMS) when compared with high-amylose maize starch (Hylon V) and waxy maize starch (Fig. 1) [94]. During the decrease in temperature program from 95 °C to 50 °C, the viscosity of NMS-LA complex increased dramatically then sharply dropped (Fig. 1b). The phenomenon may be interpreted in the following possible ways: firstly, a part of the starch-LA complex and amylopectin double helices is completely dissociated at 95 °C, during which, amylose and amylopectin leached out to disperse in the aqueous phase and amylose took on a random coil configuration [95]. Secondly, in the cooling process, high concentrations of amylose may start to aggregate, complex with LA and entangle with amylopectin to form a network, and then the starch paste showed a higher viscosity. In addition, with the continuous decrease of temperature, LA competed with amylose to form starch-LA complex rather than amylose/amylopectin network, which resulted in a low paste viscosity.

It has been reported that V-amylose formation with fatty acid is reduced at high concentration (up to 10% solids) [29, 92, 93], but other studies using flavor

compounds, such as menthone, decanal, and fenchone, have shown that gelation is induced at low starch concentrations [96–98]. Therefore, the starch-ligand concentration ratio directly affects the formation of V-complex during starch gelatinization. Other factors should also be included, for instance, plant source, lipid acyl chain length, and lipid molecular conformation, which can affect starch gel rigidity [92]. Additionally, the aqueous dispersions of dried V-amylose complexes show high spread ability and have rheological properties similar to commercial shortening at high concentration [99]. Starch pasting for a short or prolonged duration also shows a similar effect with a reduced power law flow index [29]. All these studies show the possibility for utilizing V-amylose as a fat replacer.

4.5 Effect of Amylose–Lipid Complex on Starch Retrogradation

The formation of V-amylose complexes can inhibit the retrogradation of starch effectively. In starch system, the formation of V-amylose complexes can compete with the retrogradation process for amylose [100, 101]. DSC results in the study indicate that the formation of amylose-monopalmitin complexes occurs preferentially in retrogradation [102, 103], and formation of the complex could further reduce the synergistic effect of starch [90]. Therefore, addition of the complexes or inducing the complex formation can decrease the staling of starch-containing foods [52]. Wang et al. [104] found that ALC could reduce the retrogradation of normal wheat starch to varying degrees depending on the length of the fatty acid chain. Purhagen et al. [105] provided evidence that the diacetyltartaric ester of monoglycerides in the pre-gelatinized flour has an anti-staling effect on gluten-free bread. The crumb softness of gluten-free bread with an emulsifier is mainly due to the formation of ALC.

5 Potential Health Benefits of ALC

As a kind of resistant starch, ALC can be classified as dietary fiber, which is beneficial to human health. The expected benefits of resistant starch for health can be listed as follows: decreases the pH of colon, improves glycemic control, and decreases the risk factors of cardiovascular disease and colon cancer [106]. There are also some specific potential health benefits of ALC: (1) hypoglycemic effects [4, 107], (2) reduced risk of colon cancer [108, 109], and (3) encapsulated bioactive compounds [110].

5.1 *Glycemic and Insulinemic Control*

Wang et al. [104] determined the digestibility of normal and waxy wheat starch with and without fatty acids after heat moisture treatment; the results showed the digestibility of starch-fatty acids sample decreased significantly after 120 min compared to starch without fatty acid. Similar results were also reported by Ai et al. [111] and Kawai et al. [112]. The formation of a complex between starch and fatty acid which is highly resistant to amylase may be responsible for its reduced susceptibility to enzymic hydrolysis [112]. The mechanism by which ALC is protected from hydrolysis by α -amylase is not well defined in literature. A possible mechanism is that ALC have compact structures and cannot form enzyme-substrate complexes with hydrolytic enzymes.

Hasjim et al. [4] found that the plasma glucose and insulin levels are lower after consumption of white bread that contains ALC than after regular white bread, indicating that bread containing ALC could result a decreased postprandial blood glucose. Similarly, after the rats were fed with starch-monostearoylglycerol complex, their postprandial insulin resistance decreased, accompanied by a decreased lipogenesis in the adipose tissue and liver [113].

The *in vivo* studies illustrated that ALC can be used to the prevention of hyperglycemia and hyperinsulinemia; in addition, hyperglycemia-induced hypoglycemia and the constant feeling of hunger can also be prevented [114, 115]. After 120 min of ingestion of ALC-containing bread, the insulinemic response was reduced to 2 mU/L (close to the baseline), while that of white bread was about 12 mU/L [4]. Researches also demonstrated that RS5 may have the ability to prevent the development of insulin resistance, an deviant caused by sustained hyperinsulinemia from frequent consumption of foods with high glycemic response [116, 117]. In conclusion, RS5 has benefits to potentially reduce the occurrence of metabolic syndrome, type 2 diabetes, obesity, hypertension, lipid abnormalities, and heart disease, all of which are associated with repeated hyperinsulinemia and insulin resistance [113, 117].

5.2 *Colon Cancer Prevention*

ALC has a potential effect on inhibiting colon cancer cells [109]. Zhao et al. [109] have shown cooked starch with lipid effectively reduced azoxymethane-induced preneoplastic lesions (precursors of colon cancer) in rat colon, providing evidence that ALC may suppress colon carcinogenesis. ALC may cause changes in gene expression in colon cells, which is a possible mechanism for its inhibition of colon cancer in this model system [108]. However, how specific changes in gene expression occur is still unclear [108]. Butyrate, which is produced during the bacterial fermentation in the large intestine with ALC and other carbohydrate as the substrates, has been shown to mediate this process.

Studies described as follows reported the regulation by ALC in the diet on colon cancer. The study selected three groups of 5-week-old male Fischer-344 rats, who received two doses (20 mg/kg body weight) of azoxymethane in 1 week apart, fed with a normal maize starch (NMS) diet until 3 days after the second injection, and then fed with selective diet (NMS, HA7, or RS-5 diet). After the 8-week treatment diet, the pH value and the weight of caecal digest were analyzed; in addition, the occurrence of the mucin-depleted foci (MDF) and aberrant crypt foci (ACF) in the colon, which can reflect the precursor lesions of chemically induced colon cancer, was also analyzed [118, 119]. Compared with those in the other two groups, a lower caecum pH and a significantly larger amount of caecal digesta and were observed in the group fed with RS 5, which may inhibit the growth of pathogenic organisms in the colon. The results showed that the average numbers of both MDF and ACF in the colon were significantly lower in the rats fed with the RS 5 diet. Interestingly, the average number of MDF was significantly lower than those rats fed with NMS and HA7 diets, while the ACF average number showed no significances with other groups [120, 121]. It is worth noting that in this study, no significant differences were found in the average daily food intake and body weight gain among the rats fed with different diets.

In another study using the same animal model and diet, it was found that the amount of feces excreted by the rats fed with RS5 and the starch and fat in the feces were significantly larger than those of other groups fed with fed with NMS and HA7. Gas chromatographic analysis showed that stearic acid (SA) was the main component of lipids extracted from rat feces of the rats fed with RS 5, and the results implied that a proportion of the (PUL-treated HA7)-SA complex product was not digested in the small intestine or fermented in the colon but discharged in the form of starch–lipid complex. The study also showed that 15% (*db*) of the ingested RS5 was not utilized by microorganisms in the digestive tract of rats. Notably, the low digestibility of RS5 did not affect the body weight gain of rats [122].

Two possible mechanisms of RS5 in reducing the amount of MDF in the colon can be concluded from the two *in vivo* rat studies. On the one hand, large amounts of feces are excreted from the colon to remove carcinogen (e.g., the injected AOM). On the other hand, FA in starch–lipid complexes may have the affinity to absorb carcinogens and remove them from colon.

5.3 Encapsulation for the Delivery of Bioactive/ Pharmaceuticals

Bioactive compounds, in the form of fatty acid esters, can be encapsulated in starch by forming ALC. The formation of V-amylose complexes has been demonstrated to improve oxidative stability, reduce volatility, and increase thermal stability, and to modulate the release properties of the flavor compounds. Ma et al. [110] evaluated the formation of amylose, amylopectin, and high-amylose maize starch inclusion

complexes with ascorbyl palmitate, retinyl palmitate, and phytosterol esters and found ascorbyl palmitate resulted in the highest complexation, followed by retinyl palmitate and phytosterol esters. Gökmen et al. [123] showed that the addition of V-amylose reduced the flax seed oil oxidation and the reduction of acrylamide and hydroxymethylfurfural (HMF) levels during the backing process of bread. The single helix structure of high-amylose maize starch was used to entrap menthol, menthone, thymol, pulegone, and terpinen-4-ol, and the complexes showed V-type X-ray diffraction patterns having 29–74% flavor retention [124]. Kim and Huber [125] encapsulated β -carotene into gelatinized corn starch by drop-wise addition, and less than 20% of β -carotene within the composites was degraded during the same period, with oxidation occurring at a much reduced rate.

Starch has potential applications in the delivery of bioactive pharmaceutical and nutrients [126]. Amylose complexes can be used to release the included molecule under pancreatic conditions, although they are not available to mouth and gastric digestion [127, 128]. This application has been confirmed by in vitro experiments with stearic acid and polyunsaturated fatty acids [129]. Besides, nano-encapsulation of conjugated linoleic acid (CLA) has been demonstrated by Lalush et al. [22] and patent application made based on complexes produced by the continuous homogenization method [127].

A recent study by Shi et al. [130] has shown the V-type single helix of granular cold-water-soluble (GCWS) starches can encapsulate ethylene gas, a natural ripener for fruits or vegetables, and show slow release properties at various temperature and relative humidity conditions. The inclusion complexes (IC) of Hylon-7 had the highest ethylene concentration (31.8%, w/w) among the five starches, and the IC of normal potato starch showed the best controlled release characteristics. As a renewable and inexpensive material, GCWS starch is a desirable solid encapsulation matrix with potential in agricultural and food applications.

6 Conclusions

The formation of amylose–lipid complex (ALC) can change many characters of starch, such as the rheological properties, digestibility, and retrogradation. ALC also has a potential role in reducing the risk of chronic diseases such as colon cancer. Additionally, ALC also has application in nano-encapsulation of bioactive or sensitive substances. The application of V-amylose as a fat substitute and protection of sensitive bioactive molecules, flavor food, and pharmaceutical ingredients can be further explored in the further.

Acknowledgements This chapter was modified from the paper published by our group in Journal of Food Hydrocolloids, 2013, 32, 365-372. The related contents are re-used with the permission.

References

1. Ai Y, Hasjim J, Jane JL. Effects of lipids on enzymatic hydrolysis and physical properties of starch. *Carbohydr Polym.* 2013;92(1):120–7.
2. Morrison WR, Milligan TP, Azudin MN. A relationship between the amylose and lipid contents of starches from diploid cereals. *J Cereal Sci.* 1984;2(4):257–71.
3. Morrison WR, Law RV, Snape CE. Evidence for inclusion complexes of lipids with V-amylose in maize, rice and oat starches. *J Cereal Sci.* 1993;18(2):107–9.
4. Hasjim J, Lee SO, Hendrich S, Setiawan S, Ai YF, Jane J. Characterization of a novel resistant-starch and its effects on postprandial plasma-glucose and insulin responses. *Cereal Chem.* 2010;87(4):257–62.
5. Jane JL, Robyt JF. Structure studies of amylose-V complexes and retrograded amylose by action of alpha amylases, and a new method for preparing amyloextrins. *Carbohydr Res.* 1984;132(1):105–18.
6. Jane JL, Robyt JF, Huang DH. ¹³C-N.M.R. study of the conformation of helical complexes of amyloextrin and of amylose in solution. *Carbohydr Res.* 1985;140(1):21.
7. Jane JL, Craig SAS, Seib PA, Hosoney RC. A granular cold water-soluble starch gives a V-type X-ray diffraction pattern. *Carbohydr Res.* 1986;150(1):c5–6.
8. Jane JL, Craig SAS, Seib PA, Hosoney RC. Characterization of granular cold water-soluble starch. *Starch-Stärke.* 2010;38(8):258–63.
9. Eliasson AC, Ljunger G. Interactions between amylopectin and lipid additives during retrogradation in a model system. *J Sci Food Agric.* 1988;44(4):353–61.
10. Seneviratne HD, Biliaderis CG. Action of α -amylases on amylose-lipid complex superstructures. *J Cereal Sci.* 1991;13(2):129–43.
11. Tufvesson F, Wahlgren M, Eliasson AC. Formation of amylose-lipid complexes and effects of temperature treatment. Part 1. Monoglycerides. *Starch-Stärke.* 2003;55(2):61–71.
12. Eerlingen RC, Delcour JA. Formation, analysis, structure and properties of type III enzyme resistant starch. *J Cereal Sci.* 1995;22(2):129–38.
13. Hasjim J, Ai Y, Jane JL. Novel applications of amylose-lipid complex as resistant starch type 5. In: Shi YC, Maningat CC, editors. *Resistant starch.* Hoboken, NJ: Wiley; 2013. p. 79–94.
14. Holm J, Björck I, Ostrowska S, Eliasson AC, Asp NG, Larsson K, et al. Digestibility of amylose-lipid complexes in-vitro and in-vivo. *Starch-Stärke.* 2010;35(9):294–7.
15. Birt DF, Boylston T, Hendrich S, et al. Resistant starch: promise for improving human health. *Adv Nutr.* 2003;4(6):587–601.
16. Obiro WC, Ray SS, Emmambux MN. V-amylose structural characteristics, methods of preparation, significance, and potential applications. *Food Rev Intl.* 2012;28(4):412–38.
17. Putseys JA, Lamberts L, Delcour JA. Amylose-inclusion complexes: formation, identity and physico-chemical properties. *J Cereal Sci.* 2010;51(3):238–47.
18. Seo TR, Kim JY, Lim ST. Preparation and characterization of crystalline complexes between amylose and C18 fatty acids. *LWT-Food Sci Technol.* 2015;64(2):889–97.
19. Derycke V, Vandeputte GE, Vermeylen R, Man W, Goderis B, Mhij K, et al. Starch gelatinization and amylose-lipid interactions during rice parboiling investigated by temperature resolved wide angle X-ray scattering and differential scanning calorimetry. *J Cereal Sci.* 2005;42(3):334–43.
20. Wulff G, Avgenaki G, Guzman MSP. Molecular encapsulation of flavours as helical inclusion complexes of amylose. *J Cereal Sci.* 2005;41(3):239–49.
21. Becker A, Hill SE, Mitchell JR. Relevance of amylose-lipid complexes to the behaviour of thermally processed starches. *Starch-Stärke.* 2001;53(3–4):121–30.
22. Lalush I, Bar H, Zakaria I, et al. Utilization of amylose-lipid complexes as molecular nanocapsules for conjugated linoleic. *Biomacromolecules.* 2005;6(1):121–30.
23. Gelders GG, Duyck JP, Goesaert H, Delcour JA. Enzyme and acid resistance of amylose-lipid complexes differing in amylose chain length, lipid and complexation temperature. *Carbohydr Polym.* 2005;60(3):379–89.

24. Putseys JA, Derde LJ, Lamberts L, Goesaert H, Delcour JA. Production of tailor made short chain amylose-lipid complexes using varying reaction conditions. *Carbohydr Polym.* 2009;78(4):854–61.
25. Fanta GF, Felker FC, Shogren RL. Formation of crystalline aggregates in slowly-cooled starch solutions prepared by steam jet cooking. *Carbohydr Polym.* 2002;48(2):161–70.
26. Fanta GF, Kenar JA, Felker FC. Nanoparticle formation from amylose-fatty acid inclusion complexes prepared by steam jet cooking. *Ind Crop Prod.* 2015;74:36–44.
27. Meng S, Ma Y, Cui J, Sun DW. Preparation of corn starch-fatty acid complexes by high-pressure homogenization. *Starch-Stärke.* 2015;66(9–10):809–17.
28. Nelles EM, Dewar J, Bason ML, Jrn T. Maize starch biphasic pasting curves. *J Cereal Sci.* 2000;31(3):287–94.
29. D’Silva TV, Taylor JRN, Emmambux MN. Enhancement of the pasting properties of teff and maize starches through wet-heat processing with added stearic acid. *J Cereal Sci.* 2011;53(2):192–7.
30. Wokadala OC, Ray SS, Emmambux MN. Occurrence of amylose-lipid complexes in teff and maize starch biphasic pastes. *Carbohydr Polym.* 2012;90(1):616–22.
31. De PT, Derossi A, Talja RA, Jouppila K, Severini C. Study of starch-lipid complexes in model system and real food produced using extrusion-cooking technology. *Innov Food Sci Emerg Technol.* 2011;12(4):610–6.
32. Kong L, Ziegler GR. Molecular encapsulation of ascorbyl palmitate in preformed V-type starch and amylose. *Carbohydr Polym.* 2014;111:256–63.
33. Nakazawa Y. Effect of annealing on starch? Palmitic acid interaction. *Carbohydr Polym.* 2004;57(3):327–35.
34. Chang F, He X, Huang Q. The physicochemical properties of swelled maize starch granules complexed with lauric acid. *Food Hydrocoll.* 2013;32(2):365–72.
35. Fu Z, Chen J, Luo S-J, Liu C-M, Liu W. Effect of food additives on starch retrogradation: a review. *Starch-Stärke.* 2015;67(1–2):69–78.
36. Eliasson AC, Kare L, editors. *Cereals in breadmaking: a molecular colloidal approach.* New York: Marcel Dekker; 1993.
37. Cornejo-Ramírez YI, Martínez-Cruz O, Del Toro-Sánchez CL, Wong-Corral FJ, Borboa-Flores J, Cinco-Moroyoqui FJ. The structural characteristics of starches and their functional properties. *CyTA-J Food.* 2018;16(1):1003–17.
38. Singh S, Singh N, Isono N, Noda T. Relationship of granule size distribution and amylopectin structure with pasting, thermal, and retrogradation properties in wheat starch. *J Agric Food Chem.* 2010;58(2):1180–8.
39. D’Silva TV. Modification of the paste properties of maize and teff starches using stearic acid. Doctoral dissertation, University of Pretoria; 2011.
40. Eliasson AC, Finstad H, Ljunger G. A study of starch-lipid interactions for some native and modified maize starches. *Starch-Stärke.* 2010;40(3):95–100.
41. Godet MC, Bizot H, Buleon A. Crystallization of amylose-fatty acid complexes prepared with different amylose chain lengths. *Carbohydr Polym.* 1995;27(95):47–52.
42. Gelders GG, Vanderstukken TC, Goesaert H, Delcour JA. Amylose-lipid complexation: a new fractionation method. *Carbohydr Polym.* 2004;56(4):447–58.
43. Karkalas J, Ma S, Morrison WR, Pethrick RA. Some factors determining the thermal properties of amylose inclusion complexes with fatty acids. *Carbohydr Res.* 1995;268(2):233–47.
44. Tufvesson F, Wahlgren M, Eliasson AC. Formation of amylose-lipid complexes and effects of temperature treatment. Part 2. Fatty acids. *Starch-Stärke.* 2003;55(3–4):138–49.
45. Tufvesson F, Eliasson AC. Formation and crystallization of amylose-monoglyceride complex in a starch matrix. *Carbohydr Polym.* 2000;43(4):359–65.
46. Heinemann C, Zinsli M, Renggli A, Escher F, Condepetit B. Influence of amylose-flavor complexation on build-up and breakdown of starch structures in aqueous food model systems. *LWT-Food Sci Technol.* 2005;38(8):885–94.

47. Zabar S, Lesmes U, Katz I, Shimoni E, Biancoped H. Studying different dimensions of amylose-long chain fatty acid complexes: molecular, nano and micro level characteristics. *Food Hydrocoll.* 2009;23(7):1918–25.
48. Eliasson AC, Krog N. Physical properties of amylose-monoglyceride complexes. *J Cereal Sci.* 1985;3(3):239–48.
49. Hinkle ME, Zobel HF. X-ray diffraction of oriented amylose fibers. III. The structure of amylose-n-butanol complexes. *Biopolymers.* 2010;6(8):1119–28.
50. Nuessli J, Sigg B, Condepetit B, Escher F. Characterization of amylose-flavour complexes by DSC and X-ray diffraction. *Food Hydrocoll.* 1997;11(1):27–34.
51. Siswoyo TA, Morita N. Physicochemical studies of defatted wheat starch complexes with mono and diacyl-sn-glycerophosphatidylcholine of varying fatty acid chain lengths. *Food Res Int.* 2003;36(7):729–37.
52. Cui R, Oates CG. The effect of amylose-lipid complex formation on enzyme susceptibility of sago starch. *Food Chem.* 1999;65(4):417–25.
53. Siswoyo TA, Morita N. Thermal properties and kinetic parameters of amylose-glycerophosphatidylcholine complexes with various acyl chain lengths. *Food Res Int.* 2002;35(8):737–44.
54. Tang MC, Copeland L. Analysis of complexes between lipids and wheat starch. *Carbohydr Polym.* 2007;67(1):80–5.
55. Jovanovich G, Anon MC. Amylose-lipid complex dissociation. A study of the kinetic parameters. *Biopolymers.* 1999;49(1):81–9.
56. Jovanovich G, Zamponi RA, Lupano CE, Anon MC. Effect of water content on the formation and dissociation of the amylose-lipid complex in wheat flour. *J Agric Food Chem.* 1992;40(10):1789–93.
57. Fanta GF, Shogren RL, Salch JH. Steam jet cooking of high-amylose starch-fatty acid mixtures. An investigation of complex formation. *Carbohydr Polym.* 1999;38(1):1–6.
58. Villwock VK, Eliasson AC, Silverio J, BeMiller JN. Starch-lipid interactions in common, waxy, ae du, and ae su2 maize starches examined by differential scanning calorimetry. *Cereal Chem J.* 1999;76(2):292–8.
59. Tapanapunnitikul O, Chaiseri S, Peterson DG, et al. Water solubility of flavor compounds influences formation of flavor inclusion complexes from dispersed high-amylose maize starch. *J Agric Food Chem.* 2008;56(1):220–6.
60. Bhosale RG, Ziegler GR. Preparation of spherulites from amylose-palmitic acid complexes. *Carbohydr Polym.* 2010;80(1):53–64.
61. Bhatnagar S, Hanna MA. Extrusion processing conditions for amylose-lipid complexing. *Cereal Chem.* 1994;71(6):587–93.
62. Biliaderis CG, Galloway G. Crystallization behavior of amylose-V complexes: structure-property relationships. *Carbohydr Res.* 1989;189(12):31–48.
63. Biliaderis CG, Page CM, Maurice TJ. Non-equilibrium melting of amylose-V complexes. *Carbohydr Polym.* 1986;6(4):269–88.
64. Buléon A, Delage MM, Brisson J, Chanzy H. Single crystals of V amylose complexed with isopropanol and acetone. *Int J Biol Macromol.* 1990;12(1):25–33.
65. Tufvesson F, Wahlgren M, Eliasson AC. Formation of amylose-lipid complexes and effects of temperature treatment. Part 1. Monoglycerides. *Starch-Starke.* 2003;55(2):61–71.
66. Yotsawimonwat S, Sriroth K, Kaewvichit S, Piyachomkwan K, Jane JL, Sirithunyalug J. Effect of pH on complex formation between debranched waxy rice starch and fatty acids. *Int J Biol Macromol.* 2008;43(2):94–9.
67. Anil G, Harold C. Effect of hydroxypropyl β -cyclodextrin on physical properties and transition parameters of amylose-lipid complexes of native and acetylated starches. *Food Chem.* 2008;108(1):14–22.
68. Tian Y, Yang N, Li Y, Xu X, Zhan J, Jin Z. Potential interaction between β -cyclodextrin and amylose-lipid complex in retrograded rice starch. *Carbohydr Polym.* 2010;80(2):581–4.

69. Zhang G, Hamaker BR. Starch-free fatty acid complexation in the presence of whey protein. *Carbohydr Polym.* 2004;55(4):419–24.
70. Mantzari G, Raphaelides SN, Exarhopoulos S. Effect of sorbitol addition on the physico-chemical characteristics of starch-fatty acid systems. *Carbohydr Polym.* 2010;79(1):154–63.
71. Tester R, Morrison W. Swelling and gelatinization of cereal starches. I. Effects of amylopectin, amylose and lipids. *Cereal Chem.* 1990;67:551–7.
72. Biliaderis CG, Tonogai JR. Influence of lipids on the thermal and mechanical properties of concentrated starch gels. *J Agric Food Chem.* 1991;39(5):833–40.
73. Mira I, Villwock VK, Persson K. On the effect of surface active agents and their structure on the temperature-induced changes of normal and waxy wheat starch in aqueous suspension. Part II: A confocal laser scanning microscopy study. *Carbohydr Polym.* 2007;68(4):637–46.
74. Eliasson AC, Larsson K, Mieziš Y. On the possibility of modifying the gelatinization properties of starch by lipid surface coating. *Starch-Stärke.* 1981;33(7):231–5.
75. Galloway GI, Biliaderis CG, Stanley DW. Properties and structure of amylose-glycerol monostearate complexes formed in solution or on extrusion of wheat flour. *J Food Sci.* 1989;54(4):950–7.
76. Ghiasi K, Varrianomarston E, Hosney RC. Gelatinization of wheat starch. II. Starch-surfactant interaction. *Cereal Chem.* 1982;59(2):86–8.
77. Larsson K. Inhibition of starch gelatinization by amylose-lipid complex formation. *Starch-Stärke.* 1980;32(4):125–6.
78. Lonkhuysen HV, Blankestijn J. Influence of monoglycerides on the gelatinization and enzymatic breakdown of wheat and cassava starch. *Starch-Stärke.* 1976;28(7):227–33.
79. Hoover R, Hadziyev D. Characterization of potato starch and its monoglyceride complexes. *Starch-Stärke.* 1981;33(9):290–300.
80. Eliasson AC, Carlson LG, Larsson K. Some effects of starch lipids on the thermal and rheological properties of wheat starch. *Starch-Stärke.* 1981;33(4):130–4.
81. Melvin MA. The effect of extractable lipid on the viscosity characteristics of corn and wheat starches. *J Sci Food Agric.* 2010;30(7):731–8.
82. Raphaelides SN, Georgiadis N. Effect of fatty acids on the rheological behaviour of maize starch dispersions during heating. *Carbohydr Polym.* 2006;65(1):81–92.
83. Kugimiya M, Donovan JW, Wong RY. Phase transitions of amylose-lipid complexes in starches: a calorimetric study. *Starch-Stärke.* 1980;32(8):265–70.
84. Biliaderis CG, Page CM, Slade L, Sirett RR. Thermal behavior of amylose. *Carbohydr Polym.* 1985;5(5):367–89.
85. Biliaderis CG, Page CM, Maurice TJ. On the multiple melting transitions of starch/monoglyceride systems. *Food Chem.* 1986;22(4):279–95.
86. Snape CE, Morrison WR, Marotvaler MM, Karkalas J, Pethrick RA. Solid state ^{13}C NMR investigation of lipid ligands in V-amylose inclusion complexes. *Carbohydr Polym.* 1998;36(2–3):225–37.
87. Raphaelides S, Georgiadis N. Effect of fatty acids on the rheological behaviour of amylo maize starch dispersions during heating. *Food Hydrocoll.* 2008;41(1):75–88.
88. Ing NK. Influence of food emulsifiers on pasting temperature and viscosity of various starches. *Starch-Stärke.* 1973;25(1):22–7.
89. Navarro AS. Modelling of rheological behaviour in starch-lipid systems. *LWT-Food Sci Technol.* 1996;29(7):632–9.
90. Singh J, Singh N, Saxena SK. Effect of fatty acids on the rheological properties of corn and potato starch. *J Food Eng.* 2002;52(1):9–16.
91. Gelders GG, Goesaert H, Delcour JA. Amylose-lipid complexes as controlled lipid release agents during starch gelatinization and pasting. *J Agric Food Chem.* 2006;54(4):1493–9.
92. Raphaelides SN. Rheological studies of starch-fatty acid gels. *Food Hydrocoll.* 1993;7(6):479–95.

93. Richardson G, Langton M, Bark A, Hermansson AM. Wheat starch gelatinization-the effects of sucrose, emulsifier and the physical state of the emulsifier. *Starch-Starke*. 2003;55(3–4):150–61.
94. Chang F, He X, Fu X, Huang Q, Jane JL. Effects of heat treatment and moisture contents on interactions between lauric acid and starch granules. *J Agric Food Chem*. 2014;62(31):7862–8.
95. Blazek J, Copeland L. Pasting and swelling properties of wheat flour and starch in relation to amylose content. *Carbohydr Polym*. 2008;71(3):380–7.
96. Nuessli J, Conde-Petit B, Trommsdorff UR, Escher F. Influence of starch flavour interactions on rheological properties of low concentration starch systems. *Carbohydr Polym*. 1995;28(2):167–70.
97. Conde-Petit B, Escher F. Gelation of low concentration starch systems induced by starch emulsifier complexation. *Food Hydrocoll*. 1992;6(2):223–9.
98. Conde-Petit B, Escher F. Complexation induced changes of rheological properties of starch systems at different moisture levels. *J Rheol*. 1995;39(39):1497–518.
99. Byars JA, Fanta GF, Felker FC. Rheological properties of starch-oil composites with high oil-to-starch ratios. *Cereal Chem*. 2011;88(3):260–3.
100. Czuchajowska Z, Sievert D, Pomeranz Y. Enzyme-resistant starch. IV. Effects of complexing lipids. *Cereal Chem*. 1991;68(5):241–6.
101. Gudmundsson M. Effects of an added inclusion-amylose complex on the retrogradation of some starches and amylopectin. *Carbohydr Polym*. 1992;17(4):299–304.
102. Sievert D, Wursch P. Thermal behavior of potato amylose and enzyme-resistant starch from maize. *J Appl Phys*. 1993;75(5):2502–6.
103. Tufvesson F, Skrabanja V, Björck I, Elmstahl HL, Eliasson AC. Digestibility of starch systems containing amylose-glycerol monopalmitin complexes. *LWT-Food Science and Technology*. 2001;34(3):131–9.
104. Wang S, Wang J, Yu J, Wang S. Effect of fatty acids on functional properties of normal wheat and waxy wheat starches: a structural basis. *Food Chem*. 2016;190:285–92.
105. Purhagen JK, Sjö ME, Eliasson A-C. The anti-staling effect of pre-gelatinized flour and emulsifier in gluten-free bread. *Eur Food Res Technol*. 2012;235(2):265–76.
106. Fuenteszaragoza E, Riquelmenavarrete MJ, Sánchezzapata E, Pérezálvarez JA. Resistant starch as functional ingredient: a review. *Food Res Int*. 2010;43(4):931–42.
107. Lau E, Zhou W, Henry CJ. Effect of fat type in baked bread on amylose-lipid complex formation and glycaemic response. *Br J Nutr*. 2016;115(12):2122.
108. Zhao Y, Ai Y, Li L, Jane JL, Hendrich S, Birt DF. Inhibition of azoxymethane-induced preneoplastic lesions in the rat colon by a stearic acid complexed high-amylose cornstarch using different cooking methods and assessing potential gene targets. *J Funct Foods*. 2014;6(1):499–512.
109. Zhao Y, Hasjim J, Li L, Jane JL, Hendrich S, Birt DF. Inhibition of azoxymethane-induced preneoplastic lesions in the rat colon by a cooked stearic acid complexed high-amylose cornstarch. *J Agric Food Chem*. 2011;59(17):9700.
110. Ma UVL, Floros JD, Ziegler GR. Formation of inclusion complexes of starch with fatty acid esters of bioactive compounds. *Carbohydr Polym*. 2011;83(4):1869–78.
111. Ai Y, Zhao Y, Nelson B, Birt DF, Wang T, Jane JL. Characterization and in vivo hydrolysis of amylose-stearic acid complex. *Cereal Chem*. 2014;91(5):466–72.
112. Kawai K, Takato S, Sasaki T, Kajiwara K. Complex formation, thermal properties, and in-vitro digestibility of gelatinized potato starch-fatty acid mixtures. *Food Hydrocoll*. 2012;27(1):228–34.
113. Takase S, Goda T, Watanabe M. Monostearoylglycerol-starch complex: its digestibility and effects on glycemic and lipogenic responses. *J Nutr Sci Vitaminol*. 1994;40(1):23.
114. Cryer PE. Symptoms of hypoglycemia, thresholds for their occurrence, and hypoglycemia unawareness. *Endocrinol Metab Clin N Am*. 1999;28(3):495–500.

115. Weinger K, Jacobson AM, Draelos MT, Finkelstein DM, Simonson DC. Blood glucose estimation and symptoms during hyperglycemia and hypoglycemia in patients with insulin-dependent diabetes mellitus. *Am J Med.* 1995;98(1):22–31.
116. Byrnes SE, Miller JC, Denyer GS. Amylopectin starch promotes the development of insulin resistance in rats. *J Nutr.* 1995;125(6):1430.
117. Higgins JA. Resistant starch: metabolic effects and potential health benefits. *J AOAC Int.* 2004;87(3):761.
118. Arakaki J, Suzui M, Morioka T, Kinjo T, Kaneshiro T, Inamine M, et al. Antioxidative and modifying effects of a tropical plant *Azadirachta indica* (Neem) on azoxymethane-induced preneoplastic lesions in the rat colon. *Asian Pac J Cancer Prev.* 2006;7(3):467–71.
119. McLellan EA, Medline A, Bird RP. Sequential analyses of the growth and morphological characteristics of aberrant crypt foci: putative preneoplastic lesions. *Cancer Res.* 1991;51(19):5270–4.
120. Kleessen B, Stoof G, Proll J, Schmiel D, Noack J, Blaut M. Feeding resistant starch affects fecal and cecal microflora and short-chain fatty acids in rats. *J Anim Sci.* 1997;75(9):2453.
121. Silvi S, Rumney CJ, Cresci A, Rowland IR. Resistant starch modifies gut microflora and microbial metabolism in human flora-associated rats inoculated with faeces from Italian and UK donors. *J Appl Microbiol.* 1999;86(3):521.
122. Hasjim J, Ai Y, Jane J-L. Novel applications of amylose-lipid complex as resistant starch Type 5. In: Shi Y-C, Maningat CC, editors. *Resistant starch: Sources, applications and health benefits.* Hoboken, NJ: Wiley; 2013. p. 79.
123. Gökmen V, Mogol BA, Lumaga RB, Fogliano V, Kaplun Z, Shimoni E. Development of functional bread containing nanoencapsulated omega-3 fatty acids. *J Food Eng.* 2011;105(4):585–91.
124. Yeo L, Thompson DB, Peterson DG. Inclusion complexation of flavour compounds by dispersed high-amylose maize starch (HAMS) in an aqueous model system. *Food Chem.* 2016;199:393–400.
125. Kim J-Y, Huber KC. Preparation and characterization of corn starch- β -carotene composites. *Carbohydr Polym.* 2016;136:394–401.
126. Lesmes U, Barchechath J, Shimoni E. Continuous dual feed homogenization for the production of starch inclusion complexes for controlled release of nutrients. *Innov Food Sci Emerg Technol.* 2008;9(4):507–15.
127. Shimoni E, Lesmes U, Ungar Y. Non-covalent complexes of bioactive agents with starch for oral delivery. *US Patent Application.* 2009; No. 12/298,162.
128. Cohen R, Orlova Y, Kovalev M, Ungar Y, Shimoni E. Structural and functional properties of amylose complexes with genistein. *J Agric Food Chem.* 2008;56(11):4212–8.
129. Lesmes U, Cohen SH, Shener Y, Shimoni E. Effects of long chain fatty acid unsaturation on the structure and controlled release properties of amylose complexes. *Food Hydrocoll.* 2009;23(3):667–75.
130. Cohen R, Schwartz B, Peri I, Shimoni E. Improving bioavailability and stability of genistein by complexation with high-amylose corn starch. *J Agric Food Chem.* 2011;59(14):7932.

Phase Transitions of Starch and Molecular Mechanisms



Shujun Wang, Chen Chao, Shiqing Huang, and Jinglin Yu

Abstract Starch is a macro-constituent and the most important glycemic carbohydrate of many cereal-based foods. Gelatinization and retrogradation are two major phase transitions that determine the susceptibility of starch to enzymatic digestion and its functional properties for food processing and storage. The molecular mechanisms and measurements of phase transitions, and factors influencing starch gelatinization and retrogradation, have been studied extensively to better understand how these processes affect the quality and nutritive properties of starchy foods. This chapter provides a comprehensive review of starch gelatinization and retrogradation, including the definition of the processes and molecular mechanisms of how they occur, as well as measurement methods and influencing factors. The review also discusses the effect of gelatinization and retrogradation on the *in vitro* enzyme digestibility of starch.

Keywords Amylose · Amylopectin · Starch gelatinization · Starch retrogradation · Starch digestibility · Measurement methods

1 Introduction

The functionality of starch in foods is determined to a large extent by the effects of hydrothermal treatments (heating in the presence of water), usually with the application of shear forces. Under these conditions, starch granules swell and lose their crystallinity and molecular organization in a process known as gelatinization. With continued heating and the application of shear, the gelatinized starch forms a paste containing starch polymer molecules dispersed among swollen granules and granule fragments. On cooling, the gelatinized starch undergoes retrogradation (or recrystallization), with the starch molecules re-associating into partially ordered

S. Wang (✉) · C. Chao · S. Huang · J. Yu
State Key Laboratory of Food Nutrition and Safety, Tianjin University of Science and Technology, Tianjin, China
e-mail: sjwang@tust.edu.cn

structures that differ from those in native granules. The rate and extent of gelatinization and retrogradation depend on a multiplicity of factors including the origin, type and concentration of the starch, the temperature, rate and duration of heating, magnitude of shear forces, and temperature, rate, and time for cooling. Interactions between starch and other components of foods can also affect gelatinization and retrogradation [1–13].

This chapter will describe briefly our current understanding of gelatinization and retrogradation and how the thermal transitions measured by differential scanning calorimetry (DSC) relate to starch gelatinization and retrogradation. The chapter will then focus on the mechanism of molecular disassembly of starch granules during these two complicated phase transitions over a wide range of water levels and on the measurement of starch gelatinization and retrogradation and factors affecting them.

2 Definition of Starch Gelatinization and Early Studies

As described above, native starch may be considered as a mixture of linear and highly branched polymers that assemble to form an ordered granular architecture. When heated in excess water, the starch granules undergo an irreversible phase transition, referred to as gelatinization, in which the highly ordered structure is disrupted. Starch gelatinization has been broadly defined as the “collapse (disruption) of molecular orders (breaking of hydrogen bonds) within the starch granule manifested in irreversible changes in properties such as water uptake, granular swelling, crystallite melting, unwinding of double helices, loss of birefringence, starch solubilisation and viscosity development” [14, 15]. On heating, water firstly enters the amorphous regions, which expand and transmit disruptive forces into the crystalline regions [16, 17]. These changes are accompanied by swelling of the granules, which under mixing conditions results in an increase in viscosity before the eventual collapse of the granules to form a paste, if the water content of the system is high enough.

Starch gelatinization has been studied extensively over the past 50 or more years using a variety of approaches including viscometric, microscopic, X-ray diffraction, nuclear magnetic resonance spectroscopy, and enzymatic methods. Early on, viscometric methods were used to study the starch gelatinization behavior, with gelatinization temperature and heat of gelatinization being obtained from consistency curves [18]. Subsequently, a Kofler hot stage microscope with polarized light was widely used to measure starch gelatinization, based on the loss of birefringence of granules [19, 20]. The temperature at which starch granules start to lose birefringence is defined as gelatinization onset temperature. Likewise, the birefringence end temperature (BEPT), when 98% of the starch granules have lost birefringence, is referred to as gelatinization conclusion temperature [21]. The loss of birefringence occurs over a broad temperature range for the whole sample (a BEPT range of 56–64 °C has been measured for 12% starch (w/w) suspensions of wheat and potato starches heated at 1.5 °C/min), whereas individual granules are observed to lose birefringence over a

much smaller temperature range, generally less than 1 °C. In another early approach, a method involving treatment of granules with the enzyme glucoamylase was developed to measure the degree of starch gelatinization [22]. The differences between measuring the loss of birefringence and the glucoamylase methods for determining the starch gelatinization temperature led to the conclusion that techniques based on measuring the loss of birefringence had limitations, especially given the polydisperse nature of starch granules in a particular sample [19].

Although optical microscopy is widely used to study the gelatinization behavior of starch granules, the measurement of gelatinization temperatures is not very accurate, and the energy absorbed during gelatinization is not determined. As a result, for quantitative measurements, DSC, which measures heat released or absorbed by a material during phase transitions or reactions, is considered the technique of choice for the precise determination of gelatinization temperature and energy absorbed by the starch–water systems during gelatinization [23]. DSC can produce a well-defined plot (thermogram) that traces endothermic energy changes during hydrothermal treatment of starch. The transition temperatures are the start temperature (T_s), defined as the inflexion point at which endothermic heat flow starts to deviate from a flat baseline; the onset temperature (T_o), the intersection point of tangents to the thermogram at T_s and the down slope of heat flow; the peak temperature (T_p), the temperature of maximum heat flow; the conclusion temperature (T_c), which is the intersection point of tangents to the trace at the up slope after T_p and an estimate of the baseline; and the end temperature (T_e), the inflexion point at which endothermic heat flow ceases to deviate from a flat baseline. The heat input/enthalpy change (ΔH) is defined as the area under the line drawn from the start temperature to the end temperature (Fig. 1). Plasticization also occurs as water enters the amorphous regions, but the energy changes are small compared to those involved in the melting of crystallites, and hence the endotherm associated with glass transitions is masked [15].

Stevens and Elton [23] first studied the application of DSC to the gelatinization of starch. They studied the DSC profiles of the starch–water system (starch/water ratio 1:2) and the influence of factors such as starch source, granule size, starch damage, and amylose content. Their study indicated that DSC is a useful physicochemical method capable of yielding both qualitative (e.g., nature of water absorption into the granules, effects of damaged starch on thermal behavior) and quantitative (temperature and energy required to gelatinize) data. Subsequently, starch gelatinization has been investigated extensively by DSC in combination with other techniques such as wide-angle X-ray diffraction (WA-XRD), small-angle X-ray scattering (SAXS), ^{13}C nuclear magnetic resonance (NMR), FTIR, and microscopy (light microscopy, electron microscopy, and light transmission) [15–17, 24]. As discussed in the next section, the gelatinization of starch granules is governed by the moisture content and temperature of the system.

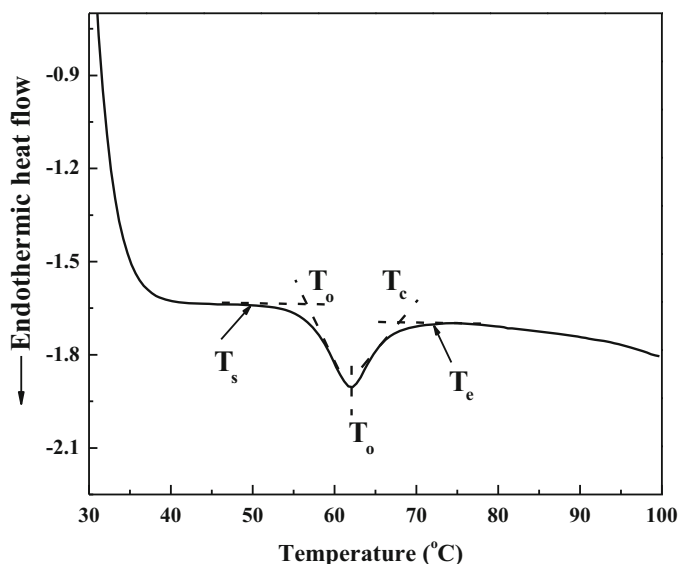


Fig. 1 A typical DSC thermogram of a wheat starch–water system (water:starch = 2:1) with a heating rate of 10 °C/min. The thermal transition temperatures are indicated as T_s , T_o , T_p , T_c , and T_e . Reproduced from [1] with permission from the Royal Society of Chemistry (2013)

3 Effect of Water Content and Temperature on the DSC Profile of Starch

With the application of DSC to characterize starch gelatinization [23, 25], researchers were able to study gelatinization over a wide range of moisture levels. One of the early DSC studies of the effect of water content on gelatinization was by Donovan on potato starch [26]. The endotherm in DSC traces is largely dependent on the water/starch ratio of the systems. At high water concentration (>66 wt% or water/starch ratio > 1.5), a single symmetrical endothermic transition appears in a temperature range of 60–80 °C in the DSC profiles (called endotherm G). As the water/starch ratio is decreased, the magnitude of this endothermic transition decreases progressively, with a concomitant development of a second high-temperature endothermic transition (referred to as endotherm M1). As the water content decreased further (30 wt%), the endotherm G disappears, whereas the endotherm M1 remains but shifts gradually to higher temperatures. Since Donovan's pioneering work, starch gelatinization monitored by DSC, in particular the effect of water content on gelatinization behavior of starch, has been the subject of intensive research. Most subsequent studies [24] have presented results generally similar to those of Donovan's observations (Fig. 2). However, several studies have obtained different DSC profiles of starch granules, for example, a gradual broadening of endotherm G was observed at increasing water/starch ratio above 1.5 for starch granules from peas (Fig. 3) [27] and wheat. These results indicate that Donovan's

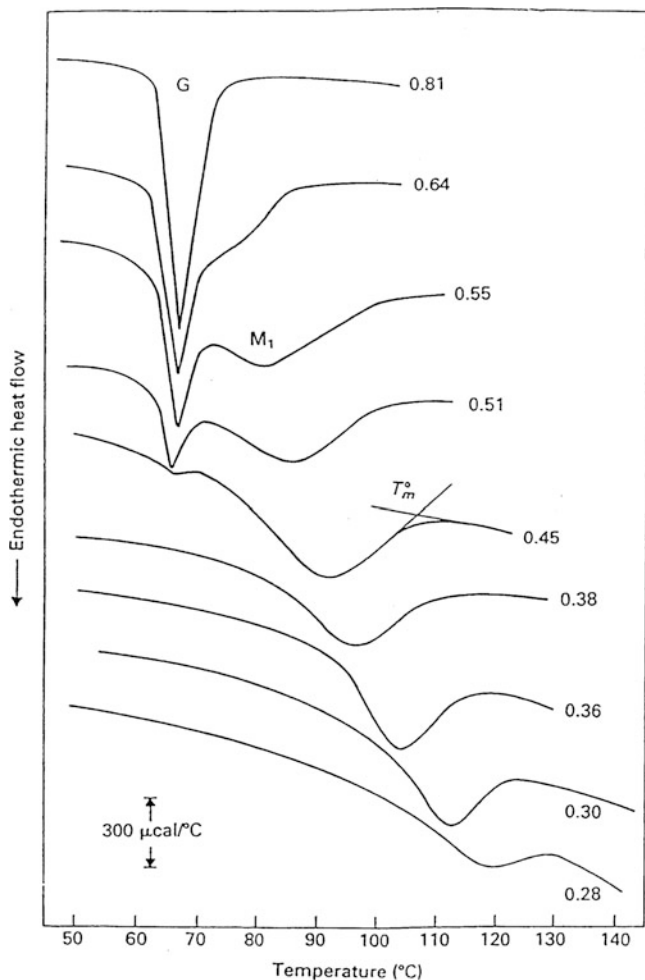


Fig. 2 DSC profiles of potato starch at different water contents (volume fraction of water indicated next to each profile). Heating rate = 10 °C/min. Reproduced from [26] with permission from the Wiley (1979)

conclusions may not provide the full mechanistic explanation for the gelatinization behavior of starch.

In addition to water content, heating conditions and starch source also influence the shape of DSC thermograms of starch–water systems. For example, endotherm G observed at high water/starch ratios does not always disappear as water content is decreased [27–34], and endotherm M1 observed at intermediate water level does not always appear, especially with rapid heating rates (Fig. 4) [27, 28, 35–37]. The rate of heating plays an important role in determining the shape of DSC thermograms of starch–water systems. At intermediate water levels (30–60 wt% moisture),

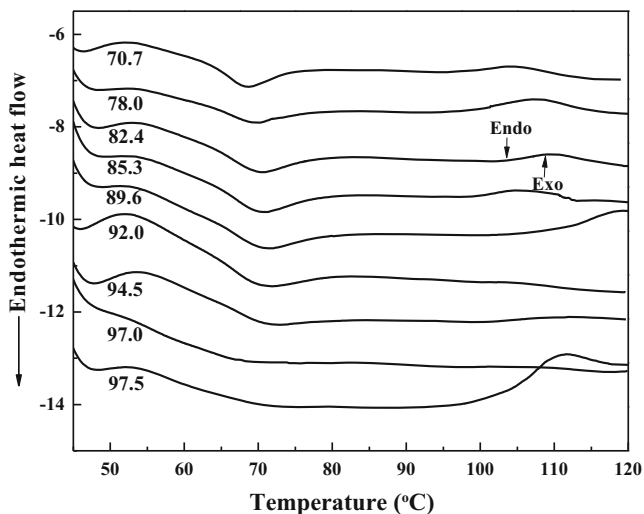


Fig. 3 DSC thermograms of native pea starch in excess water (numbers under each line represent the moisture content in wt%). The heating rate was 10 °C/min. Reproduced from [27] with permission from the American Chemical Society (2012)

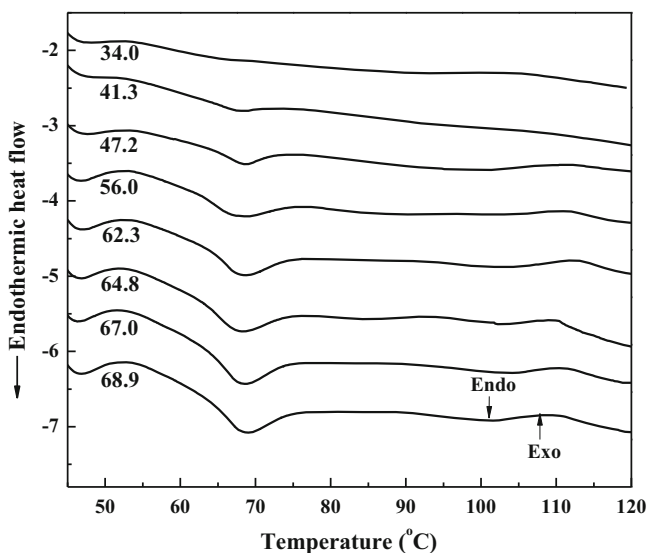


Fig. 4 DSC thermograms of native pea starch in limited water (numbers under each line represent the moisture content in wt%). The heating rate was 10 °C/min. Reproduced from [27] with permission from the American Chemical Society (2012)

increasing the heating rate can result in the gradual convergence of the endotherms G and M1 and eventual disappearance of endotherm M1 [28, 35–38]. In addition to water content and heating rate, the reference (an empty pan or a pan with water or silicon oil), types of DSC pans, and moisture equilibration time prior to heating may also influence the thermograms of starch–water systems [39].

When heated to higher temperatures, the DSC thermogram of starch–water mixtures may display multiple endothermic and exothermic transitions rather than only G and/or M1, especially for low-water content systems (<30 wt%). An additional transition that may occur is the endotherm M2, often observed at 95–125 °C with normal cereal starches. This endotherm has been attributed to the phase transition of amylose–lipid complexes [33, 40–44]. However, the M2 endothermic transition was also observed with waxy maize starches and referred to as endotherm Z [45], which was assumed not to be related to the phase transition of amylose–lipid complex due to the low amount of amylose in waxy starches. Rather, it was considered to be related in some way to the M1 endotherm and attributed to the annealing of amylopectin crystallites during heating [45–47].

4 Proposed Mechanism of Granule Disassembly During Starch Gelatinization

DSC endothermic transitions have generally been hypothesized to be related to the solvent-assisted melting of starch crystallites. At high water content (water/starch > 1.5 or 2), the single endothermic transition occurring at 50–80 °C has long been assumed to represent the complete gelatinization of starch granules. This assumption originated from DSC data of potato starch [26]. However, there is now considerable experimental evidence that is inconsistent with this assumption. Firstly, swelling of starch granules is incomplete in this amount of water [27, 48–50]. Secondly, some structural order was still present at the end of DSC endothermic transition (i.e., T_c), and that further disruption occurred on further heating beyond T_c , clearly indicating that DSC endotherm obtained at water/starch ratios used in many experiments (2:1 to 4:1) do not represent the complete gelatinization behavior of starch [33, 40, 51–53]. Finally, endotherm G obtained at water/starch 2:1 broadened progressively with increasing water content in the high range of water content (≥ 70 wt%). The peak and conclusion temperatures were observed to increase with increasing water/starch ratios at high water content. Similarly, an increase in enthalpy of endotherm G with increasing water content has also been reported for starches from wheat, rice, potato, legumes, and maize [27, 34, 37, 54–59]. According to these findings, Wang and Copeland [27] concluded that at water/starch ratio of 2:1, the single DSC endotherm reflects the partial swelling of starch granules rather than their complete gelatinization. The gradual broadening of the endotherm G in the high range of water content from 65 to 96.7% (water/starch ratio of 1.5:1 to 25:1) reflects the changes from limited swelling to maximum swelling of starch granules (mainly amylopectin

molecules) and partial dissolution of starch polymers (mainly amylose molecules). Endothermic transitions of different types of starch granules were observed over a wide range of water/starch ratios in the DSC to reflect different aspects of the swelling behavior. For wheat and pea starches, endotherm G reflects the change from limited swelling to maximum swelling with partial leaching of starch polymer molecules. For potato and waxy starches with very high swelling power, endotherm G only reflects swelling of starch granules. However, the swelling behavior of high-amylose starch during DSC heating is not as easily characterized [60]. In addition, a recent study has shown that the gelatinization endotherm involves not only the initial water uptake and swelling of amorphous regions in starch granules (within T_p) but also the melting of starch crystallites (beyond T_p) [51]. At low water content (<34 wt %), the single high-temperature DSC endotherm M1 is assumed to be related to the true melting of starch crystallites (i.e., without the assistance of water). Heating starch at low moisture for prolonged times leads to pyrodextrinization.

The nature of the biphasic endothermic G and M1 transitions of starch–water systems at medium water content (34–66 wt%) has been the subject of extensive research, leading to the proposal of several models to interpret experimental observations. Firstly, a swelling-driven melting theory was proposed by Donovan [26], who argued that the gelatinization of a starch–water system occurs initially in amorphous regions of the granule. The first G endotherm was suggested to result from the swelling-driven crystalline disruption, in which the swelling of the amorphous regions is considered to “strip” polymer chains from the surface of crystallites, while the M1 endotherm represents the melting of the remaining, less hydrated crystallites. A second, crystallite stability model, proposed by Evans and Haisman [61], considers starch granules to consist of crystallites of variable stability. According to this second model, the biphasic endotherm represents the progressive melting of crystallites with increasing stabilities: the less stable crystallites are melted first in sufficient water, followed by the true melting of remaining more stable crystallites in the absence of free water. This model has been supported by subsequent studies [29, 56, 62, 63]. A third model, proposed by Nakazawa et al. [64] and Slade and Levine [65], has been referred to as the sequential phase transition model. The G endotherm is considered to reflect primarily plasticization in amorphous regions, whereas the M1 endotherm reflects non-equilibrium melting of crystallites. A fourth, three-stage phase transition model proposed by Biliaderis et al. [37] suggested that the biphasic transitions in DSC thermograms taken at medium water content represent, in turn, partial melting, recrystallization, and final melting. According to this model, starch as a semicrystalline material is thought to undergo reorganization during heating in DSC experiments, similar to the process of annealing. As a result, starch granules are proposed to undergo a partial melting of crystallites followed by the reorganization of remaining crystallites, and the final melting of reorganized crystallites at higher temperature, which occurs in the course of two endotherms G and M [37].

Although these models are all reasonable, they are based solely on the interpretation of DSC data without taking structural changes into account. Based on SAXS, WA-XRD, dynamic mechanical analysis, and NMR data on structural changes

during heating a dilute starch–water system, Waigh, Gidley, Komanshek, and Donald [66] proposed a novel interpretation of Donovan’s results. Their approach was based on the assumption that hydrated amylopectin has a similar structure to that of a branched side-chain liquid-crystalline polymer of a smectic or nematic type. At excess water conditions (>66 wt% water), a two-stage process involved in starch gelatinization occurs, namely, a slow smectic-nematic/isotropic transition followed by the fast helix-coil transition (Fig. 5a). At intermediate water conditions (34~66 wt % water), the first endotherm G is associated with the smectic-nematic/isotropic transition and the second M1 corresponding to the helix-coil transition. At low water level (<34 wt% water), a direct transition from glassy nematic/isotropic to amorphous state occurs at elevated temperature (Fig. 5b).

5 Exothermic Transitions of Starch–Water Systems

The DSC profiles of starch–water systems have been proposed to also contain some exothermic transitions. The first proposed and widely accepted exothermic transition is related to the phase transition of amylose–lipid complexes [44]. This exothermic transition, which is usually observed to overlap with the preceding adjacent endotherm, has been attributed to the formation of the amylose–lipid complex [33, 40].

Hence, the exothermic transition was assumed to be related to the crystallization of amylose–lipid complexes by two possible mechanisms: (a) aggregation of leached amylose–lipid complexes present in native starch into Vh orthorhombic crystalline packing and (b) in situ crystallization of leached (solubilized) amylose in the presence of available endogenous lipids (Fig. 6) [33]. Recently, Wang and Copeland [27] concluded, from studies on the effect of water content on swelling power and solubility of pea starch granules, that the recrystallization of leached amylose–lipid complexes seems implausible at water/starch ratios of 1.5 to 2:1, since no amylose leaches out of the granules under these conditions. Hence, the annealing of amorphous type I amylose–lipid complexes according to mechanism (b) may contribute to the exothermic transition during DSC heating. However, the gradual development of the V-amylose pattern could also be caused by the gradual disappearance of predominant crystalline diffraction peaks of native starch crystals, which may have masked the presence of V-amylose contribution in native starch, rather than the crystallization of amylose–lipid complexes. In the study of pea starch granules, the exothermic transition could not be related to the crystallization of amylose–lipid complexes due to the tiny amount of lipid (0.04~0.08%) present in pea starch and the similarity of the DSC thermograms of native and defatted pea starch. Hence, the exothermic transition observed for all of the pea starch–water systems was explained to represent the phase transition due to the condensation of water from vapor to liquid [27, 49]. Wang et al. [60] proposed that this phase transition occurs by the following mechanisms. Firstly, water is absorbed into the granules, causing them to swell and giving rise to endotherm G. With increasing temperature, the liquid water molecules redistribute in the swollen granules, concomitant with ongoing melting of

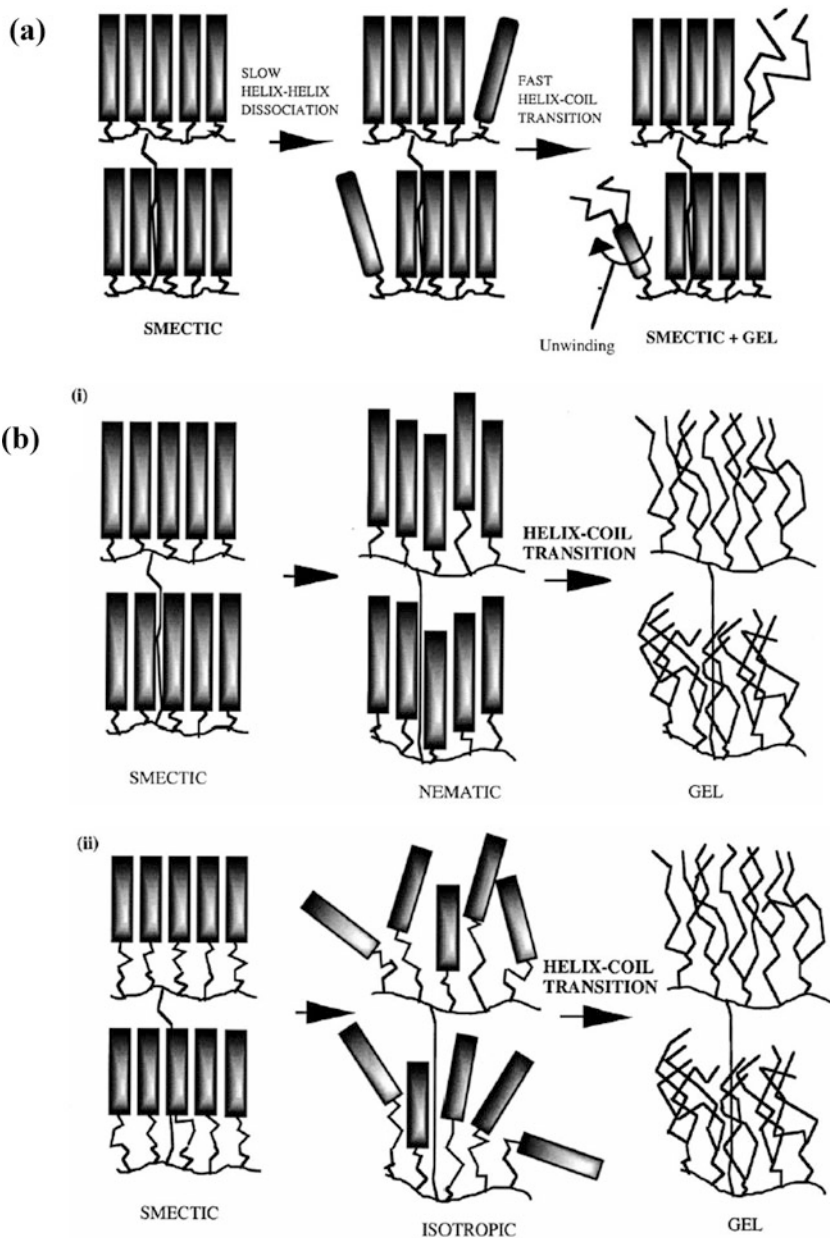


Fig. 5 The molecular disassembly of starch granules during gelatinization in excess water (a) and in limiting water (b). (i) represents the molecular disassembly of B-type starch; (ii) represents the molecular disassembly of A-type starch. Reproduced from [66] with permission from the Wiley (2000)

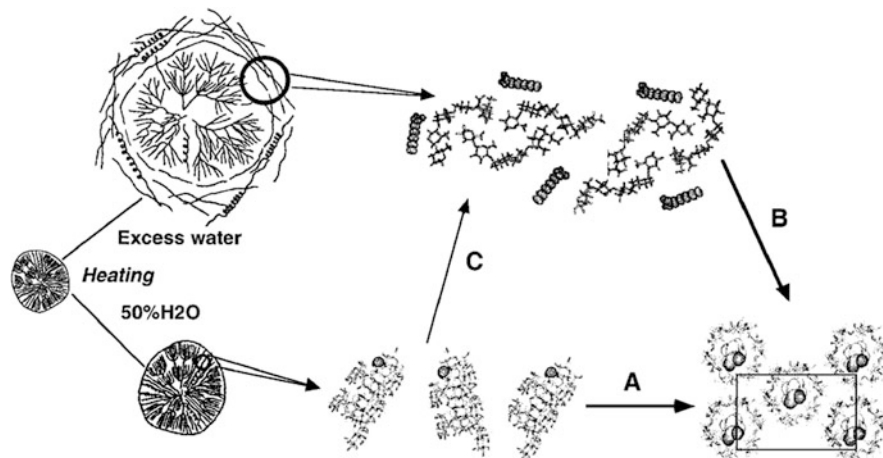


Fig. 6 Possible mechanisms involved in the crystallization of amylose–lipid complexes upon heating: (A) at low and intermediate water contents (low swelling and leaching), packing of isolated inclusion complexes pre-existing in native starch granules into V_h orthorhombic crystalline form; (B) in excess water (high swelling and leaching), crystallization of solubilized amylose in the presence of lipids; and (C) in excess water, possible melting of single inclusion complexes present in native starch before crystallization. Reproduced from [32] with permission from the Wiley (1999)

residual crystallites, before the water molecules vaporize and escape from the starch gel. The condensation of water droplets on the inside of the pan lids results in the DSC exothermic transition.

In DSC studies using a low-temperature gradient, the second endotherm M1 observed at intermediate water content was identified as an exothermic transition following the first endotherm G [34, 52]. In this case, the main endothermic transition G was associated with the melting of crystalline parts of starch granules followed by unwinding of amylopectin double helices [34]. The exothermic transition following the endotherm G was associated with the formation of amorphous hydrogen-bonded network between free ends of unwound amylopectin double helices and other amylopectin branch chains [34, 66] or amylose [52]. At low moisture content, an exothermic transition separating a biphasic M1/M2 endotherm was reported for potato starch. These three combined endotherm and exotherm transitions have been explained in terms of the following sequence of events: (1) melting of B-type crystals, (2) recrystallization into A-type crystallites, and (3) melting of A-type crystallites [67].

6 Measurement of the Extent of Starch Gelatinization

The extent of starch gelatinization is the key factor in determining the digestibility and nutritional properties of starchy foods. As discussed previously, water content and temperature are the two key factors that influence starch gelatinization, with different hydrothermal protocols, as well as the use of stirring, resulting in differences in the extent of starch gelatinization. Various experimental approaches have been developed to estimate the degree of starch gelatinization [68–70]. These include enzymatic measurement of starch degradation, DSC thermograms (particularly enthalpy change), measurement of birefringence using polarized light microscopy, measuring changes in crystallinity by X-ray diffractometry, spin–spin relaxation time in nuclear magnetic resonance (NMR) spectroscopy, and amylose–lipid complex formation. Of these, measuring the susceptibility of the starch to enzymatic hydrolysis and DSC studies are the two used most commonly.

Enzymatic methods have been widely used to determine the extent of gelatinization of starch granules [22, 71–73]. These methods generally involve incubating the starch with α -amylase and/or amyloglucosidase for a fixed time and measuring amount of starch degraded. This approach is based on the assumption of a linear relationship between extent of gelatinization and susceptibility for enzymatic degradation and is thus an indirect method since it does not measure changes in the structure of starch. DSC has become the dominant method for monitoring gelatinization, mainly because of inter-laboratory variations in the conditions for enzymatic hydrolysis and because the assumption of linearity between gelatinization and enzymatic degradation may not be true. Holm et al. [72] have shown that the enzymatic method tends to overestimate extent of gelatinization. And recently, Wang et al. [74] concluded that the extent of structural order is not the key determinant of the *in vitro* enzymatic digestibility of cooked starch.

The various methods to determine the extent of starch gelatinization measure a specific but often different property of the starch. As a result, the extent of gelatinization of the same sample measured by one method may be different from that determined by another method [75]. Moreover, the overall extent of starch gelatinization is an average of the gelatinization behavior of the many starch granules in a sample. Depending on the conditions for hydrothermal processing, a starch sample that is not 100% gelatinized may include granules that are close to the raw state (zero gelatinization), granules in different stages of partial gelatinization, as well as completely gelatinized granules [70]. Even with vigorous processing, remnants of granules (granule ghosts), with only partially disentangled amylopectin clusters, may remain [76].

7 Definition of Starch Retrogradation and Molecular Mechanism

When starch is heated in the presence of water and subsequently cooled, the disrupted amylose and amylopectin chains can gradually reassociate into a different ordered structure in a process termed retrogradation. A schematic representation of changes that occur in a starch–water mixture during heating, cooling, and storage is shown in Fig. 7 [77]. Starch retrogradation is usually accompanied by a series of physical changes such as increased viscosity and turbidity of pastes, gel formation, exudation of water, and increased degree of crystallinity with the appearance of B-type crystalline polymorphs [78]. The rearrangement and association of the outermost short branches of amylopectin (DP about 15) can result in the formation of some B-type polymorphs [79, 80]. Dispersed amylose chains form double-helical associations of 40–70 glucose units through hydrogen bonding [81, 82]. Starch retrogradation is not favored by chains that are too short or too long, with the optimum size range being between about 14 and 24 [83]. The retrogradation of rice starch may be influenced genetically by Wx and SSIIa genes, which are responsible for amylose and amylopectin synthesis, respectively [84].

For nonwaxy starch, retrogradation results in the transformation of a starch paste into a firm gel consisting of a three-dimensional network. Waxy starch pastes on retrogradation form a soft gel which contains aggregates but no network [85]. In general, stronger starch gels are associated with a higher amylose content

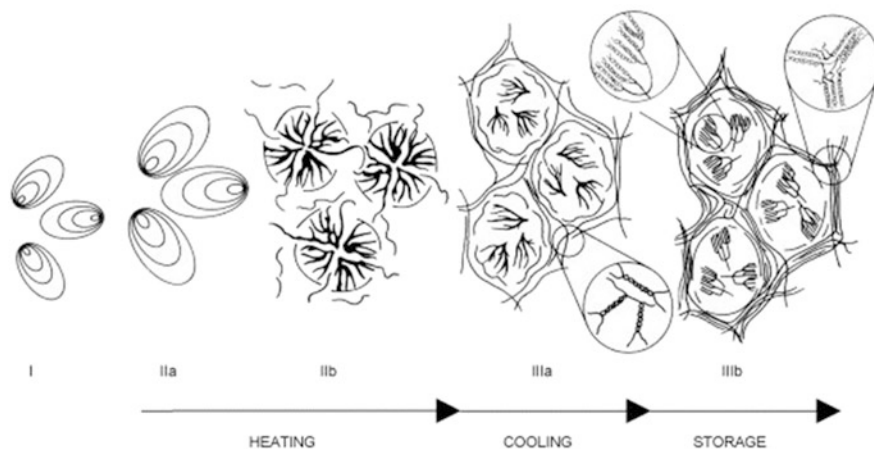


Fig. 7 Schematic representation of changes that occur in a starch–water mixture during heating, cooling, and storage. (I) Native starch granules; (II) gelatinization, associated with swelling [a] and amylose leaching and partial granule disruption [b], resulting in the formation of a starch paste; (III) retrogradation, formation of an amylose network (gelation/amylose retrogradation) during cooling of the starch paste [a] and formation of ordered or crystalline amylopectin molecules (amylopectin retrogradation) during storage [b]. Reproduced from [77] with permission from the Elsevier Ltd. (2005)

[86]. Amylose-based networks are considered to provide starch gels with elasticity and strength against deformation [85, 87], whereas soft gels containing aggregates in the absence of networks display easier penetrability and greater stickiness and adhesiveness. The reduced availability of amylose for intermolecular hydrogen bonding disrupts long-range interactions within the gel, resulting in decreased cohesiveness of the structure.

Retrogradation is an ongoing process, which initially involves rapid recrystallization of amylose molecules followed by a slow recrystallization of amylopectin molecules. Amylose retrogradation determines the initial hardness of a starch gel and the stickiness and digestibility of processed foods. The long-term developments of gel structure and crystallinity of processed starch, which are involved in the staling of bread and cakes, are considered to be due to retrogradation of amylopectin [88–90]. Because of its industrial significance, methods for monitoring starch retrogradation and ways to retard it have been investigated extensively, as will be detailed in the next sections.

8 Methods Used to Study Starch Retrogradation

As starch retrogradation is a complex process involving a series of molecular and physicochemical events, a diversity of physical and chemical methods has been applied to investigate the changes that take place in starch properties. These methods include various thermal, rheological, spectroscopic and chromatographic techniques, X-ray diffraction and scattering, mechanical tests, and microscopic imaging. Additionally, the kinetics of recrystallization of aging gelatinized starch has been modeled using the Avrami equation [91, 92]. These various techniques provide information on specific molecular characteristics or transitions as well as on changes in the material as a whole [93–97]. DSC has proven to be an extremely valuable and sensitive tool to characterize starch retrogradation, although no single method can give a complete picture of retrogradation properties at both macroscopic and molecular levels [96, 98]. The measurement methods are summarized in Table 1 [99].

8.1 Thermal Analysis

When a system is heated, absorption or release of heat or loss of mass usually occurs as a result of phase transitions (such as melting or crystallization) or chemical reactions (e.g., chemical decomposition). The realignment of disrupted amylose and amylopectin molecules to form a partially ordered structure and the exudation of water from starch gels can be monitored by several techniques of thermal analysis, including differential scanning calorimetry (DSC), differential thermal analysis (DTA), and thermogravimetry (TG). DSC is a technique that measures energy changes in a material subjected to programmed heating or cooling. The transition

Table 1 Methods used to measure starch retrogradation

Method types	Techniques	Properties measured
Thermal analysis	DSC	Transition temperatures, enthalpy change (ΔH) of crystallite melting
	DTA	Temperature differences between the sample and a reference during a thermal program
	TGA	The mass loss of the sample
Rheological analysis	RVA	Pasting viscosities during programmed heating and cooling of a starch suspension
	TPA	Hardness, cohesiveness, adhesiveness, elasticity, and brittleness of the viscoelastic sample
Spectroscopic analysis	FTIR	Order in crystalline regions and the state of organization of the double helices localized inside crystallites
Method types	Techniques	Properties measured
	NIR	Molecular changes of starch gel during retrogradation
	Raman	Internal vibrations of molecules;
		continuous measurement of starch retrogradation at the molecular level
	NMR	^1H NMR analyzes the mobility of starch polymer chains ^{13}C CP/MAS NMR investigates molecular organization of starch granule at a shorter distance scale (double helices) and amorphous single chains
X-ray diffraction	WAXD	Long-range ordered structure of starch
	SAXS	Repetitive crystalline and amorphous lamellae
Microscopic analysis	SEM AFM	Surface morphology of starch granules and retrograded starch gels
Physical methods	Turbidity Syneresis	Changes in density distribution of gelatinized starch paste
Other methods	Blue value determination	Retrogradation of amylose during starch retrogradation
	Resistance of starch to hydrolysis	Resistance of starch to enzymatic hydrolysis during retrogradation

Reproduced from [99] with permission from the Wiley (2015)

temperatures (onset, T_o ; peak, T_p ; and conclusion, T_c) and enthalpy change (ΔH) due to crystallite melting or formation of ordered structures can be derived from DSC thermograms. In the case of retrograded starch, the DSC endotherm provides quantitative measures of enthalpy change and transition temperatures for the melting of recrystallized amylopectin [96]. By investigating 14 rice cultivars, researchers suggested that the degree of retrogradation has a positive correlation with the degree of crystallinity and gelatinization temperature it suffered [100]. DTA and TG, which measure, respectively, the difference in temperature between the sample and a reference and the mass loss of a sample as a function of temperature, have been used to study retrogradation of rice starches differing in amylose content [101, 102]. The degree of retrogradation was characterized by measuring the mass

loss of bound water or the differential temperature (ΔT) of gelatinized and retrograded starch samples [101, 102].

8.2 *Rheological Methods*

Development of viscoelastic properties of starch during retrogradation can be monitored using rheological or mechanical techniques to measure large or small deformations. Large deformation tests can be conducted using uniaxial compression, texture profile analysis (TPA), the Brabender Amyloviscograph, or the Rapid Visco Analyzer (RVA). The application of large forces or shearing stresses during measurement causes permanent structural disruption of the material or shear-thinning, making the study of viscoelastic properties of the system difficult. Hence, the results may not reflect the actual changes of the gelatinized starch during retrogradation [103–105]. In many food processing operations, the viscoelastic materials are often subjected to high shear conditions that cause varying degrees of deformation, resulting in nonlinear viscoelastic behavior. To overcome these drawbacks, small deformation dynamic mechanical devices have been developed, which allow the viscoelastic properties to be measured nondestructively. Low-deformation methods include the dynamic oscillatory test, creep compliance/recovery test, and stress relaxation [106–108]. The last two tests are also known as static procedures. The information obtained by small dynamic rheological testing is useful to study gelation mechanisms, molecular interactions during gel formation, and development of gel modulus (resistance to deformation) during aging. To fully understand the viscoelastic properties of starch gels, the combination of two or more methods is usually necessary. However, there have been few studies aimed at correlating information obtained from large and small deformation measurements [96].

Of the rheological methods mentioned, TPA and pasting analysis are the most commonly used to study starch retrogradation in model starch gels and food systems. In a TPA test, the sample is compressed uniaxially, the compressive force is then removed, and the sample is re-compressed. Such a compressive sequence represents 2 “bites.” From the output of the instrument, one is able to measure five primary characteristics of a gel: hardness, cohesiveness, adhesiveness, elasticity (also called springiness), and brittleness (also called fracturability). Moreover, several additional texture characteristics such as gumminess (hardness \times cohesiveness) and chewiness (hardness \times cohesiveness \times springiness) can be derived [109]. In general, starch retrogradation contributes to the increase of hardness and decrease of adhesiveness of cooked rice during storage [110, 111].

The tendency of a gelatinized starch to retrograde can also be studied from its pasting behavior, usually by observing changes in pasting viscosities during programmed heating and cooling of a starch suspension using a Brabender Amyloviscograph or Rapid Visco Analyzer (RVA). From the traces of either of these instruments, five characteristic parameters can be obtained: peak viscosity,

trough viscosity, breakdown viscosity, final viscosity, and setback viscosity. Of these parameters, setback is defined as the difference between final viscosity and trough viscosity, and its magnitude is considered to reflect the retrogradation tendency of amylose in a starch paste. Typically, starch presenting higher setback values has a greater tendency for retrogradation [112].

8.3 Spectroscopic Methods

Vibrational spectroscopy includes several techniques, the most important of which are infrared (IR) and Raman spectroscopy. Both of these complementary techniques are usually required to fully characterize the vibrational modes of a molecule. Although some vibrations may give rise to signals in both the Raman and IR regions of the electromagnetic spectrum, Raman spectroscopy is best at detecting symmetrical vibrations of nonpolar groups, whereas IR spectroscopy is best for asymmetrical vibrations of polar groups [113]. IR and Raman spectroscopy have been used extensively to study the molecular changes during starch retrogradation, as described in the following sections.

IR Spectroscopy The technique of Fourier transform mid-infrared (FTIR) spectroscopy in combination with attenuated total reflectance (ATR) has been used to follow starch retrogradation. The wavelength range from 800 to 1300 cm^{-1} corresponds mainly to C–O and C–C stretching vibrations and is sensitive to changes in polymer conformation and starch hydration [114]. The spectral band at 995 cm^{-1} is very sensitive to water content. Bands at 1047 and 1022 cm^{-1} reflect the amounts of ordered and amorphous regions, respectively [115, 116]. The absorbance ratios of 1047/1022 cm^{-1} and 1022/995 cm^{-1} are assumed to represent, respectively, the order in more crystalline regions and the state of organization of the double helices localized inside crystallites. On retrogradation, the 1047/1022 cm^{-1} and 995/1022 cm^{-1} ratios increase, consistent with an increased organization of structure [117, 118]. Other characteristic bands were also observed to be affected by retrogradation. A weak shoulder at about 2852 cm^{-1} , which overlaps the band for the $-\text{CH}_2$ symmetrical stretching vibration, was observed to increase with retrogradation of normal starch. The increased intensity of this shoulder was attributed to the unwinding of protein [119]. An alternative explanation is that it may be related to the formation of amylose–lipid complex during retrogradation. In addition to the above well-characterized bands, other bands at 1743, 1650, 1537, 1418, 1373, and 1242 cm^{-1} also change as retrogradation progresses, although the reasons for this are not well understood. These bands may be assigned to conjugated carbonyl and carboxyl groups and C–O vibrations [120, 121].

Near-infrared reflectance (NIR) spectroscopy is another technique for acquiring information on molecular changes during retrogradation of gelatinized starch [97, 122, 123]. In a study of retrogradation behavior of rice paste [123], the NIR spectra of rice gels were characterized by small peaks at approximately

10,583–10,383 cm^{-1} and by major peaks at 8871–8655, 7297, 7097, 5430, 5245, and 4474 cm^{-1} . The peak at 10,383 cm^{-1} was attributed to the second overtone of symmetrical and asymmetrical stretching of O–H of water. Absorbances at 8871 and 8655 cm^{-1} are due to the C–H stretching vibration of starch molecules. The peak at 7297 cm^{-1} arises from the C–H stretching vibrations of starch and cellulose molecules, the one at 7097 cm^{-1} from the first overtone of O–H of water. The absorption bands at 5245 and 4474 cm^{-1} are due to the combination of water and C–H stretching and the bending of starch molecules, respectively [122, 124]. These major NIR peaks change with retrogradation, reflecting the molecular modifications of starch and water. However, the relationship between the changes in these NIR spectral bands and structural changes in retrograded starch is not well understood.

Raman Spectroscopy Raman spectroscopy is used widely to probe molecular vibrations that are sensitive to the chemical environment around individual atoms [125]. For starch the characteristic Raman spectral bands at 3200, 2900, 930, and 477 cm^{-1} are associated with amylose and amylopectin molecules. The two most intense spectral bands, at around 480 cm^{-1} and between 2900 and 3100 cm^{-1} , are attributed to vibrations in the pyranose ring of glucose and C–H stretching, respectively. Bands around 860 and 930 cm^{-1} are assigned to the C(1)-H and CH_2 deformations and C–O–C skeletal mode vibrations of the α -1,4 glycosidic linkages. A band at 1127 cm^{-1} is attributed to the contribution of two main vibrational modes, C–O stretching and C–O–H deformation. The vibrational modes that are dependent upon the crystal structure of amylose occur at approximately 1440, 1340, and 1200 cm^{-1} . These bands are associated with a complex of vibrations among CH_2 , C–O–H, and C–C–H [126–129].

Raman spectroscopy is a nondestructive technique that allows continuous measurement of starch retrogradation at the molecular level. Starch retrogradation can be monitored based on the full widths at half-height of peaks (FWHHs), shifts in the position of Raman bands at about 480 cm^{-1} and from the spectral features of the C–H stretching modes between 2800 and 3050 cm^{-1} [130]. The FWHH of the spectral feature of the C–H stretching modes between 2800 and 3050 cm^{-1} and shifts of Raman band at 480 cm^{-1} of potato, maize, and wheat starches varied with the storage time of the gel [130]. Retrogradation of potato starch led to the most remarkable changes in the FWHH at 2900 cm^{-1} and shift of the band at 480 cm^{-1} , whereas wheat starch showed the least changes on retrogradation. In a study of starch retrogradation in maize tortillas [117], the band at 480 cm^{-1} was observed to disappear gradually as retrogradation proceeded. Other bands at 1459, 1127, and 856 cm^{-1} were also observed to decrease in intensity with ongoing retrogradation, although the significance of these changes is not known. Prediction of the retrogradation degree in starch can also base on the combination of MIR and Raman spectroscopy which are more accurate than that based on a single technique [131].

8.4 Nuclear Magnetic Resonance Spectroscopy

Nuclear magnetic resonance (NMR) as an analytical technique can be dated to the mid-twentieth century, when proton nuclear magnetic resonance (^1H NMR) was observed in liquid water and paraffin wax [132, 133]. Subsequently, several other magnetically active nuclei such as ^{13}C , ^{19}F , and ^{31}P were used for the analysis of biological and pharmaceutical compounds and their mixtures [134]. As a noninvasive and nondestructive technique, NMR has become a central analytical method in food science [135], including for the study of starch retrogradation. The most frequently used NMR technique in the study of starch retrogradation is low-resolution ^1H NMR, which is capable of analyzing the mobility of starch polymer chains [136]. The starch molecules in the more mobile liquid (gelatinized) and less mobile solid-like (retrograded) state can be differentiated by the spin–spin relaxation time (T_2). As retrogradation proceeds, the signal attributed to protons in the solid phase of starch gels increases, while the signal from the liquid component decreases [137]. A decrease in the T_2 value for a population of exchangeable protons in a gel network of a crustless crumb stored at 4 °C compared to 23 °C was interpreted as showing that cool storage led to increased strength of the starch network [138, 139]. A decrease in the molecular mobility of the liquid component was observed by decreases in ^{17}O T_2 (the liquid transverse relaxation rate), ^1H D_0 (the rate of H^1 diffusion coefficient), and T_{2A} (the liquid transverse relaxation time). The value for T_{2B} (the solid transverse relaxation time) did not change with concentration or time, indicating that the mobility of the solid component does not change over time despite the conversion of the highly mobile starch fraction to the less mobile solid state during retrogradation [140].

Wu et al. [141] and Wu and Eads [142] studied polymer immobilization during aging of waxy maize starch gels using ^1H nuclear magnetic cross-relaxation spectroscopy. From the normalized amplitude of the liquid ^1H signal (single resonance), the Z-spectrum could be obtained, which is a reflection of immobile protons in the sample. At the same moisture content, different starch samples showed different Z-spectra, indicative of different mobilities of protons in the solid fraction [143]. For example, a narrower line shape is indicative of more mobile protons in the solid phase. An observed increase in the area and width of the Z-spectral line shape for waxy starch gels during aging was dependent on concentration and storage time [142, 143].

High-resolution solid-state ^{13}C NMR has been increasingly applied to the study of starch retrogradation using a special technique referred to as cross-polarization and magic-angle spinning (CP/MAS) NMR spectroscopy. ^{13}C CP/MAS NMR has been used to investigate molecular organization of starch granules at a shorter distance scale than X-ray diffraction and to obtain information on ordered helices and amorphous single chains. The two broad shoulders at 103.2 and 82.4 ppm are assigned to the amorphous domains for C-1 and C-4 [144]. These two domains are generally used to estimate the proportion of amorphous, single, and double-helical material in starch samples. On gelatinization, the increase in intensity of the C-4

resonance at 82 ppm was clearly evident, reflecting the loss of crystalline structure and increase in proportion of amorphous areas. On retrogradation, the intensity of this peak decreased with aging of a starch gel, indicating the development of rigid structures due to the interaction of starch chains. Meanwhile, the double helix content increased with aging of the starch gel [118, 145].

8.5 X-ray Diffraction

X-ray diffraction (XRD) techniques are used widely for phase identification of a crystalline material and to provide information on crystal structure and unit cell dimensions, as reviewed by Blazek and Gilbert [146]. As a semicrystalline material, native starch granules present three distinct X-ray diffraction patterns (A, B, and C) and varying degrees of crystallinity. XRD detects long-range ordered structures involving regular and repeated arrangement of double helices, thereby reflecting the three-dimensional order of starch crystallinity. The technique is less sensitive to irregularly packed structures, small chain aggregates, or isolated single helices [147]. The XRD pattern is an average of many granules, and therefore XRD does not pick up variability between or within granules. The changes in long-range ordered structure of starch gels during retrogradation have been studied extensively by XRD. During gelatinization, the crystalline structure of starch granules is disrupted, which is usually detected by an amorphous halo in the X-ray diffraction patterns of fully gelatinized starch samples. The formation of new crystallites in freeze-dried retrograded starch can be distinguished by XRD [148].

The extent to which crystallites develop and the type of polymorphs formed as a result of retrogradation are influenced by many factors, such as storage temperature, water content of gelatinized starch samples, extent of gelatinization, and amylopectin chain length [118, 149]. In most cases, retrograded starch presents a typical B-type X-ray diffraction pattern, irrespective of whether it was present as A- or B-type polymorphs in its native state [78]. Hellman et al. [150] found that the type of crystals developed in aged cereal starch gels depend on water content. Samples containing more than 43% water presented a B-type pattern on aging, whereas those containing less than 29% moisture gave an A-type pattern. Samples with moisture content of between 29 and 43% displayed a C-type pattern [151]. The development of crystalline polymorphs is also influenced by retrogradation temperature. Storage at low temperature results in the formation of B-type polymorphs, whereas high temperature leads to the formation of A- and V-type polymorphs [152].

Starch retrogradation can also be monitored by small-angle X-ray scattering (SAXS), which is used less often compared to XRD. SAXS measures variations in the distribution of electron density between two phases, such as amorphous and crystalline lamellae or amorphous and crystalline growth rings in starch. The average total thickness of the crystalline and amorphous lamellae can be obtained from the SAXS patterns [146]. When reorganization of a starch gel reaches a sufficient level of ordering, Bragg peaks corresponding to lamellae can be observed

[146, 153]. Retrogradation at low temperature leads to the formation of lamellar peaks of long-range periodicity, but this peak was not observed for starch retrograding at high temperature [152].

8.6 *Measurement of Turbidity and Syneresis*

Turbidity, as measured by absorbance of light at 620 nm, may be used to characterize the retrogradation behavior of dilute starch pastes (<2%, w/w starch). The changes in density distribution due to the aggregation of amylose and/or amylopectin chains reduce the transmission of light [87]. Many studies have shown that there is a rapid increase in the turbidity during the early stage of storage of gelatinized starch dispersions, which remains largely unchanged or increases only slowly after 48 or 72 h storage [154, 155]. The rapid increase in turbidity during the first 24 h reflects the formation of networks, resulting mainly from interactions between AM chains that were leached out of the granules during gelatinization [118, 156]. The changes in turbidity during storage of starch pastes are consistent with rapid retrogradation of amylose [87]. The increase in turbidity of starch pastes during storage has been reported to be affected by factors such as granule swelling, granule remnants, leached amylose and amylopectin, and amylose and amylopectin chain lengths [157].

Syneresis is a process in which a gel contracts on standing and exudes liquid. While syneresis is a physical characteristic of most gels, it can be used to assess the freeze-thaw stability of starch by measuring the water exuded from a gel on standing or after freezing and thawing [158]. Syneresis increases with the number of freeze-thaw cycles, in part due to enhanced amylopectin retrogradation in the starch-rich phase [159]. A low syneresis value on freezing and thawing is indicative of slow retrogradation of starch gels due to strong interactions between dispersed amylose/amylopectin and water molecules [160].

8.7 *Other Methods*

Blue Value Determination Starch can form an inclusion complex with polyiodide ions, which gives rise to a characteristic deep blue color. Amylose content of native starch is often determined colorimetrically from the iodine complexation. In amorphous domains, the conformation of amylose chains appears to be mainly in a single helical state or random coil. Dispersed amylose on retrogradation may form double-helical associations of 40–70 glucose units, which cannot accommodate the iodine. As a result, amylose gradually loses its ability to form a blue complex with iodine if double-helical associations occur between amylose chains on retrogradation. The blue value, which was defined as the absorbance at 635 nm of 10 mg anhydrous starch in 100 mL diluted I₂-KI solution at 20 °C, can be used to monitor the starch

retrogradation progress. As the blue complex is formed mainly with amylose molecules, the blue value determined during starch retrogradation predominantly reflects retrogradation of amylose. According to the blue value, the amount of soluble amylose in cooked starch decreased rapidly with storage time during the first 8 h after cooking and then underwent little change after 24 h at 20 °C [161].

Resistance of Retrograded Starch to Enzymatic Hydrolysis The resistance of starch to enzymatic hydrolysis can be used as a measure of starch retrogradation. The formation of ordered structures such as double helices and/or crystallites as a result of retrogradation increases the resistance of starch to enzymatic hydrolysis [162, 163]. To evaluate the degree of starch retrogradation by enzymatic hydrolysis, the selection of enzymes used for starch digestion is very important. As hydrolytic enzymes differ in specificity and activity towards retrograded starch [96], measures of starch retrogradation will depend on the type and amount of the particular enzymes used. The most commonly used enzymes are pancreatic α -amylase, although *Bacillus subtilis* α -amylase and β -amylase and pullulanase are also used. Heat-stable α -amylase at high temperature is not recommended since under these conditions retrograded starch almost completely hydrolyzed [164]. According to methods developed by Kainuma et al. [165] and Tsuge et al. [166], nondigestible retrograded starch can be determined colorimetrically with iodine after gelatinized starch has been digested by *Bacillus subtilis* α -amylase.

Imaging Methods Microstructures formed by the reassociation of dispersed starch molecules can be distinguished by scanning electron microscopy (SEM) or atomic force microscopy (AFM). For starch gels containing amylose, extended molecular networks containing discrete rod-shaped structures with average dimensions of 52.1 ± 12.4 nm in length, 35.2 ± 6.3 nm in width, and 0.9 ± 0.5 nm in height can be clearly observed by AFM [85]. In contrast, gels of waxy starch and starches mixed with lipids were observed to contain mainly aggregated globular structures with a diameter between 20 and 60 nm and height of 0.5–1 nm under AFM [85].

Retrogradation behavior of starch gels can also be visualized by SEM and TEM images. Upon storage and dehydration, a “cell-wall” structure with fractal-like networks and well-defined pores in the gel can be observed under SEM or TEM [167–170]. The matrix surrounding the pores appears increasingly stronger and thicker with longer storage time. The storage temperature also has important effects on the apparent fractal microstructure of retrograded starch gels, with smaller cavities formed at low temperature than at higher temperatures [168]. This observation was interpreted in terms of lower temperature reducing mobility of water and starch, thus yielding an aggregated structure rather than a globular structure [168]. The average fractal dimensions of the retrograded starch samples increased with storage time. Moreover, a good correlation was found between fractal dimensions and retrogradation enthalpies [167, 168]. In addition to fractal dimensions, the lacunarity (gaps or holes) can also be used as an indicator of the homogeneity of retrograded starch gels. The lacunarity of retrograded maize starch gels increased with storage time and correlated well with the enthalpy of retrogradation [168]. These results indicated that the fractal features extracted from SEM images

of retrograded starch gels can be used to characterize the extent of retrogradation [167, 168].

In summary, probing changes in a sole parameter over time may not provide an adequate description of retrogradation. The methods described for characterizing methods of starch retrogradation measure different events that occur during the reassociation of amylose and amylopectin chains following starch gelatinization. The changes involved may not occur simultaneously. For example, the development of gel modulus during storage can lag behind the formation of crystallites as measured by DSC and X-ray diffraction, depending on starch concentration [79]. The rate of modulus (G') development in aging nonwaxy starch gels is often much faster than the rate of increase of retrogradation enthalpy (ΔH) [107]. Furthermore, retrogradation kinetics determined by different methods on the same sample may not be in agreement [171]. Choosing the appropriate methods to monitor starch retrogradation in food products should depend on the physical and/or chemical characteristics of samples as well as an appreciation of the limitations of the methods.

9 Factors Influencing Starch Retrogradation

Starch retrogradation is mostly taken to be an undesirable process that occurs during the storage of starchy foods. Retardation or inhibition of starch retrogradation is of special interest and a challenge for the food industry and an area where great efforts have been made to study the influencing factors. As discussed subsequently, water content, starch source, and storage conditions are all well-known factors that can greatly influence starch retrogradation. The presence of food components such as lipids, carbohydrates, salts, proteins, or peptides has also been shown to play a significant role in retarding the rate of starch retrogradation.

9.1 Water Content

In the processing and storage of foods, water plays a crucial role in starch gelatinization and retrogradation. The effect of water content on starch gelatinization has been reviewed by Wang and Copeland [1]. The rate and extent of starch retrogradation is also largely dependent on water content. The effect of water content on starch retrogradation, as determined by measuring DSC enthalpy change of recrystallized amylopectin, displayed a parabolic shape, with maximum retrogradation occurring in starch gels at 40–45% water content [172]. However, Jouppila et al. [173] showed that the rate of retrogradation, as determined by the Avrami equation, was independent of water content at high temperature; the half-time for maximum retrogradation was 5.2 days at 60 °C but only 34 min at 80 °C.

The effect of water content on starch retrogradation is influenced by amylose content, which can also affect amylopectin crystallization [174]. When the water content was below 20% or above 90%, no retrogradation was observed by DSC for corn and wheat starch [174, 175]. As the water content was reduced to 80%, retrogradation occurred for nonwaxy corn starch, but was not observed in waxy starch. When the water content was decreased further to 70%, retrogradation occurred for both waxy and nonwaxy starches, with the former exhibiting smaller enthalpies, indicating that the retrogradation of starch is facilitated in the presence of amylose [174, 176, 177]. When the water content was 60%, starch retrogradation was not affected by amylose content [174]. For the low water contents, Wang et al. [178] conclude that enthalpy change of retrograded starch at low water contents involves the melting of recrystallized starch during storage and residual starch crystallites after DSC gelatinization and that the endothermic transition of retrograded starch gels does not fully represent the retrogradation behavior of starch. Very low or high water contents do not favor the occurrence of starch retrogradation.

9.2 Storage Conditions

Temperature and length of storage are the major determinants of the extent of starch retrogradation. In general, retrogradation is rapid initially and then slows down. The onset temperature and enthalpy change for the melting of retrograded starch molecules increase with storage time at constant temperature, whereas the conclusion temperature exhibits little change [118, 149, 179–181]. These observations indicate that longer storage facilitates the formation of more starch crystallites with a higher degree of perfection. As was noted for enthalpy change, the relative crystallinity, double helix content, and the IR absorbance ratio of $1047/1022\text{ cm}^{-1}$ all increase with storage time, indicating the increasing formation of starch crystallites and molecular order [118, 149, 179, 182]. The hardness and springiness of retrograded starch gels increase during the initial stage of storage at a constant temperature but then change only slightly on longer storage [181, 183, 184]. In comparison, holding gels under cycled temperatures of 4/30 °C results in hardness and springiness developing and remaining more or less the same during the whole process [181].

The most common temperature conditions for studying starch retrogradation are isothermal storage at 4, 25, or 30 °C or temperature cycling between 4 and 25 °C (or 30 °C). Generally, the storage of starch gels at 4 °C induces faster crystallization of amylopectin than at 25 or 30 °C. Temperature cycling (4/30 °C) led to smaller melting enthalpy of retrogradation products, higher melting onset temperatures, and lower melting temperature range, compared with isothermal storage at 4 °C, indicating that temperature cycles inhibited the formation of crystallites but enhanced their homogeneity and stability [148, 180]. Similarly, the DSC melting temperature range of waxy potato starch products stored at cycles of 4/25 °C shifted towards lower values compared with storage at 25 °C, indicating that less crystallites are formed during retrogradation under temperature-cycled conditions [179, 185,

[186]. However, in another study, storage at 4 °C resulted in the lowest T_o , T_p , T_c , $T_c - T_o$, and enthalpy change, compared with storage at 25 °C and temperature cycles of 4/25 °C, indicating that storage at 4 °C inhibited generation of crystallites and decreased the perfection of starch crystallites. The cycled temperature (4/30 °C) storage could promote the recrystallization and induce the digestibility than the isothermal storage [187]. Clearly, the type of starch and experimental conditions will influence how starch retrogrades.

9.3 Gelatinization Temperature Range

Previous studies of starch retrogradation rarely considered the initial thermal treatment, but some experiments have shown that heating to various temperatures above the range of gelatinization may profoundly affect amylopectin retrogradation. Keetels [188] discovered that the heating temperature to 70, 90, and 120 °C clearly generated the different rate of retrogradation. This would mainly be caused by further disentanglement of the starch molecules and a more extensive separation of amylose and amylopectin at a higher temperature. Different initial heating temperatures and amylopectin structures can result in different enthalpies of retrogradation for various starch, which may be due to varying extents of residual molecular order in starch materials that are commonly presumed to be fully gelatinized [189, 190]. Liu et al. [191] have investigated the retrogradation behavior after multi-endotherms of the gelatinization of corn starch, such as G, M1, M2, and Z endotherms by DSC. It was found that a certain thermal treatment temperature could affect the residual endotherm above this treatment temperature. The time-dependent retrogradation of corn starch is mainly due to G and M1 endotherms. The temperature and enthalpy of the melting of amylose–lipid complexes M2 and nonlipid complex amylose Z were not affected by aging time. Partial gelatinization of starch on retrogradation can also affect the retrogradation behavior [149], the retrogradation enthalpies of 68 and 70 °C were almost four times as high as that of 64 °C, and the 25 °C and 64 °C had dominant A-type crystalline pattern, while 68 and 70 °C showed dominant B-type crystalline pattern. These results showed that studies of starch retrogradation should take into account the thermal history of the samples even if temperatures are above the gelatinization temperature range.

9.4 Additives

Many additives are used to retard retrogradation of starch in foods independent of storage time or temperature. These additives can be grouped into carbohydrates, salts, amino acids/proteins/peptides, lipids, and other food components such as polyols, polyphenols, emulsifiers, citric acid, and amylase. Table 2 summarizes a large number of studies on the effect of additives on starch retrogradation. The table

Table 2 Methods used to measure starch retrogradation

Additives			Influences
Carbohydrates	Monosaccharides	Glucose	Inhibition of retrogradation of rice, wheat, sweet potato, oat, corn, and tapioca starch
			Increased retrogradation of oat starch
		Ribose	Inhibition of retrogradation of rice and wheat starch
		Fructose	Inhibition of retrogradation of rice, wheat, sweet potato, oat, corn, and tapioca starch
			Increased retrogradation of oat starch
	Oligosaccharides	Sucrose	Inhibition of retrogradation of rice, wheat, sweet potato, oat, corn, acorn, and tapioca starch
			Increased rate of rice starch retrogradation
			Little effect on retrogradation of tapioca starch
		Maltose	Suppressed retrogradation of rice starch
		Lactose	Inhibited pastry crumb retrogradation
		β -Cyclodextrin (β -CD)	Reduced the rate of retrogradation of amylose and normal rice starch, but not waxy rice starch
		Hydroxypropyl- β -CD (HP- β -CD)	More effective than β -CD in retarding retrogradation of high amylose rice starch
		Low molecular weight dextrans	Retarded starch retrogradation
		Malto-oligosaccharides	Inhibition of rice starch retrogradation and retarded bread staling
	Polysaccharides	β -Glucan	Significant inhibition of retrogradation of rice starch
Carboxymethyl cellulose (CMC)		Concentration-dependent inhibition of wheat and sweet potato starch retrogradation	

(continued)

Table 2 (continued)

Additives		Influences
	Tea polysaccharide	More effective than CMC in inhibiting wheat starch retrogradation
	Soya-bean soluble polysaccharide (SSPS)	Increase the short-term (24 h) retrogradation of wheat starch and retarded long-term retrogradation more effectively than GA
	Gum arabic (GA)	Increased short-term (24 h) retrogradation of wheat starch
		Retarded retrogradation of sweet potato starch
	Xanthan gum	Increased retrogradation of wheat starch
		Decreased retrogradation of sweet potato starch and tapioca starch
		No effect on retrogradation of corn and wheat starch amylopectins
		Enhanced short-term retrogradation of tapioca starch but retarded long-term retrogradation
	Pentosans	Water-soluble pentosans slowed the rate of amylopectin retrogradation in wheat starch gels
		Water-insoluble pentosans slowed the rate of retrogradation of both amylose and amylopectin in wheat starch gels
	Locust bean gum	Retarded retrogradation of tapioca, rice, sweet potato starch, and wheat starch
		Increased short-term retrogradation of wheat starch
	Pullulan	Inhibited short-term retrogradation of amylose and long-term retrogradation of amylopectin
	Guar gum	Inhibited the retrogradation of wheat and sweet potato starch

(continued)

Table 2 (continued)

Additives			Influences
			No effect on retrogradation of tapioca starch
		Okra gum	Inhibited the retrogradation of wheat and corn starch
		Corn fiber gum	Inhibited the retrogradation of maize starch
		Pectin	Reduced potato starch retrogradation
		Inulin	Reduced potato starch retrogradation
		Konjac glucomannan	Retarded long-term retrogradation of tapioca, maize, wheat, and potato starch; increased short-term retrogradation of wheat starch
		Tara gum	Increased short-term retrogradation of wheat starch
			Inhibit long-term retrogradation of wheat starch
		Iota-carrageenan	Increased short-term retrogradation in the presence or absence of salts
			Retarded structural ordering during retrogradation
		Alginate	Retarded the retrogradation of sweet potato starch
		Gellan	Retarded the retrogradation of sweet potato starch
		Hydroxypropylmethylcellulose (HPMC)	Decreased the hardening rate of the bread crumb and retarded the amylopectin retrogradation
Salts		Li^+ , Mg^{2+} , and Ca^{2+}	Decreased retrogradation of rice starch
		K^+ and Na^+	Decreased retrogradation of amaranth, corn, wheat, rice, and tapioca starch
Proteins	Soy protein	Soybean 7S globulin	Retarded retrogradation of corn starch
		Soybean 11S globulin	Promoted retrogradation of corn starch

(continued)

Table 2 (continued)

Additives			Influences
		Soy protein isolate (SPI)	Little effect on retrogradation of corn starch
	Wheat protein	Gluten	Retarded retrogradation of wheat starch
			Little effect on wheat starch retrogradation
		Glutenin	Retarded retrogradation of wheat starch
		Albumins, globulins, gliadins	Promoted wheat starch retrogradation
	Soy or pea protein hydrolysates		Retarded maize and corn starch retrogradation
	Amino acids	Alkaline amino acids (Arg and Lys)	Decreased retrogradation of rice, potato, and sweet potato starch
		Acidic amino acids (Asp and Glu)	Increased retrogradation of potato starch
			Decreased retrogradation of sweet potato starch
Lipids		Free fatty acids	Retarded corn and rice starch retrogradation
		Monoglycerides	Reduced waxy corn starch and waxy maize starch retrogradation
		Triglycerides	No effect on starch retrogradation
			Retarded corn and potato starch retrogradation
Other additives	Polyols		Inhibited retrogradation of potato starch
	Polyphenols	Tea polyphenols	Retarded starch retrogradation of rice starch
	Rutin		Retarded retrogradation of normal and high-amylose rice starches
	Amylases		Retarded starch retrogradation or bread staling
	Emulsifiers/surfactants	Cetyltrimethylammonium bromide (CTAB)	Retarded starch retrogradation
		Sodium dodecyl sulfate (SDS)	Retarded starch retrogradation
		Sodium stearyl lactylate (SSL)	Retarded starch retrogradation
	Citric acid		Increased retrogradation of low pH starch gels

Reproduced from [99] with permission from the Wiley (2015)

is included to illustrate the diversity of results, sometimes conflicting, obtained with starches from different sources under different experimental conditions.

Carbohydrates Carbohydrates that are widely used as additives to retard starch retrogradation include monosaccharides such as glucose, ribose, and fructose; oligosaccharides such as sucrose, maltose, and lactose; β -cyclodextrin and hydroxypropyl- β -cyclodextrin; and polysaccharides like crude tea polysaccharide, β -glucan, konjac glucomannan, carboxymethyl cellulose (CMC), soybean-soluble polysaccharide (SSPS), gum arabic (GA), iota-carrageenan, pectin, xanthan gum, and guar gum. In most cases, the addition of carbohydrates can inhibit the extent of retrogradation of starch gels, although exceptions were observed in the presence of sucrose [192]. The extent to which starch retrogradation is inhibited is largely influenced by the type and concentration of carbohydrate. The mechanisms for the inhibition of starch retrogradation are explained in terms of competition for water between starch and the other carbohydrates.

Glucose, ribose, fructose, sucrose, maltose, and water-soluble maltodextrins all can retard starch retrogradation. Many studies have shown disaccharides to be more effective than monosaccharides as inhibitors of starch retrogradation [193–197]. However, in a few cases disaccharides increased the rate of starch retrogradation [198], and sucrose and glucose increased the extent of starch retrogradation [11, 192]. The effect of oligosaccharides on starch retrogradation does not always follow a consistent trend. In some studies, inhibition of starch retrogradation decreased with increasing molecular weight of oligosaccharides [199, 200], although this observation was not noted by others [201, 202].

Inconsistent results have also been reported with monosaccharides. In one study, hexoses (with the exception of galactose) were more effective than pentoses in retarding the retrogradation of starch [195], whereas in another study glucose was less effective than ribose, which almost completely suppressed starch retrogradation [199, 203].

β -Cyclodextrin and hydroxypropyl- β -cyclodextrin, which are used widely in the food, cosmetic, and pharmaceutical industries, have also been used in studies of starch retrogradation. The addition of β -cyclodextrin can retard the short- and long-term retrogradation of amylose-containing starch, which has been attributed to the interaction between amylose and β -cyclodextrin to form an amylose- β -cyclodextrin-lipid complex [204]. β -Cyclodextrin did not retard retrogradation of waxy starch. The extent of retrogradation of normal and high-amylose rice starch decreases with increasing concentration of β -cyclodextrin [204]. Hydroxypropyl β -cyclodextrin was more effective in retarding retrogradation of high-amylose rice starch than was β -cyclodextrin [94]. In another study, hydroxypropyl- β -cyclodextrin increased short-term amylose retrogradation but had little effect on long-term amylopectin retrogradation [205].

Nonstarch hydrocolloidal polysaccharides, particularly guar gum, xanthan gum, and carrageenan and, to a lesser extent, konjac glucomannan, pentosans, gellan, pectin, pullulan, alginate, inulin, okra gum, locust bean gum, corn fiber gum, carboxymethylcellulose, hydroxypropylmethylcellulose, and tea polysaccharide,

have all been studied for their effect on starch retrogradation [17, 206–212]. As pointed out by BeMiller (2011) [17], no general conclusions on the effect of hydrocolloids on starch retrogradation have been reached. The addition of hydrocolloids can increase, decrease, or have no effect on the extent of starch retrogradation, depending on the paste/gel preparation method, storage temperature and time, and measurement techniques of starch retrogradation. In general, hydrocolloids seem to promote short-term retrogradation and retard long-term retrogradation, presumably by primarily affecting amylose–amylose interactions and amylopectin–amylopectin associations, respectively [17]. The addition of CFG (corn fiber gum) was observed that retards the retrogradation of starch gels during long-term storage [213]. The sodium alginate was observed to retard the retrogradation of starch because hydrogen bonding between sodium alginate and amylose molecules restricts the combination of amylose and amylopectin [214]. The inhibition of starch retrogradation by hydrocolloids is largely concentration-dependent.

β -Glucan is a food constituent noted for its thickening, gelling, and stabilizing properties and for its potential beneficial effects on human health [215]. The commonly used β -glucans are from cereals such as barley and oats and also microbial sources including yeast and bacteria. Similar to mono- and oligosaccharides, β -glucans can also significantly retard the retrogradation of rice starch gels during refrigerated storage. Water-soluble oat and barley β -glucans were more effective in retarding starch retrogradation than the insoluble curdlan and yeast β -glucans [215]. The retardation effect on starch retrogradation decreased with increasing ratio of β -glucans to starch [216].

Salts Salt, especially sodium chloride (NaCl), is commonly added to dough formulations at concentrations below 2% (flour basis) in the preparation of cereal-based products, to improve the microstructure, physical characteristics, and sensory properties of the finished products [217–220]. The addition of NaCl during processing or storage can alter greatly the extent of starch gelatinization and retrogradation. In comparison with gelatinization, the effect of NaCl on starch retrogradation has attracted relatively little attention. In the presence of NaCl, the extent of retrogradation is generally decreased when starch gels are stored at 4 or 25 °C [192, 217, 221]. However, the addition of 5% NaCl increased the extent of starch retrogradation of starch gels stored at –20 °C [221].

Proteins/Polypeptides/Amino Acids Proteins are often key components of starchy foods and can play an important role in contributing to their quality and nutrition. Addition of protein to starchy foods has been shown to influence starch retrogradation. Addition of soybean 7S globulin retarded retrogradation and decreased retrogradation enthalpy of corn starch gel. In contrast, addition of soybean 11S globulin promoted starch retrogradation and increased the retrogradation enthalpy. On the other hand, the addition of soy protein isolate had little effect on retrogradation properties of corn starch [222]. Wheat gluten protein has also been investigated but was found to have little effect on the retrogradation of amylopectin [223]. Of the albumin, globulin, gliadin, and glutenin fractions from wheat flour, only glutenin

was reported to retard retrogradation of wheat starch, whereas the other three wheat protein fractions promoted starch retrogradation [224].

Soy and pea protein hydrolysates have also been shown to retard maize starch retrogradation [119, 225], as have free amino acids [226–228]. The addition of the alkaline amino acid arginine decreased syneresis of potato starch, whereas the acidic amino acids aspartate and glutamate increased it [227]. AGCPH (anti-listerial grass carp protein hydrolysate), which can bind with granule remnants and amylopectin, also can reduce the degree of crystallinity and retrogradation of starch [229].

Lipids Lipids are macro-constituents of many cereal and starchy foods. Although a minor component by weight, lipids can have a significant role in determining the properties of starch and starch-based foods. Lipids can interact with starch to form inclusion complexes by entrapment in the amylose helical cavity [230]. The addition of lipids to, or the presence of free lipids in, starch-based food systems generally retard starch retrogradation after food processing followed by storage [231]. For different types of lipids, the shorter the fatty acid chain, the more effective retardation of starch retrogradation [198]. The effect of lipids in retarding starch retrogradation is interpreted in different ways. During starch retrogradation, amylose is more easily retrograded by reassociation into double helices. The addition of lipid in starch–water systems can hinder water penetration into granules and granule swelling and, in turn, amylose leaching during heating. As a result, the mobility of amylose molecules is constrained, resulting in slower amylose retrogradation [232]. Additionally, the formation of amylose–lipid complexes during heating and/or storage could inhibit the cross-linking and formation of double helical structures between amylose molecules, which would also slow their retrogradation. The presence of amylose–lipid complexes could also hinder the crystallization of amylopectin. Lipids have also been proposed to complex with the outer branches of amylopectin and thereby may inhibit starch retrogradation in a more direct way [230, 233–236]. However, there is limited experimental evidence for the interaction between lipids and the outer branches of amylopectin molecules, and hence this proposal needs further investigation for its effect on starch retrogradation.

Other Food Additives With the objective of seeking effective inhibitors of starch retrogradation, other food additives like polyols, polyphenols, emulsifiers, citric acid, and amylase have also been studied for their effect on starch retrogradation. Polyols were shown to inhibit the retrogradation/recrystallization of starch [237]. The GBE (α -1,4-glucan branching enzyme) treatment may restrain retrogradation, which was considered to be the absence of amylose and the abundance of amylopectin with shorter chain length [238]. The effect of maltogenic α -amylase on starch retrogradation has been studied. It inhibited retrogradation of waxy maize starch, which might be due to the fact that a higher proportion of short outer AP chains cannot participate in the formation of double helices [239]. The influence of polyols on starch retrogradation depends on the number of hydroxyl groups, with more hydroxyl groups exhibiting greater effectiveness in retarding the recrystallization of potato starch [194]. The addition of tea polyphenols to rice starch significantly retarded starch retrogradation in a concentration-dependent manner

[240]. Similarly, addition of the flavonoid rutin also greatly retarded the retrogradation of normal and high-amylose rice starches. The retrogradation of normal rice starch was completely inhibited by the addition of rutin, as measured by DSC [241].

Emulsifiers can also retard starch retrogradation and are used as antistaling agents in starchy foods. The addition of sodium dodecyl sulfate, cetyltrimethylammonium bromide (CTAB), and monoglycerides decreased the retrogradation of starch, which was explained as being due to complex formation between amylopectin and the emulsifiers/surfactants [235, 237]. The addition of emulsifiers/surfactants in the dough can significantly delay the firming of breads or cakes [89, 242, 243].

Thermostable amylases are used extensively in commercial bread formulations to retard bread-staling. As reviewed by Fadda et al. [89] and Fu et al. [244], the retardation of bread-staling is considered to be due to the formation of low-molecular-weight dextrans, which reduce the ability of the residual starch to retrograde by interfering in the reassociation of starch chains [245]. The effect of citric acid on starch retrogradation has also been studied. Citric acid increased retrogradation of low-pH starch gels, which was attributed to the promotion of faster reassociation of shorter chains [246].

The overall picture that emerges on the effect of additives on starch retrogradation needs considerable refinement. There are inconsistencies in the literature, which may reflect different experimental materials or conditions. Nevertheless, it seems that agents that compete with starch for water, or reduce the effectiveness of leached amylose to form a gel network, are able to retard or inhibit retrogradation. On the other hand, additives that could facilitate the interaction of amylose and/or amylopectin chains may induce more rapid retrogradation of starch.

10 Conclusions

Starch gelatinization and retrogradation are determined by a combination of variables—the type of starch, the polydispersity of granules, the moisture content of the system, temperature and rate of heating and cooling, and shear forces. Food additives can greatly alter the rate and extent of starch retrogradation, by competition for water with starch or by interfering with the reassociation of starch chains. Although there have been many studies on starch gelatinization and retrogradation, the results usually relate to a specific combination of conditions, making generalizations about functional properties of the products of hydrothermal processing difficult. Many starchy foods have been processed under low moisture conditions, which lead to incomplete gelatinization. Starch processed in this way may contain a complex mixture of granules ranging from minimally to completely disrupted, which can generate a multitude of aggregated starch forms on retrogradation. More studies are needed of gelatinization and retrogradation in low-moisture systems, to increase our understanding of the processing behavior and nutritional properties of starch.

Acknowledgment The authors gratefully acknowledge the financial support from the National Natural Science Foundation of China (31871796) and Natural Science Foundation of Tianjin City (17JCQJC45600). This chapter was modified from the papers published by our group in Comprehensive Reviews in Food Science and Food Safety, 2015, 14(5), 568-585 and Food & Function, 2013, 4(11), 1564-1580. The related materials are reused with the permission.

References

1. Wang S, Copeland L. Molecular disassembly of starch granules during gelatinization and its effect on starch digestibility: a review. *Food Funct.* 2013;4(11):1564-80.
2. Li D, Fayet C, Homer S. Effect of NaCl on the thermal behaviour of wheat starch in excess and limited water. *Carbohydr Polym.* 2013;94(1):31-7.
3. Wajiras R, Chika O, Davids J. DSC enthalpic transitions during starch gelatinisation in excess water, dilute sodium chloride and dilute sucrose solutions. *J Sci Food Agric.* 2009;89(12):2156-64.
4. Considine T, Noisuwan A, Hemar Y, Wilkinson B, Bronlund J, Kasapis S. Rheological investigations of the interactions between starch and milk proteins in model dairy systems: a review. *Food Hydrocoll.* 2011;25(8):2008-201725.
5. Noisuwan A, Bronlund J, Wilkinson B, Hemar Y. Effect of milk protein products on the rheological and thermal (DSC) properties of normal rice starch and waxy rice starch. *Food Hydrocoll.* 2008;22(1):174-83.
6. Chiotelli E, Pilosio G, Meste ML. Effect of sodium chloride on the gelatinization of starch: a multimeasurement study. *Biopolymers.* 2002;63(1):41-58.
7. Samutsri W, Suphantharika M. Effect of salts on pasting, thermal, and rheological properties of rice starch in the presence of non-ionic and ionic hydrocolloids. *Carbohydr Polym.* 2012;87(2):1559-68.
8. Sopade PA, Halley PJ, Junming LL. Gelatinisation of starch in mixtures of sugars. II. Application of differential scanning calorimetry. *Carbohydr Polym.* 2004;58(3):311-21.
9. Ahmad FB, Williams PA. Effect of sugars on the thermal and rheological properties of sago starch. *J Agric Food Chem.* 2001;49(3):1578-86.
10. Maauf AG, Che MY, Asbi BA, Junainah AH, Kennedy JF. Gelatinisation of sago starch in the presence of sucrose and sodium chloride as assessed by differential scanning calorimetry. *Carbohydr Polym.* 2001;45(4):335-45.
11. Gunaratne A, Ranaweera S, Corke H. Thermal, pasting, and gelling properties of wheat and potato starches in the presence of sucrose, glucose, glycerol, and hydroxypropyl β -cyclodextrin. *Carbohydr Polym.* 2007;70(1):112-22.
12. Kohyama K, Nishinari K. Effect of soluble sugars on gelatinization and retrogradation of sweet potato starch. *J Agric Food Chem.* 1991;39(8):1406-10.
13. Hardin M. Macromolecular interactions during gelatinisation and retrogradation in starch-whey systems as studied by rapid visco-analyser. *Int J Food Eng.* 2006;2(4):1-17.
14. Atwell WA, Hood LF, Lineback DR, Zobel HF, Varriano-Marston E. The terminology and methodology associated with basic starch phenomena. *Cereal Foods World.* 1988;33(3):306-11.
15. Biliaderis CG. Structural transitions and related physical properties of starch. In: BeMiller J, Whistler R, editors. *Starch*. 3rd ed. New York: Academic; 2009. p. 293-372.
16. Ratnayake WS, Jackson DS. Starch gelatinization. *J Appl Polym Sci.* 1975;19(2):221-68.
17. BeMiller JN. Pasting, paste, and gel properties of starch-hydrocolloid combinations. *Carbohydr Polym.* 2011;86(2):386-423.
18. Ii JWM, Pacsu E. Starch studies. Gelatinization of starches in water and in aqueous pyridine. *Indengchem.* 1942;34(7):807-12.

19. Goering KJ, Fritts DH, Allen GD. A comparison of loss of birefringence with the percent gelatinization and viscosity on potato, wheat, rice, corn, cow cockle, and several barley starches. *Cereal Chem.* 1974;51:764–71.
20. Leach HW. Gelatinization of starch. In: Whistler RL, Paschal EF, editors. *Starch: chemistry and technology*. New York: Academic; 1965. p. 289–307.
21. Watson SA. Determination of starch gelatinization temperature. In: Whistler RL, editor. *Methods in carbohydrate chemistry*. New York: Academic; 1964. p. 240–2.
22. Shetty RM, Lineback DR, Seib PA. Determining the degree of starch gelatinization. *Cereal Chem.* 1974;51:364–75.
23. Stevens DJ, Elton GH. Thermal properties of starch/water system. Part I. Measurement of heat of gelatinisation by differential scanning calorimetry. *Starch-Stärke.* 1971;23(1):8–11.
24. Goldstein A, Nantanga KKM, Seetharaman K. Molecular interactions in starch-water systems: effect of increasing starch concentration. *Cereal Chem.* 2010;87(4):370–5.
25. Wootton M, Bamunuarachchi A. Application of differential scanning calorimetry to starch gelatinization. I. Commercial native and modified starches. *Starch-Stärke.* 1979;31(6):201–4.
26. Donovan JW. Phase transitions of starch-water system. *Biopolymers.* 1979;18(2):263–75.
27. Wang S, Copeland L. Phase transitions of pea starch over a wide range of water content. *J Agric Food Chem.* 2012;60(25):6439–46.
28. Patel B, Seetharaman K. Effect of heating rate at different moisture contents on starch retrogradation and starch-water interactions during gelatinization. *Starch-Stärke.* 2010;62(10):538–46.
29. Garcia V, Colonna P, Bouchet B, Gallant DJ. Structural changes of cassava starch granules after heating at intermediate water contents. *Starch-Stärke.* 1997;49(5):171–9.
30. Tomka I. Thermoplastic starch. In: Levine H, Slade L, editors. *Water relationships in foods*. New York: Springer; 1991. p. 627–37.
31. Steeneken PAM, Woortman AJJ. Identification of the thermal transitions in potato starch at a low water content as studied by preparative DSC. *Carbohydr Polym.* 2009;77(2):288–92.
32. Jang JK, Pyun YR. Effect of moisture content on the melting of wheat starch. *Starch-Stärke.* 1996;48(2):48–51.
33. Le Bail P, Bizot H, Ollivon M, Keller G, Bourgaux C, Buléon A. Monitoring the crystallization of amylose-lipid complexes during maize starch melting by synchrotron X-ray diffraction. *Biopolymers.* 1999;50(1):99–110.
34. Randzio SL, Flis-Kabulska I, Grolier JPE. Reexamination of phase transformations in the starch-water system. *Macromolecules.* 2002;35(23):8852–9.
35. Liu H, Lelièvre J. Effects of heating rate and sample size on differential scanning calorimetry traces of starch gelatinized at intermediate water levels. *Starch-Stärke.* 1991;43(6):225–7.
36. Fredriksson H, Silverio J, Andersson R, Eliasson AC, Åman P. The influence of amylose and amylopectin characteristics on gelatinization and retrogradation properties of different starches. *Carbohydr Polym.* 1998;35(3–4):119–34.
37. Biliaderis CG, Page CM, Maurice TJ, Juliano BO. Thermal characterization of rice starches: a polymeric approach to phase transitions of granular starch. *J Agric Food Chem.* 1986;34(1):6–14.
38. Garcia V, Colonna P, Lourdin D, Buleon A, Bizot H, Ollivon M. Thermal transitions of cassava starch at intermediate water contents. *J Therm Anal.* 1996;47(5):1213–28.
39. Yu L, Christie G. Measurement of starch thermal transitions using differential scanning calorimetry. *Carbohydr Polym.* 2001;46(2):179–84.
40. Derycke V, Vandeputte GE, Vermeulen R, Man W, Goderis B, Mhij K, et al. Starch gelatinization and amylose-lipid interactions during rice parboiling investigated by temperature resolved wide angle X-ray scattering and differential scanning calorimetry. *J Cereal Sci.* 2005;42(3):334–43.
41. Jovanovich G, Añón MC. Amylose-lipid complex dissociation. A study of the kinetic parameters. *Biopolymers.* 2015;49(1):81–9.

42. Raphaelides S, Karkalas J. Thermal dissociation of amylose-fatty acid complexes. *Carbohydr Res.* 1988;172(1):65–82.
43. Biliaderis CG, Page CM, Slade L, Sirett RR. Thermal behavior of amylose-lipid complexes. *Carbohydr Polym.* 1985;5(5):367–89.
44. Kugimiya M, Donovan JW, Wong RY. Phase transitions of amylose-lipid complexes in starches: a calorimetric study. *Starch-Stärke.* 1980;32(8):265–70.
45. Russell PL. Gelatinisation of starches of different amylose/amylopectin content. A study by differential scanning calorimetry. *J Cereal Sci.* 1987;6(2):133–45.
46. Liu P, Xie F, Li M, Liu X, Yu L, Halley PJ, et al. Phase transitions of maize starches with different amylose contents in glycerol-water systems. *Carbohydr Polym.* 2011;85(1):180–7.
47. Maurice TJ, Slade L, Sirett RR, Page CM. Polysaccharide-water interactions-thermal behavior of rice starch. In: Simatos D, Multon SL, Nijhoff M, editors. *Influence of water on food quality and stability.* Dordrecht: Nijhoff M; 1985. p. 211–27.
48. Wang S, Copeland L. New insights into loss of swelling power and pasting profiles of acid hydrolyzed starch granules. *Starch-Stärke.* 2012;64(7):538–44.
49. Wang S, Copeland L. Nature of thermal transitions of native and acid-hydrolysed pea starch: does gelatinization really happen? *Carbohydr Polym.* 2012;87(2):1507–14.
50. Tester RF, Morrison WR. Swelling and gelatinization of cereal starches. I. Effects of amylopectin, amylose, and lipids. *Cereal Chem.* 1990;67(6):551–7.
51. Wang S, Zhang X, Wang S, Copeland L. Changes of multi-scale structure during mimicked DSC heating reveal the nature of starch gelatinization. *Sci Rep.* 2016;6:28271.
52. Vermeylen R, Derycke V, Delcour JA, Goderis B, Reynaers H, Koch MHJ. Gelatinization of starch in excess water: beyond the melting of lamellar crystallites. A combined wide-and small-angle X-ray scattering study. *Biomacromolecules.* 2006;7(9):2624–30.
53. Jenkins PJ, Donald AM. Gelatinisation of starch: a combined SAXS/WAXS/DSC and SANS study. *Carbohydr Res.* 1998;308(1):133–47.
54. Biliaderis CG, Maurice TJ, Vose JR. Starch gelatinization phenomena studied by differential scanning calorimetry. *J Food Sci.* 1980;45(6):1669–74.
55. Wong RBK, Lelievre J. Comparison of the crystallinities of wheat starches with different swelling capacities. *Starch-Stärke.* 1982;34(5):159–61.
56. Cruz-Orea A, Pitsi G, Jamée P, Thoen J. Phase transitions in the starch-water system studied by adiabatic scanning calorimetry. *J Agric Food Chem.* 2002;50(6):1335–44.
57. Fukuoka M, Ohta K-I, Watanabe H. Determination of the terminal extent of starch gelatinization in a limited water system by DSC. *J Food Eng.* 2002;53(1):39–42.
58. Tananuwong K, Reid DS. DSC and NMR relaxation studies of starch-water interactions during gelatinization. *Carbohydr Polym.* 2004;58(3):345–58.
59. Liu H, Yu L, Xie F, Chen L. Gelatinization of cornstarch with different amylose/amylopectin content. *Carbohydr Polym.* 2006;65(3):357–63.
60. Wang S, Li C, Yu J, Copeland L, Wang S. Phase transition and swelling behaviour of different starch granules over a wide range of water content. *LWT-Food Sci Technol.* 2014;59(2):597–604.
61. Evans ID, Haisman DR. The effect of solutes on the gelatinization temperature range of potato starch. *Starch-Stärke.* 1982;34(7):224–31.
62. Liu H, Lelievre J, Ayoung-Chee W. A study of starch gelatinization using differential scanning calorimetry, X-ray, and birefringence measurements. *Carbohydr Res.* 1991;210:79–87.
63. Liu H, Lelièvre J. A differential scanning calorimetry study of melting transitions in aqueous suspensions containing blends of wheat and rice starch. *Carbohydr Polym.* 1992;17(2):145–9.
64. Nakazawa F, Noguchi S, Takahashi J, Takada M. Thermal equilibrium state of starch-water mixture studied by differential scanning calorimetry. *Agric Biol Chem.* 1984;48(11):2647–53.
65. Slade L, Levine H. Non-equilibrium melting of native granular starch: part I. Temperature location of the glass transition associated with gelatinization of A-type cereal starches. *Carbohydr Polym.* 1988;8(3):183–208.

66. Waigh TA, Gidley MJ, Komanshek BU, Donald AM. The phase transformations in starch during gelatinisation: a liquid crystalline approach. *Carbohydr Res.* 2000;328(2):165–76.
67. Vermeulen R, Derycke V, Delcour JA, Goderis B, Reynaers H, Koch MHJ. Structural transformations during gelatinization of starches in limited water: combined wide- and small-angle X-ray scattering study. *Biomacromolecules.* 2006;7(4):1231–8.
68. Li Q, Xie Q, Yu S, Gao Q. New approach to study starch gelatinization applying a combination of hot-stage light microscopy and differential scanning calorimetry. *J Agric Food Chem.* 2013;61(6):1212–8.
69. Baks T, Ngene IS, Van Soest JGG, Janssen AEM, Boom RM. Comparison of methods to determine the degree of gelatinisation for both high and low starch concentrations. *Carbohydr Polym.* 2007;67(4):481–90.
70. Parada J, Aguilera JM. Starch matrices and the glycemic response. *Food Sci Technol Int.* 2011;17(3):187–204.
71. Liu K, Han J. Enzymatic method for measuring starch gelatinization in dry products in situ. *J Agric Food Chem.* 2012;60(17):4212–21.
72. Holm J, Lundquist I, Björck I, Eliasson AC, Asp NG. Degree of starch gelatinization, digestion rate of starch in vitro, and metabolic response in rats. *Am J Clin Nutr.* 1988;47(6):1010–6.
73. Di Paola RD, Asis R, Aldao MAJ. Evaluation of the degree of starch gelatinization by a new enzymatic method. *Starch-Stärke.* 2003;55(9):403–9.
74. Wang S, Wang S, Liu L, Wang S, Copeland L. Structural orders of wheat starch do not determine the in vitro enzymatic digestibility. *J Agric Food Chem.* 2017;65(8):1697–706.
75. Svihus B, Uhlen AK, Harstad OM. Effect of starch granule structure, associated components and processing on nutritive value of cereal starch: a review. *Anim Feed Sci Technol.* 2005;122(3):303–20.
76. Debet MR, Gidley MJ. Why do gelatinized starch granules not dissolve completely? Roles for amylose, protein, and lipid in granule “ghost” integrity. *J Agric Food Chem.* 2007;55(12):4752–60.
77. Goesaert H, Brijs K, Veraverbeke WS, Courtin CM, Gebruers K, Delcour JA. Wheat flour constituents: how they impact bread quality, and how to impact their functionality. *Trends Food Sci Technol.* 2005;16(1):12–30.
78. Hoover R, Hughes T, Chung HJ, Liu Q. Composition, molecular structure, properties, and modification of pulse starches: a review. *Food Res Int.* 2010;43(2):399–413.
79. Ring SG, Colonna P, I’Anson KJ, Kalichevsky MT, Miles MJ, Morris VJ, et al. The gelation and crystallisation of amylopectin. *Carbohydr Res.* 1987;162(2):277–93.
80. Hoover R. Composition, molecular structure, and physicochemical properties of tuber and root starches: a review. *Carbohydr Polym.* 2001;45(3):253–67.
81. Jane JL, Robyt JF. Structure studies of amylose-V complexes and retrograded amylose by action of alpha amylases, and a new method for preparing amyloextrins. *Carbohydr Res.* 1984;132(1):105–18.
82. Leloup VM, Colonna P, Ring SG, Roberts K, Wells B. Microstructure of amylose gels. *Carbohydr Polym.* 1992;18(3):189–97.
83. Shi YC, Seib PA. The structure of four waxy starches related to gelatinization and retrogradation. *Carbohydr Res.* 1992;227(92):131–45.
84. Yang F, Chen Y, Tong C, Huang Y, Xu F, Li K, et al. Association mapping of starch physicochemical properties with starch synthesis-related gene markers in nonwaxy rice (*Oryza sativa L.*). *Mol Breed.* 2014;34(4):1747–63.
85. Tang MC, Copeland L. Investigation of starch retrogradation using atomic force microscopy. *Carbohydr Polym.* 2007;70(1):1–7.
86. Ishiguro K, Noda T, Kitahara K, Yamakawa O. Retrogradation of sweet potato starch. *Starch-Stärke.* 2000;52(1):13–7.
87. Miles MJ, Morris VJ, Orford PD, Ring SG. The roles of amylose and amylopectin in the gelation and retrogradation of starch. *Carbohydr Res.* 1985;135(2):271–81.

88. Tran UT, Okadome H, Murata M, Homma S, Ohtsubo K. Comparison of Vietnamese and Japanese rice cultivars in terms of physicochemical properties. *Food Sci Technol Res.* 2001;7(4):323–30.
89. Fadda C, Sanguinetti AM, Del Caro A, Collar C, Piga A. Bread staling: updating the view. *Compr Rev Food Sci Food Saf.* 2014;13(4):473–92.
90. Gray JA, Bemiller JN. Bread staling: molecular basis and control. *Compr Rev Food Sci Food Saf.* 2003;2(1):1–21.
91. Mua JP, Jackson DS. Retrogradation and gel textural attributes of corn starch amylose and amylopectin fractions. *J Cereal Sci.* 1998;27(2):157–66.
92. McIver RG, Axford DWE, Colwell KH, Elton GAH. Kinetic study of the retrogradation of gelatinised starch. *J Sci Food Agric.* 1968;19(10):560–3.
93. Yao Y, Ding X. Pulsed nuclear magnetic resonance (PNMR) study of rice starch retrogradation. *Cereal Chem.* 2002;79(6):751.
94. Tian Y, Yang N, Li Y, Xu X, Zhan J, Jin Z. Potential interaction between β -cyclodextrin and amylose-lipid complex in retrograded rice starch. *Carbohydr Polym.* 2010;80(2):581–4.
95. Tian Y, Li Y, Xu X, Jin Z, Jiao A, Wang J, et al. A novel size-exclusion high performance liquid chromatography (SE-HPLC) method for measuring degree of amylose retrogradation in rice starch. *Food Chem.* 2010;118(2):445–8.
96. Karim AA, Norziah MH, Seow CC. Methods for the study of starch retrogradation. *Food Chem.* 2000;71(1):9–36.
97. Bao J, Shen Y, Jin L. Determination of thermal and retrogradation properties of rice starch using near-infrared spectroscopy. *J Cereal Sci.* 2007;46(1):75–81.
98. Russell PL. The ageing of gels from starches of different amylose/amylopectin content studied by differential scanning calorimetry. *J Cereal Sci.* 1987;6(2):147–58.
99. Wang S, Li C, Copeland L, Niu Q, Wang S. Starch retrogradation: a comprehensive review. *Compr Rev Food Sci Food Saf.* 2015;14(5):568–85.
100. Kong X, Zhu P, Sui Z, Bao J. Physicochemical properties of starches from diverse rice cultivars varying in apparent amylose content and gelatinisation temperature combinations. *Food Chem.* 2015;172:433–40.
101. Tian Y, Li Y, Xu X, Jin Z. Starch retrogradation studied by thermogravimetric analysis (TGA). *Carbohydr Polym.* 2011;84(3):1165–8.
102. Tian Y, Xu X, Xie Z, Zhao J, Jin Z. Starch retrogradation determined by differential thermal analysis (DTA). *Food Hydrocoll.* 2011;25(6):1637–9.
103. Vandeputte GE, Vermeylen R. Rice starches. III. Structural aspects provide insight in amylopectin retrogradation properties and gel texture. *J Cereal Sci.* 2003;38(1):61–8.
104. Jankowski T. Influence of starch retrogradation on the texture of cooked potato tuber. *Int J Food Sci Technol.* 2010;27(6):637–42.
105. Hallberg LM, Chinachoti P. A fresh perspective on staling: the significance of starch recrystallization on the firming of bread. *J Food Sci.* 2002;67(3):1092–6.
106. Shiraishi K, Lauzon RD, Yamazaki M, Sawayama S, Sugiyama N, Kawabata A. Rheological properties of cocoyam starch paste and gel. *Food Hydrocoll.* 1995;9(2):69–75.
107. Biliaderis CG, Zawistowski J. Viscoelastic behavior of aging starch gels: effects of concentration, temperature, and starch hydrolysates on network properties. *Cereal Chem.* 1990;67(3):240–6.
108. Akuzawa S, Sawayama S, Kawabata A. Dynamic viscoelasticity and stress relaxation in starch pastes. *J Texture Stud.* 1995;26(5):489–500.
109. Rosenthal AJ. Texture profile analysis-how important are the parameters? *J Texture Stud.* 2010;41(5):672–84.
110. Yu S, Ma Y, Sun D-W. Effects of freezing rates on starch retrogradation and textural properties of cooked rice during storage. *LWT-Food Sci Technol.* 2010;43(7):1138–43.
111. Yu S, Ma Y, Sun D-W. Impact of amylose content on starch retrogradation and texture of cooked milled rice during storage. *J Cereal Sci.* 2009;50(2):139–44.

112. Zaidul ISM, Norulaini NAN, Omar AKM, Yamauchi H, Noda T. RVA analysis of mixtures of wheat flour and potato, sweet potato, yam, and cassava starches. *Carbohydr Polym.* 2007;69(4):784–91.
113. Larkin P, editor. *Infrared and Raman spectroscopy: principles and spectral interpretation.* Amsterdam: Elsevier; 2011.
114. Htoon A, Shrestha AK, Flanagan BM, Lopezrubio A, Bird AR, Gilbert EP, et al. Effects of processing high amylose maize starches under controlled conditions on structural organisation and amylase digestibility. *Carbohydr Polym.* 2009;75(2):236–45.
115. Wang S, Luo H, Zhang J, Zhang Y, He Z, Wang S. Alkali-induced changes in functional properties and in vitro digestibility of wheat starch: the role of surface proteins and lipids. *J Agric Food Chem.* 2014;62(16):3636.
116. Soest JGV, Wit DD, Tournois H, Vliegenthart JFG. The influence of glycerol on structural changes in waxy maize starch as studied by Fourier transform infra-red spectroscopy. *Polymer.* 1994;35(22):4722–7.
117. Flores-Morales A, Jiménez-Estrada M, Mora-Escobedo R. Determination of the structural changes by FT-IR, Raman, and CP/MAS ¹³C NMR spectroscopy on retrograded starch of maize tortillas. *Carbohydr Polym.* 2012;87(1):61–8.
118. Ambigaipalan P, Hoover R, Donner E, Liu Q. Retrogradation characteristics of pulse starches. *Food Res Int.* 2013;54(1):203–12.
119. Lian X, Zhu W, Wen Y, Li L, Zhao X. Effects of soy protein hydrolysates on maize starch retrogradation studied by IR spectra and ESI-MS analysis. *Int J Biol Macromol.* 2013;59(4):143.
120. Thygesen LG, Lokke MM, Micklander E, Engelsen SB. Vibrational microspectroscopy of food. Raman vs. FT-IR. *Trends Food Sci Technol.* 2003;14(1–2):50–7.
121. Nuopponen MH, Wikberg HI, Birch GM, Jääskeläinen AS, Maunu SL, Vuorinen T, et al. Characterization of 25 tropical hardwoods with Fourier transform infrared, ultraviolet resonance Raman, and ¹³C-NMR cross-polarization/magic-angle spinning spectroscopy. *J Appl Polym Sci.* 2006;102(1):810–9.
122. Cho SY, Choi SG, Rhee C. Determination of degree of retrogradation of cooked rice by near infrared reflectance spectroscopy. *Korean J Food Sci Technol.* 1998;6(1):355–9.
123. Mariotti M, Sinelli N, Catenacci F, Pagani MA, Lucisano M. Retrogradation behaviour of milled and brown rice pastes during ageing. *J Cereal Sci.* 2009;49(2):171–7.
124. Barton FE, Himmelsbach DS, McClung AM, Champagne EL. Two-dimensional vibration spectroscopy of rice quality and cooking. *Cereal Chem.* 2002;79(1):143–7.
125. Li-Chan ECY. The applications of Raman spectroscopy in food science. *Trends Food Sci Technol.* 1996;7(11):361–70.
126. Wang S, Copeland L. Effect of acid hydrolysis on starch structure and functionality: a review. *Crit Rev Food Sci Nutr.* 2015;55(8):1081–97.
127. Socrates G, editor. *Infrared and Raman characteristic group frequencies: tables and charts.* Chichester: Wiley; 2004.
128. Schuster KC, Urlaub E, Gapes JR. Single-cell analysis of bacteria by Raman microscopy: spectral information on the chemical composition of cells and on the heterogeneity in a culture. *J Microbiol Methods.* 2000;42(1):29–38.
129. Kizil R, Irudayaraj J, Seetharaman K. Characterization of irradiated starches by using FT-Raman and FTIR spectroscopy. *J Agric Food Chem.* 2002;50(14):3912–8.
130. Fechner PM, Wartewig S, Kleinebudde P, Neubert RHH. Studies of the retrogradation process for various starch gels using Raman spectroscopy. *Carbohydr Res.* 2005;340(16):2563–8.
131. Hu X, Shi J, Zhang F, Zou X, Holmes M, Zhang W, et al. Determination of retrogradation degree in starch by mid-infrared and Raman spectroscopy during storage. *Food Anal Methods.* 2017;10(11):3694–705.
132. Purcell EM, Torrey HC, Pound RV. Resonance absorption by nuclear magnetic moments in a solid. *Phys Rev.* 1946;69(1–2):37.
133. Bloch F. Nuclear induction. *Phys Rev.* 1946;70(7–8):460.

134. Malet-Martino M, Holzgrabe U. NMR techniques in biomedical and pharmaceutical analysis. *J Pharm Biomed Anal.* 2011;55(1):1–15.
135. Bertocchi F, Paci M. Applications of high-resolution solid-state NMR spectroscopy in food science. *J Agric Food Chem.* 2008;56(20):9317–27.
136. Ablett S. Overview of NMR applications in food science. *Trends Food Sci Technol.* 1992;3:246–50.
137. Teo CH, Seow CC. A pulsed NMR method for the study of starch retrogradation. *Starch-Stärke.* 1992;44(8):288–92.
138. Bosmans GM, Lagrain B, Fierens E, Delcour JA. The impact of baking time and bread storage temperature on bread crumb properties. *Food Chem.* 2013;141(4):3301–8.
139. Bosmans GM, Lagrain B, Deleu LJ, Fierens E, Hills BP, Delcour JA. Assignments of proton populations in dough and bread using NMR relaxometry of starch, gluten, and flour model systems. *J Agric Food Chem.* 2012;60(21):5461–70.
140. Lewen KS, Paeschke T, Reid J, Molitor P, Schmidt SJ. Analysis of the retrogradation of low starch concentration gels using differential scanning calorimetry, rheology, and nuclear magnetic resonance spectroscopy. *J Agric Food Chem.* 2003;51(8):2348–58.
141. Wu JY, Bryant RG, Eads TM. Detection of solid-like components in starch using cross-relaxation and Fourier transform wide line proton NMR methods. *J Agric Food Chem.* 1992;40(3):449–55.
142. Wu JY, Eads TM. Evolution of polymer mobility during ageing of gelatinized waxy maize starch: a magnetization transfer ^1H NMR study. *Carbohydr Polym.* 1993;20(1):51–60.
143. Vodovotz Y, Vittadini E, Sachleben JR. Use of ^1H cross-relaxation nuclear magnetic resonance spectroscopy to probe the changes in bread and its components during aging. *Carbohydr Res.* 2002;337(2):147–53.
144. Gidley MJ, Bociek SM. Molecular organization in starches: a carbon ^{13}C CP/MAS NMR study. *J Am Chem Soc.* 1985;107(24):7040–4.
145. Baik M-Y, Dickinson LC, Chinachoti P. Solid-state ^{13}C CP/MAS NMR studies on aging of starch in white bread. *J Agric Food Chem.* 2003;51(5):1242–8.
146. Blazek J, Gilbert EP, Copeland L. Effects of monoglycerides on pasting properties of wheat starch after repeated heating and cooling. *J Cereal Sci.* 2011;54(1):151–9.
147. Gidley MJ, Cooke D. Aspects of molecular organization and ultrastructure in starch granules. *Biochem Soc Trans.* 1991;19(3):551.
148. Zhou X, Lim ST. Pasting viscosity and in vitro digestibility of retrograded waxy and normal corn starch powders. *Carbohydr Polym.* 2012;87(1):235–9.
149. Fu ZQ, Wang LJ, Li D, Zhou YG, Adhikari B. The effect of partial gelatinization of corn starch on its retrogradation. *Carbohydr Polym.* 2013;97(2):512.
150. Hellmann N, Feirchild B, Senti F. The bread staling problem. Molecular organization of starch upon aging of concentrated starch gels at various moisture. *Cereal Chem.* 1954;31:495–505.
151. Osella CA, Sánchez HD, Carrara CR, de la Torre MA, Pilar BM. Water redistribution and structural changes of starch during storage of a gluten-free bread. *Starch-Stärke.* 2005;57(5):208–16.
152. Shama K, Shimoni E, Bianco-Peled H. Small angle X-ray scattering of resistant starch type III. *Biomacromolecules.* 2004;5(1):219–23.
153. Suzuki T, Chiba A, Yarno T. Interpretation of small angle X-ray scattering from starch on the basis of fractals. *Carbohydr Polym.* 1997;34(4):357–63.
154. Wang S, Yu J, Gao W, Pang J, Yu J, Xiao P. Characterization of starch isolated from *Fritillaria* traditional Chinese medicine (TCM). *J Food Eng.* 2007;80(2):727–34.
155. Wang S, Gao W, Jia W, Xiao P. Crystallography, morphology and thermal properties of starches from four different medicinal plants of *Fritillaria* species. *Food Chem.* 2006;96(4):591–6.
156. Perera C, Hoover R. Influence of hydroxypropylation on retrogradation properties of native, defatted and heat-moisture treated potato starches. *Food Chem.* 1999;64(3):361–75.

157. Jacobson MR, Obanni M, Bemiller JN. Retrogradation of starches from different botanical sources. *Cereal Chem.* 1997;74(5):511–8.
158. Hoover R, Ratnayake WS. Starch characteristics of black bean, chick pea, lentil, navy bean and pinto bean cultivars grown in Canada. *Food Chem.* 2002;78(4):489–98.
159. Yuan RC, Thompson DB. Freeze-thaw stability of three waxy maize starch pastes measured by centrifugation and calorimetry. *Cereal Chem.* 1998;75(4):571–3.
160. Liu J, Wang B, Lin L, Zhang J, Liu W, Xie J, et al. Functional, physicochemical properties and structure of cross-linked oxidized maize starch. *Food Hydrocoll.* 2014;36:45–52.
161. Jankowski T. Influence of starch retrogradation on the texture of cooked potato tuber. *Int J Food Sci Technol.* 1992;27(6):637–42.
162. Eerlingen RC, Jacobs H, Delcour J. Enzyme-resistant starch. 5. Effect of retrogradation of waxy maize starch on enzyme susceptibility. *Cereal Chem.* 1994;71(4):351–5.
163. Cui R, Oates CG. The effect of retrogradation on enzyme susceptibility of sago starch. *Carbohydr Polym.* 1997;32(1):65–72.
164. Sievert D, Pomeranz Y. Enzyme-resistant starch. I. Characterization and evaluation by enzymatic, thermoanalytical, and microscopic methods. *Cereal Chem.* 1989;66(4):342–7.
165. Kainuma K, Matsunaga A, Itagawa M, Kobayashi S. New enzyme system-beta-amylase-pullulanase-to determine the degree of gelatinization and retrogradation of starch or starch products. *J Jpn Soc Starch Sci.* 1981;28(4):235–40.
166. Tsuge H, Hishida M, Iwasaki H, Watanabe S, Goshima G. Enzymatic evaluation for the degree of starch retrogradation in foods and foodstuffs. *Starch-Stärke.* 1990;42(6):213–6.
167. Wu Y, Lin Q, Chen Z, Wu W, Xiao H. Fractal analysis of the retrogradation of rice starch by digital image processing. *J Food Eng.* 2012;109(1):182–7.
168. Utrilla-Coello RG, Bello-Perez LA, Vernon-Carter EJ, Rodriguez E, Alvarez-Ramirez J. Microstructure of retrograded starch: quantification from lacunarity analysis of SEM micrographs. *J Food Eng.* 2013;116(4):775–81.
169. Putaux J-L, Buleon A, Chanzy H. Network formation in dilute amylose and amylopectin studied by TEM. *Macromolecules.* 2000;33(17):6416–22.
170. Charoenrein S, Tatirat O, Rengsutthi K, Thongngam M. Effect of konjac glucomannan on syneresis, textural properties and the microstructure of frozen rice starch gels. *Carbohydr Polym.* 2011;83(1):291–6.
171. Roulet P, MacInnes WM, Würsch P, Sanchez RM, Raemy A. A comparative study of the retrogradation kinetics of gelatinized wheat starch in gel and powder form using X-rays, differential scanning calorimetry and dynamic mechanical analysis. *Food Hydrocoll.* 1988;2(5):381–96.
172. Zeleznak KJ, Hosney RC. The role of water in the retrogradation of wheat starch gels and bread crumb. *Cereal Chem.* 1986;63(5):407–11.
173. Jouppila K, Kansikas J, Roos YH. Factors affecting crystallization and crystallization kinetics in amorphous corn starch. *Carbohydr Polym.* 1998;36(2-3):143–9.
174. Zhou X, Wang R, Yoo SH, Lim ST. Water effect on the interaction between amylose and amylopectin during retrogradation. *Carbohydr Polym.* 2011;86(4):1671–4.
175. Longton J, LeGrys GA. Differential scanning calorimetry studies on the crystallinity of ageing wheat starch gels. *Starch-Stärke.* 1981;33(12):410–4.
176. Sievert D, Würsch P. Thermal behavior of potato amylose and enzyme-resistant starch from maize. *Cereal Chem.* 1993;70:333–8.
177. Klucinec JD, Thompson DB. Amylopectin nature and amylose-to-amylopectin ratio as influences on the behavior of gels of dispersed starch. *Cereal Chem.* 2007;79(1):24–35.
178. Wang S, Li C, Zhang X, Copeland L, Wang S. Retrogradation enthalpy does not always reflect the retrogradation behavior of gelatinized starch. *Sci Rep.* 2016;6:20965.
179. Xie YY, Hu XP, Jin ZY, Xu XM, Chen HQ. Effect of temperature-cycled retrogradation on in vitro digestibility and structural characteristics of waxy potato starch. *Int J Biol Macromol.* 2014;67:79–84.

180. Zhou X, Baik B-K, Wang R, Lim S-T. Retrogradation of waxy and normal corn starch gels by temperature cycling. *J Cereal Sci.* 2010;51(1):57–65.
181. Park EY, Baik B-K, Lim S-T. Influences of temperature-cycled storage on retrogradation and in vitro digestibility of waxy maize starch gel. *J Cereal Sci.* 2009;50(1):43–8.
182. Zhang L, Hu X, Xu X, Jin Z, Tian Y. Slowly digestible starch prepared from rice starches by temperature-cycled retrogradation. *Carbohydr Polym.* 2011;84(3):970–4.
183. Singh H, Lin JH, Huang WH, Chang YH. Influence of amylopectin structure on rheological and retrogradation properties of waxy rice starches. *J Cereal Sci.* 2012;56(2):367–73.
184. Ji Y, Zhu K, Qian H, Zhou H. Staling of cake prepared from rice flour and sticky rice flour. *Food Chem.* 2007;104(1):53–8.
185. Niba LL. Processing effects on susceptibility of starch to digestion in some dietary starch sources. *Int J Food Sci Nutr.* 2003;54(1):97–109.
186. Mangala SL, Udayasankar K, Tharanathan RN. Resistant starch from processed cereals: the influence of amylopectin and non-carbohydrate constituents in its formation. *Food Chem.* 1999;64(3):391–6.
187. Shi M, Gao Q. Recrystallization and in vitro digestibility of wrinkled pea starch gel by temperature cycling. *Food Hydrocoll.* 2016;61:712–9.
188. Keetels C, Van Vliet T, Walstra P. Gelation and retrogradation of concentrated starch systems: 2. Retrogradation *Food Hydrocolloids.* 1996;10(3):355–62.
189. Fisher DK, Thompson DB. Retrogradation of maize starch after thermal treatment within and above the gelatinization temperature range. *Cereal Chem.* 1997;74(3):344–51.
190. Liu Q, Thompson DB. Retrogradation of du wx and su2 wx maize starches after different gelatinization heat treatments. *Cereal Chem.* 1998;75(6):868–74.
191. Liu H, Yu L, Chen L, Li L. Retrogradation of corn starch after thermal treatment at different temperatures. *Carbohydr Polym.* 2007;69(4):756–62.
192. Chang SM, Liu LC. Retrogradation of rice starches studied by differential scanning calorimetry and influence of sugars, NaCl and lipids. *J Food Sci.* 1991;56(2):564–6.
193. Wang YJ, Jane J. Correlation between glass transition temperature and starch retrogradation in the presence of sugars and maltodextrins. *Cereal Chem.* 1994;71(6):527–31.
194. Smits ALM, Kruiskamp PH, Van Soest JGG, Vliegthart JFG. The influence of various small plasticisers and malto-oligosaccharides on the retrogradation of (partly) gelatinised starch. *Carbohydr Polym.* 2003;51(4):417–24.
195. Katsuta K, Nishimura A, Miura M. Effects of saccharides on stabilities of rice starch gels. 1. Mono- and disaccharides. *Food Hydrocoll.* 1992;6(4):387–98.
196. Katsuta K, Miura M, Nishimura A. Kinetic treatment for rheological properties and effects of saccharides on retrogradation of rice starch gels. *Food Hydrocoll.* 1992;6(2):187–98.
197. Aee LH, Hie KN, Nishinari K. DSC and rheological studies of the effects of sucrose on the gelatinization and retrogradation of acorn starch. *Thermochim Acta.* 1998;322(1):39–46.
198. Germani R, Ciacco CF, Rodriguez-Amaya DB. Effect of sugars, lipids and type of starch on the mode and kinetics of retrogradation of concentrated corn starch gels. *Starch-Stärke.* 1983;35(11):377–81.
199. Cairns P, I'Anson KJ, Morris VJ. The effect of added sugars on the retrogradation of wheat starch gels by X-ray diffraction. *Food Hydrocoll.* 1991;5(1–2):151–3.
200. Katsuta K, Nishimura A, Miura M. Effects of saccharides on stabilities of rice starch gels. 2. Oligosaccharides. *Food Hydrocoll.* 1992;6(4):399–408.
201. Rojas JA, Rosell CM, De Barber CB. Role of maltodextrins in the staling of starch gels. *Eur Food Res Technol.* 2001;212(3):364–8.
202. Durán E, León A, Barber B, de Barber CB. Effect of low molecular weight dextrins on gelatinization and retrogradation of starch. *Eur Food Res Technol.* 2001;212(2):203–7.
203. I'Anson KJ, Miles MJ, Morris VJ, Besford LS, Jarvis DA, Marsh RA. The effects of added sugars on the retrogradation of wheat starch gels. *J Cereal Sci.* 1990;11(3):243–8.
204. Tian Y, Li Y, Manthey FA, Xu X, Jin Z, Deng L. Influence of β -cyclodextrin on the short-term retrogradation of rice starch. *Food Chem.* 2009;116(1):54–8.

205. Gunaratne A, Kong X, Corke H. Functional properties and retrogradation of heat-moisture treated wheat and potato starches in the presence of hydroxypropyl β -cyclodextrin. *Starch-Stärke*. 2010;62(2):69–77.
206. Zhou Y, Wang D, Zhang L, Du X, Zhou X. Effect of polysaccharides on gelatinization and retrogradation of wheat starch. *Food Hydrocoll*. 2008;22(4):505–12.
207. Witczak T, Witczak M, Ziobro R. Effect of inulin and pectin on rheological and thermal properties of potato starch paste and gel. *J Food Eng*. 2014;124:72–9.
208. Qiu S, Yadav MP, Chen H, Liu Y, Tatsumi E, Yin L. Effects of corn fiber gum (CFG) on the pasting and thermal behaviors of maize starch. *Carbohydr Polym*. 2015;115:246–52.
209. Pongsawatmanit R, Chantaro P, Nishinari K. Thermal and rheological properties of tapioca starch gels with and without xanthan gum under cold storage. *J Food Eng*. 2013;117(3):333–41.
210. Correa MJ, Ferrero C, Puppo C, Brites C. Rheological properties of rice-locust bean gum gels from different rice varieties. *Food Hydrocoll*. 2013;31(2):383–91.
211. Chen L, Ren F, Zhang Z, Tong Q, Rashed MMA. Effect of pullulan on the short-term and long-term retrogradation of rice starch. *Carbohydr Polym*. 2015;115:415–21.
212. Alamri MS, Mohamed AA, Hussain S. Effects of alkaline-soluble okra gum on rheological and thermal properties of systems with wheat or corn starch. *Food Hydrocoll*. 2013;30(2):541–51.
213. Qiu S, Yadav MP, Zhu Q, Chen H, Liu Y, Yin L. The addition of corn fiber gum improves the long-term stability and retrogradation properties of corn starch. *J Cereal Sci*. 2017;76:92–8.
214. Li Q-Q, Wang Y-S, Chen H-H, Liu S, Li M. Retardant effect of sodium alginate on the retrogradation properties of normal cornstarch and anti-retrogradation mechanism. *Food Hydrocoll*. 2017;69:1–9.
215. Banchathanakij R, Supphantharika M. Effect of different β -glucans on the gelatinisation and retrogradation of rice starch. *Food Chem*. 2009;114(1):5–14.
216. Satrapai S, Supphantharika M. Influence of spent brewer's yeast β -glucan on gelatinization and retrogradation of rice starch. *Carbohydr Polym*. 2007;67(4):500–10.
217. Day L, Fayet C, Homer S. Effect of NaCl on the thermal behaviour of wheat starch in excess and limited water. *Carbohydr Polym*. 2013;94(1):31–7.
218. Uthayakumaran S, Batey I, Day L, Wrigley C. Salt reduction in wheat-based foods-technical challenges and opportunities. *Food Aust*. 2011;63(4):137–40.
219. Nunes MHB, Moore MM, Ryan LAM, Arendt EK. Impact of emulsifiers on the quality and rheological properties of gluten-free breads and batters. *Eur Food Res Technol*. 2009;228(4):633–42.
220. Miller RA, Hosney RC. Role of salt in baking. *Cereal Foods World*. 2008;53(1):4–6.
221. Baker LA, Rayas-Duarte P. Freeze-thaw stability of amaranth starch and the effects of salt and sugars. *Cereal Chem*. 1998;75(3):301–7.
222. Yu S, Jiang LZ, Kopparapu NK. Impact of soybean proteins addition on thermal and retrogradation properties of nonwaxy corn starch. *J Food Process Preserv*. 2015;39(6):710–8.
223. Ottenhof MA, Farhat IA. The effect of gluten on the retrogradation of wheat starch. *J Cereal Sci*. 2004;40(3):269–74.
224. Lian X, Guo J, Wang D, Li L, Zhu J. Effects of protein in wheat flour on retrogradation of wheat starch. *J Food Sci*. 2014;79(8):1505–11.
225. Ribotta PD, Colombo A, Rosell CM. Enzymatic modifications of pea protein and its application in protein-cassava and corn starch gels. *Food Hydrocoll*. 2012;27(1):185–90.
226. Lockwood S, King JM, Labonte DR. Altering pasting characteristics of sweet potato starches through amino acid additives. *J Food Sci*. 2008;73(5):373–7.
227. Chen W, Zhou H, Yang H, Cui M. Effects of charge-carrying amino acids on the gelatinization and retrogradation properties of potato starch. *Food Chem*. 2015;167:180–4.
228. An HJ, King JM. Using ozonation and amino acids to change pasting properties of rice starch. *J Food Sci*. 2009;74(3):C278–83.
229. Xiao J, Zhong Q. Suppression of retrogradation of gelatinized rice starch by anti-listerial grass carp protein hydrolysate. *Food Hydrocoll*. 2017;72:338–45.

230. Putseys JA, Lamberts L, Delcour JA. Amylose-inclusion complexes: formation, identity and physico-chemical properties. *J Cereal Sci.* 2010;51(3):238–47.
231. Copeland L, Blazek J, Salman H, Tang MC. Form and functionality of starch. *Food Hydrocoll.* 2009;23(6):1527–34.
232. Becker A, Hill SE, Mitchell JR. Relevance of amylose-lipid complexes to the behaviour of thermally processed starches. *Starch-Stärke.* 2001;53(3–4):121–30.
233. Nakazawa Y, Wang YJ. Effect of annealing on starch-palmitic acid interaction. *Carbohydr Polym.* 2004;57(3):327–35.
234. Huang JJ, White PJ. Waxy corn starch: monoglyceride interaction in a model system. *Cereal Chem.* 1993;70:42–7.
235. Gudmundsson M, Eliasson AC. Retrogradation of amylopectin and the effects of amylose and added surfactants/emulsifiers. *Carbohydr Polym.* 1990;13(3):295–315.
236. Eliasson AC, Ljunger G. Interactions between amylopectin and lipid additives during retrogradation in a model system. *J Sci Food Agric.* 1988;44(4):353–61.
237. Miura M, Nishimura A, Katsuta K. Influence of addition of polyols and food emulsifiers on the retrogradation rate of starch. *Food Struct.* 1992;11(3):5.
238. Li W, Li C, Gu Z, Qiu Y, Cheng L, Hong Y, et al. Relationship between structure and retrogradation properties of corn starch treated with 1, 4- α -glucan branching enzyme. *Food Hydrocoll.* 2016;52:868–75.
239. Grewal N, Faubion J, Feng G, Kaufman RC, Wilson JD, Shi YC. Structure of waxy maize starch hydrolyzed by maltogenic α -amylase in relation to its retrogradation. *J Agric Food Chem.* 2015;63(16):4196–201.
240. Wu Y, Chen Z, Li X, Li M. Effect of tea polyphenols on the retrogradation of rice starch. *Food Res Int.* 2009;42(2):221–5.
241. Zhu F, Wang Y-J. Rheological and thermal properties of rice starch and rutin mixtures. *Food Res Int.* 2012;49(2):757–62.
242. Gujral HS, Haros M, Rosell CM. Starch hydrolyzing enzymes for retarding the staling of rice bread. *Cereal Chem.* 2003;80(6):750–4.
243. Seyhun N, Sumnu G, Sahin S. Effects of different emulsifier types, fat contents, and gum types on retardation of staling of microwave-baked cakes. *Mol Nutr Food Res.* 2003;47(4):248–51.
244. Fu Z, Chen J, Luo SJ, Liu CM, Liu W. Effect of food additives on starch retrogradation: a review. *Starch-Stärke.* 2015;67(1–2):69–78.
245. Goesaert H, Leman P, Bijttebier A, Delcour JA. Antifirming effects of starch degrading enzymes in bread crumb. *J Agric Food Chem.* 2009;57(6):2346–55.
246. Hirashima M, Takahashi R, Nishinari K. The gelatinization and retrogradation of cornstarch gels in the presence of citric acid. *Food Hydrocoll.* 2012;27(2):390–3.

Rheological, Pasting, and Textural Properties of Starch



Shujun Wang and Fei Ren

Abstract Native starch is an important raw material used in the industry. Rheological, pasting, and textural properties of starch are the major functional properties to determine its applications. Key rheological properties of starch include rheology of starch during heating, viscosity of starch paste, and rheological features of starch gel. The pasting properties of starch are commonly quantified by measuring changes in viscosity during the heating and cooling of starch dispersions. The textural characteristics of starch gels have an important role in the classification of sensory and quality of foods. In this this chapter, the rheological, pasting, and textural properties of starch from different botanical sources are compared, and the impacts of other ingredients (sugars, salts and lipids) on the properties are summarized. The relationship of starch functionalities with food quality is also summarized. The information provided will be useful for the applications of starch in the industry.

Keywords Starch · Rheology · Pasting property · Texture · Food quality

1 Introduction

Starch is the main component of many edible plants and widely used in food, material, chemical, and medical industries [1]. Starch occurs naturally as semicrystalline granules with hierarchical structure, which is composed of amylose molecules (mostly unbranched) and amylopectin molecules (highly branched) [2]. The rheological behavior, pasting, and textural properties of starch are the main functional characteristics that determine its application [3, 4], which are largely affected by the structural changes in starch during gelatinization and retrogradation. As a starch suspension is heated to gelatinization temperature, the starch granules absorb water and swell, the amylopectin double helices dissociate, and the amylose molecules

S. Wang (✉) · F. Ren

State Key Laboratory of Food Nutrition and Safety, Tianjin University of Science and Technology, Tianjin, China

e-mail: sjwang@tust.edu.cn

© Springer Nature Singapore Pte Ltd. 2020

S. Wang (ed.), *Starch Structure, Functionality and Application in Foods*,
https://doi.org/10.1007/978-981-15-0622-2_7

121

leach out, leading to the formation of a starch paste or gel [5, 6]. Upon cooling, the dissociated starch chains recrystallize gradually into an ordered structure, the viscoelasticity and hardness of starch gel gradually increase [7]. Currently, many methods have been used to characterize the rheological, pasting, and textural properties of starch. The Brabender Viscograph and Rapid Visco Analyser (RVA) have been widely used for the determination of pasting properties of starch [1, 8, 9]. Researchers generally use a dynamic rheometer for studying the rheological behavior of a starch paste or gel [10–13]. The textural characteristics of starch are the main indicators of the sensory and quality of starchy foods, measured by the texture analyzer [14]. Quality and shelf-life of starch-based foods are largely controlled by starch functional characteristics. Therefore, this chapter will summarize the rheological, pasting properties, and texture of starch and their effects on food quality.

2 Rheological Behavior of Starch

Starch shows different deformation and flow characteristics under the action of external forces, which is called the rheological behavior of starch [15]. The elastic or storage modulus (G'), viscous or loss modulus (G''), and loss tangent ($\tan \delta$) are the main parameters that describe the rheological behavior of starch. A $\tan \delta$ value of <1 means a more elastic and solid material, whereas $\tan \delta > 1$ describes a more viscous and liquid material [12]. The rheological properties of starch are related closely to the gelatinization and retrogradation of starch, including the rheological behavior of starch during gelatinization, the rheology of starch paste, and the viscoelasticity of starch gel during and after retrogradation [16].

During gelatinization, the G' value of starch progressively increases with temperature to a maximum (peak G') and then drops with continued heating. Simultaneously, the G'' value of starch shows similar changes. The dynamic rheological behavior of starch during heating is determined by source and structure of the starch. Starch with larger sized granules has higher G' , G'' values and lower $\tan \delta$, as observed with potato, rice, and wheat starches [17, 18]. During heating, the G' and G'' values of starch increase with the increasing amylose content [17, 19, 20]. In other words, waxy starches (composed almost entirely of amylopectin) have generally the lowest G' and G'' values [18]. The rheological behavior of starch during gelatinization is also determined by the lipids and proteins in starch. The peak G' of maize starch occurs at a higher temperature as the protein content of starch increases because the protective effect of proteins on starch granular integrity [21]. The lipids in starch decrease the G' and G'' values during cooking, due to the formation of amylose–lipid complexes, which inhibits the swelling of starch granules [22].

The fluid rheology of starch is of special significance for improving the quality of food [23]. In general, the fluid behavior of starch at steady-state flow is studied after starch gelatinization [24]. Viscosity is an important parameter to characterize the rheological behaviors of starch paste, considering starch is widely used as thickener

in yoghurt, breads, puddings, and other foods. After heating, the viscosity of starch paste shows generally a non-Newtonian fluid behavior that the shear stress fails to increase linearly with increasing shear rate [13]. The Bingham model, power law model, and Herschel–Bulkley model are used to the mathematically model the rheology of starch pastes [25]. Under steady-state shearing, starch pastes formed exhibit decreasing viscosity with increasing shear rate (i.e., shear-thinning behavior) [26], which is caused by shear-induced disruption of the swollen granules and leached starch components orienting themselves in the direction of stirring. The steady-state viscosity of starch pastes increases with increasing starch concentration, whereas it decreases at higher temperature [26, 27].

Upon cooling and storage, starch paste can form a viscoelastic gel. The elastic modulus (G') is an important indicator of gel strength. During retrogradation, the gelation of amylose firstly favors the development of starch gel structure [28], so the G' value of starch gel increases generally with increasing amylose content [29]. Then, the recrystallization of amylopectin is beneficial to the long-term development of gel structure [30]. Almost all non-waxy starches at a concentration of 6–8 wt% can form strong gels after retrogradation [31, 33]. Additives can also affect the viscoelasticity of starch gels. The addition of salt to starch leads to the difference in starch gel structures. The gel strength of starch increased as Na_2SO_4 , MgCl_2 , CaCl_2 , NaCl , and KCl were added into the starch but decreased with the addition of NaI , NaSCN , KI , and KSCN [32]. Fatty acids are conducive to the formation of starch gel [33], whereas sugars decrease the gel strength of starch [34].

3 Pasting Properties of Starch

Under controlled temperature profiles and shear forces, the changes that occur in starch-water systems throughout gelatinization and granule disruption are defined as pasting [35]. The pasting properties of starch can be quantified by measuring the viscosity of starch suspensions during heating and cooling. During heating, the viscosity increases to maximum and then decreases with further heating as a function of the changes in starch granules [36]. During cooling, the viscosity of starch paste increases with time, which is indicative of starch retrogradation [37]. A Rapid Visco Analyser (RVA) is most commonly used in the routine analysis of starch pasting properties. The RVA profiles provide information on pasting temperature (T_p), peak viscosity (PV, ability of granules to swell before rupturing), breakdown (BD, stability of hot paste to shear force), setback (SB, initial retrogradation of starch paste on cooling), and final viscosity (FV) [30].

Pasting properties of starch are determined by the starch structures. Amylopectin is the main component responsible for swelling of starch granules and increases in viscosity during heating, whereas amylose is often intertwined with amylopectin, limiting the swelling of starch granules. Hence, the peak viscosity (PV) of a starch paste decreases with increasing amylose content, such that waxy starches generally display a lower T_p and higher PV than the corresponding non-waxy starch

[38]. Upon cooling, a non-waxy starch has a greater setback (SB) value than its waxy variety, which is due to the amylose primarily favoring the short-term development of starch gel during cooling. Lipids, phosphomonoesters, and other minor components in starch granules have significant effects on the pasting behavior. During heating, amylose–lipid complexes that may have formed can be entangled with amylopectin molecules, inhibiting granule swelling and resulting in the increase of paste temperature (T_p) and the decrease of peak viscosity (PV). Wheat and barley starches showed higher T_p and lower PV than other normal cereal starches. The larger amounts of phospholipids in these two starches bind readily to amylose [39]. However, as the endogenous lipids of wheat starch are removed by sodium dodecyl sulfate, the starch exhibits similar T_p and PV compared with cassava starch and waxy corn starch [40, 41]. In contrast, the potato starch is negatively charged and mutually exclusive between granules as a result of the presence of phosphomonoesters in starch molecules, which can enhance the swelling of starch granules, greatly decrease the T_p , and increase the PV. Additionally, the large granule size of potato starch also contributes to the great increase of PV during cooking.

The presence of food additives such as proteins, lipids, salts, or sugars has also been shown to play a significant role in improving the pasting properties of starch. Addition of proteins generally retards the pasting process of starches, which is due to the competition for water between proteins and starch granules inhibiting the progression of starch gelatinization, leading to the delayed formation of viscosity peak [42]. As mentioned above, the addition of lipids increases the pasting temperature and decreases the viscosity of starch paste due to the formation of amylose–lipid complexes, which impede the swelling of starch granules [32, 43]. Recently, starch–protein–lipid ternary complexes have attracted attention due to interactions among these macronutrients during cooking influencing sensory, texture, and digestibility properties of finished foods. The formed starch–protein–fatty acid ternary complexes show higher viscosities than those of binary complex during the cooling and holding stages due to the emulsifying action of proteins [42, 44]. The addition of sugars such as sucrose, glucose, fructose, maltose, galactose, and lactose can increase the viscosity of starch [45, 46]. During cooking, the salt had the least effect on the pasting properties of almost all starches [40, 47]. However, the cation of salt can shield the negative charge of phosphomonoesters and reduce the charge repulsion, resulting in the formation of a low viscosity of potato starch paste [48].

4 Textural Properties of Starch

Textural properties of starch gels are very important criteria to evaluate the performance of starch in a food system. Upon retrogradation, non-waxy starch pastes transform into a firm gel of tree-dimensional networks, whereas waxy starch pastes form a soft gel consisting of aggregates [49]. In general, stronger starch gels are associated with higher amylose content [50]. Amylose-based networks provide the

elasticity and strength of starch gels against deformation [49], while soft gels containing aggregates show greater penetration, stickiness, and adhesion [30]. Amylose retrogradation determines the initial hardness of a starch gel and the stickiness and digestibility of processed foods [30]. On the other hand, retrogradation of amylopectin determines the long-term development of gel structure and crystallinity of processed starch involving in the staling of bread and cakes [51].

Texture profile analysis (TPA) is the most commonly used to study the textural properties of starch gels and starch-based food systems. In a TPA test, the sample is subjected to twice cyclic processes of exerting and removing compressive force, and five primary characteristics of a gel are obtained: hardness, cohesiveness, adhesiveness, elasticity (also called springiness), and brittleness (also called fracturability) [30]. Moreover, several additional texture characteristics such as gumminess (hardness \times cohesiveness) and chewiness (hardness \times cohesiveness \times springiness) can be derived [30]. Among these texture characteristics, the hardness of starch gels has an important role in the classification of sensory and quality of starch-based foods [14]. In general, the hardness of starch is positively correlated with starch concentration [52]. As mentioned above, due to amylose crystallization (short-term) and amylopectin retrogradation (long-term), the hardness of starch gels increases with time [13]. The hardness of starch gels increases during the initial stage of storage at a constant temperature but then changes only slightly on longer storage [53]. In comparison, freeze-thaw cycle treatment results in hardness developing and remaining more or less the same during the whole process [54]. Under the same conditions, maize, wheat, and potato starches show similar hardness values which are higher compared with that of a tapioca starch gel [52]. This is due to the relatively low amylose content of tapioca starch and the large loss of granular integrity in the gel [55].

In contrast to amylose content, lipid content is negatively correlated with gel hardness. The formation of amylose–lipid complexes reduces the amount of amylose available for network formation [40]. Additives such as sugars are commonly used in starch-based foods in order to optimize the process operation and cause some textural modification [45]. The increased gel hardness in wheat and potato starch in the presence of sucrose, glucose, and glycerol has been reported [45]. This increased gel hardness has been attributed to the formation of a strong amylose gel matrix network via changes of conformational ordering and intermolecular association of amylose chains [45]. Polymeric constituents of food, such as proteins, also affect the textural properties of the starch gel. A mixed gel of oat starch and skim milk powder was harder than mixed gels of oat starch–whey protein concentrate and of oat starch–whey lactalbumin mixed gels [4], which is explained as being due to casein micelles, soluble milk minerals, and lactose in milk providing more junction zones for an intermolecular association of amylose continuous network [45].

5 Relationship with Food Quality

Starch is widely used in many food formulations to improve quality attributes and shelf-life. The two main uses are as thickening and gelling agents which are determined by the rheological, pasting, and textural properties of starch. After heating to above the gelatinization temperature, starch suspensions can develop significant viscosity. The viscosity of the resultant starch paste determines its thickening power of starch for various applications [56]. As thickening agents, starch has been used in soups, gravies, salad dressings, sauces, and toppings. The shear thinning behavior of starch paste is also of practical relevance for many food products, such as processed cheeses, yoghurts, and foods produced by extrusion [5, 57]. After cooling and storage, some starch pastes can form viscoelastic gels. Maize starch gels with different hardness have been classified into the five dietary groups, which provides valuable information on standard criteria and guidelines for diets customized for the elderly [14]. As a gelling agents, starch is extensively used in products like jam, jelly, marmalade, and restructured and low-calorie foods [58].

6 Conclusions

This chapter provides a summary of the rheological, pasting, and textural properties of starch. The relationship of these properties with food quality contributes to an understanding of starch functionality and its applications in the food industry. In complex food systems, the rheological, pasting properties, and texture of starches are influenced by other food components such as proteins, lipids, and salts, which affect the quality and shelf-life of food. Therefore, future work should construct a food model composed of starch and other food components, investigating the effect of the interactions among food constituents on the functionality of starch and the quality of relevant starch-based foods.

Acknowledgments The authors gratefully acknowledge the financial support from the National Natural Science Foundation of China (31871796) and Natural Science Foundation of Tianjin City (17JCQJC45600).

References

1. Liu W, Budtova T. Dissolution of unmodified waxy starch in ionic liquid and solution rheological properties. *Carbohydr Polym.* 2013;93(1):199–206.
2. Pérez S, Bertoft E. The molecular structures of starch components and their contribution to the architecture of starch granules: a comprehensive review. *Starch-Stärke.* 2010;62(8):389–420.
3. Berski W, Ziobro R. Pasting and gel characteristics of normal and waxy maize starch in glucose syrup solutions. *J Cereal Sci.* 2018;79:253–8.

4. Kumar L, Brennan M, Zheng H, Brennan C. The effects of dairy ingredients on the pasting, textural, rheological, freeze-thaw properties and swelling behaviour of oat starch. *Food Chem.* 2018;245:518–24.
5. Considine T, Noisuwan A, Hemar Y, Wilkinson B, Bronlund J, Kasapis S. Rheological investigations of the interactions between starch and milk proteins in model dairy systems: a review. *Food Hydrocoll.* 2011;25(8):2008–17.
6. Ren F, Dong D, Yu B, Hou Z, Cui B. Rheology, thermal properties, and microstructure of heat-induced gel of whey protein-acetylated potato starch. *Starch-Stärke.* 2017;69(9–10):1600344.
7. Hoover R, Hughes T, Chung HJ, Liu Q. Composition, molecular structure, properties, and modification of pulse starches: a review. *Food Res Int.* 2010;43(2):399–413.
8. Wiesenborn DP, Orr PH, Casper HH, Tacke BK. Potato starch paste behavior as related to some physical/chemical properties. *J Food Sci.* 1994;59(3):644–8.
9. Wang S, Luo H, Zhang J, Zhang Y, He Z, Wang S. Alkali-induced changes in functional properties and in vitro digestibility of wheat starch: the role of surface proteins and lipids. *J Agric Food Chem.* 2014;62(16):3636–43.
10. Kaur L, Singh N, Sodhi NS. Some properties of potatoes and their starches II. Morphological, thermal and rheological properties of starches. *Food Chem.* 2002;79(2):183–92.
11. Kong X, Kasapis S, Bao J, Corke H. Influence of acid hydrolysis on thermal and rheological properties of amaranth starches varying in amylose content. *J Sci Food Agric.* 2012;92(8):1800–7.
12. Nep EI, Ngwuluka NC, Kemas CU, Ocheke NA. Rheological and structural properties of modified starches from the young shoots of *Borassus aethiopicum*. *Food Hydrocoll.* 2016;60:265–70.
13. Li G, Zhu F. Effect of high pressure on rheological and thermal properties of quinoa and maize starches. *Food Chem.* 2018;241:380–6.
14. Kim Y, Kim HJ, Cho W, Ko S, Park SK, Lee S. Classification of starch gel texture for the elderly diets based on instrumental and sensory methodology. *J Texture Stud.* 2017;48(5):357–61.
15. Tabilo-Munizaga G, Barbosa-Cánovas GV. Rheology for the food industry. *J Food Eng.* 2005;67(1–2):147–56.
16. Ai Y, Jane JL. Gelatinization and rheological properties of starch. *Starch-Stärke.* 2015;67(3–4):213–24.
17. Singh J, Singh N. Studies on the morphological, thermal and rheological properties of starch separated from some Indian potato cultivars. *Food Chem.* 2001;75(1):67–77.
18. Singh N, Singh J, Kaur L, Singh Sodhi N, Singh GB. Morphological, thermal and rheological properties of starches from different botanical sources. *Food Chem.* 2003;81(2):219–31.
19. Tsai ML, Li CF, Lif CY. Effects of granular structures on the pasting behaviors of starches. *Cereal Chem.* 1998;74(6):750–7.
20. Freitas RA, Paula RC, Feitosa JPA, Rocha S, Sierakowski MR. Amylose contents, rheological properties and gelatinization kinetics of yam (*Dioscorea alata*) and cassava (*Manihot utilissima*) starches. *Carbohydr Polym.* 2004;55(1):3–8.
21. Singh N, Shevkani K, Kaur A, Thakur S, Parmar N, Singh VA. Characteristics of starch obtained at different stages of purification during commercial wet milling of maize. *Starch-Stärke.* 2014;66(7–8):668–77.
22. Singh J, Singh N, Saxena SK. Effect of fatty acids on the rheological properties of corn and potato starch. *J Food Eng.* 2002;52(1):9–16.
23. Marcotte M, Art H, Ramaswamy HS. Rheological properties of selected hydrocolloids as a function of concentration and temperature. *Food Res Int.* 2001;34(8):695–703.
24. Lagarrigue S, Alvarez G. The rheology of starch dispersions at high temperatures and high shear rates: a review. *J Food Eng.* 2001;50(4):189–202.
25. Che LM, Li D, Wang LJ, Özkan N, Chen XD, Mao ZH. Rheological properties of dilute aqueous solutions of cassava starch. *Carbohydr Polym.* 2008;74(3):385–9.

26. Nguyen QD, Jensen CTB, Kristensen PG. Experimental and modelling studies of the flow properties of maize and waxy maize starch pastes. *Chem Eng J*. 1998;70(2):165–71.
27. Dintzis FR, Bagley EB. Effects of thermomechanical processing on viscosity behavior of corn starches. *J Rheol*. 1995;39(6):1483–95.
28. Hansen LM, Hosney RC, Faubion JM. Oscillatory rheometry of starch-water systems: effect of starch concentration and temperature. *Cereal Chem*. 1991;68(4):347–51.
29. Lu ZH, Sasaki T, Li YY, Yoshihashi T, Li LT, Kohyama K. Effect of amylose content and rice type on dynamic viscoelasticity of a composite rice starch gel. *Food Hydrocoll*. 2009;23(7):1712–9.
30. Wang S, Li C, Copeland L, Niu Q, Wang S. Starch retrogradation: a comprehensive review. *Compr Rev Food Sci Food Saf*. 2015;14(5):568–85.
31. Wang YJ, White P, Pollak L. Physicochemical properties of starches from mutant genotypes of the Oh43 inbred line. *Cereal Chem*. 1993;70(2):199–203.
32. Ahmad FB, Williams PA. Effect of salts on the gelatinization and rheological properties of sago starch. *J Agric Food Chem*. 1999;47(8):3359–66.
33. Ai Y, Hasjim J, Jane JL. Effects of lipids on enzymatic hydrolysis and physical properties of starch. *Carbohydr Polym*. 2013;92(1):120–7.
34. Ahmad FB, Williams PA. Effect of sugars on the thermal and rheological properties of sago starch. *J Agric Food Chem*. 1999;49(3):401–12.
35. Wang S, Copeland L. Effect of acid hydrolysis on starch structure and functionality: a review. *Crit Rev Food Sci Nutr*. 2015;55(8):1081–97.
36. Adebowale KO, Lawal OS. Functional properties and retrogradation behaviour of native and chemically modified starch of mucuna bean (*Mucuna pruriens*). *J Sci Food Agric*. 2003;83(15):1541–6.
37. Singh J, Kaur L, McCarthy OJ. Factors influencing the physico-chemical, morphological, thermal and rheological properties of some chemically modified starches for food applications-a review. *Food Hydrocoll*. 2007;21(1):1–22.
38. Collado LS, Mabesa RC, Corke H. Genetic variation in the physical properties of sweet potato starch. *J Agric Food Chem*. 1999;47(10):4195.
39. Jane JL, Chen YY, Lee LF, Mcpherson AE, Wong KS, Radosavljevic M, et al. Effects of amylopectin branch chain length and amylose content on the gelatinization and pasting properties of starch. *Cereal Chem*. 1999;76(5):629–37.
40. Ai Y, Nelson B, Birt DF, Jane JL. In *vitro* and in *vivo* digestion of octenyl succinic starch. *Carbohydr Polym*. 2013;98(2):1266–71.
41. Debet MR, Gidley MJ. Three classes of starch granule swelling: influence of surface proteins and lipids. *Carbohydr Polym*. 2006;64(3):452–65.
42. Wang S, Yu J, Cai J, Wang S, Chao C, Copeland L. Toward a better understanding of starch-monoglyceride-protein interactions. *J Agric Food Chem*. 2018;66(50):13253–9.
43. Chao C, Yu J, Wang S, Copeland L, Wang S. Mechanisms underlying the formation of complexes between maize starch and lipids. *J Agric Food Chem*. 2018;66(1):272–8.
44. Zheng M, Chao C, Yu J, Copeland L, Wang S, Wang S. Effects of chain length and degree of unsaturation of fatty acids on structure and in *vitro* digestibility of starch-protein-fatty acid complexes. *J Agric Food Chem*. 2018;66(8):1872–80.
45. Gunaratne A, Ranaweera S, Corke H. Thermal, pasting, and gelling properties of wheat and potato starches in the presence of sucrose, glucose, glycerol, and hydroxypropyl β -cyclodextrin. *Carbohydr Polym*. 2007;70(1):112–22.
46. Chantaro P, Pongsawatmanit R. Influence of sucrose on thermal and pasting properties of tapioca starch and xanthan gum mixtures. *J Food Eng*. 2010;98(1):44–50.
47. Jyothi AN, Sasikiran K, Sajeev MS, Revamma R, Moorthy SN. Gelatinisation properties of cassava starch in the presence of salts, acids and oxidising agents. *Starch-Stärke*. 2005;57(11):547–55.
48. Shi X, Bemiller JN. Effects of food gums on viscosities of starch suspensions during pasting. *Carbohydr Polym*. 2002;50(1):7–18.

49. Tang MC, Copeland L. Investigation of starch retrogradation using atomic force microscopy. *Carbohydr Polym.* 2007;70(1):1–7.
50. Sandhu K, Singh N. Some properties of corn starches II: Physicochemical, gelatinization, retrogradation, pasting and gel textural properties. *Food Chem.* 2007;101(4):1499–507.
51. Fadda C, Sanguinetti AM, Del Caro A, Collar C, Piga A. Bread staling: updating the view. *Compr Rev Food Sci Food Saf.* 2014;13(4):473–92.
52. Waterschoot J, Gomand SV, Fierens E, Delcour JA. Production, structure, physicochemical and functional properties of maize, cassava, wheat, potato and rice starches. *Starch-Stärke.* 2015;67(1–2):14–29.
53. Singh H, Lin JH, Huang WH, Chang YH. Influence of amylopectin structure on rheological and retrogradation properties of waxy rice starches. *J Cereal Sci.* 2012;56(2):367–73.
54. Park EY, Baik BK, Lim ST. Influences of temperature-cycled storage on retrogradation and in vitro digestibility of waxy maize starch gel. *J Cereal Sci.* 2009;50(1):43–8.
55. Karam LB, Grossmann MVE, Silva RSSF, Ferrero C, Zaritzky NE. Gel textural characteristics of corn, cassava and yam starch blends: a mixture surface response methodology approach. *Starch-Stärke.* 2005;57(2):62–70.
56. Kaur A, Shevkani K, Singh N, Sharma P, Kaur S. Effect of guar gum and xanthan gum on pasting and noodle-making properties of potato, corn and mung bean starches. *J Food Sci Technol.* 2015;52(12):8113–21.
57. Kumar L, Brennan MA, Mason SL, Zheng H, Brennan CS. Rheological, pasting and micro-structural studies of dairy protein-starch interactions and their application in extrusion-based products: a review. *Starch-Stärke.* 2017;69(1–2):1600273.
58. Saha D, Bhattacharya S. Hydrocolloids as thickening and gelling agents in food: a critical review. *J Food Sci Technol.* 2010;47(6):587–97.

Starch Modification and Application



Shujun Wang, Jinwei Wang, Yi Liu, and Xia Liu

Abstract Starch occurs widely in nature and is the second largest biomass on earth after cellulose and one of the most abundant bio-renewable materials. The properties of native starch do not always meet the requirements for a multitude of industrial applications. Functional limitations of native starch can be overcome by modifications to broaden its applications in papermaking, pharmaceuticals, medicine, food, and other industries. In this chapter, we describe in detail the main methods for the modification of starch used in recent years. These methods involve physical, chemical, and biological modifications. We also discuss applications of modified starch in industries and propose potential applications of modified starch materials for the future.

Keywords Starch · Physical modification · Chemical modification · Biological modification · Starch applications

1 Introduction

Starch, a major storage reserve polysaccharide in plants, is used widely in the food and nonfood industries [1–3]. Native starch is used as a texture stabilizer and conditioner in food systems, but limitations such as low shear resistance, thermal resistance, and high tendency towards retrogradation limit its use in industrial applications [4, 5]. To overcome these deficiencies and widen the utilization of starch, physical, chemical, and enzymatic modifications of native starch are carried out [6]. Physical modifications are usually environmentally “green” and safe for industrial production and are simple and easy for commercialization. Physical modifications include hydrothermal (heat-moisture and annealing), microwave, ultrahigh pressure (UHP), irradiation, and ultrasonic treatment. Chemical

S. Wang (✉) · J. Wang · Y. Liu · X. Liu

State Key Laboratory of Food Nutrition and Safety, Tianjin University of Science and Technology, Tianjin, China

e-mail: sjwang@tust.edu.cn

© Springer Nature Singapore Pte Ltd. 2020

S. Wang (ed.), *Starch Structure, Functionality and Application in Foods*,

https://doi.org/10.1007/978-981-15-0622-2_8

modifications are mostly practiced for food starches, generally by derivatization such as etherification, esterification, cross-linking, oxidization, and acid hydrolysis of starch [7]. Enzymatic modification mainly involves treatment of starch using hydrolyzing enzymes, showing several advantages including fewer by-products, more specific hydrolysis products, and higher yield, better process control, and finalized products with specific characteristics [8]. The most common enzymes for starch modification include endo- and exo-amylases, debranching enzymes, and transferases.

All of these modification methods tend to change the starch structures and therefore affect functional properties and digestibility of starch, which determine the applications of starch in food industries. This chapter will summarize the definitions and classifications of modified starches by considering physical, chemical, and enzymatic treatment and their applications in food systems.

2 Physical Modification of Starch

The physical modification of starch refers to as treatments of starch by means of thermal mechanical force or physical field and does not result in breakdown or chemical reaction of the D-glucopyranosyl units of the starch polymer molecules [9]. Starch physical modification is generally divided into three categories: hydrothermal treatment, physical field treatment, and other physical treatments (Fig. 1). After physical modification, starch functionality is often altered differently, depending on the extent of modification [9].

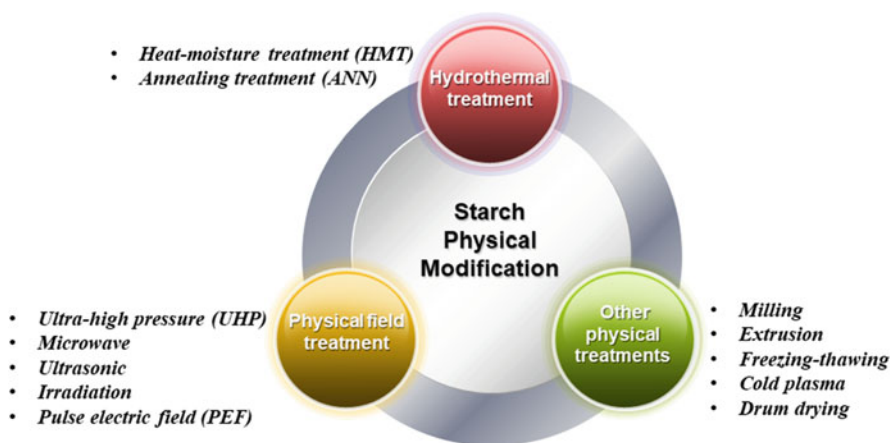


Fig. 1 Common physical modification of starch

2.1 Heat-Moisture Treatment (HMT)

Heat-moisture treatment (HMT) is a process in which starch with a low moisture content (water content $\leq 35\%$) is heated at temperatures of 80–140 °C for 15 min ~ 72 h [9–11]. The factors that influence the effects of HMT on starch include the type of starch, amylose content, heating temperature, water content, and so on. In some studies, HMT did not damage the morphology of starch granules, including the size and shape of starch granules [12, 13]. However, other studies have shown that potato and corn starch granules had cracked after HMT [14]. Through repeated HMT of sweet potato starch, the more repetitions, the more serious the damage of starch granules [15]. These changes in morphology may be due to partial gelatinization of starch granules. The impact of HMT on gelatinization characteristics is not consistent, for example, the enthalpy changes (ΔH) of starch increase, decrease, or even remain unchanged after HMT treatment. Regarding the decrease in ΔH , one explanation is that HMT destroys some of the double helices present in crystalline and amorphous regions in starch granules [13]. Another explanation is that gelatinization occurs in the process of HMT, in which unstable amylose and amylopectin molecules become disorganized [16]. Generally, HMT leads to an increase in the thermal transition temperatures (onset temperature (T_o), peak temperature (T_p), and conclusion temperature (T_c)) of starch. There are two reasons for this. Firstly, the unstable starch granules are disrupted, leading to the remaining stable granules requiring higher temperatures to be broken down [17]. Secondly, crystallite perfections may occur, which then need higher temperatures for disruption [18]. A recent study showed that HMT destroys the long- and short-range ordered structure of wheat and yam starches [17] and changed other functional properties, such as decreasing starch solubility, swelling power, amylose leaching, and peak viscosity (PV).

2.2 Annealing Treatment

Annealing (ANN) is a process in which starch is heated with excess water to below the gelatinization temperature of starch but above the glass transition temperature [19–21]. The annealing conditions reported in different references vary greatly. The temperature has a great influence on the effect of annealing. Usually, the higher annealing the temperature is, the more obvious the changes of the structure and functional properties of the starch after annealing are. Several studies showed that annealing does not change the morphology of starch granules [22–24], while some studies found that pores on the surface of the starch granules became larger and more numerous [25–27]. In most studies, the ΔH of starch remained unchanged or increased after annealing, whereas few studies reporting ΔH decreased. Annealing increases T_o , T_p , and T_c and decreases the gelatinization temperature change ($\Delta T: T_c - T_o$), which is due to the formation of more complete crystallites [27]. Most

studies showed that the crystallinity of annealed starch remained unchanged or increased, rather than decreased. Annealing can result in the transformation of the crystalline type of starch, for example, ANN increased the content of B-type polymorph in C-type starch [25] and changed A + B type to A-type pattern [27–29]. Similar to HMT, annealing treatment decreased solubility, swelling power, amylose leaching, and peak viscosity of starch.

2.3 *Ultrahigh Pressure Treatment*

Ultrahigh pressure (UHP) technology was initially used to sterilize and kill enzymes. Regardless of the size and shape of samples, UHP can uniformly and instantaneously act on starch granules. Gelatinization of starch occurs when the pressure reaches a certain level [30, 31]. With increasing pressure, the degree of structural destruction gradually increases. When the starch is completely gelatinized, swollen starch granule is often observed to remain relatively intact [32, 33]. This is a typical characteristic of starch treated by UHP compared with other treatments. After UHP treatment, A-type and C-type starch often presents the characteristic XRD peaks of B-type polymorph, whereas B-type starch often remains unchanged [31, 34–37]. This may be due to a small amount of B-type starch naturally present in the A-type or C-type starch [34], which is disrupted preferentially compared with the more resistant B-type starch. After the A-type starch is gelatinized, the B-type starch is highlighted. There is little information on the influence of UHP on texture properties, swelling power, and viscosity.

2.4 *Microwave Treatment*

Microwaves are electromagnetic waves with a frequency range between 300 and 300,000 MHz. Microwaves interact with polar molecules and charge particles of food to generate heat. Frequency, water content, and treatment time are the main factors affecting starch modification in microwave treatment [38, 39]. When treated at a low temperature (≤ 65 °C), the morphology of starch (e.g., wheat starch) granules was little changed [38, 39]. When the temperature is high enough (≥ 90 °C), the starch granules swelled and may be completely destroyed [38, 40]. Under low moisture (water content $\leq 35\%$), microwave treatment is in some ways similar to HMT. In this case, starch crystallites become more ordered than the native starch. The XRD pattern for B-type potato starch changes into A-type, whereas the pattern for A-type maize starches remained unchanged [41, 42]. These changes in X-ray pattern may be attributed to (1) loss of water from the central channel of the B-unit cell and (2) the double helices move into the central channel, which was initially occupied by the vaporized water molecules [41]. Generally, microwave treatment causes damage to starch structure, with the

higher frequency and moisture content leading to the greater degree of damage. Starch treated with microwave showed decreased melting enthalpy, swelling power, and solubility and increased gelatinization temperatures.

2.5 *Gamma Irradiation Treatment*

Gamma irradiation can produce free radicals to alter the starch structure. Gamma irradiation hardly causes evident morphological changes in starch granules. However, some studies indicated that the surface of the starch granule showed cracks or holes [43, 44]. The relative crystallinity decreases with the increase of radiation dose. In most studies, gamma irradiation had little or no effect on T_o , T_p , T_c , and ΔH [45–47]. The swelling power and viscosity parameters were observed to decrease in most reports [48–50].

2.6 *Ultrasonic Treatment*

Ultrasound is a sound wave of frequency that is higher than 16 kHz, which is inaudible to human ears. Ultrasonic treatment hardly changes the size and shape of starch granules but leads to holes on the surface of starch granules [51, 52]. An important reason for the change of starch granules is cavitation (formation of bubbles of gases) [53]. The effects on relative crystallinity are related to the time and intensity of treatment and the environment. In most studies, ultrasound decreases viscosity and increases solubility and the swelling power of starch. The effect of ultrasound on starch thermal properties is contradictory and remains to be further explored.

2.7 *Other Methods*

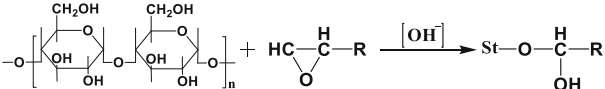
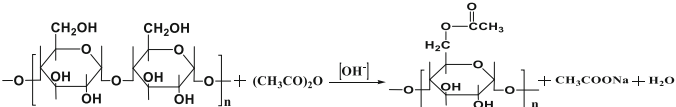
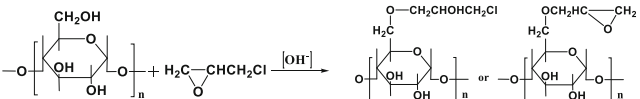
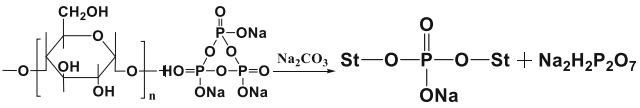
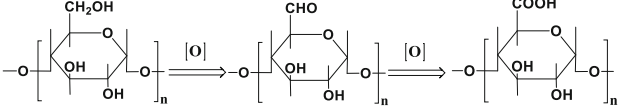
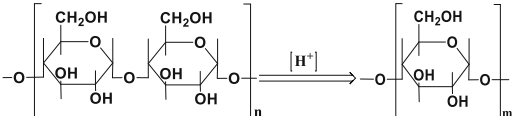
During processing of grains or starchy materials, starch granule can also be modified physically. Milling is a very important process for cereal grains. During the milling of cereal grains or starch alone, starch granules are often damaged, leading to the disruption of starch crystallites and granule morphology. The degree of damage to starch is dependent on the time of grinding and the magnitude of mechanical force [54, 55]. Extrusion is a processing technology for starch modification or preparation of some low moisture cereal-based foods. During extrusion, starch granules are gelatinized, and amylopectin molecules are fragmented due to high pressure, temperature, and mechanical force during extrusion [56, 57]. Drum drying as a method for food processing is found to change the functional properties of starch, which are determined by the water content, drying time, and temperature [58]. Other methods,

such as freezing-thawing [59], cold plasma [60], and pulsed electric field [61] treatments are also reported and still remain to be studied.

3 Chemical Modification of Starch

The chemical and functional changes by chemical substitution of starch depend on the source of starch, reaction conditions (reactant concentration, reaction time, pH, and presence of catalyst), substituent types, degree of substitution, and distribution of substituent in the starch molecules [62]. Some chemical modification reactions of starch are presented in Table 1.

Table 1 Representative chemical modifications of starch

Modification type	Reaction scheme
Etherification	
Esterification	
Cross-linking	<p>A</p>  <p>B</p> 
Oxidation	
Acid hydrolysis	

St Starch

3.1 *Etherification*

Hydroxypropylated starches (HPS) are usually prepared by etherifying native starch with propylene oxide in the presence of an alkaline catalyst [63]. The introduction of hydroxypropyl groups of starch chains destroys the inter- and intramolecular hydrogen bonds, thereby weakening the starch granular structure, resulting in increased freedom of movement of starch chains in amorphous regions [63].

3.2 *Esterification*

Starch esterification involves the conversion of three available hydroxyl groups of glucosyl residues to alkyl or aryl derivatives. Acetylation is one of the popular chemical methods of starch esterification, which is achieved with either acetic anhydride or vinyl acetate in the presence of an alkaline catalyst such as NaOH, $\text{Ca}(\text{OH})_2$, and Na_2CO_3 [64, 65]. Acetylated starch can be divided into three types according to the degree of substitution (DS). Low DS (0.01–0.2) starch esters, which are soluble in cold water, are the most common type of acetylated starch [66]. Starch acetates with low DS are usually synthesized by using acetate anhydride in an alkaline solution. Native starch is activated by the alkali to generate a more reactive starch alkoxide derivative that reacts with acetic anhydride to form starch acetates [67]. Medium DS (0.1–0.3) starch esters are generally less water-soluble than the low DS starch esters [68]. The high DS (2–3) starch esters are insoluble in water but are soluble in organic solvents. Acetylation occurs mainly in the amorphous regions and the outer lamellae of crystalline regions [69]. The acetylation introduces bulky acetyl groups onto starch chains, resulting in structural reorganization due to steric hindrance; this leads to the repulsion between starch molecules, which promotes the penetration of water into the amorphous regions of granules and increases the swelling capacity [70]. After acetylation, swelling power and solubility of corn, potato, and rice starches were increased greatly [71, 72]. In addition to the DS values, the differences in the granule size distribution, physicochemical composition, and granule stiffness between starches may also account for the changes in swelling power and solubility of acetylated starch. Waxy starch shows increased swelling power after acetylation because amylopectin in waxy starch has a more open structure than in non-waxy starch, which allows rapid water penetration and increases swelling power [73].

Starch modification with the dicarboxylic acid anhydride, such as octenyl succinic anhydride (OSA), is a desirable form of starch esterification. OSA can react with starch to form OSA starch containing both hydrophilic and hydrophobic groups [74, 75]. Amphiphilic polymers have a wide range of industrial applications, especially in emulsification, encapsulation, films and coatings, and gel production. In recent years, OSA starch has attracted much attention due to its desirable stability, encapsulation, interface, heat, nutrition, and rheological properties [76].

3.3 *Cross-Linking*

Cross-linking is a commonly used chemical modification method, in which native starch reacts with various reagents such as sodium trimetaphosphate (STMP), sodium tripolyphosphate (STPP), epichlorohydrin (ECH), and phosphoryl chloride (POCl_3). In the presence of neutral salts and at $\text{pH} > 11$, POCl_3 is an efficient cross-linking agent [4]. STMP is also an efficient cross-linking agent and one of the most important food additives [4]. ECH is poorly soluble in water and partially decomposes into glycerol; hence water-soluble POCl_3 and STMP are often used preferentially. In addition, the ECH cross-links are found to be less uniformly distributed compared with STMP ones [77]. In cross-linking reaction using ECH and STMP, both reagents attack inside the starch granules, whereas cross-linking with POCl_3 only occurs on the surface of the granule [78]. The final products are usually divided into three categories based on the cross-linking agents used. The first is mono-starch phosphate, which is prepared by esterifying starch with orthophosphoric acid, sodium or potassium orthophosphate, or STPP. The second category is starch diphosphate, which is produced when native starch reacts with STMP or POCl_3 . The third type of cross-linked starch is starch diphosphate, which results from combination of starch monophosphate and starch diphosphate. The type of cross-linking agents is the major determinant for the changes in functional properties of treated starches. The viscosity of the cross-linked starch prepared with STMP and STPP drops to close to zero, the gelatinization temperatures are increased, and enthalpy of gelatinization is slightly decreased [79]. Generally, cross-linking plays a key part of altering the properties of native starches, such as increased solubility, thermomechanical shearing, and paste stability [80, 81].

3.4 *Oxidation*

Starch oxidation involves the introduction of carbonyl and carboxyl functional groups onto starch chains and the depolymerization of starch molecules. The most commonly used oxidants include potassium permanganate, sodium hypochlorite, hydrogen peroxide, and persulfate. The properties of oxidized starch derivatives may be improved, depending on the method of oxidation and the properties of reagents used [82]. The oxidation reaction occurs primarily at the C-2, C-3, and C-6 hydroxyls on a D-glucopyranosyl unit [83]. Oxidized starch has a lower viscosity, better paste stability and film-forming ability, and lower molecular weight compared with the original starch. Sodium hypochlorite is the oldest and most popular commercial oxidant. Factors that affect hypochlorite oxidation include temperature, pH, hypochlorite concentration, source, and structure of starch [7]. Compared with native starch, sodium hypochlorite-oxidized soybean starch exhibits decreased pasting temperature, peak and breakdown viscosities, and gelatinization and retrogradation enthalpies [84]. Ozonized starch has similar pasting properties as chemically

oxidized starch with a low concentration of sodium hypochlorite and had no toxic residues [85]. Starch subjected to 10 min of ozonolysis is comparable to the starch prepared by the commonly alkaline oxidation method [86].

3.5 *Acid Hydrolysis*

Acid hydrolysis is one of the oldest starch modification methods, with the derived degradation products having many applications. Preparation of acid-thinned starch involves treating the concentrated starch paste (36–40% solids) in an inorganic acid solution (HCl or H₂SO₄) at a temperature below the gelatinization temperature for a specified time, depending on the required viscosity or degree of conversion [67]. The mechanism of acid hydrolysis involves the attack of glucosidic oxygen atoms of starch by hydroxide ion, causing the cleavage of starch chains. Acid hydrolysis of starch proceeds by randomly cleaving both α -(1,4) and α -(1,6) bonds and shortening the chain length over time. The α -(1,4) bonds and amorphous regions containing α -(1,6) bonds are more accessible to acid penetration and hydrolysis. Acid modification involves a two-stage attack on starch granules. Both amylose and amylopectin are attacked in the early stages of acid hydrolysis, whereas attack preferentially occurs in the amorphous regions followed by the crystalline regions at a slower rate [87].

Acid hydrolysis causes a significant increase in double helix content, due to the preferential hydrolysis of amorphous regions and retrogradation of free amylose that is released [88]. When starch granules are subjected to acid hydrolysis, the relative crystallinity increases with hydrolysis time. Several hypotheses have been proposed to interpret the increased crystallinity in the early stages of acid hydrolysis. Firstly, the cleavage of some amylose chains running through the amorphous region may allow the newly released chain ends rearrange into a more crystalline structure. Secondly, the reordering of crystal structure during acid hydrolysis may lead to an increase in crystallinity because the water channels in the crystallite cavities are partially filled by double helices. Thirdly, an increase in crystallinity may also be due to the retrogradation of hydrolyzed free amylose into double helices, which rearrange into crystalline regions that are resistant to acid hydrolysis. Acid hydrolysis modifies the structure of starches, making them behave differently when heated in water, such as decreased intrinsic viscosity and hot paste viscosity and increased gel strength and water solubility and film-forming ability [89].

4 Enzymatic Modification for Starch

During enzymatic modification of starch, enzymes such as α -amylase (AM), β -amylase, glucoamylase, debranching enzymes, cyclodextrin glycosyltransferase, and glucose isomerase are often used. The enzymatic hydrolysis of starch and its derivatives is shown in Fig. 2.

4.1 Endo- and Exo-amylases

The endo-amylases can cleave α -(1,4) glycosidic bonds within amylose and amylopectin chains but not the α -(1,6) glycosidic bonds in amylopectin [90]. The products of hydrolysis are oligosaccharides of varying chain lengths and have the α -configuration on the C-1 of the reducing glucose unit produced. The α -amylase (1, 4- α -D-glucan glucanohydrolases) is a well-known endo-amylase, which hydrolyzes in a random fashion at any (1,4)-linkages within the starch chain to rapidly reduce the molecular size of starch [8]. The α -amylase can generate pores at the surface of starch granules, with pore size depending on the type and level of enzyme used [91].

The exo-amylases either exclusively cleave α -(1,4) glycosidic bonds such as β -amylase or cleave both α -(1,4) and α -(1,6) glycosidic bonds from the nonreducing ends of the starch chains such as amyloglucosidase (AMG) or glucoamylase and α -glucosidase. Exo-amylases act on the external glucose residues of amylose or amylopectin and thus produce only glucose (glucoamylase and α -glucosidase), or maltose and β -limit dextrin (β -amylase) [92]. β -Amylase (1, 4- α -D-glucan

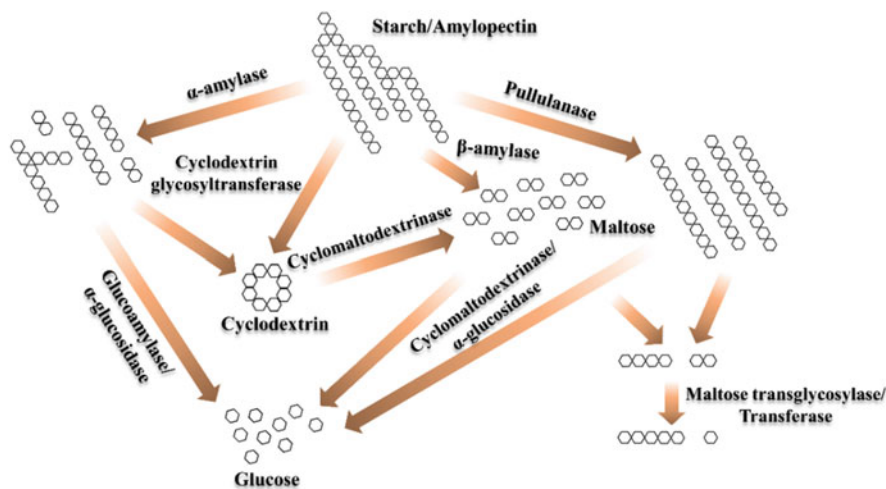


Fig. 2 Enzymatic hydrolysis of starch and its derivatives

maltohydrolases) and glucoamylase/amyloglucosidase (1, 4- α -D-glucan glucosidase, AMG) are well-known exo-amylases and also convert the anomeric configuration of the liberated maltose from α to β . The former can only hydrolyze α -(1,4) glycosidic bonds, while the latter not only hydrolyze α -(1,4) glycosidic bonds but also hydrolyze α -(1,6) glycosidic bonds and α -(1,3) glycosidic bonds. Glucoamylase and α -glucosidase have different substrate preferences: α -glucosidase preferentially acts on short maltooligosaccharides and releases glucose with an α -configuration, while glucoamylase specifically hydrolyzes long-chain polysaccharides. Glucoamylases have also been found in a variety of microorganisms [92]. β -Amylases are widely found in higher plants and also in certain microorganisms such as some *Bacillus* strains and *Clostridium thermosulfurogenes*; the latter is found to produce amylases with thermostable properties [93, 94]. The enzyme modification by β -amylase/transglucosidase results in many cracks on the starch granule surface. The enzymatically modified starch has higher solubility but lower swelling capacity and pasting viscosity compared with native starch [91]. Enzymatic treatment of corn starch increased gelatinization temperatures and enthalpy change [8].

Cyclodextrins are produced by an intramolecular transglycosylation reaction in which the enzyme cleaves the α -1,4 glycosidic bond and connects both reducing and nonreducing ends [95, 96]. Cyclodextrins with neither reducing ends nor nonreducing ends are resistant to amylolytic enzymes. Cyclomaltodextrinase catalyzes the hydrolysis of cyclodextrins to form the corresponding linear maltooligosaccharides. In contrast to the extensive information on amylolytic enzymes, research on cyclomaltodextrinase is limited to a few microorganisms. To date, only two strains, *Bacillus macerans* and *Bacillus coagulans*, are known to produce this enzyme [97, 98].

4.2 Debranching Enzymes

The debranching enzymes isoamylase and type I pullulanase exclusively hydrolyze α -(1,6) glycosidic bonds. The major difference between pullulanase and isoamylase is the ability to hydrolyze pullulan, a polysaccharide with a repeating unit of maltotriose that is α -(1,6) linked [99, 100]. Pullulanase was first discovered in 1961 [101] and has attracted great interest due to its specific action on the α -(1,6) glycosidic bonds in starch, amylopectin, pullulan, and related oligosaccharides, which, during the saccharification process, has enables a complete and efficient conversion of the branched polysaccharides into small fermentable sugars [102]. Pullulanase is produced by mesophilic organisms like *Klebsiella aerogenes* [101]. The optimum temperature for maximum activity of pullulanase is around 60 °C, which is very beneficial for the saccharification of starch to generate glucose syrups in the industry. Pullulanase is generally used in combination with amyloglucosidase and α - or β -amylase [90, 101, 103]. Isoamylase, discovered in 1949, is elaborated by a number of microorganisms like *K. aerogenes* and *Pseudomonas* spp. and can only hydrolyze the α -(1, 6) bond in amylopectin [104]. These

enzymes specifically degrade amylopectin to produce linear glucans. Glucoamylase from *Sclerotium rolfisii* has also been found to have an important effect on pullulan [105].

4.3 *Transferases*

Transferases hydrolyze an α -(1,4) glycosidic bond of a donor molecule and transfer the cleaved residue from the donor to a glycosidic acceptor with the formation of a new glycosidic bond. Enzymes such as amyloamylase and cyclodextrin glycosyltransferase form a new α -(1,4) glycosidic bond [104]. Cyclodextrin glycosyltransferases have very low hydrolytic activity and produce cyclic oligosaccharides with six, seven, or eight glucose residues and highly branched, high molecular weight cyclodextrin glycosyltransferase limit dextrans. In terms of the type of enzymatic reaction, amyloamylase is very similar to cyclodextrin glycosyltransferase. The major difference is that amyloamylase performs a transglycosylation reaction to produce a linear product, while cyclodextrin glycosyltransferase generates a cyclic product [106, 107].

5 Applications of Modified Starch

Changes of starch functional properties are accomplished by modification reactions, of which physical modifications are green and efficient methods. UHP reduces the swelling and viscosity of starch. Microwaves change the morphology and crystallinity of starch, while ultrasound modifies the swelling of granules and pastes. Milling and extrusion can also physically modify starch granules. Physical modification of starch has been used widely for the preparation of various noodles, convenience foods, and fried foods. For noodles, high paste viscosity and breakdown, low gelatinization temperature, and high starch swelling power are ideal characteristics [108]. Baking biscuits is similar to HMT. The degree of gelatinization is small due to the low water content and a relatively low baking temperature [109]. Starch can be used to produce environmentally friendly edible films. Films require starch with high amylose content to achieve favorable tensile strength and elongation, characteristics that can be obtained by modification reactions [110, 111].

Demands for chemically modified starches are increasing the growth of food industries [6]. Etherification improves the clarity of starch pastes, increases viscosity, reduces syneresis, and increases freeze-thaw stability [112]. Therefore, it is widely used in food applications such as gravy, dipping, sauces, fruit pie fillings, and puddings. Esterification results in lower gelatinization temperature and retrogradation, lower tendency to form gels, and higher paste clarity [113], which makes it useful as an emulsion stabilizer in refrigerated and frozen foods and for packaging. Cross-linked starch has higher stability of granules towards swelling, high

temperature, and high shear and acidic conditions [114]; it is used widely as viscosifiers and texturizers in soups, sauces, gravies, bakery, and dairy products [4]. Oxidized starch has low viscosity, high clarity, and low temperature stability [115] and can be used in batter and bread for coating various foodstuffs, in confectionery as binders and film formers, and in dairy as texturizers. Acid-hydrolyzed starch has low paste viscosity and high gel strength and water solubility, which makes it useful as gelling agent in the production of gum and processed cheese loaves, as fat replacers/fat mimetic in low-fat butter spread/margarine, low-fat mayonnaise, low-fat milk type products, and low-fat ice cream, as well as in slowly digestible cookies that are rich in resistant starch [89].

Enzymatic modification of starch has many applications in the food industry as a green method. Originally, α -amylases were added during dough preparation to generate fermentable compounds. α -Amylases also have an anti-stalling effect on bread baking, and they improve the softness retention of baked goods [116]. In addition to the saccharification or liquefaction of starch, these enzymes are also used to prepare viscous and stable starch solutions for the sizing of textile fibers, the clarification of haze formed in beer or fruit juices, and the pretreatment of animal feed to improve digestibility. Starch is treated with α -amylase and transglucosidase to produce new branched structures with a slowly digestible character [117]. The fungal α -amylase (AM) or amyloglucosidase (AMG) to obtain porous starch is used in a variety of food applications [8]. The most important uses of glucoamylase are the production of high-glucose syrups (96–98% glucose) and high-fructose syrups (55% fructose) [118, 119]. Cyclomaltodextrinase was used to modify rice starch to produce low-amylose starch products. The complex formed by organic molecules with cyclomaltodextrins can stabilize light-, heat-, and oxygen-sensitive materials in starch granules and provide slow release property besides providing special tastes, odors, and flavors to the starch granules. The branching enzyme is claimed to increase shelf life and loaf volume of baked goods. The main application of pullulanase is starch saccharification, and the most important industrial application of pullulanase is the production of high-glucose (30–50% glucose; 30–40% maltose) or high-maltose (30–50% maltose; 6–10% glucose) syrups [104, 120]. Pullulanase also finds minor applications in the manufacturing of low-calorie beer and in the baking industry as the anti-stalling agent to improve texture, volume, and flavor of bakery products [104]. It is expected that starch modified with amyloamylases may find application in the food industry as a plant-based alternative to gelatin. Amyloamylase-treated potato starch showed thermoreversible gelation at concentrations of 3% (w/v) or more, thus making it comparable to gelatin [121]. Amyloamylase-modified potato starch has been used as a fat replacer and enhancer of creaminess in yoghurt [122]. The cyclodextrin glycosyltransferases were mainly used for the industrial production of cyclodextrins. Cyclodextrin glycosyltransferases can also be used to produce novel glycosylated compounds. One commercial application is the glycosylation of the potent sweetener stevioside, isolated from the leaves of the plant *Stevia rebaudiana*, thereby increasing solubility and reducing bitterness [123].

6 Conclusions

The inherent defects of native starches, such as insolubility in cold water, low shear resistance, high tendency to retrograde, and high glycemic response after cooking, can be overcome by physical, chemical, or enzymatic modification. The modification of starch improves the functional properties of native starch or delivers new functionality to modified starches. Hence, the modified starches have been used widely in many food and nonfood industries. In the future, novel modification methods or techniques are required to produce starches with more diversified and promising properties for wider industrial applications.

References

1. Burrell MM. Starch: the need for improved quality or quantity-an overview. *J Exp Bot.* 2003;54(382):451–4566.
2. Balat M, Balat H, Öz C. Progress in bioethanol processing. *Prog Energy Combust Sci.* 2008;34(5):551–73.
3. Wang J, Ren F, Yu J, Copeland L, Wang S, Wang S. Toward a better understanding of different dissolution behavior of starches in aqueous ionic liquids at room temperature. *ACS Omega.* 2019;4(6):11312–9.
4. Singh J, Kaur L, McCarthy OJ. Factors influencing the physico-chemical, morphological, thermal and rheological properties of some chemically modified starches for food applications-a review. *Food Hydrocoll.* 2007;21(1):1–22.
5. Wang J, Ren F, Huang H, Wang Y, Copeland L, Wang S, et al. Effect of CaCl_2 pre-treatment on the succinylation of potato starch. *Food Chem.* 2019;288:291–6.
6. Abbas KA, Khalil SK, Anis Shobirin MH. Modified starches and their usages in selected food products: a review study. *J Agric Sci.* 2010;2(2):90–100.
7. Ashogbon AO, Akintayo ET. Recent trend in the physical and chemical modification of starches from different botanical sources: a review. *Starch-Stärke.* 2014;66(1–2):41–57.
8. Dura A, Blaszcak W, Rosell CM. Functionality of porous starch obtained by amylase or amyloglucosidase treatments. *Carbohydr Polym.* 2014;101(2):837–45.
9. Anil G. Heat-moisture treatment of starch. In: Sui Z, Kong X, editors. *Physical modifications of starch.* Singapore: Springer; 2018. p. 15–36.
10. Jacobs H, Delcour JA. Hydrothermal modifications of granular starch, with retention of the granular structure: a review. *J Agric Food Chem.* 1998;46(8):2895–905.
11. Silva WM, Biduski B, Lima KO, Pinto VZ, Hoffmann JF, Vanier NL, et al. Starch digestibility and molecular weight distribution of proteins in rice grains subjected to heat-moisture treatment. *Food Chem.* 2017;219(15):260–7.
12. Ams B, Bartz J, Radunz M, Evangelho JAD, Pinto VZ, Zavareze EDR, et al. Impact of heat-moisture treatment on rice starch, applied directly in grain paddy rice or in isolated starch. *LWT-Food Sci Technol.* 2015;60(2):708–13.
13. Gunaratne A, Hoover R. Effect of heat–moisture treatment on the structure and physicochemical properties of tuber and root starches. *Carbohydr Polym.* 2002;49(4):425–37.
14. Kawabata A, Takase N, Miyoshi E, Sawayama S, Kimura T, Kudo K. Microscopic observation and X-ray diffractometry of heat/moisture-treated starch granules. *Starch-Stärke.* 1994;46(12):463–9.

15. Huang TT, Zhou DN, Jin ZY, Xu XM, Chen HQ. Effect of repeated heat-moisture treatments on digestibility, physicochemical and structural properties of sweet potato starch. *Food Hydrocoll.* 2016;54:202–10.
16. Hormdok R, Noomhorm A. Hydrothermal treatments of rice starch for improvement of rice noodle quality. *LWT-Food Sci Technol.* 2007;40(10):1723–31.
17. Wang S, Wang S, Guo P, Liu L, Wang S. Multiscale structural changes of wheat and yam starches during cooking and their effect on in vitro enzymatic digestibility. *J Agric Food Chem.* 2017;65(1):156–66.
18. Sun Q, Dai L, Nan C, Xiong L. Effect of heat moisture treatment on physicochemical and morphological properties of wheat starch and xylitol mixture. *Food Chem.* 2014;143:54–9.
19. Jayakody L, Hoover R. Effect of annealing on the molecular structure and physicochemical properties of starches from different botanical origins-a review. *Carbohydr Polym.* 2008;74(3):691–703.
20. Tester RF, Debon SJ. Annealing of starch-a review. *Int J Biol Macromol.* 2000;27(1):1–12.
21. Tester RF, Debon SJJ, Karkalas J. Annealing of wheat starch. *J Cereal Sci.* 1998;28(3):259–72.
22. Wang S, Wang J, Yu J, Wang S. A comparative study of annealing of waxy, normal and high-amylose maize starches: the role of amylose molecules. *Food Chem.* 2014;164(20):332–8.
23. Jayakody L, Hoover R, Liu Q, Donner E. Studies on tuber starches III. Impact of annealing on the molecular structure, composition and physicochemical properties of yam (*Dioscorea sp.*) starches grown in Sri Lanka. *Carbohydr Polym.* 2009;76(1):145–53.
24. Adebowale KO, Afolabi TA, Oluowolabi BI. Hydrothermal treatments of finger millet (*Eleusine coracana*) starch. *Food Hydrocoll.* 2005;19(6):974–83.
25. Wang S, Wang J, Wang S, Wang S. Annealing improves paste viscosity and stability of starch. *Food Hydrocoll.* 2017;62:203–11.
26. Xu M, Saleh ASM, Gong B, Li B, Jing L, Gou M, et al. The effect of repeated versus continuous annealing on structural, physicochemical, and digestive properties of potato starch. *Food Res Int.* 2018;111:324–33.
27. Waduge RN, Hoover R, Vasanthan T, Gao J, Li J. Effect of annealing on the structure and physicochemical properties of barley starches of varying amylose content. *Food Res Int.* 2006;39(1):59–77.
28. Genkina NK, Wasserman LA, Noda T, Tester RF, Yuryev VP. Effects of annealing on the polymorphic structure of starches from sweet potatoes (*Ayamurasaki* and *Sunnyred* cultivars) grown at various soil temperatures. *Carbohydr Res.* 2004;339(6):1093–8.
29. Gomes AMM, Silva CEMD, Ricardo NMPS, Sasaki JM, Germani R. Impact of annealing on the physicochemical properties of unfermented cassava starch ("*Polvilho Doce*"). *Starch-Stärke.* 2004;56(9):419–23.
30. Douzals J, Marechal P, Coquille J, Gervais P. Microscopic study of starch gelatinization under high hydrostatic pressure. *J Agric Food Chem.* 1996;44(6):1403–8.
31. Katopo H, Song Y, Jane JL. Effect and mechanism of ultrahigh hydrostatic pressure on the structure and properties of starches. *Carbohydr Polym.* 2002;47(3):233–44.
32. Stute R, Heilbronn, Klingler RW, Boguslawski S, Eshtiaghi MN, Knorr D. Effects of high pressures treatment on starches. *Starch-Stärke.* 1996;48(11–12):399–408.
33. Stolt M, Oinonen S, Autio K. Effect of high pressure on the physical properties of barley starch. *Innovative Food Sci Emerg Technol.* 2000;1(3):167–75.
34. Wang J, Zhu H, Li S, Wang S, Wang S, Copeland L. Insights into structure and function of high pressure-modified starches with different crystalline polymorphs. *Int J Biol Macromol.* 2017;102:414–24.
35. Guo Z, Zeng S, Lu X, Zhou M, Zheng M, Zheng B. Structural and physicochemical properties of lotus seed starch treated with ultra-high pressure. *Food Chem.* 2015;186(1):223–30.
36. Li W, Zhang F, Liu P, Bai Y, Gao L, Shen Q. Effect of high hydrostatic pressure on physicochemical, thermal and morphological properties of mung bean (*Vigna radiata L.*) starch. *J Food Eng.* 2011;103(4):388–93.

37. Hibi Y, Matsumoto T, Hagiwara S. Effect of high pressure on the crystalline structure of various starch granules. *Cereal Chem.* 1993;70(6):671–6.
38. Palav T, Seetharaman K. Mechanism of starch gelatinization and polymer leaching during microwave heating. *Carbohydr Polym.* 2006;65(3):364–70.
39. Anderson AK, Guraya HS. Effects of microwave heat-moisture treatment on properties of waxy and non-waxy rice starches. *Food Chem.* 2006;97(2):318–23.
40. Lewandowicz G, Jankowski T, Fornal J. Effect of microwave radiation on physico-chemical properties and structure of cereal starches. *Carbohydr Polym.* 2000;42(2):193–9.
41. Luo Z, He X, Fu X, Luo F, Gao Q. Effect of microwave radiation on the physicochemical properties of normal maize, waxy maize and amylomaize V starches. *Starch-Stärke.* 2006;58(9):468–74.
42. Lewandowicz G, Fornal J, Walkowski A. Effect of microwave radiation on physico-chemical properties and structure of potato and tapioca starches. *Carbohydr Polym.* 1997;34(4):213–20.
43. Chung HJ, Liu Q. Molecular structure and physicochemical properties of potato and bean starches as affected by gamma-irradiation. *Int J Biol Macromol.* 2010;47(2):214–22.
44. Lee JS, Ee ML, Chung KH, Othman Z. Formation of resistant corn starches induced by gamma-irradiation. *Carbohydr Polym.* 2013;97(2):614–7.
45. Chung HJ, Liu Q. Effect of gamma irradiation on molecular structure and physicochemical properties of corn starch. *J Food Sci.* 2010;74(5):353–61.
46. Kong X, Zhou X, Sui Z, Bao J. Effects of gamma irradiation on physicochemical properties of native and acetylated wheat starches. *Int J Biol Macromol.* 2016;91:1141–50.
47. Bashir K, Aggarwal M. Physicochemical, thermal and functional properties of gamma irradiated chickpea starch. *Int J Biol Macromol.* 2017;97:426–33.
48. Polesi LF, Junior MDDM, Sarmiento SBS, Canniatti-Brazaca SG. Starch digestibility and physicochemical and cooking properties of irradiated rice grains. *Rice Sci.* 2017;24(1):48–55.
49. Gul K, Singh AK, Sonkawade RG. Physicochemical, thermal and pasting characteristics of gamma irradiated rice starches. *Int J Biol Macromol.* 2016;85:460–6.
50. Byungryol B, Yu JY, Hyunseong Y, Juwoon L, Myungwoo B, Baik BK, et al. Physicochemical properties of waxy and normal maize starches irradiated at various pH and salt concentrations. *Starch-Stärke.* 2010;62(1):41–8.
51. Sujka M, Jamroz J. Ultrasound-treated starch: SEM and TEM imaging, and functional behaviour. *Food Hydrocoll.* 2013;31(2):413–9.
52. Sujka M. Ultrasonic modification of starch-impact on granules porosity. *Ultrason Sonochem.* 2017;37:424–9.
53. Zhu J, Li L, Chen L, Li X. Study on supramolecular structural changes of ultrasonic treated potato starch granules. *Food Hydrocoll.* 2012;29(1):116–22.
54. Tran TTB, Shelat KJ, Tang D. Milling of rice grains. The degradation on three structural levels of starch in rice flour can be independently controlled during grinding. *J Agric Food Chem.* 2011;59(8):3964–73.
55. Li E, Dhital S, Hasjim J. Effects of grain milling on starch structures and flour/starch properties. *Starch-Stärke.* 2014;66(1–2):15–27.
56. Thymi S, Krokida MK, Pappa A, Maroulis ZB. Structural properties of extruded corn starch. *J Food Eng.* 2005;68(4):519–26.
57. Gomez MH, Aguilera JM. A physicochemical model for extrusion of corn starch. *J Food Sci.* 1984;49(1):40–3.
58. Valous NA, Gavrieliidou MA, Karapantsios TD, Kostoglou M. Performance of a double drum dryer for producing pregelatinized maize starches. *J Food Eng.* 2002;51(3):171–83.
59. Kumar L, Brennan M, Zheng H, Brennan C. The effects of dairy ingredients on the pasting, textural, rheological, freeze-thaw properties and swelling behaviour of oat starch. *Food Chem.* 2018;245:518–24.
60. Thirumdas R, Trimukhe A, Deshmukh RR, Annapure US. Functional and rheological properties of cold plasma treated rice starch. *Carbohydr Polym.* 2017;157:1723–31.

61. Han Z, Zeng XA, Yu SJ, Zhang BS, Chen XD. Effects of pulsed electric fields (PEF) treatment on physicochemical properties of potato starch. *Innov Food Sci Emerg Technol.* 2009;10(4):481–5.
62. Huber KC, Bemiller JN. Location of sites of reaction within starch granules. *Cereal Chem.* 2001;78(2):173–80.
63. Seow CC, Thevamalar K. Internal plasticization of granular rice starch by hydroxypropylation: effects on phase transitions associated with gelatinization. *Starch-Stärke.* 2010;45(3):85–8.
64. Huang J, Schols HA, Jin Z, Sulmann E, Agj V. Characterization of differently sized granule fractions of yellow pea, cowpea and chickpea starches after modification with acetic anhydride and vinyl acetate. *Carbohydr Polym.* 2007;67(1):11–20.
65. Wang Y, Wang L. Characterization of acetylated waxy maize starches prepared under catalysis by different alkali and alkaline-earth hydroxides. *Starch-Stärke.* 2015;54(1):25–30.
66. Elomaa M, Asplund T, Soininen P, Laatikainen R, Peltonen S, Hyvarinen S, et al. Determination of the degree of substitution of acetylated starch by hydrolysis, ¹H NMR and TGA/IR. *Carbohydr Polym.* 2004;57(3):261–7.
67. Thirathumthavorn D, Charoenrein S. Thermal and pasting properties of acid-treated rice starches. *Starch-Stärke.* 2005;57(5):217–22.
68. Pu H, Chen L, Li X. An oral xolon-targeting controlled release system based on resistant starch acetate: synthesization, characterization, and preparation of film-coating pellets. *J Agric Food Chem.* 2011;59(10):5738–45.
69. Chen ZG, Schols HA, Agj V. Differently sized granules from acetylated potato and sweet potato starches differ in the acetyl substitution pattern of their amylose populations. *Carbohydr Polym.* 2004;56(2):219–26.
70. Lawal OS. Succinyl and acetyl starch derivatives of a hybrid maize: physicochemical characteristics and retrogradation properties monitored by differential scanning calorimetry. *Carbohydr Res.* 2004;339(16):2673–82.
71. Singh J, Kaur L, Singh N. Effect of acetylation on some properties of corn and potato starches. *Starch-Stärke.* 2004;6(12):586–601.
72. González Z, Pérez E. Effect of acetylation on some properties of rice starch. *Starch-Stärke.* 2015;54(3–4):148–54.
73. Liu H, Ramsden L, Corke H. Physical properties of cross-linked and acetylated normal and waxy rice starch. *Starch-Stärke.* 1999;51(7):249–52.
74. Bhosale R, Singhal R. Effect of octenylsuccinylation on physicochemical and functional properties of waxy maize and amaranth starches. *Carbohydr Polym.* 2007;68(3):447–56.
75. Sweedman MC, Tizzotti MJ, Schäfer C, Gilbert RG. Structure and physicochemical properties of octenyl succinic anhydride modified starches: a review. *Carbohydr Polym.* 2013;92(1):905–20.
76. Wang S, Li T, Wang S, Copeland L. Effects of hydrothermal-alkali and freezing-thawing pre-treatments on modification of corn starch with octenyl succinic anhydride. *Carbohydr Polym.* 2017;175:361–9.
77. Shiftan D, Ravenelle F, Mateescu MA, Marchessault RH. Change in the V/B polymorph ratio and T₁ relaxation of epichlorohydrin crosslinked high amylose starch excipient. *Starch-Stärke.* 2015;52(6–7):186–95.
78. Carmona-Garcia R, Sanchez-Rivera MM, Méndez-Montelvo G, Garza-Montoya B, Bello-Pérez LA. Effect of the cross-linked reagent type on some morphological, physicochemical and functional characteristics of banana starch (*Musa paradisiaca*). *Carbohydr Polym.* 2009;76(1):117–22.
79. Shi M, Gu F, Wu J, Yu S, Gao Q. Preparation, physicochemical properties, and in vitro digestibility of cross-linked resistant starch from pea starch. *Starch-Stärke.* 2013;65(11–12):947–53.
80. Ratnayake WS, Jackson DS. Phase transition of cross-linked and hydroxypropylated corn (*Zea mays L.*) starches. *LWT-Food Sci Technol.* 2008;41(2):346–58.

81. Majzoobi M, Radi M, Farahnaky A, Jamalians J, Tongdang T. Physico-chemical properties of phosphoryl chloride cross-linked wheat starch. *Iran Polym J*. 2009;18(6):491–9.
82. Santanderortega MJ, Stauner T, Loretz B, Ortegavinuesa JL, Bastosgonzález D, Wenz G, et al. Nanoparticles made from novel starch derivatives for transdermal drug delivery. *J Control Release*. 2010;141(1):85–92.
83. Kuakpetoon D, Wang YJ. Characterization of different starches oxidized by hypochlorite. *Starch-Stärke*. 2015;53(5):211–8.
84. Adebawale KO, Lawal OS. Functional properties and retrogradation behaviour of native and chemically modified starch of mucuna bean (*Mucuna Pruriens*). *J Sci Food Agric*. 2003;83(83):1541–6.
85. Chan HT, Bhat R, Karim AA. Physicochemical and functional properties of ozone-oxidized starch. *J Agric Food Chem*. 2009;57(13):5965–70.
86. Oladebeye AO, Oshodi AA, Amoo IA, Karim AA. Functional, thermal and molecular behaviours of ozone-oxidised cocoyam and yam starches. *Food Chem*. 2013;141(2):1416–23.
87. Wang L, Wang YJ. Structures and physicochemical properties of acid-thinned corn, potato and rice starches. *Starch-Stärke*. 2015;53(11):570–6.
88. Atichokudomchai N, Varavinit S, Chinachoti P. A study of ordered structure in acid-modified tapioca starch by ¹³C CP/MAS solid-state NMR. *Carbohydr Polym*. 2004;58(4):383–9.
89. Wang S, Copeland L. Effect of acid hydrolysis on starch structure and functionality: a review. *Crit Rev Food Sci Nutr*. 2015;55(8):1081–97.
90. Norman BE. The use of debranching enzymes in dextrose syrup production. *Starch-Stärke*. 1982;157–79.
91. Keeratiburana T, Hansen AR, Soontaranon S, Blennow A, Tongta S. Porous high amylose rice starch modified by amyloglucosidase and maltogenic α -amylase. *Carbohydr Polym*. 2020;230:115611.
92. Pandey A, Soccol CR, Soccol VT. Biopotential of immobilized amylases. *Indian J Microbiol*. 2000;40(1):1–14.
93. Hyun HH, Zeikus JG. Regulation and genetic enhancement of beta-amylase production in *Clostridium thermosulfurogenes*. *J Bacteriol*. 1985;164(3):1162–70.
94. Taniguchi H, Odashima F, Igarashi M, Maruyama Y, Nakamura M. Characterization of a potato starch-digesting bacterium and its production of amylase. *J Agric Chem Soc Jpn*. 1982;46(8):2107–015.
95. Jacob J, Geßler K, Hoffmann D, Sanbe H, Koizumi K, Smith SM, et al. Band-flip and kink as novel structural motifs in α -(1 \rightarrow 4)-d-glucose oligosaccharides. Crystal structures of cyclodeca- and cyclotetradecaamylose. *Carbohydr Res*. 1999;322(3–4):228–46.
96. Veen BAVD, Uitdehaag JCM, Dijkstra BW, Dijkhuizen L. Engineering of cyclodextrin glycosyltransferase reaction and product specificity. *Biochim Biophys Acta*. 2000;1543(2):336–60.
97. Kitahata S, Taniguchi M, Beltran SD, Sugimoto T, Okada S. Purification and some properties of cyclodextrinase from *Bacillus coagulans*. *J Agric Chem Soc Jpn*. 1983;47(7):1441–7.
98. Depinto JA, Campbell LL. Purification and properties of the cyclodextrinase of *Bacillus macerans*. *Biochemistry*. 1968;7(1):121–5.
99. Bender H, Lehmann J, Wallenfels K. Pullulan, an extracellular glucan from *Pullularia pullulans*. *Biochim Biophys Acta*. 1959;36(2):309–16.
100. Barnett C, Smith A, Scanlon B, Israillides CJ. Pullulan production by *Aureobasidium pullulans* growing on hydrolysed potato starch waste. *Carbohydr Polym*. 1999;38(3):203–9.
101. Saha BC, Zeikus JG. Novel highly thermostable pullulanase from thermophiles. *Trends Biotechnol*. 1989;7(9):234–9.
102. Hii SL, Tan JS, Ling TC, Ariff AB. Pullulanase: role in starch hydrolysis and potential industrial applications. *Enzyme Res*. 2012;2012(1):921362.
103. Hassan KS, James B. Effect of pullulanase and α -amylase on hydrolysis of waxy corn starch. *Starch-Stärke*. 2010;42(12):482–6.

104. Maarel MJEC, Bvd V, JCM U, Leemhuis H, Dijkhuizen L. Properties and applications of starch-converting enzymes of the α -amylase family. *J Biotechnol.* 2002;94(2):137–55.
105. Kelkar HS, Deshpande MV. Purification and characterization of a pullulan-hydrolyzing glucoamylase from *Sclerotium rolfssii*. *Starch-Stärke.* 1993;45(10):361–8.
106. Kaur B, Ariffin F, Bhat R, Karim AA. Progress in starch modification in the last decade. *Food Hydrocoll.* 2012;26(2):398–404.
107. Takaha T, Smith SM. The functions of 4- α -glucanotransferases and their use for the production of cyclic glucans. *Biotechnol Genet Eng Rev.* 1999;16(1):257–80.
108. Panozzo JF, McCormick KM. The rapid viscoanalyser as a method of testing for noodle quality in a wheat breeding programme. *J Cereal Sci.* 1993;17(1):25–32.
109. Luyten H, Vliet TV. Influence of a filler on the rheological and fracture properties of food materials. In: Carter RE, editor. *Rheology of food, pharmaceutical and biological materials with general rheology.* Barking: Elsevier Applied Science; 1990. p. 43–56.
110. Dhall RK. Advances in edible coatings for fresh fruits and vegetables: a review. *Crit Rev Food Sci Nutr.* 2013;53(5):435–50.
111. Jiménez A, Talens P, Chiralt A. Edible and biodegradable starch films: a review. *Food Bioprocess Technol.* 2012;5(6):2058–76.
112. Lee HL, Yoo B, Lee HL, Yoo B. Effect of hydroxypropylation on physical and rheological properties of sweet potato starch. *LWT-Food Sci Technol.* 2011;44(3):765–70.
113. Shah A, Masoodi FA, Gani A, Ashwar BA. Physicochemical, rheological and structural characterization of acetylated oat starches. *LWT-Food Sci Technol.* 2017;80:19–26.
114. Zhao J, Chen Z, Jin Z, Buwalda P, Gruppen H, Schols HA. Effects of granule size of cross-linked and hydroxypropylated sweet potato starches on their physicochemical properties. *J Agric Food Chem.* 2015;63(18):4646–54.
115. Sukhija S, Singh S, Riar CS. Effect of oxidation, cross-linking and dual modification on physicochemical, crystallinity, morphological, pasting and thermal characteristics of elephant foot yam (*Amorphophallus paeoniifolius*) starch. *Food Hydrocoll.* 2016;55:56–64.
116. Sahlstrom S, Brathen E. Effects of enzyme preparations for baking, mixing time and resting time on bread quality and bread staling. *Food Chem.* 1997;58(1):75–80.
117. Miao M, Xiong S, Jiang B, Jiang H, Cui SW, Zhang T. Dual-enzymatic modification of maize starch for increasing slow digestion property. *Food Hydrocoll.* 2014;38(6):180–5.
118. Abraham TE, Jamuna R, Bansilal CV, Ramakrishna SV. Continuous synthesis of glucoamylase by immobilized fungal mycelium of *Aspergillus niger*. *Starch-Stärke.* 2010;43(3):113–6.
119. Berghofer E, Sarhaddar S. Production of glucose and high fructose syrup by enzymatic direct hydrolysis of cassava roots. *Process Biochem.* 1988;23(6):188–94.
120. Gomes I, Gomes J, Steiner W. Highly thermostable amylase and pullulanase of the extreme thermophilic eubacterium *rhodothermus marinus*: production and partial characterization. *Bioresour Technol.* 2003;90(2):207–14.
121. Maarel MJEC, Capron I, GJW E, Bos HT, Kaper T, Binnema DJ, et al. A novel thermoreversible gelling product made by enzymatic modification of starch. *Starch-Stärke.* 2010;57(10):465–72.
122. Arnoc A, Velde FVD, Marjaw K, Maurits B, Leo M, Arjen S, et al. Improved creaminess of low-fat yoghurt: the impact of amyloamylase-treated starch domains. *Food Hydrocoll.* 2009;23(3):980–7.
123. Pedersen S, Dijkhuizen L, Dijkstra B, Jensen BF, Jørgensen ST. A better enzyme for cyclodextrins. *ChemTech.* 1995;25(12):19–25.

In Vitro Starch Digestion: Mechanisms and Kinetic Models



Bin Zhang, Haiteng Li, Shaokang Wang, Shahid Ahmed Junejo, Xingxun Liu, and Qiang Huang

Abstract This chapter briefly introduces the concept of “physiologically resistant starch” and “enzyme-resistant starch” and their health benefits. The emphasis of this chapter is two fundamental mechanisms which determine starch digestibility in food, including (1) physical barriers that slow down digestive enzyme access/binding to starch and (2) starch structural features that limit the enzyme action once bound to starch. Commonly used in vitro kinetic models and the starch digestive enzymes (i.e., pancreatic α -amylase and amyloglucosidase) are also discussed at the end of this chapter.

Keywords Starch digestion · Resistant starch · Digestion kinetics · Digestive enzymes

B. Zhang (✉)

School of Food Science and Engineering, Center for Discipline Innovation of Food Nutrition and Human Health (111 Center), Guangdong Province Key Laboratory for Green Processing of Natural Products and Product Safety, South China University of Technology, Guangzhou, China

Department of Applied Biology and Chemical Technology, The Hong Kong Polytechnic University, Kowloon, Hong Kong, China
e-mail: zhangb@scut.edu.cn

H. Li

Centre for Nutrition and Food Sciences, The University of Queensland, Brisbane, QLD, Australia

S. Wang · S. A. Junejo · Q. Huang

School of Food Science and Engineering, Center for Discipline Innovation of Food Nutrition and Human Health (111 Center), Guangdong Province Key Laboratory for Green Processing of Natural Products and Product Safety, South China University of Technology, Guangzhou, China

X. Liu

School of Food Science and Engineering, Nanjing University of Finance and Economics, Nanjing, China

1 Introduction

Starch is the most abundant nutrient in the global diet and provides most important source of energy in the human diet. Starch has multiple structure levels, from nm to mm size scales, including individual chains, double helices, crystalline and amorphous lamellae, blocklets, growth rings, and intact granules [1, 2]. During starch biosynthesis, starch chains assemble into the semicrystalline granules. The complex structure of starch contributes to its nutritional functionality, such as digestion rate and extent (location) in the human digestive tract, which further impacts on human health. The term physiologically resistant starch (RS) is defined as the portion of starch that cannot be absorbed in the small intestine of healthy individuals and becomes a fermentable substrate for colonic microbiota [3]. RS lowers the glycemic index and insulin responses, potentially reducing the risk of developing type 2 diabetes, obesity, and cardiovascular disease, as reviewed elsewhere [4]. Colonic fermentation of resistant starch into short-chain fatty acids particularly butyrate could protect colonic epithelial cells from DNA damage and lowers the risk of colon-related diseases [5, 6]. These health benefits stimulated the interest in both quantity and quality of dietary starch that maintains the state of good health of an individual. However, research on human starch digestion is very challenging due to the complexity of the human digestive system involving multiple enzymes and hormonal control. Therefore, RS is normally reported through *in vitro* methods that simulate *in vivo* conditions and referred as “enzyme-resistant starch (ERS).” It is noteworthy that ERS is a method-oriented and measurement concept. It is now known that the amount of ERS in a given starchy food is under kinetic rather than thermodynamic control. *In vitro* methods generally oversimplify the digestion conditions/mechanisms in human digestion tracts and may not completely reflect starch digestion *in vivo* [7–9]. However, *in vitro* digestion approach is practical and reproducible to evaluate RS level and understand rate-determining features of starch digestibility [10]. This chapter focuses on two fundamental mechanisms which determine starch digestibility (rate and extent) within a food matrix. Commonly used starch digestive enzymes (i.e., pancreatic α -amylase and amyloglucosidase) and *in vitro* kinetic models will be discussed as well.

2 Fundamental Mechanisms

Resistant starch can be classified into four categories based on the origins: physically inaccessible starch, granular (B- or some C-type polymorph) starch, retrograded starch, and chemically modified starch [11]. In recent years, starch–lipid complex was proposed to be a new resistant starch source [12–15]. While this traditional classification indicates that ERS is definitely indigestible during enzymatic digestion, recent evidences suggest that starch digestibility is controlled by kinetics [16, 17]. Enzymatic reaction involves several steps: diffusion of enzymes to the

solid surface, adsorption/binding, and catalysis. There are two fundamental mechanisms in determining the extent and rate of starch digestion [15, 18]: (1) barriers that slow down or prevent digestive enzyme access/binding to starch and (2) starch structural features that limit enzyme action after initial binding.

Within the starch granules or food matrices, there are multiple features that slow down or prevent diffusion and adsorption processes. For example, in raw plant-based foods, intact cell walls (e.g., whole or partly milled grains) hinder enzymatic diffusion, due to the limiting porosity of the wall matrix [19]. When starch is encapsulated in cell or tissue structure, intact plant cell wall restricts the enzyme diffusion in individual isolated legume cells [20]. In addition, the presence of other dietary components could also limit the enzymatic binding to starch, e.g., non-starch polysaccharides (e.g., arabinoxylans and β -glucan), which enhance viscosity and proteins which absorb amylases. For instance, the digestion kinetics has been observed to be slower in condensed protein products such as pasta [21]. According to current understanding, the diffusion and adsorption of the enzyme to the starch granule surface is a key step in granular starch hydrolysis [21]. The absence of pores and channels limits the accessibility of digestive enzymes, which is generally found in B-type granular starch, contributing to its resistant nature [22–26].

Starch structural features, such as local molecular density and chemical structure, also could slow down or prevent enzyme hydrolysis. The enzymatic resistance mechanism for the retrograded starch and starch–lipid complex is that double/single helices render the α -1,4 glucosidic linkages inaccessible to amylase. Crystallinity alone does not always result in an increase in ERS content, as evidenced by that high-amylose starches with reduced crystallinity have increased level of enzymatic resistance than counterparts [27–29]. It is suggested that the local molecular density of starch chains controls the digestion rate and extent, which represents another mechanism of achieving local molecular density [29]. Chemical modification (e.g., hydroxypropylation, octenylsuccinylation, and chemical cross-linking) involves the introduction of functional groups into the starch molecule, reducing the extent of the enzyme-catalyzed hydrolysis [30].

3 Starch Digestive Enzymes

For enzyme action on polymers, there are three distinct action patterns: single chain, multichain, and multiple-attack [31]. In the single chain action, once the enzyme forms an active enzyme-substrate (ES) complex, it catalyzes a reaction in a “zipper” fashion toward one end of the chain. The multichain pattern is the classical random action in which the enzyme catalyzes the hydrolysis of only one bond per effective encounter. In the multiple-attack action, once the enzyme is forming ES complex, the enzyme catalyzes the hydrolysis of several bonds before it dissociates and forms a new active ES complex with another polymer chain [31].

The digestion of starch or starch-containing food is achieved by two types of enzymes in the mammalian digestion tract: (a) salivary and pancreatic α -amylases

and (b) intestinal brush border glucoamylases, maltase-glucoamylase, and sucrase-isomaltase [32]. Two kinds of enzyme, i.e., porcine pancreatic or human salivary α -amylase and fungal amyloglucosidase, are normally adopted to mimic in vitro starch digestion. Amyloglucosidase is an exo-acting enzyme like the intestinal brush border enzymes that are not yet available commercially. The enzyme reaction is highly dependent on temperature and pH parameters, although the condition was generally fixed at the optimal pH and at the temperature around 37 °C [10]. The actions of two commercially used starch digestive enzymes used in in vitro digestion models, i.e., α -amylase and amyloglucosidase, are briefly reviewed here.

3.1 α -Amylase

Salivary and pancreatic α -amylases (EC 3.2.1.1) in mammals digest starch molecules endo-wisely at inner α -(1 \rightarrow 4) linkages of starch chains. The end products of α -amylase digestion have α -configuration at the anomeric carbon of the reducing end. However, product specificities of α -amylases depend on their sources, resulting from the differences in length, folding, and amino acid sequences of the enzyme protein [31]. Human salivary and porcine pancreatic α -amylases are two commercially available amylases for in vitro starch digestion/RS measurement, showing a multiple-attack digestion pattern on starch molecules [33]. The end products mainly are maltose, maltotriose, maltotetraose, and α -limit dextrins. Very little amount of glucose is released from α -amylase digestion. Only maltotriose and maltotetraose could be slowly converted to maltose and glucose after prolonged incubation through the subsidiary binding site (see Fig. 1). The former gives nearly three times as much glucose as the latter [34]. Porcine pancreatic α -amylase shows five D-glucose binding subsites, with catalytic groups located between the second and third subsites from the reducing end subsite (Fig. 1) [35]. Human salivary α -amylase shows six D-glucose binding subsites, and the catalytic groups are also located between the second and third subsites [36]. Porcine pancreatic α -amylase shows an average of seven hydrolytic cleavages occurring per productive encounter, and human salivary α -amylase shows three hydrolytic cleavages [31, 37].

3.2 Amyloglucosidase

Another starch degradation enzyme used in in vitro digestion is amyloglucosidase (EC 3.2.1.3) usually from *Aspergillus niger*. Amyloglucosidase-I (AMG-I) has an N-terminal starch-binding domain, which is for hydrolyzing granular starches and distinct from the active site (C-terminal catalytic domain) (see Fig. 2) [38]. It can hydrolyze both α -1,4 and α -1,6 glycosidic linkages and produces β -D-glucose from the nonreducing ends of starch chains. The specific activity toward the α -1,6 linkage is only 0.2% compared to the α -1,4 linkage [39]. Amyloglucosidase has a multichain

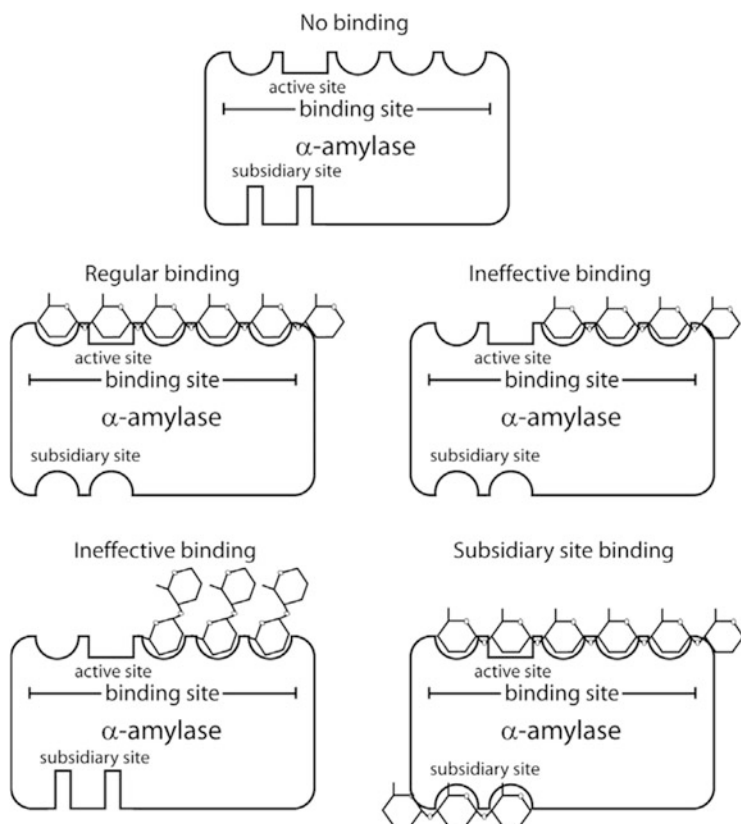


Fig. 1 Schematic drawing of the binding sites of porcine pancreatic α -amylase. The enzyme is first shown unbound; then regular binding without inhibition is presented. Ineffective binding shows how the enzyme might be bound in the instances of competitive inhibition. Binding at the subsidiary site, which opens up only on occupation of the catalytic site by the substrate, brings about uncompetitive inhibition. Reproduced from [10] with permission from Elsevier Ltd. (2010)

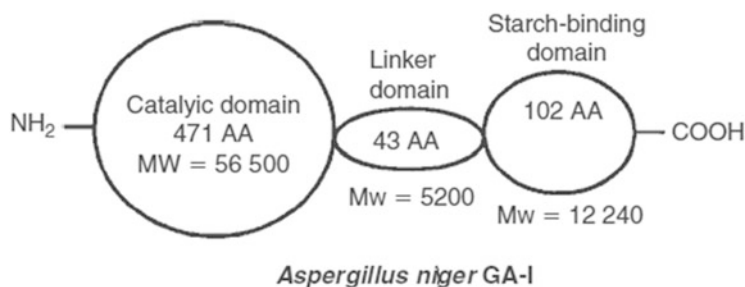


Fig. 2 Schematic representation of the domain structure of amyloglucosidase-I from *Aspergillus niger*. Reproduced from [40] with permission from Elsevier Ltd. (2009)

digestion mechanism. Amyloglucosidase has “pocket like” active sites, which generate only a single and low molecular weight product. After breaking the glycosidic bond, the starch chain must dissociate first and leave the active sites before releasing end products [40].

4 Kinetic Models

Starch digestion involves an interaction between solid substrate (e.g., starch granules, food matrix) and enzymes in solution. Even when starch is gelatinized, it is not a true solution, and its structure will be greatly influenced by the botanical source and previous processing history. The starch digestion rate is a determinant of the metabolic response to a meal, which is better expressed by kinetics rather than thermodynamics. The *in vitro* starch digestion kinetic models are summarized here, including studies of first-order and Michaelis–Menten kinetics, which are more focusing on prolonged and initial digestion stage, respectively.

4.1 First-Order Kinetics

When starch or starch-containing foods are hydrolyzed by amylase or combined with amyloglucosidase *in vitro*, the rate of reaction decreases as the time is extended and plots of the quantity of hydrolyzed starch fraction against time are logarithmic [17]. The natural substrate decay of an exponential reaction fits a first-order equation as follows [41]:

$$C_t = C_\infty (1 - e^{-kt})$$

where t is the digestion time (min), C_t is the concentration of digestion products at incubation time t , C_∞ is the corresponding concentration at infinite time, and k is a pseudo-first-order rate constant (min^{-1}). It would be difficult to obtain the precise value of C_∞ , unless enzymatic digestion allows a long enough incubation time. Butterworth used a modified Guggenheim method to obtain the reaction rate without knowing the value of C_∞ [17]. The equation is shown as below.

$$\ln(dC_t/dt) = -kt + \ln(C_\infty k)$$

Obviously, a plot of $\ln(dC_t/dt)$ against t is linear with the slope of $-k$ and intercept of $\ln(C_\infty k)$. The rate constant is a function of the fixed amylase concentration used in the digestion [17] and is therefore pseudo-first order. Poulsen et al. refer to this plot as a “log of slope” or logarithm of the slope (LOS) plot, and the slope is sensitive to changes in k occurring during a reaction [42]. To use the LOS plot requires

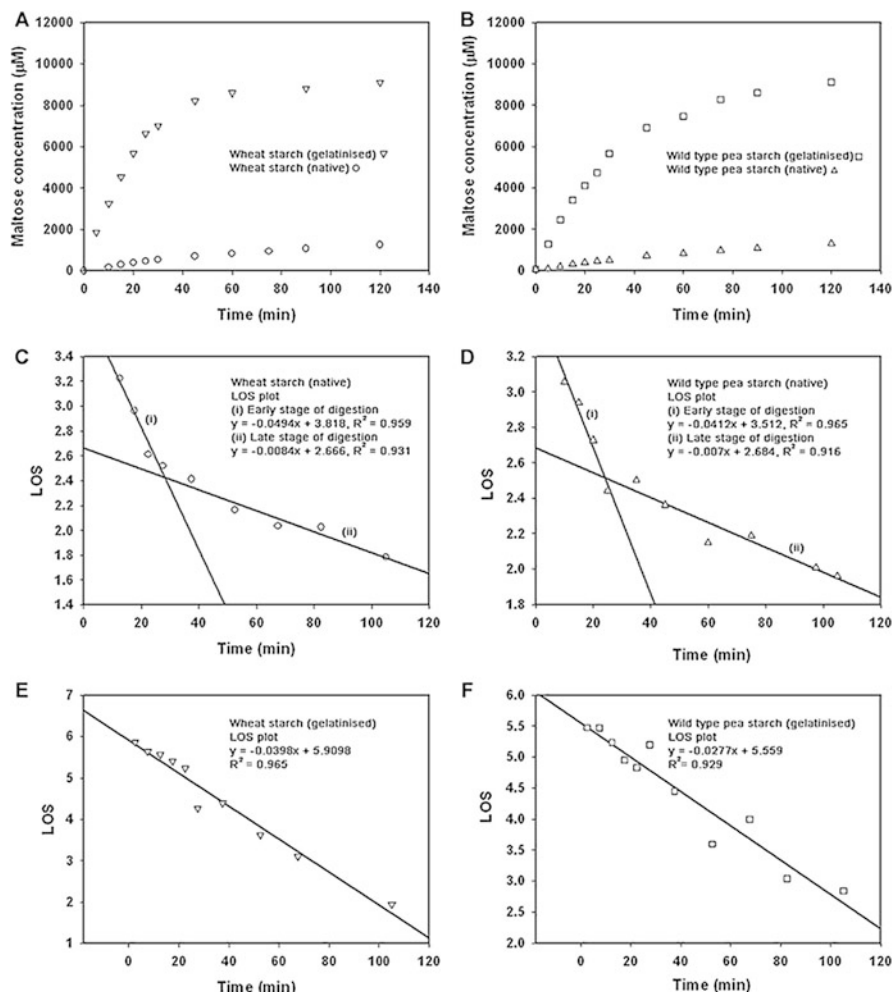


Fig. 3 In vitro starch digestion kinetic profiles and fitting data of native and cooked starches (native and cooked wheat (a) and pea (b) starches; fitting data for native wheat (c) and pea (d), cooked wheat (e) and pea (f) starches). Reproduced from [17] with permission from Elsevier Ltd. (2012)

determination of the slope of a digestibility curve at several time points. The digestion rate constant could be unique under the conditions of characteristic amylase and starch concentration.

The enzymatic digestion profiles and LOS plots of native and cooked starches are shown in Fig. 3. The pancreatic amylase concentration of 0.165 IU/mL was used for cooked starches, and the enzymatic digestion profiles of both starches fitted well to first-order kinetics and are single-phase processes. The enzymatic concentration increased to 0.33 IU/mL for native starches, and fitting plots of both starches revealed a discontinuity and showed a two-phase digestion profile. The fast digestion

phase (<20 min) is believed to be the presence of readily digested starch polymers on the granule surface, whereas the subsequent phase is the main single-rate digestion process (Fig. 3c, d). Therefore, there are no distinct structural fractions existed in rapidly and slowly digestible starches in starch or food matrices, and the amount of digested fraction is under kinetic more than thermodynamic control [28, 43]. Even the enzyme-resistant starch fraction can be further digested by more enzyme or longer hydrolysis time. It should be noted that the first-order kinetic model cannot be directly fitted in some cases, such as (1) under low enzyme concentration, which gives a linear kinetic profile resulting in zero-order kinetics [44], (2) presence of strong inhibitory products [45], and (3) structural and molecular changes occurring during the digestion process such as high-amylose maize starch [28, 46].

LOS plots could characterize multiple stages of the first-order kinetics, and the slope of each stage represents a velocity coefficient. LOS plots are linear if starch substrates are digested at a single rate. However, for some special substrates, the digestion process may have many linear phases [47]. Thus, the whole kinetic profile can be expressed by a piecewise function as follows:

$$C_t = \begin{cases} C_1 + C_{1\infty}(1 - e^{-k_1t}), & 0 \leq t \leq t_1 \\ C_2 + C_{2\infty}(1 - e^{-k_2t}), & t_1 \leq t \leq t_2 \\ \dots \\ C_n + C_{n\infty}(1 - e^{-k_nt}), & t_{n-1} \leq t \leq t_n \end{cases} \quad (1)$$

where n represents the number of phases of starch digestion and each phase has a corresponding k_n and $C_{n\infty}$.

Zou et al. characterized pasta structure and composition in order to reveal how the gluten network decreases digestion rate of the encapsulated starch granules [47]. Figure 4 showed that the presence or absence of pepsin does not affect the starch digestion rate for hard macaroni wheat flour and the starch extracted from the flour, indicating that the natural protein component in the flour has little effect on the starch digestion rate. The authors also found two distinct stages of enzymatic digestion profile, and the starch is digested in the initial stage with a higher rate constant (k_1), while the rate constant of the latter stage (k_2) is slower [47]. After pepsin hydrolysis, there is a significant increase in k_1 value and no obvious change for k_2 value. It seems that pepsin hydrolysis is confined to the external regions and penetrates the inner gluten network with difficulty, and hence the compacted gluten network could retard the starch digestion rate. For pasta powder samples, the LOS plots also show two distinct stages: fast phase represents the starch digestion without the gluten network barrier, whereas slow phase reflects starch granules entrapped with a gluten network with a slow digestion rate [47]. Either grinding process or pepsin hydrolysis could destroy compact gluten structure, which determines the starch digestion rate in pasta.

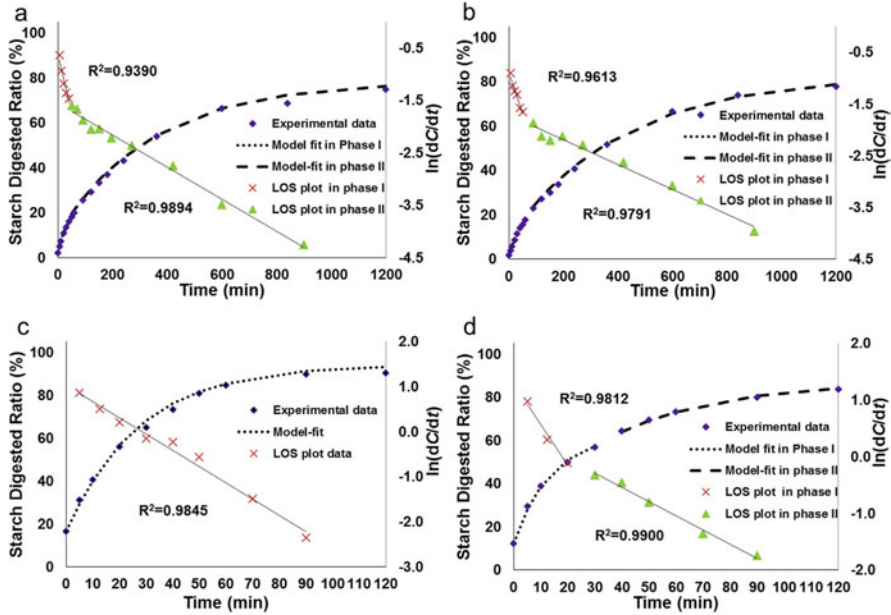


Fig. 4 In vitro starch digestion kinetic profiles, fitting curves, and LOS plots from pasta (a, b), pasta powder (c, d) with pepsin treatment (a, c) or without pepsin treatment (b, d). Reproduced from [47] with permission from Elsevier Ltd. (2015)

4.2 Michaelis–Menten Kinetics and Lineweaver–Burk Plots

Michaelis and Menten proposed a relationship between reaction rate and substrate concentration in 1913, which is one of the simplest and best-known models of enzyme kinetics. According to an intermediate compound theory proposed by Henri and Wurtz, when an enzyme catalyzes a chemical reaction, the enzyme is first combined with the substrate to form an intermediate complex (ES) and then generates the product (P) and releases the enzyme subsequently. The mechanism is presented as follows:



where E is the enzyme, S is the substrate, and P is the product. E and S combine to give an enzyme-substrate complex (ES). The chemical reactions happen at the second step to breakdown ES and generate a product with a first-order catalytic constant k_{cat} (also called k_2 or the turnover number). Initial enzyme reaction rate can be obtained by the Michaelis–Menten plots with three hypotheses: (a) the enzyme

concentration in the reactions is small relative to the substrate concentration; (b) only initial rate conditions are considered. Very little product accumulation happens, and the formation of ES from $E + P$ is negligible; (c) steady-state assumption. Although the compounds can also be broken down into products and enzymes, the decomposition rate is much smaller than the degradation rate; as a result, it will not affect the equilibrium between the substrate, enzymes, and compounds. ES concentration remains unchanged when the ES breakdown rate equals the ES formation rate.

$$\frac{d[P]}{dt} = \frac{V_{\max}[S]}{K_m + [S]} \quad (3)$$

where K_m is the Michaelis–Menten constant, V_{\max} is the maximum rate of the reaction, and $[P]$ is the concentration of the product. The relationship between the K_m and the rate constants in the reaction scheme is as follows:

$$K_m = \frac{K_{-1} + K_2}{K_{+1}} \quad (4)$$


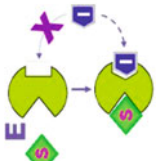
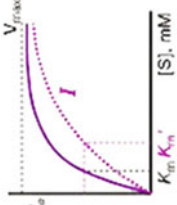
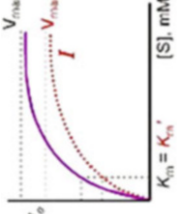
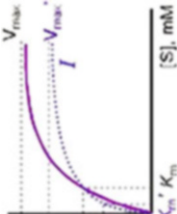
It is difficult to estimate V_{\max} from the position of an asymptote; as in the plot of a rectangular hyperbola, the linear transform of the Michaelis–Menten equation (Lineweaver–Burk linear transform) is often used.

$$\frac{1}{v} = \frac{1}{V_{\max}} + \frac{K_m}{V_{\max}[S]} \quad (5)$$

Recently, Michaelis–Menten kinetics is the most common method used to study the mechanism of inhibitors to enzymatic action. The interaction modes of inhibitors can be judged according to the Lineweaver–Burk double reciprocal curve, which is the foundation to investigate the inhibition mechanism. Michaelis–Menten kinetics shows the relationship between the initial rate of the enzymatic reaction (v) and substrate concentration (S). K_m , with the unit generally as mol/L, represents the substrate concentration when reaction rate (v) reaches a half of the V_{\max} ($K_m = [S]$ at $0.5 V_{\max}$), determined by the nature of enzyme, rather than the concentration of enzyme. Thus different types of enzymes can be identified according to the value of K_m . In this region of the curve, enzyme is almost completely saturated with the substrate, so the reaction relative to the substrate is a zero-level reaction, which means that increasing the substrate has little effect on the reaction rate and the constant value approaching the reaction rate is called the maximum reaction rate (V_{\max}).

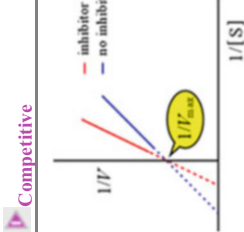
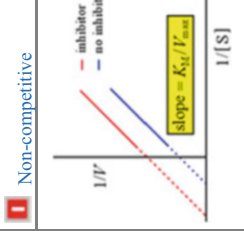
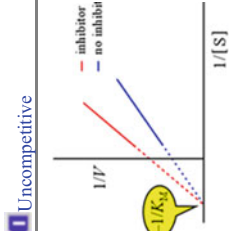
Table 1 shows the mechanism of competitive, noncompetitive, and uncompetitive inhibition. Competitive inhibition kinetics has the following characteristics: when the inhibitor is present, Michaelis–Menten constant (K_m) increases and the maximum reaction rate (V_{\max}) remains unchanged. In noncompetitive inhibition kinetics,

Table 1 The mechanism of competitive, noncompetitive inhibition, and uncompetitive inhibition

	<p>Competitive</p>  <p>Substrate</p> <p>Compete for active site</p> <p>Inhibitor</p>		<p>Uncompetitive</p> 
<p>Inhibitory mechanisms and instructions</p>	$E + S \rightleftharpoons ES \longrightarrow E +$ $+ I \rightleftharpoons EI$	$E + S \rightleftharpoons ES \longrightarrow E +$ $+ I \rightleftharpoons EI$ $EI + S \rightleftharpoons EI/S$	$E + S \rightleftharpoons ES \longrightarrow E +$ $+ I \rightleftharpoons E/S$
<p>Michaelis–Menten plots</p>			

(continued)

Table 1 (continued)

<p>Lineaver-Burk double reciprocal plots</p>	<p> Competitive</p> <p>inhibitor (red dashed line), no inhibitor (blue solid line). The lines intersect on the y-axis at $1/V_{max}$. The slope is K_M/V_{max}.</p>	<p> Non-competitive</p> <p>inhibitor (red dashed line), no inhibitor (blue solid line). The lines intersect on the x-axis. The slope is K_M/V_{max}.</p>	<p> Uncompetitive</p> <p>inhibitor (red dashed line), no inhibitor (blue solid line). The lines are parallel and intersect on the y-axis at $-1/K_M$.</p>
	<p>V_{max} unchanged, K_m raised</p>	<p>V_{max} reduced, K_m reduced</p>	<p>V_{max} reduced, K_m unchanged</p>

K_m remains unchanged, and V_{max} decreases when the inhibitor is present. There are some limitations for the Michaelis–Menten kinetics, for example, the estimated K_m and V_{max} often have a relatively large error when the substrate concentration is low.

Lineweaver–Burk double reciprocal graphs can be used to distinguish competitive, noncompetitive, and hybrid competitive inhibition. Further, Dixon and Cornish–Bowden equations are used to obtain inhibition constant (K_i).

Dixon equation is the curve under the condition of different substrate concentrations, with the reciprocal of the initial velocity reaction rate ($1/v$) as the ordinate and the inhibitor concentration (i) as the abscissa, and Cornish–Bowden equation is the curve under the condition of a series of substrate concentrations (a) with a/v as the ordinate and i as the abscissa. Therefore, it is more helpful in revealing the complex case of the interaction between enzyme and inhibitors using these two equations together [48]. In addition, competitive inhibition constant (K_{ic}) and noncompetitive inhibition constant (K_{iu}) can be obtained through the curve. By definition, K_{ic} refers to the dissociation of complex compounds formed by inhibitors and enzymes, so $1/K_{ic}$ characterizes the combination of inhibitors and enzymes.

Among them, the initial reaction rate (v) is the slope of the plot with time as the abscissa and reducing sugar content as the ordinate. The value of K_{ic} and K_{iu} can be obtained by Dixon equation. For different inhibitors and enzymes, the applicable Dixon equation is different. For competitive inhibition, the applicable equation is shown in Eq. (6).

$$v = \frac{V_{max}a}{K_m \left(1 + \frac{i}{K_{ic}}\right) + a} \quad (6)$$

For hybrid inhibition, the applicable equation is shown in Eq. (7):

$$v = \frac{V_{max}a}{K_m \left(1 + \frac{i}{K_{ic}}\right) + a \left(1 + \frac{i}{K_{iu}}\right)} \quad (7)$$

where V_{max} represents the maximum reaction rate, a represents the concentration of starch, K_m represents the Michaelis constant, i represents the concentration of the inhibitor protein, and v represents the initial reaction rate.

Taking the reciprocals of both sides of the Dixon equation, we can get a linear plot with i as the abscissa and $1/v$ as the vertical, where $K_{ic} = -i$, and the value of K_{ic} can be obtained by the absolute value of the abscissa of the intersection of different linear curves with different starch concentrations.

The value of K_{iu} cannot be obtained directly from the Dixon equation, but it can be obtained from the Cornish–Bowden equation, with a/v as the ordinate and i as the abscissa. For hybrid inhibition, the applicable Cornish–Bowden equation is shown in Eq. (8) [49].

$$\frac{v}{a} = \frac{V_{\max}}{K_m \left(1 + \frac{i}{K_{ic}}\right) + a \left(1 + \frac{i}{K_{iu}}\right)} \quad (8)$$

Similarly, taking the reciprocals of both sides of Cornish–Bowden equation, a linear plot with i as the abscissa and a/v as the vertical will be obtained, where $K_{iu} = -i$, and similar to the above, the value of K_{iu} can be obtained by the absolute value of the abscissa of the intersection of different linear curves with different starch concentrations.

5 Conclusions

From nutritional perspectives, RS is physiologically useful to reduce the risk factors of obesity and type 2 diabetes. Focusing on the two fundamental but rate-determining steps of the conversion of starch substrate into absorbable products allows a better understanding of starch digestibility. Instead of only comparing experimental data of starch digestion, the digestion curves can be modeled by kinetic equations (first-order kinetics and Michaelis–Menten kinetics and the derivations). The kinetic analysis helps evaluate the role of non-starch components within starch foods and starch structural features in determining starch digestibility. Greater understanding of the structural basis in determining starch digestibility would help to design starch foods with enhanced nutritional outcomes.

In a real food system, there are complex mechanisms, i.e., the interactions among starch, amylases, and non-starch components, which may significantly impact on starch digestion and need more investigations. Furthermore, advanced in vitro methods imitating complex physiological processes, e.g., mastication habits, intestinal passage rate, and colonic fermentation by human microbiota, provide opportunities to better understand deeper nutritional functionality of RS.

Acknowledgments We thank the National Natural Science Foundation of China (31701546), the Natural Science Foundation of Guangdong Province (2017A030313207), and the 111 Project (B17018). Bin Zhang thanks the Hong Kong Scholar Program (XJ2019049), Pearl River Talent Recruitment Program of Guangdong Province (2017GC010229), and the Pearl River Nova Program of Guangzhou (201906010079).

References

1. Svihus B, Hervik AK. Digestion and metabolic fates of starch, and its relation to major nutrition-related health problems: a review. *Starch-Starke*. 2016;68(3–4):302–13.
2. Wang SJ, Li CL, Copeland L, Niu Q, Wang S. Starch retrogradation: a comprehensive review. *Compr Rev Food Sci Food Saf*. 2015;14(5):568–85.
3. Englyst HN, Cummings JH. Digestion of the polysaccharides of some cereal foods in the human small-intestine. *Am J Clin Nutr*. 1985;42(5):778–87.

4. Li H, Gidley MJ, Dhital S. High-amylose starches to bridge the “fiber gap”: development, structure, and nutritional functionality. *Compr Rev Food Sci Food Saf.* 2019;18:362–79.
5. Van Munster IP, Tangerman A, Nagengast FM. Effect of resistant starch on colonic fermentation, bile-acid metabolism, and mucosal proliferation. *Dig Dis Sci.* 1994;39(4):834–42.
6. Topping DL, Bajka BH, Bird AR, Clarke JM, Cobiac L, Conlon MA, Morell MK, Toden S. Resistant starches as a vehicle for delivering health benefits to the human large bowel. *Microb Ecol Health Dis.* 2008;20(2):103–8.
7. Hasjim J, Lavau GC, Gidley MJ, Gilbert RG. In vivo and in vitro starch digestion: are current in vitro techniques adequate? *Biomacromolecules.* 2010;11(12):3600–8.
8. Tovar J, Bjorck IM, Asp NG. Incomplete digestion of legume starches in rats: a study of precooked flours containing retrograded and physically inaccessible starch fractions. *J Nutr.* 1992;122(7):1500–7.
9. Faisant N, Champ M, Colonna P, Buleon A. Structural discrepancies in resistant starch obtained in-vivo in humans and in-vitro. *Carbohydr Polym.* 1993;21(2–3):205–9.
10. Dona AC, Pages G, Gilbert RG, Kuchel PW. Digestion of starch: in vivo and in vitro kinetic models used to characterise oligosaccharide or glucose release. *Carbohydr Polym.* 2010;80(3):599–617.
11. Englyst HN, Kingman SM, Cummings JH. Classification and measurement of nutritionally important starch fractions. *Eur J Clin Nutr.* 1992;46:S33–50.
12. Ai YF, Hasjim J, Jane JL. Effects of lipids on enzymatic hydrolysis and physical properties of starch. *Carbohydr Polym.* 2013;92(1):120–7.
13. Zhang B, Huang Q, Luo FX, Fu X. Structural characterizations and digestibility of debranched high-amylose maize starch complexed with lauric acid. *Food Hydrocoll.* 2012;28(1):174–81.
14. Hasjim J, Lee SO, Hendrich S, Setiawan S, Ai Y, Jane JL. Characterization of a novel resistant-starch and its effects on postprandial plasma-glucose and insulin responses. *Cereal Chem.* 2010;87(4):257–62.
15. Zhang B, Dhital S, Gidley MJ. Densely packed matrices as rate determining features in starch hydrolysis. *Trends Food Sci Technol.* 2015;43(1):18–31.
16. Zhang B, Wang K, Hasjim J, Li EP, Flanagan BM, Gidley MJ, Dhital S. Freeze-drying changes the structure and digestibility of B-polymorphic starches. *J Agric Food Chem.* 2014;62(7):1482–91.
17. Butterworth PJ, Warren FJ, Grassby T, Patel H, Ellis PR. Analysis of starch amylolysis using plots for first-order kinetics. *Carbohydr Polym.* 2012;87(3):2189–97.
18. Dhital S, Warren FJ, Butterworth PJ, Ellis PR, Gidley MJ. Mechanisms of starch digestion by alpha-amylase: structural basis for kinetic properties. *Crit Rev Food Sci Nutr.* 2017;57:875–92.
19. Li H, Gidley MJ, Dhital S. Wall porosity in isolated cells from food plants: implications for nutritional functionality. *Food Chem.* 2019;279:416–25.
20. Dhital S, Bhattarai RR, Gorham J, Gidley MJ. Intactness of cell wall structure controls the in vitro digestion of starch in legumes. *Food Funct.* 2016;7:1367–79.
21. Fardet A, Hoebler C, Baldwin PM, Bouchet B, Gallant DJ, Barry JL. Involvement of the protein network in the in vitro degradation of starch from spaghetti and lasagne: a microscopic and enzymic study. *J Cereal Sci.* 1998;27(2):133–45.
22. Warren FJ, Royall PG, Gaisford S, Butterworth PJ, Ellis PR. Binding interactions of alpha-amylase with starch granules: the influence of supramolecular structure and surface area. *Carbohydr Polym.* 2011;86(2):1038–47.
23. Blazek J, Gilbert EP. Effect of enzymatic hydrolysis on native starch granule structure. *Biomacromolecules.* 2010;11(12):3275–89.
24. Dhital S, Shrestha AK, Gidley MJ. Effect of cryo-milling on starches: functionality and digestibility. *Food Hydrocoll.* 2010;24(2–3):152–63.
25. Blazek J, Copeland L. Amylolysis of wheat starches. I. Digestion kinetics of starches with varying functional properties. *J Cereal Sci.* 2010;51(3):265–70.

26. Tahir R, Ellis PR, Butterworth PJ. The relation of physical properties of native starch granules to the kinetics of amylolysis catalysed by porcine pancreatic alpha-amylase. *Carbohydr Polym.* 2010;81(1):57–62.
27. Lopez-Rubio A, Htoon A, Gilbert EP. Influence of extrusion and digestion on the nanostructure of high-amylose maize starch. *Biomacromolecules.* 2007;8(5):1564–72.
28. Htoon A, Shrestha AK, Flanagan BM, et al. Effects of processing high amylose maize starches under controlled conditions on structural organisation and amylase digestibility. *Carbohydr Polym.* 2009;75(2):236–45.
29. Zhang B, Dhital S, Flanagan BM, Luckman P, Halley PJ, Gidley MJ. Extrusion induced low-order starch matrices: enzymic hydrolysis and structure. *Carbohydr Polym.* 2015;134:485–96.
30. Han JA, BeMiller JN. Preparation and physical characteristics of slowly digesting modified food starches. *Carbohydr Polym.* 2007;67(3):366–74.
31. Robyt JF, French D. Multiple attack hypothesis of alpha-amylase action: action of porcine pancreatic human salivary and *Aspergillus oryzae* alpha-amylases. *Arch Biochem Biophys.* 1967;122(1):8–16.
32. Nichols BL, Avery S, Sen P, et al. The maltase-glucoamylase gene: common ancestry to sucrase-isomaltase with complementary starch digestion activities. *Proc Natl Acad Sci.* 2003;100(3):1432–7.
33. Hizukuri S. Starch: analytical aspects. In: Eliasson AC, editor. *Carbohydrates in food.* New York: CRC; 1996. p. 347–430.
34. Robyt JF. Enzymes in the hydrolysis and synthesis of starch. In: Whistler RL, Bemiller JN, Paschall EF, editors. *Starch: chemistry and technology.* 2nd ed. Cambridge: Academic; 1986. p. 87–123.
35. Robyt JF, French D. Action pattern of porcine pancreatic alpha-amylase in relationship to substrate binding site of enzyme. *J Biol Chem.* 1970;245(15):3917–27.
36. Kandra L, Gyemant G. Examination of the active sites of human salivary alpha-amylase (HSA). *Carbohydr Res.* 2000;329(3):579–85.
37. Abdullah M, French D, Robyt JF. Multiple attack by alpha-amylases. *Arch Biochem Biophys.* 1966;114(3):595–63.
38. Takahashi T, Kato K, Ikegami Y, Irie M. Different behavior towards raw starch of 3 forms of glucoamylase from a *Rhizopus* Sp. *J Biochem.* 1985;98(3):663–71.
39. Norouzzian D, Akbarzadeh A, Scharer JM, Young MM. Fungal glucoamylases. *Biotechnol Adv.* 2006;24(1):80–5.
40. Robyt JF. Enzymes and their action on starch. In: Bemiller JN, Whistler RL, editors. *Starch chemistry and technology.* 3rd ed. Cambridge: Academic; 2009. p. 237–92.
41. Goni I, Garcia-Alonso A, Saura-Calixto F. A starch hydrolysis procedure to estimate glycemic index. *Nutr Res.* 1997;17(3):427–37.
42. Poulsen BR, Ruiter G, Visser J, et al. Determination of first order rate constants by natural logarithm of the slope plot exemplified by analysis of *Aspergillus niger* in batch culture. *Biotechnol Lett.* 2003;25(7):565–71.
43. Zhang B, Dhital S, Gidley MJ. Synergistic and antagonistic effects of α -amylase and amyloglucosidase on starch digestion. *Biomacromolecules.* 2013;12(6):1945–54.
44. Warren FJ, Zhang B, Waltzer G, Gidley MJ, Dhital S. The interplay of α -amylase and amyloglucosidase activities on the digestion of starch in in vitro enzymic systems. *Carbohydr Polym.* 2015;117:192–200.
45. Warren FJ, Butterworth PJ, Ellis PR. Studies of the effect of maltose on the direct binding of porcine pancreatic alpha-amylase to maize starch. *Carbohydr Res.* 2012;358:67–71.
46. Lopez-Rubio A, Flanagan BM, Shrestha AK, Gidley MJ, Gilbert EP. Molecular rearrangement of starch during in vitro digestion: toward a better understanding of enzyme resistant starch formation in processed starches. *Biomacromolecules.* 2008;9(7):1951–8.

47. Zou W, Sissons M, Gidley MJ, Gilbert RG, Warren FJ. Combined techniques for characterising pasta structure reveals how the gluten network slows enzymic digestion rate. *Food Chem.* 2015;188:559–68.
48. Cornish-Bowden A, Eisenthal R. Statistical considerations in the estimation of enzyme kinetic parameters by the direct linear plot and other methods. *Biochem J.* 1974;139(3):721–30.
49. Eisenthal R, Cornish-Bowden A. The direct linear plot. A new graphical procedure for estimating enzyme kinetic parameters. *Biochem J.* 1974;139(3):715–20.

Digestibility of Starches for Human Health



Les Copeland

Abstract This chapter considers the digestibility of starch in relation to its nutritional qualities and influences on human health. Rapidly digested starch (RDS) is associated with poor postprandial glycaemic and insulinemic control. Excessive dietary exposure over the long term increases the risks for obesity and diet-related illnesses. Slowly digested starch (SDS) moderates these postprandial responses and has a key role in producing satiety and limiting food intake. Starch that is not digested in the upper human gut is a good source of fermentable food for the gut microbiota, which are now recognised as having an essential role in the health of the host.

Keywords Starch digestibility · Rapidly digested starch · Slowly digested starch · Resistant starch · Human health

1 Introduction

Starch is a macro-constituent of many foods and the main source of glycaemic (glucose releasing) carbohydrate in the human diet. It usually contributes 50–70% of dietary energy. The energy density of starch-rich foods and their low satiety effects are contributing factors to obesity and diet-related illnesses. Hence, the digestibility and postprandial glycaemic effect of starchy foods are of considerable interest for nutrition and health. This chapter will consider the nutritional qualities of starch and their relationship to human health and risk factors for disease.

L. Copeland (✉)

Sydney Institute of Agriculture, School of Life and Environmental Sciences, The University of Sydney, Sydney, NSW, Australia

e-mail: les.copeland@sydney.edu.au

© Springer Nature Singapore Pte Ltd. 2020

S. Wang (ed.), *Starch Structure, Functionality and Application in Foods*,

https://doi.org/10.1007/978-981-15-0622-2_10

169

2 Nutritional Importance of Starch

Glucose is an energy source for all tissues in the human body. However, the brain, kidneys, red blood cells and reproductive tissues have specific requirements for a reliable supply of glucose to support normal physiological functioning. The brain alone uses 20–25% of total basal metabolic energy expenditure even though it accounts for less than 10% of body weight [1]. Glucose is also the main energy source for foetal growth [2–4], and females during pregnancy and lactating mothers have additional requirements for glucose. Under normal circumstances, the body's essential glucose requirements are met from dietary glycaemic carbohydrate and gluconeogenesis from noncarbohydrate sources, such as the glycerol part of glycerolipids, some amino acids (e.g. alanine) or short-chain fatty acids (SCFAs) produced in fermentations by gut microflora and absorbed into the bloodstream [5–7]. Gluconeogenesis can contribute about 20–30% of the glucose needs in humans. Nevertheless, there is still debate about the minimum daily requirement of dietary glycaemic carbohydrate considered essential in adult humans [4, 8].

Glucose is a strong reducing agent and therefore a chemically reactive molecule. Complex hormonal and metabolic controls normally maintain blood glucose levels within a narrow concentration range to avoid adverse physiological consequences of insufficient availability of glucose to meet essential metabolic needs (hypoglycaemia) or too high concentrations (hyperglycaemia) that can cause chemical damage to tissues. Postprandial glucose metabolism is complex and influenced by many factors that vary between individuals, including physiology, age and state of health. The gut microbiome also plays an important role [9, 10]. If blood glucose is elevated, hormones produced by the gut induce pancreatic islet cells to release insulin, which interacts with specific receptors and stimulates glucose uptake by the tissues. Other hormones act to slow the rate of gastric emptying and reduce food intake [10]. Glucose excess to immediate metabolic requirements can be stored in the liver as glycogen, which acts as a transient buffer for glucose in the bloodstream. Glycogen can also be stored in muscle, but from there it is then no longer available to other tissues. As the capacity of the liver and muscle to lay down glycogen reserves is finite, excess glucose is then diverted to lipogenesis. Prolonged excess of nutrient intake increases the risk of insulin insensitivity, obesity, type-2 diabetes and other diet-related diseases, which are increasing around the world [9, 11].

The availability of readily digestible dietary starch is considered to have been a key factor in the evolution of modern humans (*Homo sapiens*) from their early hominin ancestors. According to a hypothesis put forward by Hardy et al. [12], the coincidence of regular consumption of starchy plant foods, the adoption of cooking and an increase in the copy number of the salivary amylase gene (*AMY1*) provided an evolutionary advantage that underpinned the rapid increases in brain size and aerobic capacity that occurred from around 2 million years ago.

3 Glycaemic Effect of Starch

The glycaemic potential of starch and starchy foods may be assessed using *in vivo* and *in vitro* testing methods. Glycaemic index (GI) is a numerical value that indicates the blood glucose-raising potential of a food. The GI is defined as the increase in blood glucose after intake of 50 g of a carbohydrate over 120 min, using either glucose or white bread as the reference value [13].

The GI value accounts for the digestion of the food, absorption of glucose from the gut and its clearance from bloodstream. Foods are classified as low GI (value <55), medium GI (56–69) and high GI (>70) [14]. High-GI foods produce a greater increase in postprandial blood glucose and an exaggerated insulin response, which over time increases body fat and weight, and eventually insulin resistance and decrease of insulin release due to exhaustion of pancreatic endocrine function. Insulin resistance prevents glucose from entering the brain, which is associated with neurodegenerative disease and cognitive decline [10].

This method for measuring GI requires testing human subjects, which is costly, time-consuming and labour intensive. A practical limit on the number of subjects that can be tested at a time reduces statistical robustness of the analyses, whereas ethical considerations prevent the testing of materials not permitted as foods. For these reasons, *in vitro* enzymic assays are often used as a proxy to assess the digestibility of food starches. *In vitro* methods are particularly useful in comparative, high-throughput studies and for ranking of multiple samples such as those from plant breeding programs. These methods can be applied to materials not able to be eaten as a food [15]. Samples within the same experiment are comparable, but variability between laboratories in the application of the experimental protocol, especially the source and amounts of enzymes used, makes comparisons between studies less reliable. Comparative advantages and limitations of *in vivo* and *in vitro* methods for assessing the glycaemic effects of food starches are shown in Table 1.

The *in vitro* tests are mostly based on methodology developed by Englyst and co-workers [16] (hereafter referred to as the Englyst method), on the principle that starch is the main glycaemic carbohydrate in foods and that cellulose and other polysaccharides in the diet are not digested in the upper gut of humans. The rate and extent of glucose release from starch are measured using a combination of digestive enzymes under defined conditions. The original method published by Englyst involved an initial acid/pepsin step to simulate the passage of the starch through the stomach. This step is not always included by others who have subsequently used this protocol. Englyst followed the pepsin treatment with a starch digestion using pancreatin (a pancreatic extract) in combination with added amyloglucosidase and invertase. Pancreatin is a source of α -amylase and also provides glucosidase, protease, lipase and nuclease activities. The actual amount of enzyme activities used for the digestions is not well defined, and the presence of proteases in pancreatin as well as many commercial pancreatic amylase preparations used nowadays is another source of uncertainty.

Table 1 Comparison of glycaemic index testing and in vitro digestion studies

Parameters	Glycaemic index	In vitro digestion
Property measured	Blood glucose raising potential of a carbohydrate-rich food	Enzymic breakdown of starch
Time required	Slow (days)	Rapid (hours)
Labour input	High	Low
Costs	High	Low
Variability	High inter- and intra-individual variability	Controlled test conditions, easily replicated
Representative of physiology	Good	Does not consider gastric emptying, glucose absorption and the heterogeneous environment of the gut
Standard for testing	Established ISO method and Australian standard	No standard testing protocol established
Other factors	Comprehensive database available	Suitable for testing novel foods

Adapted from [15] with permission from the Elsevier Ltd. (2012)

Englyst et al. [16] proposed a terminology that correlated with results obtained from in vivo studies with ileostomates using a variety of substrates. The amount of glucose released in vitro under their defined conditions within 20 min was said to represent rapidly digested starch (RDS), whereas glucose released from starch more slowly (between 20 and 120 min) was designated as slowly digested starch (SDS). Starch that was undigested after 2 h was classified as resistant starch (RS). This value may be an underestimation, as some starches are considered to take closer to 4 h to pass out of the small intestine. It is important to recognise that rapidly and slowly digested starch and resistant starch are physiological concepts, not chemical entities. As discussed by Dhital et al. [17], they represent kinetic stages in the enzymic breakdown of starch under a specific set of experimental conditions. This raises questions about the comparability of the values obtained for RDS, SDS and RS between studies and with values initially obtained by Englyst. Both RDS and SDS are regarded nutritionally as glycaemic starches as they cause the uptake of glucose into the bloodstream. Resistant starch has no glycaemic effect as it escapes digestion in the upper gut. SDS and RS are associated with health benefits through better blood glucose control and the provision of substrates to promote growth of beneficial microflora in the colon [18].

Although Englyst's method is based on mimicking physiological processes that occur in the hydrolysis of starch by digestive enzymes, there are questions about the comparability of in vitro methods, which measures the enzymic breakdown of starch under fixed experimental conditions with a process that varies between individuals and includes chewing, the mixing effects of muscle contraction, viscosity effects, the concentration of digesta by removal of water, absorption of glucose into the bloodstream and the metabolic clearance of glucose from the bloodstream [19].

An often-used modification of the Englyst method, which seeks to correlate *in vitro* starch hydrolysis with GI values for the same food, gives rise to an 'estimated GI' or eGI value as described by Goni et al. [20]. Using samples of common foods cooked in boiling water until considered edible, the percentage of starch hydrolysed *in vitro* after 90 min was found to correlate best with actual GI values. A hydrolysis index (HI) was calculated from measurements of total starch and enzyme-digestible starch (i.e. total starch minus enzyme-resistant starch) and the area under the curve for the test food as a proportion of the curve for corn starch as a reference [19]. Similarly, a strong correlation was obtained between the hydrolysis percentage at 120 min and GI values for potatoes, indicating that the glycaemic response to the potatoes was largely dependent on the percentage of starch hydrolysed by 120 min [21].

4 Starch Digestion

The digestibility of foods is influenced by many factors including size of particles, composition and structure of the food matrix and the digestive health of the individual. In general, rapidly digested foods tend to have higher glycaemic potential, whereas foods digested slowly provide more fermentable substrates for the gut microbiota. Particle size is affected by milling and processing and the breaking up of food by chewing. Chewing also serves to mix the substrate and salivary amylases into a bolus, which protects the enzyme and allows digestion to continue to some extent in the low-pH environment of the stomach [22]. Access of digestive enzymes to the substrate is the rate-limiting step in the hydrolysis of starch and is a major determinant of the rate of glucose release and postprandial metabolism [17, 23]. Plant cell wall material is not digested in the upper gut and provides a barrier between food substrates and the enzymes. Entrapment of starch in the gluten matrix is a major factor in lowering the rate of starch digestion in pasta [24].

Starch depolymerisation in the upper gut of humans is mediated by α -amylases, which cleave the α -1,4 glycosidic bonds to produce linear and branched dextrins. Amyloglucosidases and isoamylases break the α -1,6 branching links. The cleavage of the α -1,6 linkages takes place at a slower rate than the α -1,4 linkages [25]. *In vitro* studies have shown starches that produce a higher proportion of branched α -limit dextrins release glucose more slowly [26]. Humans have two forms of α -amylase: one in saliva (encoded by the *AMY1* genes) and the other form secreted by the pancreas into the small intestine (encoded by the *AMY2* genes). *Homo sapiens* have between 2 and 20 gene copies of *AMY1*, whereas other primates have only two copies. The potential for greater expression of amylase means greater ability to digest starch. A strong correlation has been shown between *AMY1* copy number and the concentration of amylase in saliva and the oral capacity for starch digestion [27, 28]. Individuals with high copy numbers of *AMY1* digest starchy foods more

rapidly and produce higher postprandial glycaemia in, whereas having low copy number is associated with colonic methane production [28].

The linear and branched dextrins released from starch are hydrolysed into free glucose by mucosal α -glucosidases at the intestinal brush border membrane for absorption into the bloodstream [29]. Several factors can modulate the rate of starch digestion and absorption of glucose. Plant-derived polyphenolic compounds in the diet can act as nonspecific inhibitors of digestion enzymes and glucose transporters [30–32], while inhibition of α -amylase by malto-oligosaccharides in hydrolysis products and by binding of the enzyme to cellulose and other food polysaccharides may also be relevant [33].

5 Starch Digestibility

Raw starch is hydrolysed slowly, with the rate influenced by various factors including varietal and genetic differences, amylose content and granule structural characteristics and surface properties. Physical and chemical properties that impede access of the enzyme to the granule surface or reduce enzyme binding to the substrate in other ways slow down enzyme action [33, 34]. For example, amylases are considered to attack the amorphous layers of the granules more readily due to the greater difficulty of access of the enzymes to glucan bonds in the more densely packed crystalline regions [35]. Waxy starches are attacked more readily than non-waxy starches as the amorphous regions contain less amylose to hinder enzyme access. The rate of hydrolysis closely approximates first-order kinetics and will therefore slow down as the concentration of substrate decreases [21].

Most starch consumed by humans has been at least partially gelatinised due to processing or cooking, which results in the disruption of the structural order of native granules. Starch granules, regardless of their source, that have been at least partially gelatinised are hydrolysed much more rapidly than intact native granules [21, 36]. The rate of enzymic hydrolysis of cooked starch is controlled by the extent of gelatinisation that occurs and subsequent aggregate formation due to retrogradation during cooling. These processes are influenced by the nature of the starch, the temperature, rate and duration of heating, water availability, shear forces and length of cooling time [36–39]. Even moderate cooking that causes no visible disruption to granules greatly increases the susceptibility of starch to hydrolysis by amylases *in vitro* [40]. Cooking also disrupts the integrity of plant cell walls so that the starch granules are more accessible to α -amylase digestion [41]. The amylolysis kinetics of cooked starch are more complex than first-order, reflecting the greater heterogeneity of the substrate [42].

Starchy foods that are digested slowly and elicit a lower glycaemic response are considered more beneficial to health and in the prevention and management of diabetes and hyperlipidaemia than foods that produce high glycaemic responses [9]. Rapidly digested starch is abundant in highly processed foods and is the most significant contributor to a rapid influx of glucose into the bloodstream and poor

glycaemic and insulin control. Slowly digested starch results in a more prolonged release of glucose giving rise to a reduced postprandial glycaemic and insulin responses [9]. Slowly digested starch, which is likely to contain a mixture of remnant crystalline clusters from partially gelatinised starch as well as retrograded starch, could be affected by small variations in the cooking and cooling conditions.

Starch breakdown products (dextrins and/or glucose) that reach the ileum are considered to have physiological benefits by triggering the ileal and colonic brakes, which stimulate hormone secretions that decrease the rate of gastric emptying and thereby reduce food intake [43]. These digestion products in the ileum are proposed act on the gut-brain axis by altering gene expression to lower production of appetite-stimulating signalling molecules and increase production of appetite-suppressing neuropeptides [44]. The result is the slowing of nutrient delivery into the bloodstream and stimulation of the satiation response in the brain and controlling food intake [19, 45]. The ileal brake has been offered as an explanation for how low-GI foods could moderate hunger levels.

6 Resistant Starch

Starch that escapes digestion in the small intestine passes into the lower gut, where it is a substrate for fermentation by the microflora. The human gastrointestinal tract is host to about 10^{14} microbial cells, which account for about 2% of the body weight and occupy multiple environmental niches. The majority of cells reside in the colon. The complexity and functional diversity of species varies between individuals, as does the impact of diet on the microbiota [46]. Functional diversity and redundancy give the gut microbiota a degree of resilience to variations in the diet and against inflammatory conditions. The gut microbiota can affect the host's resistance to inflammatory and autoimmune conditions and influence brain function and cognitive abilities. Dietary variations have been demonstrated to drive changes in the composition and function of gut microflora [47]. However, the extent to which changes in the gut microflora are causative of disease or provide a biomarker for abnormalities remains to be definitively determined.

The resistance of starch to digestion may be due to many factors: its intrinsic structural properties; effects of the food matrix in limiting access by hydrolytic enzymes; retrogradation; the extent of structural changes during processing; chemical modifications; and interactions with other food constituents. Resistant starch has properties similar to readily fermentable dietary fibre. Health benefits of traditional Indian and African diets are attributed to being rich in resistant starch [48]. As discussed elsewhere in this book, the properties and different forms of resistant starch have been reviewed extensively in the literature (e.g. [49, 50]) and will not be covered here.

The short-chain fatty acids (SCFAs) acetate, propionate and butyrate are major products of the microbial fermentations and are considered to play important beneficial physiological roles [5–7, 46]. However, as much of the information on the fate

of SCFAs produced by fermentation in the gut comes from animal models due to the difficulty of performing experiments with humans, caution is needed in the interpretation of results to humans. Short-chain fatty acid produced by gut microflora lowers the pH of the colon, creating a less favourable environment for harmful microbes and affecting the absorption of nutrients, including reducing the bioavailability of toxic amines. SCFAs act as signalling metabolites involved in regulating energy homeostasis and glucose and lipid fluxes and helping to modulate inflammation [5–7]. SCFAs absorbed into the bloodstream enter pathways of carbohydrate and lipid metabolism in the liver. They can supply up to about 10% of the energy for host metabolism. The energy yield from nondigestible carbohydrate will vary depending on the efficiencies of fermentation and of absorption of the SCFA products [46]. Propionate is mainly incorporated into gluconeogenesis, whereas acetate is mostly assimilated into lipid biosynthesis [5–7]. Fermentation of resistant starch produces a high level of butyrate, which is the main energy source of colonocytes and helps to inhibit their malignant transformation [51].

7 Conclusions

The digestive fate of starch determines its nutritional qualities and their relationship to human health. Rapidly digested starch is associated with poor postprandial glycaemic and insulinemic control. Excessive dietary exposure over the long term increases the risks for obesity and diet-related illnesses. Slowly digested starch moderates these postprandial responses and has a key role in producing satiety and limiting food intake. On the other hand, starch that is not digested in the upper human gut is good source of fermentable food for the gut microbiota, which are now recognised as having an essential role in the health of the host. Exploring the complexity of the interplay between starch properties and its digestion, the gut microbiota, diet and health will no doubt be a topic of research interest for years to come.

References

1. Fonseca-Azevedo K, Herculano-Houzel S. Metabolic constraint imposes tradeoff between body size and number of brain neurons in human evolution. *Proc Natl Acad Sci USA*. 2012;109(45):18571–6.
2. Herrera E. Metabolic adaptations in pregnancy and their implications for the availability of substrates to the fetus. *Eur J Clin Nutr*. 2000;54:47–51.
3. Baumann MU, Deborde S, Illsley NP. Placental glucose transfer and fetal growth. *Endocrine*. 2002;19(1):13–22.
4. Trumbo P, Schlicker S, Yates AA, Poos M. Dietary reference intakes for energy, carbohydrate, fiber, fat, fatty acids, cholesterol, protein and amino acids. *J Acad Nutr Diet*. 2002;102(11):1621–30.

5. den Besten G, van Eunen K, Groen AK, Venema K, Reijngoud DJ, Bakker BM. The role of short-chain fatty acids in the interplay between diet, gut microbiota, and host energy metabolism. *J Lipid Res.* 2013;54(9):2325–40.
6. Byrne CS, Chambers ES, Morrison DJ, Frost G. The role of short chain fatty acids in appetite regulation and energy homeostasis. *Int J Obes.* 2015;39(9):1331–8.
7. Morrison DJ, Preston T. Formation of short chain fatty acids by the gut microbes and their impact on human metabolism. *Gut Microbes.* 2016;7(3):189–200.
8. Bier DM, Brosnan JT, Flatt JP, Hanson RW, Heird W, Hellerstein MK, et al. Report of the IDECG working group on lower and upper limits of carbohydrate and fat intake. *Eur J Clin Nutr.* 1999;53:S177–8.
9. Svihus B, Hervik AK. Digestion and metabolic fates of starch, and its relation to major nutrition-related health problems: a review. *Starch-Stärke.* 2016;68(3–4):302–13.
10. Pfeiffer AFH, Keyhani-Nejad F. High glycemic index damage-pivotal role of GIP and GLP-1. *Trends Endocrinol Metab.* 2018;29(5):289–99.
11. Hyseni L, Atkinson M, Bromley H, Orton L, Lloyd-Williams F, McGill R, et al. The effects of policy actions to improve population dietary patterns and prevent diet-related non-communicable diseases: scoping review. *Eur J Clin Nutr.* 2017;71(6):694–711.
12. Hardy K, Brand-Miller J, Browne KD, Thomas MG, Copeland L. The importance of dietary carbohydrate in human evolution. *Q Rev Biol.* 2015;90(3):251–68.
13. Jenkins DJ, Kendall CW, Augustin LS, Franceschi S, Hamidi M, Marchie AJ, et al. Glycemic index: overview of implications in health and disease. *Am J Clin Nutr.* 2002;76(1):266S–73S.
14. International Standards Organization Standard 26, 642. Food products: determination of the glycaemic index (GI) and recommendation for food classification. 2010. <https://www.iso.org/standard/43633.html>
15. Ek KL, Brand-Miller J, Copeland L. Glycemic effect of potatoes. *Food Chem.* 2012;133(4):1230–40.
16. Englyst HN, Kingman SM, Cummings JH. Classification and measurement of nutritionally important starch fractions. *Eur J Clin Nutr.* 1992;46(Suppl 2):S33–50.
17. Dhital S, Warren FJ, Butterworth PJ, Ellis PR, Gidley MJ. Mechanisms of starch digestion by α -amylase-structural basis for kinetic properties. *Crit Rev Food Sci Nutr.* 2017;57(5):875–92.
18. Englyst KN, Englyst HN, Hudson JH, Cole TJ, Cummings JH. Rapidly available glucose in foods: an in vitro measurement that reflects the glycemic response. *Am J Clin Nutr.* 1999;69(3):448–54.
19. Magallanes-Cruz PA, Flores-Silva PC, Bello-Perez LA. Starch structure influences its digestibility: a review. *J Food Sci.* 2017;82(9):2016–23.
20. Goni I, Garcia-Alonso A, Saura-Calixto F. A starch hydrolysis procedure to estimate glycemic index. *Nutr Res.* 1997;17(3):427–37.
21. Ek KL, Wang S, Copeland L, Brand-Miller JC. Discovery of a low-glycaemic index potato and relationship with starch digestion in vitro. *Br J Nutr.* 2014;111(4):699–705.
22. Butterworth PJ, Warren FJ, Ellis PR. Human α -amylase and starch digestion: an interesting marriage. *Starch-Stärke.* 2011;63(7):395–405.
23. Edwards CH, Grundy MML, Grassby T, Vasilopoulou D, Frost GS, Butterworth PJ, et al. Manipulation of starch bioaccessibility in wheat endosperm to regulate starch digestion, postprandial glycemia, insulinemia, and gut hormone responses: a randomized controlled trial in healthy ileostomy participants. *Am J Clin Nutr.* 2015;102(4):791–800.
24. Zou W, Sissons M, Gidley MJ, Gilbert RG, Warren FJ. Combined techniques for characterising pasta structure reveals how the gluten network slows enzymic digestion rate. *Food Chem.* 2015;188:559–68.
25. Zhang G, Hamaker BR. Slowly digestible starch: concept, mechanism, and proposed extended glycemic index. *Crit Rev Food Sci Nutr.* 2009;49(10):852–67.
26. Kittisuban P, Lee B-H, Suphantharika M, Hamaker BR. Slow glucose release property of enzyme-synthesized highly branched maltodextrins differs among starch sources. *Carbohydr Polym.* 2014;107(1):182–91.

27. Mandel AL, Peyrot des Gachons C, Plank KL, Alarcon S, Breslin PAS. Individual differences in *AMY1* gene copy number, salivary-amylase levels, and the perception of oral starch. *PLoS One*. 2010;5(10):e13352.
28. Atkinson FS, Hancock D, Petocz P, Brand-Miller JC. The physiologic and phenotypic significance of variation in human amylase gene copy number. *Am J Clin Nutr*. 2018;108(4):737–48.
29. Lin AHM, Lee BH, Nichols BL, Quezada-Calvillo R, Rose DR, Naim HY, et al. Starch source influences dietary glucose generation at the mucosal α -glucosidase level. *J Biol Chem*. 2012;287(44):36917–21.
30. Zhu F. Interactions between starch and phenolic compound. *Trends Food Sci Technol*. 2015;43(2):129–43.
31. Simsek M, Quezada-Calvillo R, Ferruzzi MG, Nichols BL, Hamaker BR. Dietary phenolic compounds selectively inhibit the individual subunits of maltase-glucoamylase and sucrase-isomaltase with the potential of modulating glucose release. *J Agric Food Chem*. 2015;63(15):3873–9.
32. Barrett AH, Farhadi NF, Smith TJ. Slowing starch digestion and inhibiting digestive enzyme activity using plant flavanols/tannins—a review of efficacy and mechanisms. *LWT-Food Sci Technol*. 2018;87:394–9.
33. Dhital S, Gidley MJ, Warren FJ. Inhibition of α -amylase activity by cellulose: kinetic analysis and nutritional implications. *Carbohydr Polym*. 2015;123:305–12.
34. Zhang B, Dhital S, Gidley MJ. Densely packed matrices as rate limiting features in starch hydrolysis. *Trends Food Sci Technol*. 2015;43(1):18–31.
35. Blazek J, Copeland L. Amylolysis of wheat starches. II. Degradation patterns of native starch granules with varying functional properties. *J Cereal Sci*. 2010;52(2):295–302.
36. Wang S, Copeland L. Molecular disassembly of starch granules during gelatinization and its effect on starch digestibility: a review. *Food Funct*. 2014;4(1):1564–80.
37. Goesaert H, Brijs K, Veraverbeke WS, Courtin CM, Gebruers K, Delcour JA. Wheat flour constituents: how they impact bread quality and how to impact their functionality. *Trends Food Sci Technol*. 2005;16(1–3):12–30.
38. Hoover R. The impact of heat-moisture treatment on molecular structures and properties of starches isolated from different botanical sources. *Crit Rev Food Sci Nutr*. 2010;50(9):835–47.
39. Wang S, Li C, Copeland L, Niu Q, Wang S. Starch retrogradation: a comprehensive review. *Compr Rev Food Sci Food Saf*. 2015;14(5):568–85.
40. Wang S, Wang S, Liu L, Wang S, Copeland L. Structural orders of wheat starch do not determine the in vitro enzymatic digestibility. *J Agric Food Chem*. 2017;65(8):1697–706.
41. Singh J, Dartois A, Kaur L. Starch digestibility in food matrix: a review. *Trends Food Sci Technol*. 2010;21(4):168–80.
42. Nhan MT, Copeland L. Genotype and environment effects on the susceptibility of wheat starch to amylolysis. *Starch-Stärke*. 2017;69(9–10):1700058.
43. Cisse F, Pletsch EA, Erickson DP, Chegeni M, Hayes AMR, Hamaker BR. Preload of slowly digestible carbohydrate microspheres decreases gastric emptying rate of subsequent meal in humans. *Nutr Res*. 2017;45:46–51.
44. Hasek LY, Phillips RJ, Zhang G, Kinzig KP, Kim CY, Powley TL, et al. Dietary slowly digestible starch triggers the gut-brain axis in obese rats with accompanied reduced food intake. *Mol Nutr Food Res*. 2018;62(5):170017.
45. Lee BH, Bello-Pérez LA, Lin AHM, Kim CY, Hamaker BR. Importance of location of digestion and colonic fermentation of starch related to its quality. *Cereal Chem*. 2013;90(4):335–43.
46. Flint HJ, Scott KP, Louis P, Duncan SH. The role of the gut microbiota in nutrition and health. *Nat Rev Gastroenterol Hepatol*. 2012;9(10):577–89.
47. David LA, Maurice CF, Carmody RN, Gootenberg DB, Button JE, Wolfe BE, et al. Diet rapidly and reproducibly alters the human gut microbiome. *Nature*. 2014;505(7484):559–63.
48. Shetty PS, Kurpad AV. Increasing starch intake in the human diet increases fecal bulking. *Am J Clin Nutr*. 1986;43(2):210–2.

49. Fuentes-Zaragoza E, Sanchez-Zapata E, Sendra E, Sayas E, Navarro C, Juana Fernandez-Lopez J, et al. Resistant starch as prebiotic: a review. *Starch-Stärke*. 2011;63(7):406–15.
50. Raigond P, Ezekiel R, Raigond B. Resistant starch in food: a review. *J Sci Food Agric*. 2015;95(10):1968–78.
51. Liu H, Wang J, He T, Becker S, Zhang G, Li D, Ma X. Butyrate: a double-edged sword for health? *Adv Nutr*. 2018;9(1):21–9.